

# **Dissertation**

**submitted to the**

**Combined Faculties for the Natural Sciences and for Mathematics**

**of the Ruperto-Carola University of Heidelberg, Germany**

**for the degree of**

**Doctor of Natural Sciences**

presented by

Florian Kohlhepp

Diploma-Biologist

born in Lohr am Main

# **Dissertation**

**submitted to the**

**Combined Faculties for the Natural Sciences and for Mathematics**

**of the Ruperto-Carola University of Heidelberg, Germany**

**for the degree of**

**Doctor of Natural Sciences**

presented by

Florian Kohlhepp

Diploma-Biologist

born in Lohr am Main

Oral examination: .....



# **EHD proteins in Apicomplexan Parasites**

Referees: Prof. Dr. Michael Lanzer  
Dr. Ann-Kristin Müller

Hiermit erkläre ich, dass ich die vorliegende Arbeit von September 2009 bis November 2012 unter Anleitung von Dr. Ann-Kristin Müller selbst durchgeführt habe und schriftlich ausgearbeitet habe. Ich habe mich keiner anderen Hilfsmittel und Quellen bedient als den hier ausdrücklich erwähnten.

.....

Datum

.....

Florian Kohlhepp

# Contents

<b>Danksagung</b>	<b>I</b>
<b>Summary</b>	<b>III</b>
<b>Zusammenfassung</b>	<b>V</b>
<b>Abbreviations</b>	<b>VII</b>
<b>1 Introduction</b>	<b>1</b>
1.1 Apicomplexa . . . . .	1
1.1.1 General . . . . .	1
1.1.2 Specific subcellular structures of apicomplexa . . . . .	1
1.1.3 Replication of the apicomplexan pathogens . . . . .	8
1.1.4 Epidemiology and pathogenicity . . . . .	14
1.2 Eps15-homology domain proteins . . . . .	23
1.2.1 Protein architecture and function . . . . .	24
1.2.2 Function . . . . .	27
1.3 Aim of this study . . . . .	29
<b>2 Materials and Methods</b>	<b>31</b>
2.1 Laboratory equipment . . . . .	31
2.2 Consumables . . . . .	32
2.3 Strains . . . . .	33
2.3.1 Bacteria strains . . . . .	33
2.3.2 Cell lines . . . . .	33
2.3.3 Parasite strains . . . . .	33
2.3.4 Mosquito strains . . . . .	33
2.3.5 Mouse strains . . . . .	33
2.4 Chemicals and reagents . . . . .	34
2.5 Oligonucleotides . . . . .	34
2.6 Antibodies . . . . .	35
2.6.1 Primary antibodies . . . . .	35
2.6.2 Secondary antibodies . . . . .	36
2.7 Media, buffers and solutions . . . . .	36
2.7.1 Media and buffers for molecular biological methods . . . . .	36
2.7.2 Media and solutions for cell culture . . . . .	37
2.7.3 Media, buffers and solutions for parasitological methods . . . . .	38
2.7.4 Buffers and solutions for biochemical methods . . . . .	39
2.7.5 Antibiotics . . . . .	41
2.8 Molecular biological methods . . . . .	41
2.8.1 Cloning of the targeting constructs for parasite transfection . . . . .	41
2.8.2 Stage-specific RNA isolation and cDNA synthesis for RT PCR . . . . .	47

2.9	Cell culture . . . . .	49
2.9.1	<i>In vitro</i> liver-stage development of <i>P. berghei</i> in human hepatoma cells Huh7 . . . . .	49
2.9.2	<i>P. falciparum</i> culture - asexual parasites . . . . .	49
2.9.3	<i>P. falciparum</i> culture - gametocytes . . . . .	50
2.9.4	Cultivation of <i>Toxoplasma gondii</i> in human foreskin fibroblasts (HFFs) . . . . .	50
2.10	Parasitological methods . . . . .	51
2.10.1	<i>Plasmodium</i> methods . . . . .	51
2.10.2	<i>Anopheles</i> mosquito methods . . . . .	56
2.10.3	<i>Toxoplasma</i> methods . . . . .	57
2.11	Animal experimental methods . . . . .	60
2.11.1	Administration of anaesthesia . . . . .	60
2.11.2	Infection of rodents with <i>Plasmodium</i> parasites . . . . .	60
2.11.3	Blood withdrawal by heart puncture . . . . .	60
2.12	Biochemical methods . . . . .	61
2.12.1	Preparation of parasite lysate for SDS-PAGE . . . . .	61
2.12.2	SDS polyacrylamide gel electrophoresis (SDS-PAGE) . . . . .	61
2.12.3	Western blot analysis . . . . .	62
2.13	<i>In silico</i> analysis of apicomplexan EHD-proteins . . . . .	62
<b>3</b>	<b>Results</b>	<b>63</b>
3.1	Establishment of a combined <i>in vitro/in vivo</i> <i>P. falciparum</i> life-cycle	63
3.1.1	<i>Plasmodium falciparum</i> asexual and sexual bloodstage <i>in vitro</i> culture . . . . .	63
3.1.2	Membrane feeding of mature gametocytes to <i>Anopheles stephensi</i> mosquitoes . . . . .	65
3.1.3	Liver-stage development of <i>Plasmodium falciparum in vitro</i> . . . . .	66
3.2	Characterization of EHD-proteins in apicomplexan parasites . . . . .	67
3.2.1	RME-1 encodes for a conserved EHD-family member in apicomplexan parasites . . . . .	67
3.2.2	<i>TgRME-1</i> localizes to not yet known subcellular structures within <i>Toxoplasma gondii</i> . . . . .	67
3.2.3	Functional analysis of RME-1 in <i>Toxoplasma gondii</i> . . . . .	71
3.2.4	Localization of <i>Plasmodium falciparum</i> EHD-protein <i>PfEHD</i> . . . . .	76
3.2.5	Protein localization of <i>TgRME-1</i> and <i>PfEHD</i> is interchangeable between apicomplexans, but differs according to the intrinsic protein architecture . . . . .	78
3.2.6	Expression and localization of the EHD-protein in <i>P. berghei</i> . . . . .	81
3.2.7	EHD gene deletion in murine <i>P. berghei</i> is not essential for blood-stage development . . . . .	81
3.2.8	EHD mutant <i>P. berghei</i> parasites develop indistinguishable from wildtype parasites during the intra-mosquito life-cycle . . . . .	88

---

3.2.9	Depletion of EHD results in developmental slow-down during late liver-stage development in <i>P. berghei</i> and protection of severe pathology in C57BL/6 mice . . . . .	92
<b>4</b>	<b>Discussion</b>	<b>95</b>
4.1	<i>Plasmodium falciparum</i> transmission . . . . .	95
4.2	Characterization of EHD-proteins in apicomplexa . . . . .	97
4.2.1	The apicomplexan EHD-protein family . . . . .	98
4.2.2	Structure of the apicomplexan EHD-proteins . . . . .	99
4.2.3	Localization and function of EHD-proteins in apicomplexa . .	102
4.2.4	Virulence of the <i>P. berghei</i> ANKA strain depleted of <i>PbEHD</i>	112
<b>5</b>	<b>Supplementary data</b>	<b>117</b>
<b>6</b>	<b>References</b>	<b>118</b>

# Danksagung

Im Laufe der Ausführung meiner Doktorarbeit ergaben sich viele berufliche und private Kontakte, die zum Gelingen dieser Arbeit beigetragen haben und denen ich zu Dank verpflichtet bin. Dies soll im Folgenden geschehen. Sollte ich dabei Personen vergessen haben, so ist dies nicht aus bösen Hintergedanken sondern purer Zerstreuung entstanden und ich bitte diejenigen um Entschuldigung.

Bedanken möchte ich mich im Folgenden besonders bei

**Ann-Kristin**, die mir die Möglichkeit gegeben hat, meine Dissertation in ihrem Labor anzufertigen. Die aus dir sprudelnden Ideen und vor allem deine motivierende Art haben mich immer wieder über Motivationstäler hinweg getragen. Ich danke dir für deine Offenheit für meine neu entstehenden Pläne und das Vertrauen in meine Person. Ich danke dir vor allem auch für dein Mentoring in Sachen Zukunftsplanung. Bitte erhalte dir deine motivierende Art!

**Markus**, der mich bereitwillig in sein Labor in Glasgow aufgenommen hat und dort meinen Horizont erweitert hat. Du hast es mir ermöglicht, Einblick in neue Arbeitsweisen und ein neues Forschungsfeld zu bekommen. Zusätzlich übernahmst du das Mentoring für ein Zweitprojekt, welches letztendlich erfolgreicherweise zum Hauptprojekt meiner Arbeit wurde. Zusätzlich danke ich dir, dass du ohne zu zögern für einen Beisitz in meinem Prüfungskomitee für meine Verteidigung nach Heidelberg reistest.

**Prof. Lanzer**. Für meine Aufnahme in seine Abteilung und seine Bereitschaft, das Erstgutachten meiner Arbeit zu übernehmen.

**Markus und Freddy**. Für die Teilnahme an meinen TAC-Meetings und vor allem auch an meinem Prüfungskomitee.

**The whole lab in Heidelberg**. You have been phenomenal and I would not want to miss working together with you. We've spent a lot of time together and you've always been there for help or a good laugh.

**The whole lab in Glasgow**. From the beginning on you've made it very easy for me integrating into your group and I quite enjoyed working in such an international atmosphere. Besides I really enjoyed hanging out for a beer or two in the pub with you guys. We really had a great time.

**Manu**. Für ihre gute Betreuung während meiner Zeit in Glasgow und ihre fort-dauernde Freundschaft.

**Roland**. Der mich gelehrt hat, was es bedeutet, Perfektionist zu sein. Ich hoffe

ich konnte mir einiges davon auch einverleiben. Du warst ein sehr guter Kollege, manchmal sogar Mentor und vor allem auch Freund. Ich hoffe wir werden noch einige Championsleague-Finals zusammen erleben (dann vielleicht mit besserem Ausgang).

**Matt.** Who brought some british (probably rather Londonish) culture into my life. I have enjoyed many a good chat and sometimes also intense discussions with you. Thank you for becoming my friend.

**Kerstin.** Die mich einen Grossteil meiner Arbeit in Heidelberg begleitet hat und immer ein offenes Ohr beim täglichen Kaffeetreff hatte. Ich freue mich sehr, dass wir auch ausserhalb des Labors Freunde geblieben sind.

**Miriam Griesheimer.** Für deine aufopferungsvolle Arbeit an allen Problemchen, die im Alltag eines Doktoranden entstehen. Was du leistest, ist mehr als pflichtbewusst!

**Tobias Spielmann und Florian Kruse.** Für eine fruchtbare Kollaboration.

**Julia.** Für die Weiterbearbeitung meines vielversprechenden Projektes und deine Korrekturen an meiner Arbeit.

**Jenny.** Für ihre Bereitschaft, mir im Labor in allen Belangen tatkräftig beizustehen, obwohl eigentlich gerade mal wieder 'ne Schulstunde war. Danke auch, für einige spassige Ethanol-Verkostungen.

**Meiner Tante Irene.** Für die finanzielle Unterstützung eines unterbezahlten Wissenschaftlers.

**Meinen Eltern.** Die mich zu dem aufwachsen haben lassen, was ich heute bin. Ihr habt es mir ermöglicht, frei von gesellschaftlichen oder kulturellen Zwängen aber mit kritischem Verstand genau das zu machen, was ich will. Ich danke euch für alles.

**Dem wichtigsten Menschen in meinem Leben, meiner Frau.** Ich danke dir für das Ertragen aller Entbehrungen der letzten 3,5 Jahre. Deine Unterstützung hat mich immer wieder angetrieben und es mir leicht gemacht, die Arbeit durchzuziehen. Ich hoffe ich kann mich irgendwann einmal revanchieren.

# Summary

A bottle neck in malaria research is the investigation of *Plasmodium falciparum* liver stage parasites because of technical issues in the infection of *Anopheles* mosquitoes with these parasites and subsequent generation of infectious sporozoites. Therefore I, in close collaboration with a colleague, established a combined *in vitro/in vivo* *P. falciparum* life-cycle in our lab. For that a protocol was established that included the generation of sexual *P. falciparum* stages in cell culture that were subsequently transmitted to *Anopheles* mosquitoes utilizing a special membrane feeding system. Later in the life-cycle sporozoites were extracted from the mosquito salivary glands to finally infect liver cells for further studies. We were able to establish a constant mosquito-infection rate for several months to perform experiments on *P. falciparum* sporozoites and exo-erythrocytic forms.

To help decipher the in apicomplexans so far mostly uncharacterized cellular process endocytosis I investigated the function and localization of an EH-domain containing dynamin-like protein in *Toxoplasma* and *Plasmodium*. It belongs to a family of eukaryotic Eps15-homology domain containing proteins (EHDs) that have been characterized in higher eukaryotes and especially vertebrates to be part of endocytic events such as vesicular trafficking and endocytic recycling. I was able to show by an *in silico* analysis that in contrast to vertebrates (four different EHDs) there is only one protein member of this family existing in each apicomplexan. Nevertheless, the apicomplexan EHD-protein has similar to all other EHD-proteins a predicted characteristic ATPase-domain (dynamin-like G-domain) and the Eps15-homology domain (EH). Through a fluorescent tagging approach I was able to show a dynamic localization of the *Toxoplasma* EHD-protein member *TgRME-1* (named after its ortholog in *C. elegans* receptor-mediated endocytosis protein 1) within the parasites. It localized to a vesicular compartment within the parasites that did not colocalize with known organelles so far. The compartment fragmented upon cellular division and is most likely involved in vesicular trafficking of supply vesicles that transport lipids or other nutrients to the newly forming daughter-cells. From the data obtained in this thesis it can be hypothesized that the *TgRME-1* labelled compartment represents a storage compartment that is filled up during the non-replicative phase and during endodyogeny helps to form daughter-cells. Structural analysis of the protein by deletion of either the G-domain or the EH-domain revealed a similar architecture of the protein compared to published data on mammalian EHDs. Investigation of the *Plasmodium berghei* EHD (*PbEHD*) with an antibody generated against the protein revealed a different localization in different parasite stages. Whereas the protein localized to several vesicular compartments in the sporozoite stage it concentrated to a single organelle-like compartment in liver-stages 24 hours after invasion. This compartment later (48 hours after invasion) also fragmented and was distributed to the newly forming merozoites during schizogony, similar to *TgRME-1*. This sub-cellular localization indicated that both proteins might share a similar function in tachyzoites of *Toxoplasma* and *Plasmodium* liver stage parasites. A phenotypical



analysis of *PbEHD* via generation of a *pbehd* (-) parasite revealed a putative function for the protein during intrahepatic development. The *pbehd* (-) liver stage parasite showed a reduced growth rate *in vivo* and *in vitro* but was still able to complete the life-cycle. *In vivo*, C57BL/6 mice infected with *pbehd* (-) parasites showed a prolonged prepatency period and did not develop experimental cerebral malaria in contrast to wildtype-infected mice. I was able to narrow down this protective effect solely to both the prolonged liver-stage phase and the involvement of the immunomodulator cytokine IL-10.

Even though a defined role for the EHD-protein in the apicomplexan parasites could not be determined in this thesis I was able to characterize its architecture and localization in *Toxoplasma gondii* and *Plasmodium berghei*. I was able to identify a so far uncharacterized compartment in these parasites that is most likely involved in endocytic-recycling and storage of nutrients such as lipids for the parasites. In addition, my studies showed that the apicomplexan EHD-protein is involved in processes of the cellular division. A better understanding of these and other mechanisms of endocytosis will lead to anti-parasitic strategies that may reduce the burden caused by apicomplexan parasites.

# Zusammenfassung

Eine kritische Engstelle der Forschung an *Plasmodium falciparum* ist die Untersuchung von Leberstadien aufgrund technischer Hindernisse bei der Infektion von *Anopheles* Stechmücken und der anschliessenden Erzeugung von infektiösen Sporozoiten. Daher etablierte ich zusammen mit einem Kollegen einen kombinierten *in vivo/in vitro* *P. falciparum*-Lebenszyklus in unserem Labor. Im Rahmen dessen wurde ein Protokoll entwickelt, das die Erzeugung von *P. falciparum*-Sexualstadien und anschliessende Übertragung des Erregers auf *Anopheles* Stechmücken beinhaltete. Im weiteren Verlauf des Lebenszykluses wurden Sporozoiten aus den Speicheldrüsen der Stechmücken extrahiert und anschliessend Leberzellen mit diesen infiziert. Es gelang uns, die Infektionsrate der Stechmücken über Monate hinweg konstant hoch zu halten, um Experimente an Sporozoiten und exo-erythrozytären Stadien von *P. falciparum* durchführen zu können.

Um zur Entzifferung des in Apicomplexa bisher weitestgehend unbekanntes Prozesses der Endozytose beizutragen, untersuchte ich die Funktion und Lokalisation eines EH-Domänen-beinhaltenen Dynamin-ähnlichen Proteins in *Toxoplasma* und *Plasmodium*. Dieses Protein gehört einer Familie von eukaryotischen Eps15-Homologie-Domänen beinhaltenen Proteinen (EHDs) an, denen in höheren Eukaryoten und speziell in Vertebraten eine Rolle bei vesikulären Transporten und endozytotischem Recycling zugesprochen werden konnte. Ich konnte mittels *in silico*-Analysen zeigen, dass im Unterschied zu Vertebraten (besitzen 4 EHD-Proteine) in Apicomplexa nur jeweils ein Protein dieser Familie vorhanden ist. Dennoch besitzt auch das EHD-Protein der Apicomplexa laut Prognosen von Datenbanken die charakteristische ATPase-Domäne (Dynamin-ähnliche G-Domäne) und die Eps15-Homologie (EH)-Domäne. Ich war in der Lage, mittels fluoreszente Tag eine dynamische Lokalisation des *Toxoplasma* EHD-proteins *TgRME-1* (benannt nach seinem Ortholog in *C. elegans*: Receptor-mediated endocytosis protein 1) zu zeigen. Das Protein befand sich innerhalb eines vesikulären Kompartiments innerhalb des Parasiten, welches in seiner Lokalisierung nicht mit einem bisher bekannten Organell übereinstimmte. Während der Zellteilung teilte sich das Kompartiment und ist hierbei höchst wahrscheinlich beteiligt an der Verteilung von Vesikeln, die Lipide oder andere Nährstoffe zu den sich neu bildenden Tochterzellen bringen. Zusätzlich kann von den in dieser Arbeit erzeugten Daten abgeleitet werden, dass es sich bei dem *TgRME-1*-Kompartiment vermutlich um einen Speicher handelt, der während der Nicht-Teilungsphase aufgefüllt wird und während der Endodyogenese die Bildung der Tochterzellen unterstützt. Die strukturelle Analyse des Proteins ergab durch Deletion von entweder der G-Domäne oder der EH-Domäne eine mit den Säuger-EHD-Proteinen vergleichbare Architektur. Die Untersuchung des EHD-Proteins in *Plasmodium berghei* (*PbEHD*) mittels eines gegen das Protein erzeugten Antikörpers ergab eine unterschiedliche Lokalisation des Proteins in verschiedenen Stadien des Erregers. Während sich das Protein in Sporozoiten in mehreren vesikulären Kompartimenten befand, war es auch in Leberstadien 24 Stunden nach der Invasion in einem

einzigem Organell-ähnlichen Kompartiment zu finden. Dieses Kompartiment teilte sich später (48 Stunden nach der Invasion) ebenfalls auf und verteilte sich während der Shizogonie auf die einzelnen Merozoiten, vergleichbar mit *TgRME-1*. Diese subzelluläre Lokalisation deutet darauf hin, dass beide Proteine eine ähnliche Funktion in Tachyzoiten von *Toxoplasma* und Leberstadien von *Plasmodium* ausführen. Eine phänotypische Analyse von *PbEHD* mittels Erzeugung eines *pbehd* (-)-Parasiten ergab eine mögliche Funktion des Proteins während der Leberstadienentwicklung. Die *pbehd* (-)-Leberstadien wuchsen langsamer *in vivo* und *in vitro*, waren aber immer noch in der Lage, den Lebenszyklus zu vervollständigen. *In vivo* zeigte sich in infizierten C57BL/6 Mäusen im Gegensatz zu mit Wildtyp infizierten Mäusen eine verlängerte Präpatenz und ein Schutz vor der Entstehung von experimenteller cerebraler Malaria (ECM). Ich war in der Lage zu zeigen, dass dieser schützende Effekt einzig der verlängerten Leberstadienphase und der Beteiligung des Zytokins IL-10 zuzuschreiben ist.

Obwohl dem EHD-Protein in Apicomplexa in dieser Arbeit keine definierte Funktion zugeordnet werden konnte, war ich dennoch in der Lage die Architektur und Lokalisation des Proteins in *Toxoplasma gondii* und *Plasmodium berghei* zu charakterisieren. Ich konnte ein bisher nicht charakterisiertes Kompartiment in diesen Parasiten identifizieren, das höchst wahrscheinlich an endozytotischem Recycling und Speicher von Nährstoffen wie beispielsweise Lipiden beteiligt ist. Zusätzlich zeigten meine Untersuchungen, dass das Apicomplexa EHD-Protein beteiligt ist an der Zellteilung der Parasiten. Ein besseres Verständnis von diesen und anderen Mechanismen der Endozytose wird dazu beitragen, anti-parasitische Strategien zu entwickeln, die die von Apicomplexa Parasiten verursachte Belastung vermindern können.

# Abbreviations

aa	amino acids
ACP	acyl-carrier protein
Amp	ampicillin
AMP	Adenosin monophosphate
APS	ammonium persulphate
ATP	Adenosin triphosphate
BBB	blood-brain barrier
bp	base pair
BNI	Bernhardt-Nocht Institut
BS	blood stage
BSA	bovine serum albumin
cDNA	complementary DNA
gDNA	genomic DNA
Cl	chloride
CM	Cytoplasma membrane/Cerebral malaria
CSP	circumsporozoite protein
C-terminus	carboxy-terminus
Da	dalton
DD	destabilization domain (ddFKBP)
dd	bidest.
ddH <sub>2</sub> O	double distilled water (Millipore)
DEPC	diethylpyrocarbonate
DHFR	dihydrofolate reductase
DHFR/TS	dihydrofolate reductase-thymidylate synthase
DIC	differential interference contrast
DMEM	Dulbecco's Modified Eagle Medium
DMSO	dimethylsulfoxid
DNA	deoxyribonucleic acid
dNTP	desoxyribonucleosid-triphosphat
<i>E. coli</i>	<i>Escherichia coli</i>
DrpB	Dynamamin-related protein B
ECM	experimental cerebral malaria
EDTA	ethylenediaminetetra acetic acid
EE	early endosome
EEF	extra-erythrocytic form
EH	Eps15-homology domain
EHD	Eps15-homology domain containing protein
ER	endoplasmic reticulum
ERC	endocytic recycling compartment
FCS	fetal calf serum

for	forward
g	gram or gravitational acceleration
G	gauge
GFP	green-fluorescent protein
GOI	gene of interest
GPI	glycophosphatidylinositol
GRA	dense granule protein
GSH	Glutathion
GTP	Guanosin triphosphate
h	hours
HFF	Human foreskin fibroblast
HRP	horseradish peroxidase
iEM	immuno-electron microscopy
IFA	immuno-fluorescence analysis
IL-10	interleukin 10
IMC	inner membrane complex
Ig	immuno-globuline
i.p.	intraperitoneal
i.v.	intravenous
iRBC	infected red blood cell
k	kilo
kb	kilobase
K/X	Ketamin/ Xylazin
l	liter
LB	Luria broth
LDL	low-density lipoprotein
LE	late endosome
L-FABP	liver fatty acid-binding protein
LS	liver stage
m	milli
M	molar
mA	milli Ampere
MHC	major histo-compatibility complex
MIC	micronemal protein
min	minute
ml	millilitre
MOPS	3-(N-morpholino)propanesulfonic acid
MPA	Mycophenolic acid
MTOC	microtubule-organizing center
MyoA	Myosin A
n	nano
Na	sodium

N-terminus	amino-terminus
OD	optical density
ODS	oocyst-derived sporozoites
ORF	open-reading frame
PbA	<i>Plasmodium berghei</i> strain ANKA
PABA	para-Aminobenzoic acid
PAGE	polyacrylamide gel electrophoresis
PBS	phosphate buffered saline
PCR	polymerase chain reaction
Pb	<i>Plasmodium berghei</i>
Pf	<i>Plasmodium falciparum</i>
PFA	paraformaldehyde
pH	potential hydrogenii
PM	plasmamembrane
P/S	penicillin and streptomycin
PV	parasitophorous vacuole
PVM	parasitophorous vacuolar membrane
RBC	red blood cell
rev	reverse
RME-1	receptor-mediated endocytosis protein 1
RNA	ribonucleic acid
ROP	Rhoptry protein
RON	Rhoptry neck protein
rpm	revolutions per minute
RT	room temperature or reverse transcriptase
-RT	without reverse transcriptase
+RT	with reverse transcriptase
s	second
SDS	sodium dodecylsulphate
SG	salivary gland
SGS	salivary gland sporozoite
Shld-1	Shield-1
SP	signal peptide
spz	sporozoite/s
TAE	Tris/acetic acid/EDTA
Taq	<i>Thermus aquaticus</i>
TBS	tris-buffered saline
TBST	tris-buffered saline/tween
TE	Tris/ EDTA
TEMED	triethylmethylethyldiamine
Tg	<i>Toxoplasma gondii</i>
TM	transmembrane domain

TRIS	tris (hydroxymethyl)-aminomethane
TVM	tubovesicular membranous network
U	units
UIS	upregulated in infective sporozoites
UTR	untranslated region
UV	ultra violet
V	Volt
VAC	vacuola compartment
vol	volume
w/o	without
WHO	World Health Organization
WT	wildtype
WTCMP	Wellcome Trust Center for Molecular Parasitology
WT	micro
XA	Xanthin
YFP	yellow-fluorescent protein

# Chapter 1

## Introduction

### 1.1 Apicomplexa

#### 1.1.1 General

Apicomplexans are unicellular eukaryotic organisms (protists) that belong, together with their two well-studied sister-lineages dinoflagellates and ciliates, to the higher order of the assemblage of the alveolates<sup>1</sup>. Alveolates are characterized by a common feature, the so-called cortical alveoli, membrane-bound vesicles that can be found in close association with the plasma membrane of the cell<sup>2</sup>. Apicomplexans and dinoflagellates probably evolved from a group of predatory flagellates, the colpodellids, that were shown to represent a sister group of the apicomplexans<sup>3</sup>. Both, apicomplexans and flagellates, share a common mechanism of attaching to the host cell (apicomplexans) or the prey (colpodellids), respectively, that is mediated by similar organelles. Whereas both sister groups, the apicomplexans and the colpodellids, kept these organelles within the course of evolution, dinoflagellates lost them. But all three clades still share an endosymbiontically taken up red alga<sup>4</sup>, the apicoplast, a remnant chloroplast, that in some alveolates still is photosynthetically active<sup>5 6</sup>. Apicomplexans belong to a monophyletic group that is almost exclusively obligate intracellular parasitic and affect human life in terms of veterinary medicine and agriculture (*Babesia*, *Theileria* and *Eimeria*) and in terms of human health (e.g. *Toxoplasma*, *Plasmodium*) on a daily basis. For an overview of pathogenic apicomplexa infecting humans see Tab. 1.1.

#### 1.1.2 Specific subcellular structures of apicomplexa

##### Apical secretory organelles

Unique to the invasive stages of apicomplexan protozoa are three types of electron-dense secretory organelles, namely **rhoptries**, **micronemes** and **dense granules** (Fig. 1.1). These organelles are carrying characteristic secreted proteins that are

Table 1.1: Apicomplexan parasites infecting humans

<b>Genera</b>	<b>Transmission</b>	<b>Disease</b>
<i>Plasmodium</i>	mosquito	malaria
<i>Toxoplasma</i>	felines/vertical	neurological/congenital
<i>Cryptosporidium</i>	fecal-oral	watery-diarrhea
<i>Isospora</i>	soil	watery-diarrhea
<i>Cyclospora</i>	soil	watery-diarrhea
<i>Sarcocystis</i>	predator-prey	rare
<i>Babesia</i>	tick	zoonotic



involved in adhesion (AMA-1, MICs) and both the formation of the moving junction and the PV/PVM (RONs, ROPs, GRAs)<sup>7</sup>, respectively. A number of key parasite ligands that are located and released from these secretory organelles mediate the interaction of the parasite with the host cell to facilitate and trigger invasion. Studies on *Plasmodium falciparum*, e.g., have shown that the invasion process requires several sequential steps like attachment to the erythrocyte surface, apical re-orientation and release of proteins of the apical organelles, with micronemes being secreted first<sup>8, 9</sup>. **Micronemes** are the smallest in size among the apicomplexan apical secretory organelles and their number per cell varies highly between different genera, species and developmental stages of apicomplexan parasites<sup>10</sup>. In general, parasite stages that are able to glide and to invade cells have more micronemes in comparison to non-invading cells who contain few if not none. The majority of microneme proteins (MICs) that are secreted upon host-cell contact have multiple adhesion-domain types that lead to interactions between the parasite and the host-cell. For this reason micronemes are secreting before all other secretory organelles since they provide the initial contact through secreting them onto the parasite surface. Not much is known about the factors triggering secretion but it has been shown that micronemal protein secretion is rapidly upregulated upon contact with the host cell<sup>8, 4</sup>. In case of *P. falciparum* external low potassium ion concentrations both internal elevated cyclic AMP (cAMP) and  $\text{Ca}^{2+}$  concentrations are involved in triggering this process<sup>20</sup>. **Rhoptries** are club shaped organelles that exist in the number of 8-12 per parasite cell and are located at the apical end of the parasite. The extended apical end of these organelles, the so-called neck, is connected to the apical pole of the parasite where rhoptry proteins can be released from the cell. Rhoptries are acidified organelles, with a pH of about 3.5-7 (depending on the maturity of the organelle)<sup>11</sup> and occupy about 10-30% of the total cell volume<sup>7</sup>. Rhoptries harbour about 30 different proteins, most of them located either within the bulbous part (rhoptry proteins, ROPs) or at the neck of the organelle (rhoptry neck proteins, RONs)<sup>12</sup>. Some of these proteins are important kinases that are essential virulence factors and are secreted upon invasion of the parasites<sup>13, 14, 15, 16</sup> (Fig. 1.2). Rhoptry proteins are produced as pro-peptides at the ER and then processed, packaged and sorted at the Golgi-apparatus into vesicular immature rhoptries. Some proteins are also delivered to the rhoptries via the endosomal pathway in multivesicular bodies and might therefore represent analogous organelles of secretory lysosomal granules of mammalian cells<sup>17, 18, 19</sup>. The external signals and signaling mechanisms responsible for secretion of rhoptry proteins are so far unknown in apicomplexan parasites<sup>20</sup>. **Dense granular** proteins are released during and after invasion of the parasites into the host cell and they remain either soluble within the PV or are integrated into the PVM or the TVM, a tubovesicular membranous network within the PV<sup>21</sup>. Dense granule proteins are thought to modify the environment within the PV, are release through an "open IMC-window"<sup>22</sup> (Fig. 1.2) and have been identified as excretory/secretory antigens in *Toxoplasma*<sup>23</sup>.

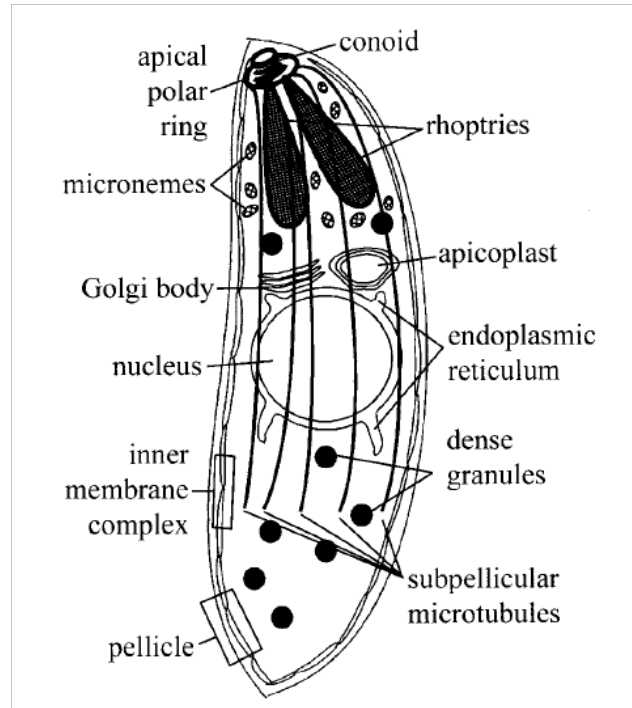


Figure 1.1: **The morphology of apicomplexan parasites.** Apicomplexa invasive stages possess several clade-specific cellular organelles in addition to the eukaryotic standard repertoire **Golgi-apparatus**, **mitochondria** (not shown in this figure), **endoplasmic reticulum** and the **nucleus**. Secretory organelles such as **rhoptries**, **micronemes** and **dense granules** contain secretable proteins that are required for motility, invasion, formation of the PVM and establishment of the PV milieu. An additional organelle is the **apicoplast**, a secondary endosymbiotic red alga, that supplies the parasite with fatty acids. The **conoid** is a spiral structure of undefined material and facilitates invasion into the host cell. It can protrude from or retract into the **apical polar ring**, a MTOC for the **subpellicular microtubules** that help to keep the parasite's elongated shape. The parasites are bounded by the **pellicle**, which consists of the **IMC** and the parasite membrane. PVM: parasitophorous vacuole membrane; PV: parasitophorous vacuole; MTOC: microtubule-organizing center; IMC: inner membrane complex; Adapted from Morrissette and Sibley, 2002<sup>47</sup>.

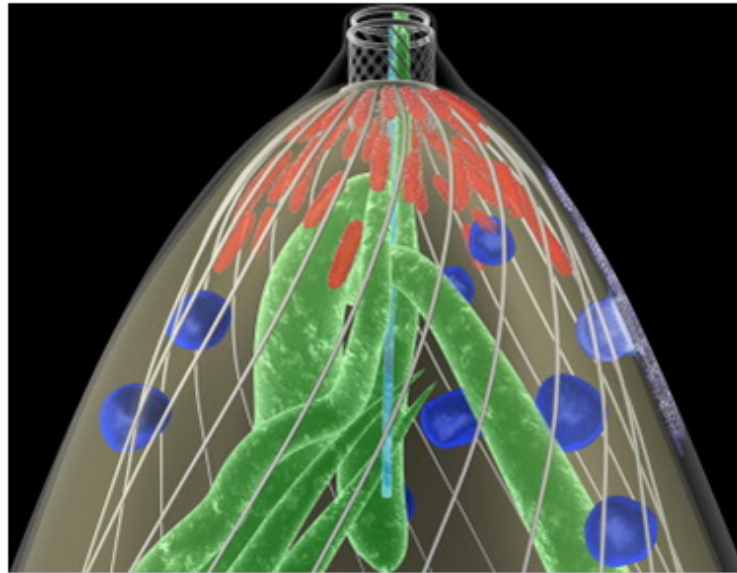


Figure 1.2: **3-D reconstruction of the secretory apical organelles during initiation of invasion.** Rhoptries (green) are secreted *one at a time* through the conoid ring at the apical tip. Micronemes (red) dock to the posterior polar conoid ring at the tip. Dense granules (dark blue) are secreting through "open IMC-windows" at the side of the apical tip. The polarity and shape of the cells is maintained by subpellicular microtubules (grey net of bundles). (Adapted from Paredes-Santos et al., 2012<sup>22</sup>)

### Apicoplast

An apicomplexa-specific organelle first identified in 1975<sup>24</sup> harbors a circular extra-chromosomal genome of prokaryotic origin, quite similar to that of plastids of plants and algae<sup>25 26 27</sup>. In contrast to the confirmed plant- or algae-like origin it has been shown that this plastid-like organelle lacks any genes involved in photosynthesis<sup>28</sup>. Comparisons of the apicoplast with photosynthetic plastids of the ancestral apicomplexan parasite, *Chromera velia*, show that these plastids all share the same ancestry and undoubtedly are of red algae origin. This alga was taken up into the parasites by endosymbiosis<sup>29</sup>. Dinoflagellates also possess this plastid and therefore the endosymbiosis of the red alga took place before dinoflagellates and apicomplexa separated<sup>5</sup> (see 1.1). Another indicator that clearly supports the endosymbiosis theory is the fact that the apicoplast possesses 3-4 membranes as observed in electron-microscopy studies<sup>30</sup>. The apicoplast occurs in all members of the phylum apicomplexa with exception of *Cryptosporidium* spp.<sup>31 32 33</sup> and possibly gregarines, as well<sup>34</sup>. For a long time no function of the apicoplast other than keeping itself alive has been suggested<sup>28 35</sup>, in addition to the observation of the obvious loss of the photosynthetic activity. On the other hand disrupting the integrity of the apicoplast by chemical or genetic intervention leading to delayed death showed that the plastid is essential for the parasite<sup>36 37</sup>. Already in 1998 parasite genome projects made it possible to identify apicoplast-specific genes involved in parasite metabolism. Waller

et al. identified genes for an apicoplast fatty acid biosynthesis system in *Toxoplasma* and *Plasmodium*, the type II fatty-acid synthesis (FASII) pathway<sup>38</sup>. Previously it had been believed that apicomplexans were not able to synthesize their own fatty acids *de novo* and these metabolites had to be scavenged from the host cell *de novo*<sup>39</sup>. One of the key proteins involved in the FASII pathway in apicomplexa is the acyl-carrier protein ACP. Conditional mutagenesis of this protein in *Toxoplasma* effects apicoplast biogenesis and results in death of the parasite<sup>39</sup>. But on the other hand this pathway was not essential for blood- and mosquito-stages, but essential for liver-stages, of *Plasmodium*, indicating for different needs of fatty-acids in these cells or other mechanisms to *de novo* synthesize or salvage these metabolites from host cells in different stages<sup>40 41</sup>. Some other *de novo* mechanisms like a FASI-pathway (most apicomplexans except *Theileria* and *Babesia*)<sup>42 43</sup> and a fatty acid elongation pathway (*Toxoplasma*)<sup>39</sup> have been identified, recently. In addition to that other apicomplexan parasites harbouring an apicoplast (*Babesia*, *Theileria*) are completely lacking the FASII synthesis machinery suggesting that they are dependent on fatty acid salvage from the host<sup>44</sup>. This leads to the question what is the potential role of the apicoplast in these organisms, something that still remains to be experimentally addressed. Since the human FASI pathway components differ from the apicomplexan FASII, this makes it, at least for the stages depending on this pathway, an interesting target for apicomplexan parasite prevention strategies<sup>45</sup>. For an overview of the processes involved in the fatty acid metabolism in *Plasmodium* liver stage parasites see Fig. 1.3<sup>46</sup>.

### Cytoskeleton

The cytoskeleton of apicomplexa consists of three different types of structural elements: **Microtubules** (and associated proteins), the **subpellicular network** (including the inner membrane complex IMC) and the combination of **actin/myosin**. The haploid stages of apicomplexa have two different forms of **microtubules**: Spindle microtubules and subpellicular microtubules (Fig. 1.4A)<sup>47</sup>. The **subpellicular microtubules** are spirally arranged and radiate from the apical polar ring down to the region of the nucleus (approximately 2/3 of the length of the parasite), where they end<sup>48 95 49 50 51 52</sup>. Underlying the inner membrane complex of the parasite the subpellicular microtubules confer both polar orientation and elongated shape of the parasite (compare Fig. 1.1, Fig. 1.2 and Fig. 1.4). Therefore replicative parasite stages lacking the subpellicular microtubules are non-motile, non-polar and non-invasive<sup>96 53</sup>. The apical polar ring (APR) (Fig. 1.1) acts as a microtubule organizing center (MTOC) and laterally associates with the minus end of the subpellicular microtubules<sup>51 54</sup>. **Spindle microtubules** are employed by replicative stages during mitosis. Since nuclear division of the parasites occurs without nuclear breakdown spindle microtubules associate with a spindle organizing structure located within nuclear envelope invaginations during this process, the so-called centrocone<sup>95 55 97 105 99 56 57 58</sup>. Close to the centrocone located is the centriol (except

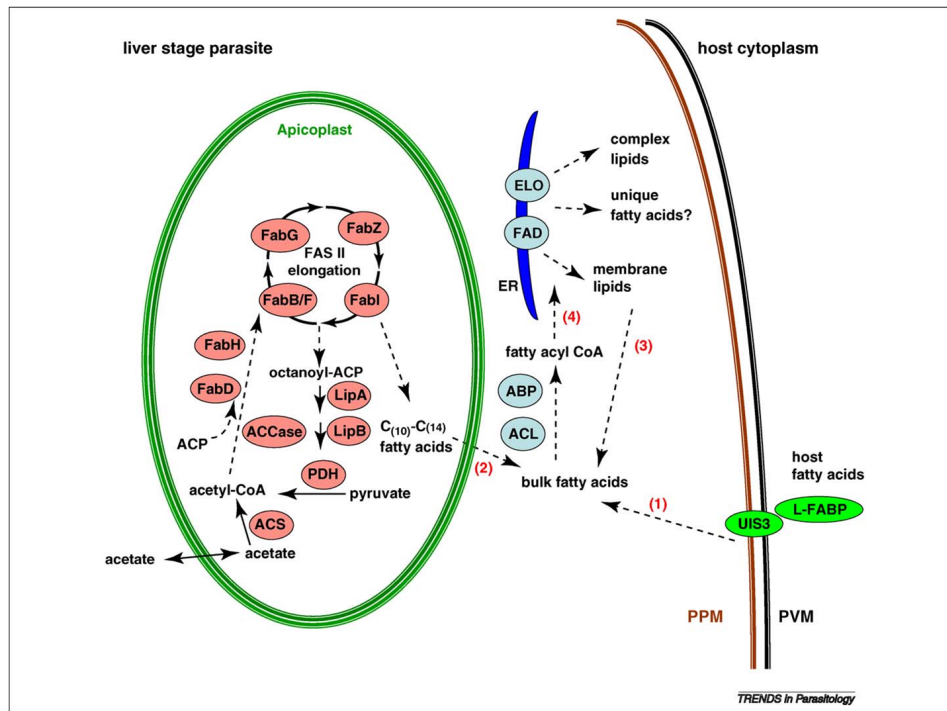


Figure 1.3: **Schematic overview of the fatty acid metabolism pathways in *Plasmodium* liver-stages.** Fatty acids in the liver-stages can be obtained in 4 different ways: Through **1)** uptake from the host cell, **2)** *de novo* synthesis via the FASII-pathway taking place in the apicoplast, **3)** recycling of membrane lipids or **4)** modification and integration into membranes. **1)** The parasite-specific PVM resident protein UIS3 is interacting with the liver host cell specific lipid carrier liver fatty acid binding protein (L-FABP) and uptake is proposedly mediated by UIS3. **2)** For the *de novo* synthesis of fatty acids in the apicoplast the main precursor is acetyl-CoA, which can be either synthesized from pyruvate by the pyruvate-dehydrogenase complex (PDH) or from acetate via the acetyl-CoA synthetase (ACS). Before going into the FASII elongation cycle, where the fatty acid chain is elongated by two carbons a cycle, acetyl-CoA is condensed with the acyl-carrier protein (ACP). Several enzymes are involved in the several steps before either octanoyl-ACP (important co-factor of the PDH) or  $C_{(10)}$  to  $C_{(14)}$  fatty acid chains are produced. **3)** Free fatty acids can be released from membrane turnover events. **4)** The activation of fatty acids to Acyl-CoA thioesters is needed for most cellular processes fatty acids are involved in. The process is mediated by the enzymes ACL (acyl-CoA synthase) and ABP (acyl-CoA binding protein). The fatty acids can then be modified by other enzymes in the endoplasmic reticulum (ER). (Adapted from Tarun et al., 2009<sup>46</sup>.)

in *Plasmodium* merozoites and *Theileria* sporozoites), a specialized MTOC, that does not seem to be necessary for nuclear division but might be necessary for apicoplast division or serve as a nucleation site for the basal body of the flagellum of microgametes<sup>59</sup>. The **subpellicular network** was first identified in *Toxoplasma gondii* (Fig. 1.4B). It was shown that a network of filaments of 8-10 nanometers in diameter is underlying the plasma membrane (PM) of the parasites creating a three-layered pellicle (PM, 2x IMC)<sup>60</sup>. Two of the main network proteins are members of the inner membrane complex (IMC) in *Toxoplasma*, *TgIMC-1* and *TgIMC-2*. These proteins are predicted to form coiled-coils similar to the ones formed by myosin in order to stabilize the network<sup>47</sup>. The IMC is directly underlying the parasite's plasma membrane and is made of large flattened vesicles in *Plasmodium* sporozoites. In other apicomplexans it is made of many cortical bound large vesicles, the alveoli (Alveolata-specific), aligned in longitudinal rows<sup>61 62</sup>. The membranes of the IMC are spiked with intramembranous particles (IMPs) that are also organized in rows and might represent transmembrane domains of proteins attached to intermediate filaments, giving the whole cytoskeleton more stability (Fig. 1.4B)<sup>47</sup>. **Actin** is expressed by two different genes in *Plasmodium*<sup>63</sup>, whereas *Toxoplasma* actin is only expressed by one<sup>64</sup>. Most of the actin molecules in apicomplexans seem to be in a monomeric state rather than existing as a polymerized form. *Toxoplasma* tachyzoites for example only have about 2% of their actin in assembled filaments<sup>64</sup> and only just a few years ago actin microfilaments could be observed in electron microscopy studies for the first time<sup>95</sup>. However, artificially stabilizing actin in *Toxoplasma* with the drug jasplakinolide showed that indeed actin monomers can form filaments in these cells and this most notably at the apical end of tachyzoites<sup>65 66</sup> (Fig. 1.4C). In addition to that, more recent studies have shown that actin filaments in *Toxoplasma* and *Plasmodium* are rather short, between 50 and 150 nm in length<sup>67</sup> and undergo rapid structural reorganization and turnover<sup>68</sup>, mediated by polymerizing and depolymerizing factors such as ADF, ARP2/ARP3 etc.<sup>69 70</sup>. In artificially hypotonically swelled *Toxoplasma* parasites  $\alpha$ -actin antibodies labeled the region between the plasma membrane and the IMC. Actin filaments have been shown to be linked to the substrate extracellular parasites are binding to by transmembrane adhesins that are reaching from the outside of the cell through the plasma membrane to the actin filaments<sup>71</sup>. One of the major roles of actin filaments in extracellular apicomplexan stages is the interaction with the substrate and formation of the motor complex together with **myosin** and other accessory proteins (Fig. 1.5) (Fig. 1.5). This actin-myosin based motor complex enables the parasites to glide on substrates (gliding motility) and to penetrate and invade cells. Apicomplexans harbor only a limited and rather uncommon repertoire of myosins including myosins of the unusual class XIV, which is restricted to this phylum<sup>72</sup>. One of the most important roles for apicomplexan myosins is exhibited by myosin A (MyoA). MyoA is anchored within the IMC by accessory proteins<sup>73 74</sup> and forms the motor protein complex for gliding motility that directly interacts with the actin-filaments (Fig. 1.5). It has long

been thought that MyoA is absolutely essential for gliding motility and invasion, since tetracyclin-inducible conditional knock-out studies showed complete blockage of invasion<sup>75 76</sup>, before recently new knock-out studies made it possible to completely knock-out MyoA while invasion to a certain degree is still possible (Nicole Andenmatten and Markus Meissner, unpublished observations).

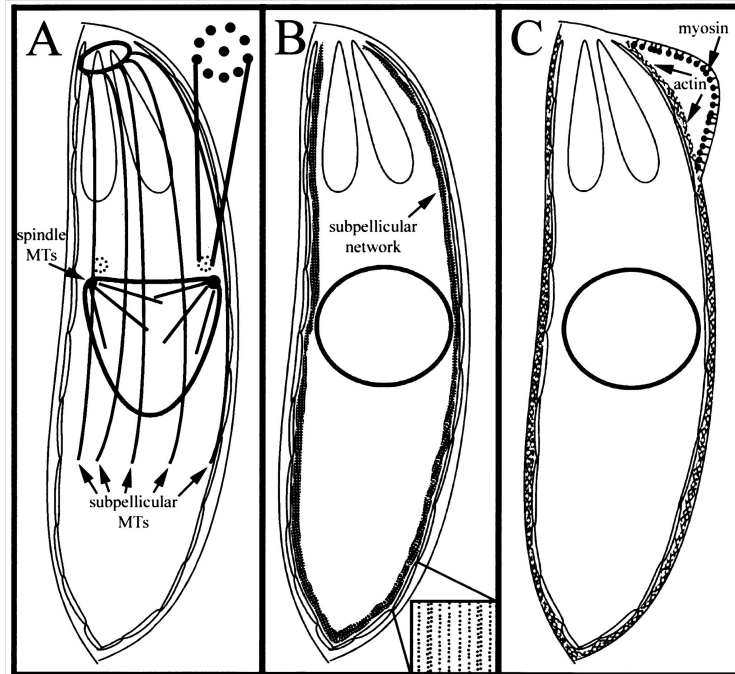


Figure 1.4: **Components of the apicomplexa cytoskeleton.** **A) Microtubules.** Subpellicular microtubules radiate from the apical polar ring (black ring at the upper end of the parasite) in close association with the cytosolic face of the IMC towards the basal end of the parasite. Spindle microtubules nucleate at the centrocones (invaginations of the nuclear membrane) during mitosis and are associated with centrioles (dotted circular structure) that might be needed for apicoplast division or serve as nucleation site for the basal body of the flagellum of sexual forms. **B)** The **subpellicular network** is an association of intermedial filaments that underlie the inner membrane complex (IMC) and is connected with this by transmembrane domains of membrane receptors to give stability and rigidity to the parasite. **C) Actin and myosin** are located between the IMC and the plasma membrane, actin associated with the IMC, myosin anchored within the plasma membrane, and form, together with other associated proteins, the motor machinery of the parasites. (Adapted from Morrissette and Sibley, 2002<sup>47</sup>.)

### 1.1.3 Replication of the apicomplexan pathogens

#### Life-cycle

Apicomplexa grow and replicate within parasitophorous vacuoles in host cells and do not undergo extracellular cell division. This means apicomplexa have to rapidly invade host cells, followed by parasite replication including cellular division, host cell

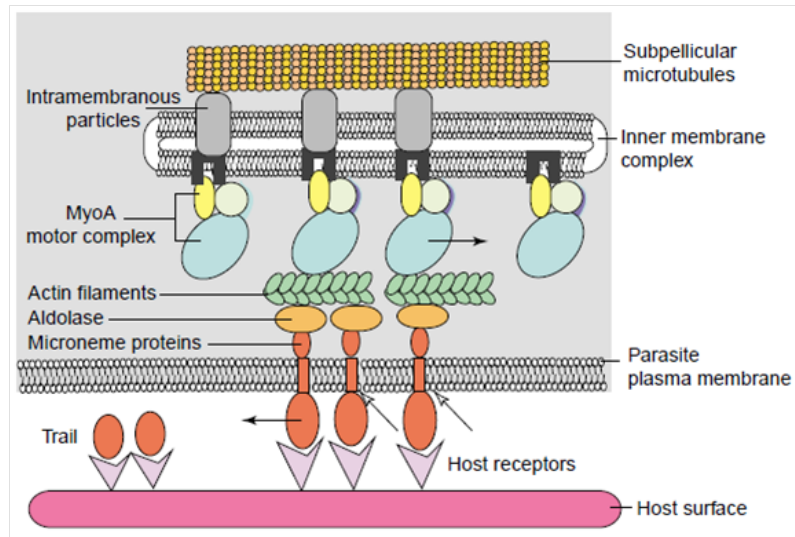


Figure 1.5: **The apicomplexan gliding machinery.** This caption shows a model for the interaction of the MyoA motor complex with the micronemal protein-host receptor complex. The MyoA motor complex is anchored within the membrane of the IMC and can bind to and move along the actin microfilaments. The actin-filaments themselves are connected with microneme-secreted transmembrane proteins located in the parasite membrane via an aldolase protein. The transmembrane proteins on the outside of the parasite can bind to host receptors thereby promoting parasite-host cell interaction and gliding of the parasite since the driving force of the MyoA-complex can be transmitted to the substrate. Black arrows indicate the movement of the complexes. Open arrows show proteolytic cleavage sites. MyoA: Myosin A; IMC: Inner membrane complex; (Adapted from Soldati and Meissner, 2004<sup>57</sup>)



lysis and reinvasion, in order to multiply and survive. Apicomplexa have developed complex life-cycles in order to colonize their hosts and to be transmitted to a new host (Fig. 1.6). Whereas *Toxoplasma* can be transmitted directly from vertebrate to vertebrate via sporozoites stages within oocysts shed within the feces from cats or via ingestion of tissue cysts by canine animals (Fig. 1.8) *Plasmodium* needs an invertebrate vector to be transmitted from one host to the other. In order to produce replicative stages, that multiply within the host cells, apicomplexa produce extracellular invasive stages (*Toxoplasma*: Tachyzoites, Bradyzoites, Sporozoites; *Plasmodium*: Merozoites, Ookinetes, Sporozoites) that possess specific organelles required for invasion. They are motile to reach and invade new host cells (Fig. 1.6). Whereas *Toxoplasma* can invade any nucleated cell of warm-blooded vertebrates<sup>77</sup>, *Plasmodium* is restricted to specific cells types such as hepatocytes and red blood-cells to productively replicate within.

### Parasitophorous vacuole (PV)

After invasion of the apicomplexans into their host cell these parasites reside within a parasitophorous vacuole surrounded by a membrane, the parasitophorous vacuole membrane (PVM)<sup>78</sup>. The PVM forms a physical barrier between the parasites and the host cell cytosol protecting the parasite from host defense mechanisms. But since the parasites are surrounded by this, and in addition to that, at least one other membrane (host cell cytoplasmic membrane) and therefore can not directly take up nutritional factors from the surrounding medium the PVM plays also a specific role in parasite-host-specific exchange. The entry of apicomplexan parasites is an active process driven by the parasites' ability to glide and to form a moving junction at the connection point between the parasite and the host cell. The invasion is therefore termed "active" instead of "induced" (bacteria) since the host cell does not take part in this process<sup>79 80 81</sup>. Therefore the parasite first attaches to the host cell and subsequently penetrates into a vacuolar invagination of the host cell membrane by forming a moving junction between the parasite and the host cell surface<sup>82</sup>. It has long been thought that the driving force of the invasion of apicomplexan parasites is the motor complex, the so-called glideosome, an acto-myosin motor located between the parasite plasma membrane and the inner membrane complex<sup>83</sup> (Fig. 1.5). But this biological dogma recently seems to have been proven wrong: Knock-out studies of protein-members of the motor-complex of *Toxoplasma gondii*, previously said to be essential for parasite invasion, did not completely abolish invasion of the parasites (Nicole Andenmatten and Markus Meissner, WTCMP Glasgow; unpublished observations). The attachment of the parasites to the host cell membrane and the invasion into it requires sequential secretion of specific proteins from apical parasite organelles (1.1.2 Apical secretory organelles), termed micronemes, dense granules and rhoptries<sup>84</sup>. These proteins and lipids, together with proteins and lipids provided by the host cell, are incorporated into the newly forming PVM<sup>81 85 86 87 88 89</sup>. The mature PVs in *Toxoplasma* and *Plasmodium* differ to some extent. The

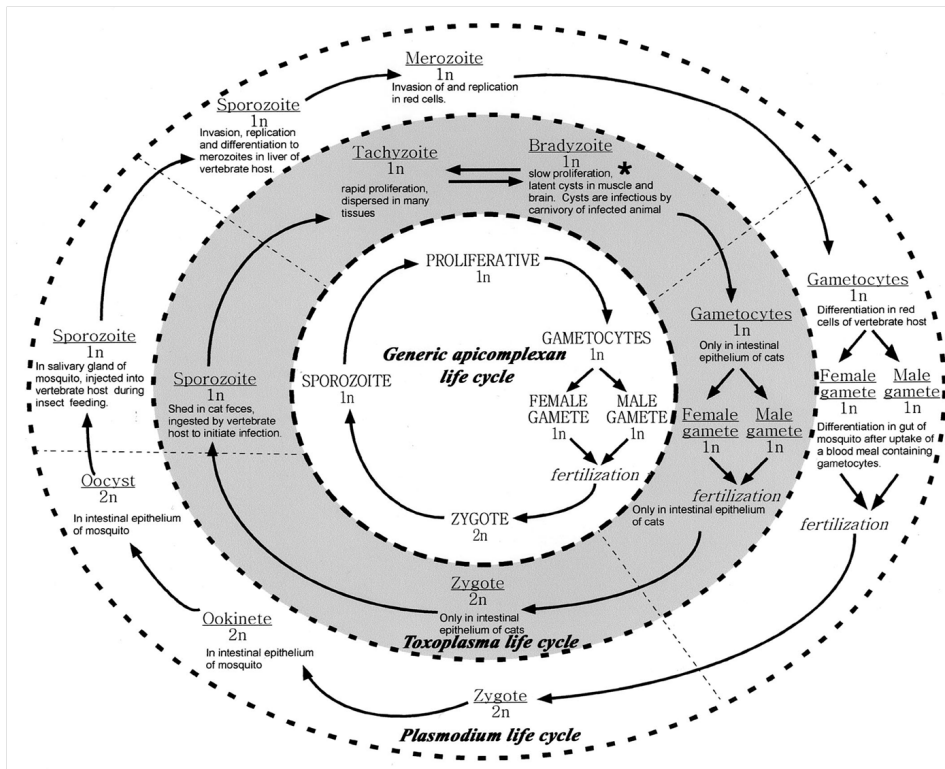


Figure 1.6: Comparison of the life-cycles of *Toxoplasma* and *Plasmodium*.

The inner and the outer white circles represent the generic apicomplexan and the *Plasmodium* life-cycle, respectively. The inner grey-shaded circle represents the *Toxoplasma* life-cycle. Rapidly proliferating haploid asexual stages of apicomplexans are able to produce sexual stages (gametocytes). Gametocytes transform into gametes of both, male and female gender, that fuse to form a diploid zygote. Via meiosis the zygotes are transformed into haploid sporozoites that are able to initiate infection in a new host individual. The sexual reproduction of *Toxoplasma* via sexual stages can take place in the intestinal epithelium of cats only, their **definite host**. Asexual reproduction, in contrast, can take place in many other warm-blooded **intermediate hosts** (vertebrates) and the replication of tachyzoites happens in many different cell-types and organs. Tachyzoites can differentiate into slowly replicating bradyzoites that form dormant cyst stages in muscle and brain tissues. These tissue cysts are then infectious to carnivorous hosts again by bypassing the sexual phase and reactivating tachyzoite production from the cysts. In contrast to *Toxoplasma*, *Plasmodium* species are restricted to a specific host and a mosquito vector that is transmitting the sporozoites to a new host individual. Whereas the *Toxoplasma* zygotes directly transform into sporozoites within the intestinal epithelium of cats *Plasmodium* zygotes transform into motile ookinetes first, that cross the midgut epithelium of the mosquito. Afterwards they transform into resident oocysts, where meiosis is going on and sporozoites are produced, that travel to the salivary glands of the vector. After maturing there, the parasites are injected upon blood-meal of the mosquito into the skin and bloodstream of a new host, to finally establish infection within liver-cells. Whereas the asexual *Toxoplasma* tachyzoites are able to infect any nucleated cell of their vertebrate host, *Plasmodium* merozoites, released by the liver cell, can only infect non-nucleated red blood-cells, where they undergo several rounds of asexual replication before they produce sexual stages again. (The figure was adapted from Morrissetti and Sibley, 2002<sup>47</sup>.)

PV in *Toxoplasma* is a wide compartment with the parasites being connected at the center and space remaining at the periphery<sup>90</sup>. The *Toxoplasma* PVM is tightly associated with host cell mitochondria and endoplasmic reticulum (ER)<sup>91</sup> and can be prolonged by long extensions reaching into the host cell cytoplasm. In *Plasmodium*, in contrast, the parasite membrane and the PVM are always tightly associated and therefore difficult to distinguish from each other in fluorescence microscopy analyses<sup>92</sup>. *Plasmodium* parasites differ in terms of the composition of their PVM according to which host-cell type they are residing in. Liver-stage parasites have, in comparison to blood-stages, different proteins residing in the PVM to achieve protein export into the PVM, the host-cell cytoplasm or beyond. In addition to that liver-stage parasites are closely associated with the host-cell ER via the PVM<sup>93</sup> to scavenge host-derived lipids, something that is not possible in intraerythrocytic.

### Replication

The replication of apicomplexans in general to create two daughter-cells or multiple progenie can occur through two different mechanisms: Whereas *Plasmodium*, *Eimeria*, *Babesia* and *Theileria* replicate through a mechanism called schizogony creating up to 64 daughter parasites<sup>94 95 96 97 98 99</sup>, in *Neospora* and *Toxoplasma* replication occurs by endodyogeny<sup>100 101 102 103</sup>. In both mechanisms the nuclear membrane remains intact throughout the whole nuclear division (cryptomitosis) and the caryokinesis occurs without chromatin condensation<sup>104 97 105 99</sup>. Both processes, endodyogeny and schizogony, are very similar and are differing mainly in the preservation of the mother cell specialization (Fig. 1.7).

**Endodyogeny** During endodyogeny two daughter-cells are formed within the mother cell. The mother cell remains polarized during the whole replication cycle and keeps the integrity of the inner membrane complex (IMC) and the subpellicular membranes (Fig. 1.7A). Therefore the mother cell preserves the ability to glide and to invade new host cells throughout the complete life-cycle even if the host cell lyses before the generation of the daughter-cells is complete. Each daughter-cell is enclosed by its own IMC and associated subpellicular microtubules and filled with the apical organelles in addition to a nucleus, mitochondrion, Golgi-apparatus and the plastid<sup>106 103 107</sup>.

**Schizogony** In parasites undergoing schizogony subpellicular membranes and the IMC are disassembled after invasion of the parasites into host cells and several rounds of nuclear divisions take place (Fig. 1.7B). At the end of each cycle up to 64 (in blood stages) or up to 30.000 (in liver stages) daughter nuclei have been formed and move to the periphery of the cell where they assemble together with new sets of the organelles, are incorporated each with their own newly formed IMC, and finally bud off from the mother cell as merozoites. During the process of schizogony, in contrast to parasites undergoing endodyogeny, parasites are not invasive any more because

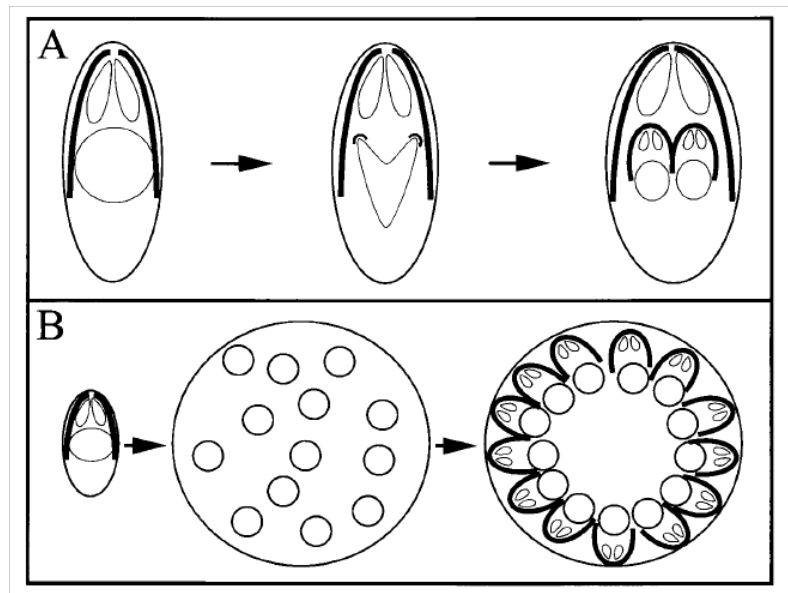


Figure 1.7: **Schematic comparison of apicomplexan endodyogeny and schizogony.** **A)** Endodyogeny is producing two daughter-cells inside the mother cell without losing the shape and polarity of the mother cell. The inner membrane complex (IMC, thick black line) and subpellicular microtubules of the mother cell remain intact throughout the whole process and the daughter-cells are forming surrounded by their own IMC. When the daughter-cell formation is complete the newly formed cells bud off from the remnants of the mother cell. **B)** During schizogony the integrity and polarity of the mother cell is lost, the parasite rounds up and subpellicular microtubules and the IMC are lost. Extensive cell growth and nuclear division takes place before single nuclei align with single sets of apical organelles, the IMC and subpellicular microtubules at the periphery of the replicating cell.(represented as white circles) (Figure adapted from Morrissetti and Sibley, 2002<sup>47</sup>.)

they lack cell polarity and the integrity of the organization of apical organelles<sup>94 95 96 99</sup>.

### 1.1.4 Epidemiology and pathogenicity

#### Toxoplasmosis and Malaria

**Toxoplasmosis** *Toxoplasma* replication and transmission follows a predator-prey system that alternates between definite (sexual reproduction) and intermediate (asexual reproduction) hosts (Fig. 1.6). It is very unique for *Toxoplasma* in its coccidian group that transmission of the parasites can occur not only between definite and intermediate host (sexual cycle), but also between two intermediate hosts by carnivorism (asexual cycle) and even between definite hosts by oocyst-contaminated feces<sup>108</sup> (Fig. 1.8). But the proportion of asexual and sexual cycles taking part in transmission vary between given environments according to the structures of the definite and intermediate host populations<sup>109</sup>. In general, *Toxoplasma* infection has been described for more than 350 host species, mostly mammals and birds, and the majority of these animals are living in a wild environment<sup>110</sup>. The contamination of this environment is linked by the stray, domestic or wild feline definite hosts shedding oocysts that are then taken up by intermediate hosts (Fig. 1.8), and therefore the seroprevalence of *Toxoplasma* in the intermediate hosts mostly depends on the felids in their environment. Most **wild** definite hosts have a seroprevalence of close to 100%, but this depends on many different environmental factors such as climatic conditions, susceptibility of the host, lifespan and feeding behaviour<sup>111 112 113</sup>. Seroprevalence in **humans** also varies quite dramatically: In general, it is assumed that about 25-30% of the world's human population is infected with *Toxoplasma* parasites<sup>114</sup>. Whereas low seroprevalences (10-30%) have been found in North America, South East Asia, Northern Europe and Sahelian countries of Africa, moderate prevalences (30-50%) have been found in Central and Southern Europe and high prevalences in Latin America and in tropical African countries<sup>108</sup>. Important factors for the seroprevalence of human populations are climatic conditions that affect the survival of oocysts in the environment, infection rates in meat producing animals, dietary habits (cooking of meat, handwashing, fertilization and collection of vegetables, kinds of meat and vegetables consumed etc.) and the domestication of cats. In addition to that, water contaminated with feces also plays a very important role in transmission of *Toxoplasma* to humans. In general, most human infections are acquired through horizontal transmission via ingestion of tissue cysts in infected meat (30-63% of all risks in Europe) or by ingestion of feline feces-contaminated soil (6-17% of all risks in Europe), water, or food with sporulated oocysts<sup>115</sup>. The fact that most cases of new *Toxoplasma* infections in Europe are caused by contaminated food is especially surprising considering the fact that tissue cysts are usually killed in deeply frozen food (below  $-12^{\circ}\text{C}$ ) after 3 days or immediately by heating them up to  $67^{\circ}\text{C}$ <sup>116 117</sup>. Two rather rare sources for an infection are the horizontal transmission of tachyzoites through the placenta from the mother to the

unborn child (congenital), happening only if the mother acquired a primary acute infection during the pregnancy, and infections related to organ transmission. For a summary of all infection risks see Fig. 1.8. **Pathogenesis during the course of the infection in humans:** After ingestion of cysts or oocysts into the human body the respective forms, bradyzoites or sporozoites, invade the small intestinal epithelium where they convert into the rapidly growing tachyzoites. The acute early steps of the infection of this tissue finally lead to a transmigration of the parasites through the epithelium to the basolateral side<sup>118</sup>, where the parasite invades monocytes. These are the key cells for disseminating the parasites through the blood flow to all organs, using them as shuttle service to cross biological barriers almost "unseen" by the immune system<sup>119 120</sup>, being able to infect almost any nucleated cell. Nevertheless, shortly after ingestion of the parasite into the human digestive tract there is a local release of chemokines by the infected cells which then leads to attraction of cells of the innate immune system<sup>121</sup>. Phagocytotic immune-cells are recruited and a Th1-based immune-reaction is generated, which, if not tightly regulated by IL-10 and TGF- $\beta$ , can result in severe tissue damage in non-healthy patients<sup>122 123</sup>. An overshooting Th1-immune-response might also be responsible for the fatality of acute *Toxoplasma* infection during pregnancy<sup>124</sup>. Normally a Th2-based immune-response leads to maternal-fetal tolerance but is destroyed by IFN $\gamma$  secretion during a *Toxoplasma* infection which can lead to serious damage if not abortion of the unborn child<sup>124 125</sup>. On the other hand, in contrast to generating an overwhelming immune-response during acute infection, *Toxoplasma* has evolved many different techniques to avoid the host cell immune system and thereby establishing a lifelong persistent infection in its host. Some of the parasite strains for example are able to get some of the secreted proteins transported into the host cell nucleus, where they interfere with pathways of the host immune system<sup>126 127</sup>. In addition to that it has also been demonstrated that the parasites are able to inhibit apoptotic mechanisms of the cells they are residing in, thereby ensuring protection from rapid clearance of intracellular tachyzoites from macrophages and oocysts from tissues and prevent alerting of the immune system<sup>128 126</sup>. In 80% of all cases in **immunocompetent** individuals an acquired infection is asymptomatic<sup>114</sup>. In all other cases in this group patients may experience fever, a swelling of cervical lymphnodes or other non-clinical symptoms. Yet, the severity of the disease outcome might be dependent on the parasite strain since recent observations showed that countries that have more virulent strains predominating generally have higher incidence rates of severe disease. This severity is usually expressed by the existence of high rates of chorioretinitis, an inflammation of the patient's eye<sup>129 130 131</sup>. But these strains can also be responsible for the generation of lethal infections in immunocompetent patients<sup>132</sup>. In contrast to immunocompetent individuals, Toxoplasmosis is always life-threatening in **immunocompromised** patients<sup>108</sup>. Among these patients people with an HIV-infection or under immunosuppressive therapies are considered at the highest risk. Especially people receiving an organ via transplantation are at a

very high risk since they can either develop Toxoplasmosis through reactivation of cysts during their immuno-suppressive therapy or via the transplanted organ, that may carry tissue-cysts itself<sup>133 134 135</sup>. In HIV patients the incidence of Toxoplasmosis is closely related to the number of CD4<sup>+</sup> T-cells, the risk increasing with decreasing cell numbers. The most affected organ in these patients is the brain, where toxoplasmic encephalitis (TE) can occur. This inflammation of the brain can lead to symptoms ranging from headache, lethargy and incoordination to loss of memory, major motor seizures and finally death<sup>136</sup>. But also other organs can be involved such as the lung, the eyes and the heart resulting in inflammation of the tissue in these organs<sup>137 138</sup>. As described above one fatal outcome of the primary infection in immunocompetent individuals can be the **congenital Toxoplasmosis** in pregnant women. Here, tachyzoites that are circulating in the mother during a recently acquired infection are transmitted to the child via vertical transmission (Fig. 1.8) through the placenta, a target tissue for parasite replication<sup>139</sup>. The severity of the disease thereby is highly dependent on the timepoint of the infection of the mother during her pregnancy. During the first trimester the placental barrier is highly efficient and only in 10% of the cases parasites pass through. This changes with the 2nd and 3rd trimester when in 30% and 60-70% of the cases, respectively, parasites can pass the barrier<sup>140</sup>. Nevertheless parasite replication at all times can lead to inflammation of the placenta and in the fetus' eye and brain tissue causing severe damage to the child and finally may lead to abortion of the child.

**Malaria** To date malaria is still one of the most dangerous and deadly neglected infectious diseases in the world. Even though the World Health Organization (WHO) reported a 50% reduction of reported malaria cases in 43 of 99 countries with ongoing transmission (Fig. 1.9) between 2000 and 2010 in their World Malaria report 2011, there are still more than 200 million malaria cases estimated each year<sup>141</sup>. Of these, more than 80% are reported in subsaharan Africa resulting in 600.000 deaths per year on this continent, mostly amongst children under the age of 5 years<sup>141</sup>. Malaria is caused by at least five different species of the apicomplexan parasite *Plasmodium* (see 1.1): *P. vivax*, *P. malariae*, *P. ovale*, *P. knowlesi* and *P. falciparum*, the latter of which causes Malaria tropica, the most severe form of all malaria diseases. Today, more than 100 different *Plasmodium* species are known, infecting a broad variety of vertebrates including mammals like humans and rodents, but also birds and reptiles. The transmission of the *Plasmodium* parasites from host to host occurs through an infectious blood meal of mosquitoes (see 1.1.3) of the genera *Culex*, *Anopheles*, *Culiceta*, *Mansonia* and *Aedes*. After transmission of the parasites in form of sporozoites by a mosquito they reach the liver (see 1.1) where they replicate and remain clinically silent. In *P. malariae*, *P. ovale* and *P. vivax* liver-stage parasites can form persistent stages, so-called hypnozoites, that can lead to disease relapses years after the initial infection. After replication within the liver-cells merozoites bud-off and detach from the surrounding tissue<sup>142</sup>. These merozoite filled vesicles are thought to be derived from the host liver cell and its membranes<sup>143</sup>.

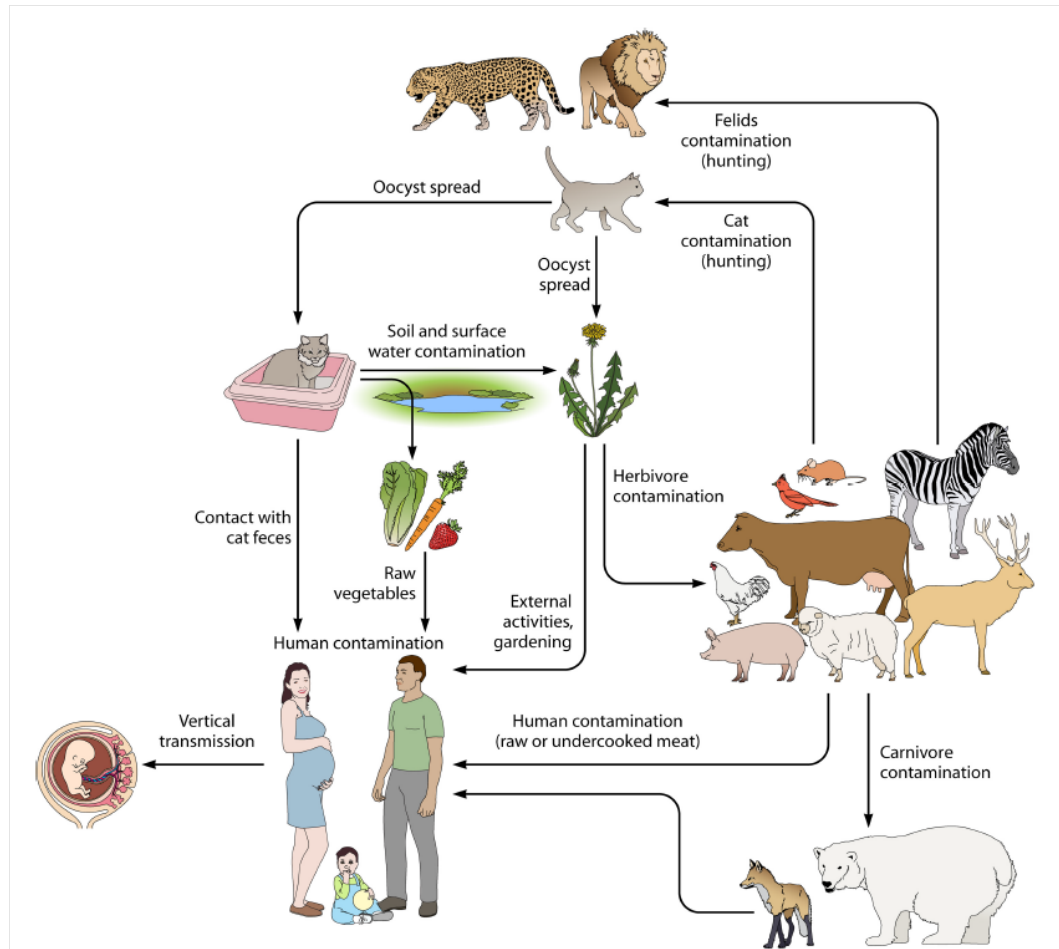


Figure 1.8: Sources of *Toxoplasma gondii* infection for humans. (Adapted from Robert-Gangneux and Darde, 2012<sup>108</sup>.)



They release merozoites into the bloodstream of the host, where they undergo asexual replication (see 1.1). It is during this phase of the parasite's life-cycle that the human host is suffering from clinical symptoms. The classical clinical symptoms of malaria are intense chills, fever and sweating<sup>144</sup>. The chills will often be accompanied by headaches, nausea and fatigue. One of the most characteristic symptoms of a malaria infection in humans is the re-occurrence of fever attacks. The frequency of these fever attacks is dependent on the speed of the asexual replication and the timing of the erythrocyte bursting. This bursting leads to a release of merozoites as well as free antigens alerting the immune system and leading to an inflammatory reaction resulting in fever<sup>145</sup>. All *Plasmodium* species infecting humans except *P. falciparum* can only invade erythrocytes of a certain age. Therefore their replication cycles and as a result the burst of the mature infected red blood cells (iRBCs) are synchronized leading to a defined pattern of fever attacks. In a *P. vivax* and a *P. ovale* infection the fever attacks are re-occurring every 48 hours (Malaria tertiana) whereas in *P. malariae* they do every 72 hours (Malaria quartana). *P. falciparum*, in contrast, can infect RBCs of any age and therefore the replication and burst of iRBCs is not synchronized, the fever-attacks are irregular. Since replication of the *Plasmodium* parasites leads to the burst of erythrocytes one of the complications of malaria is anemia. *P. falciparum*, in contrast to the other parasite strains, can also cause additional complications of the infection called **severe malaria**. Severe malaria is characterized by acute renal failure, lung edema, severe anemia and acidosis<sup>146</sup>. One reason for the higher virulence of *P. falciparum* is its ability to express variant surface antigens like PfEMP-1 on the iRBC surface that subvert immunity and mediate sequestration from blood circulation to avoid spleen-dependent killing mechanisms by sticking to endothelial cells<sup>147</sup>. This ability to sequester is one of the most important features involved in both cerebral malaria (described below) and pregnancy-associated malaria (PAM)<sup>148</sup>, both complications of severe malaria. PfEMP-1 protein variants are expressed by members of the var gene family that have different exons lying in subtelomeric regions of the chromosomes. The var genes undergo genetic recombinations of different subregions that can more or less randomly be recombined through antigenic switching to express different protein variants that are selected throughout the course of the infection<sup>147 149 150</sup>. Some of the variants lead to adhesion in different tissues like the placental chondroitin-sulfate A (CSA) or the brain. The different adhesion properties are thought to be mainly determined by specific PfEMP-1s that can bind to ICAM-1, CD36, CSA or other endothelial receptors and lead to agglutination and rosetting and other interactions in the tissue capillaries<sup>151</sup>. Var genes can be separated into different groups according to the genome architecture and genes within these groups are more likely to recombine with each other than with others<sup>152 153 154</sup>. Variants expressed by different groups seem to have different influence on the clinical outcome of the disease<sup>155</sup>. Whereas some of the var gene groups seem to be more associated with mild malaria others are with severe malaria. For example variants that do not bind to

CD36, a tissue marker that is only expressed in low numbers in the brain, are associated with severe complications such as cerebral malaria<sup>156 157</sup>. In addition, most of these variants also do support iRBC rosetting, which is consistently associated with severe malarial infections in children and partly with the development of cerebral malaria<sup>158 159 153</sup>. This led to the conclusion that at least partially specific surface proteins expressed by variant parasite genes (*var*) on iRBCs involved in binding to specific tissues like the brain (ICAM-1) or the placenta (CSA) are responsible for the clinical outcome of malaria infections<sup>152</sup>.

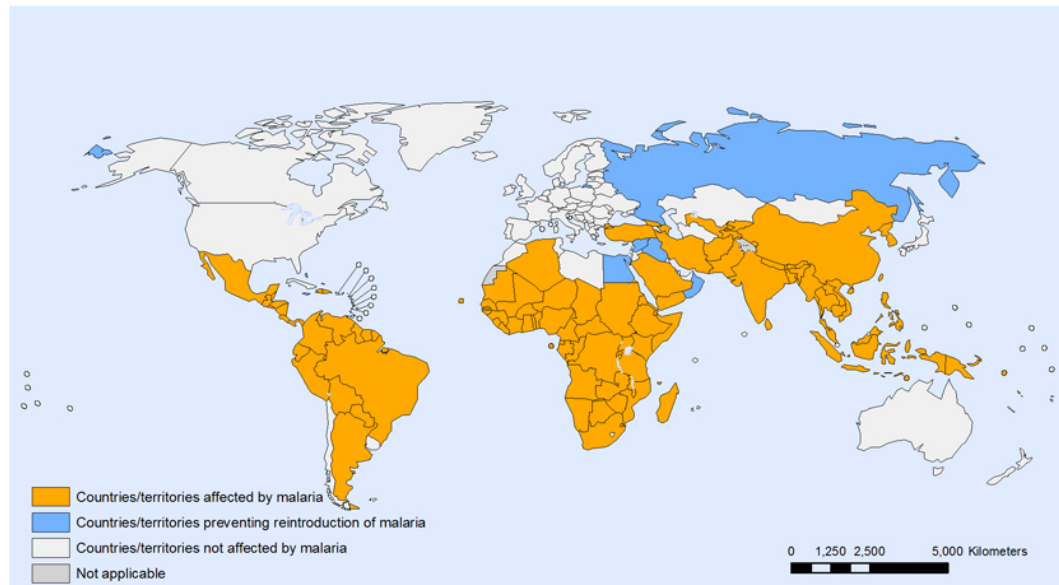


Figure 1.9: **Countries and territories affected by Malaria in 2010.** This map was adapted from the WHO Malaria report 2010.

### Cerebral malaria and experimental cerebral malaria

Cerebral malaria (CM) is a life-threatening complication of severe malaria infections (see 1.1.4) in humans. The mechanisms are not fully understood in detail, yet. One of the reasons for this is the difficult to study the parasitological and immunological events within the affected organ, the brain, ante-mortem<sup>160</sup>. Therefore a mouse model system has been found that is supposed to mimic cerebral malaria events and was called experimental cerebral malaria (ECM). It is currently highly under debate if this ECM model system is of added value to the scientific CM community and if its study is at all relevant to the humane CM disease<sup>160</sup>. Nevertheless, it is the only system generating a similar *Plasmodium*-caused severe disease phenotype in a model organism closely related to humans. Therefore, even if not directly comparable to human CM, can give clues to what mechanisms may be underlying the generation of the disease<sup>161</sup>.

**Human cerebral malaria** The WHO defines CM as an unrousable coma that is not attributable to other causes than a severe malaria (see 1.1.4) infection<sup>162</sup>. Whereas

adults generally are resistant to developing severe malaria, very young children are at a high risk of developing **severe** malarial **anemia**. In contrast to that, older children, who have had at least one previous malaria infection already, seem to be at increasing risk of developing **cerebral** malaria<sup>163</sup>. Therefore the epidemiology of severe malaria leads to the assumption of a major role of the immune system in both initiation of (in children) and protection from (adults) cerebral malaria<sup>160</sup>. Field studies have shown that about 1% of all diagnosed *P. falciparum* infections progress into CM. In about 10-20% of these CM patients the outcome is fatal leading to 300.000-500.000 deaths per year<sup>160</sup>. In the last few years it has been shown that the generation of CM is most likely caused by a combination of a host-immune response to the parasite and the parasites' ability to sequester in the brain of its host. Cerebral malaria can rapidly develop in infected patients after 2-3 days of fever with coma being the standard definition of CM. Early clinical symptoms like headache, fits, vomiting and diarrhea can not be distinguished from symptoms generated by meningitis, encephalitis and febrile convulsions<sup>160</sup>. But these can rapidly progress into more severe symptoms and finally coma if immediate medical treatment is not provided. Two of the main pathological characteristics of CM have been seen in post-mortem analyses of brain sections of patients having died of CM. In these sections haemorrhaging into the white matter of the brain tissue, indicating a leakage of the blood-brain barrier (BBB) and sequestration of iRBCs within cerebral capillaries could be observed<sup>164</sup>. In addition to that, accumulated and adherent leukocytes like monocytes and macrophages could be found sequestered together with the infected cells and infiltrated into the brain tissue<sup>165</sup>. It is known, that endothelial receptors in the brain play a very important role for **sequestration** of malaria parasites during CM within the brain. One of the best studied receptors involved in iRBC sequestration is ICAM-1<sup>166 167</sup>. It has been shown that ICAM-1 is upregulated on cerebral vasculature endothelium<sup>157 166</sup> during malaria infections and that iRBC are binding to ICAM-1 molecules *in vitro*<sup>168 169 170</sup>. In addition to that, there is evidence that the binding of iRBCs to ICAM-1 *in vivo* is associated with the risk of developing CM, even though there is conflicting data on that matter<sup>160</sup>. Therefore other receptors like VCAM-1, E-Selectin and ELAM-1 might be involved since they have been shown to be upregulated in CM as well<sup>171 172 169</sup>. Rather than just single receptor molecules being involved most likely *P. falciparum*-cytoadherence is a multi-step process in which many different receptors are involved initiating first contact, mediating rolling of the parasites and finally firm adhesion<sup>173 174</sup>. A widely accepted model assumed for a long time that symptoms of CM were solely due to blockage of the blood flow in brain microvessels by sequestered iRBCs<sup>175</sup>. In this model parasites adhere to brain endothelial cells via surface proteins that interact with endothelial receptors, combined with rosetting of infected and non-infected red blood cells, thereby impairing blood flow leading to hypoxia, hypoglycemia and built up of toxic waste products. This rapidly would lead to irreversible tissue damage<sup>160</sup>. This being the only cause for CM symptoms is currently under debate<sup>176 177 178</sup>. Be-

cause, even though parasite sequestration is usually seen in CM brains, there is also deaths attributable to CM according to WHO guidelines that do not show sequestration<sup>179 180 164</sup>. In addition, parasite sequestration has also been observed in patients that did not develop CM<sup>172 181</sup>. One of the other factors that might contribute to the development of CM during severe malarial infections is the **host immune system**. Highly characteristic cytokine profiles associated with acute severe malaria prove evidence for the involvement of the immune response in the generation of CM. Elevated levels of pro-inflammatory cytokines in the patients plasma such as  $\text{TNF}\alpha$ ,  $\text{IFN}\gamma$  and increased production of anti-inflammatory cytokines such as IL-10 have been observed consistently during the course of cerebral malaria<sup>182 183</sup>. Also high concentrations of inflammatory cytokines in the cerebrospinal fluid could be associated with the severity of the disease<sup>184</sup>. Nevertheless, most of the data acquired on immune-cells and factors involved in the development of human CM were gained from **peripheral** fluids. This is especially crucial when it comes to the analysis of the involvement of T-lymphocyte subsets in the development of CM. So far only data comparing peripheral blood T-cell populations in CM and non-CM cases could be analyzed due to the inability to collect cells from crucial tissues at key time-points<sup>185</sup>. Since it is hypothesized that there has to be a major migration of T-cell subsets to the brain tissue in order to play a prominent role there, this explains the lack of knowledge still present how exactly the immune system is involved in the development of CM<sup>160</sup>. Therefore an experimental system is still needed to understand the mechanisms behind the disease.

**Experimental cerebral malaria** The best accepted experimental model of CM is the *Plasmodium berghei* ANKA (PbA) model<sup>160</sup>. Infection of susceptible inbred mice, including the strains C57BL/6 and CBA, with this rodent malaria strain leads to severe cerebral pathological symptoms such as ataxia, fitting, respiratory distress and ultimately coma<sup>186</sup>. Depending on the genetic background of the host and on the specific parasite clone the onset of clinical signs after infection is typically between 5-10 days post-infection<sup>186</sup>. As seen in humans upon the first occurrence of clinical signs of the infection usually there is a rapid decline of the condition of the animals with death occurring within 4 or 5 hours after the onset of neurological signs<sup>160</sup>. It has been observed in mice showing signs of ECM that there is disruption of the blood-brain barrier with blood-leakage into the cortex and other regions of the brain<sup>177 187</sup>, accumulation of iRBCs in blood vessels<sup>188 189</sup> and signs of perivascular inflammation in these regions<sup>190</sup>. Other factors, like cognitive dysfunction and impaired visual memory<sup>191</sup> during the course of a PbA infection lead to a progressing decline of the general animal condition that has recently been made evaluable by the definition of a "coma and behaviour scale" documenting the progress for the assessment of ECM in a murine model<sup>192</sup>. As shown for human CM, also the susceptibility of mice to ECM is depending on genetic and environmental factors, such as the genetic background (BALB/C vs. C57BL/6) and the age. It has been shown, for example, that differences in the expression profile of genes in the brain of

susceptible mice, compared with resistant mice, involve metabolic energy pathways, immune activation, apoptosis and neuroprotection/-toxicity<sup>193 194 195</sup>. But most of the characteristics involved are yet to be determined<sup>160</sup>. Since parasite sequestration in the brain is assumed to be one of the main factors involved in generation of CM in humans the obvious question arises: Do PbA parasites also sequester in the brain of mice showing signs of ECM and if yes, which parasite and host receptors are involved in this? Indeed, PbA infected RBCs have been shown to be accumulated in brain capillaries of mice showing signs of ECM on light and electron microscopy level<sup>196 197 189</sup>. But it is not yet understood if the sequestration of the parasites indeed is mediated by strong adherence, comparable to human CM, or rather tight junctions or even only weak interactions<sup>160</sup>. In terms of receptors possibly involved in PbA sequestration it has recently been shown that CD36-mediated sequestration is involved in blocking of blood vessels in lung and adipose tissue but not in the brain<sup>198</sup>. This has been interpreted as evidence for PbA-sequestration not being important for the development of ECM in the PbA model<sup>199</sup>. Nevertheless, even in human CM the role of CD36 for the sequestration in the brain is under debate and the possibility of other endothelial receptors like ICAM-1 being involved is very high (as discussed above). Additionally, it has been shown that at least the number of parasites residing in the brain, shown by the parasite biomass present, is directly correlated with the risk of ECM<sup>200 201 202</sup>. In line with the observation that CD36-mediated sequestration does not play a major role in the generation of ECM it has been shown that other endothelial receptors like ICAM-1, VCAM-1 and P-selectin are upregulated on brain endothelial cells in ECM-susceptible mice during a PbA infection<sup>182 183</sup>. These results are in good agreement with the observations in human brains affected by CM. In addition, ICAM-1 or P-selectin deficient mice did not develop ECM, while leukocyte attachment in these mice in the brain was not impaired, suggesting a major role of both ICAM-1 and P-selectin for iRBC sequestration in these mice<sup>203 204 205</sup>. As described above, parasite proteins involved in sequestration of the human malaria parasite *P. falciparum* include variant antigenic proteins expressed by *var* genes. There is no known homolog of *var* genes in other malaria species but a protein family exists, the *Plasmodium* interspersed repeat (*pir*) family, that is believed to be involved in antigenic variation and has been identified in *P. vivax* a decade ago<sup>206</sup>. Since then members of the *pir* family have been investigated also in rodent malaria parasites like the *cirs* (*P. chabaudi*), the *birs* (*P. berghei*) and the *yirs* (*P. yoelii*)<sup>207 208 209</sup>. But a connection to *P. berghei*-induced ECM could so far not be made<sup>160</sup>. The lack of information about receptors involved in the generation of the cerebral symptoms makes a detailed comparison of CM and ECM quite difficult, but the majority of **immunological** features of human CM are recapitulated during a PbA infection in C57BL/6 mice and can be compared<sup>160</sup>. Like in human CM, the susceptibility of mouse strains to ECM has been directly correlated with the strength of a pro-inflammatory immune environment in response to the parasite<sup>210 211 201</sup>. A great variety of experiments in the field of ECM immunology

has led to the conclusion, that a balance between Th-1 to regulatory T-cell responses is determining the outcome of a PbA infection<sup>212 200 213</sup>, whereas manipulation of the Th2-response (for example through ablation of the IL-4R) does not have a major influence<sup>214</sup>. As already observed in human CM, also in ECM circulating cytokines lead to an upregulation of the expression of endothelial receptors as well as increased expression of chemokines in leukocytes. Thereby, one of the most important family of leukocytes involved in the development of ECM seems to be CD8<sup>+</sup>-T cells. It has been shown that CD8<sup>+</sup>-T-cells accumulate in the brain of susceptible but not resistant mice immediately before the onset of neurological signs and it is believed that these cells can directly cause the disruption of the blood brain barrier via secretion of perforin, a pore-forming protein<sup>215</sup>. In addition to that depletion of CD8<sup>+</sup>-T cells either early (from start of the infection) or late (between day 4 and 5 post-infection) completely inhibits the development of ECM in these mice<sup>216 217 218</sup>. The interplay between the innate and the adaptive immune response also seems to play a major role since it has recently been shown that NK cell-derived IFN $\gamma$  is required for the upregulation of co-stimulatory receptors on CD8<sup>+</sup> T cells and for their subsequent migration to and sequestration in the brain of susceptible mice<sup>219 220</sup>. Even though CD4<sup>+</sup>-T cell depletion during early stages protects from development of ECM, their role during coma stage of the infection is somehow contradictory. Whereas they do not seem to play a role in some studies<sup>217</sup>, in others their depletion also at later timepoints of an PbA infection prevents from ECM and an adoptive transfer of PbA-specific CD4<sup>+</sup>-T cells has been shown to reduce parasite burden and prevent ECM in susceptible mice<sup>220 221</sup>. Therefore a role of CD4<sup>+</sup>-T cells during the generation ECM can not be ruled out and this topic needs some further investigation.

## 1.2 Eps15-homology domain proteins

For the uptake of nutrients and signalling molecules membrane-bound receptors on mammalian cells and other organisms need to be internalized and processed. In addition to that, the expression of adhesion molecules on the surface, ion channels and the retrieval of synaptic vesicles in neurons need to be fine regulated<sup>222</sup>. But not all of the receptors and membrane-bound proteins that are internalized are directed to protein degradation. Some of the receptors need to be recycled back to the surface of the cell by a process called endocytic recycling. Here, first receptors are collected into the early endosome (EE) and then transported back to the plasma membrane. This can happen either directly (fast recycling) or through an organelle first (slow recycling), that is called endocytic recycling compartment (ERC)<sup>223 224</sup> (Fig. 1.10). One of the key groups of proteins involved in endocytic recycling is the family of the Rab-GTPases (Rabs)<sup>225 226</sup>. Rabs are cycling between an inactive (GDP-bound) and an active state (GTP-bound), which has a high affinity for effector proteins, such as SNARE proteins e.g. These proteins mediate fusion between vesicles and target organelles and they themselves promote vesicular transport, fission of and fusion with membranes<sup>227</sup>. Recently, another protein family has been identified that is

involved in the regulation of endocytic recycling events, the Eps15-homology domain (EHD) protein family. EHD-proteins have been identified in many different eukaryotic organisms but are best studied in mammalian cells and in model organisms such as *Drosophila melanogaster* and *Caenorhabditis elegans*. EHD-proteins have been linked to Rab-proteins in a few studies not because of direct interaction but through mutual interaction partners<sup>228 229 230</sup>. Whereas there are four different members of EHD-proteins in mammals, EHD1 to EHD4, there is only one ortholog in both, *Drosophila* (Past-1) and *C. elegans* (Receptor-mediated endocytosis protein 1, Rme-1). In the following, I will mainly focus on the mammalian EHD-protein family members since most functional and structural data have been obtained for this family.

### 1.2.1 Protein architecture and function

EHD-proteins have a molecular mass of about 60 kDa and contain several distinct architectural features: They harbor a **G-domain** at the N-terminal part of the protein, followed by a **helical middle domain** and an **EH-domain** at the C-terminus (N-terminus in plant orthologs)<sup>282</sup> (Fig. 3.5). The proteins are able to bind and hydrolyze ATP, oligomerize around membrane tubules and use the energy created by ATP-hydrolysis to pinch off vesicles from membranes.

#### G-domain

The G-domain harbours the nucleotide binding site of EHD-proteins and is predicted to be similar to the nucleotide binding site-domain found in Ras and dynamin family GTPases in the first place<sup>231</sup>, which is the reason why the domain has been named G-domain. Later, it could be shown that EHD2 indeed is a P-loop-containing NTPase (Guanosin-recognition motive: NKxD; P-loop motive: GQYSTGKT), binding and hydrolyzing nucleoside-triphosphates, but instead of binding to GTP alone, it has a way higher affinity for ATP<sup>283 282</sup>. Upon nucleotide binding EHD-proteins are able to dimerize (Fig. 1.11 A) which then makes them able to bind to membranes. It has been shown that nucleotide-binding of the G-domain is a prerequisite for the protein to dimerize and to oligomerize *in vivo* since nucleotide-free mutants of EHD2 could not bind to lipids anymore and the protein remained cytosolic<sup>282</sup>. A recently developed model<sup>232</sup> (Fig. 1.11 B) proposes a mechanism in which the binding of ATP to the G-domain of an EHD-protein leads to an initial dimerization step (Fig. 1.11 A), upon which the dimer undergoes conformational change and becomes able to bind to lipid bilayers. The dimerization is mediated by a highly conserved hydrophobic interphase within the G-domain (Fig. 1.11 A). After the binding the dimer is able to oligomerize with other dimers to form a ring around membrane tubules and is finally able to pinch off vesicles upon ATP-hydrolysis (Fig. 1.11 B). This function as so-called "membrane bender" has been characterized for EHD2 *in vitro*, because it was shown that this protein tubulates liposomes, forms ring-like oligomers around the tubules and induces the ATP-hydrolysis upon

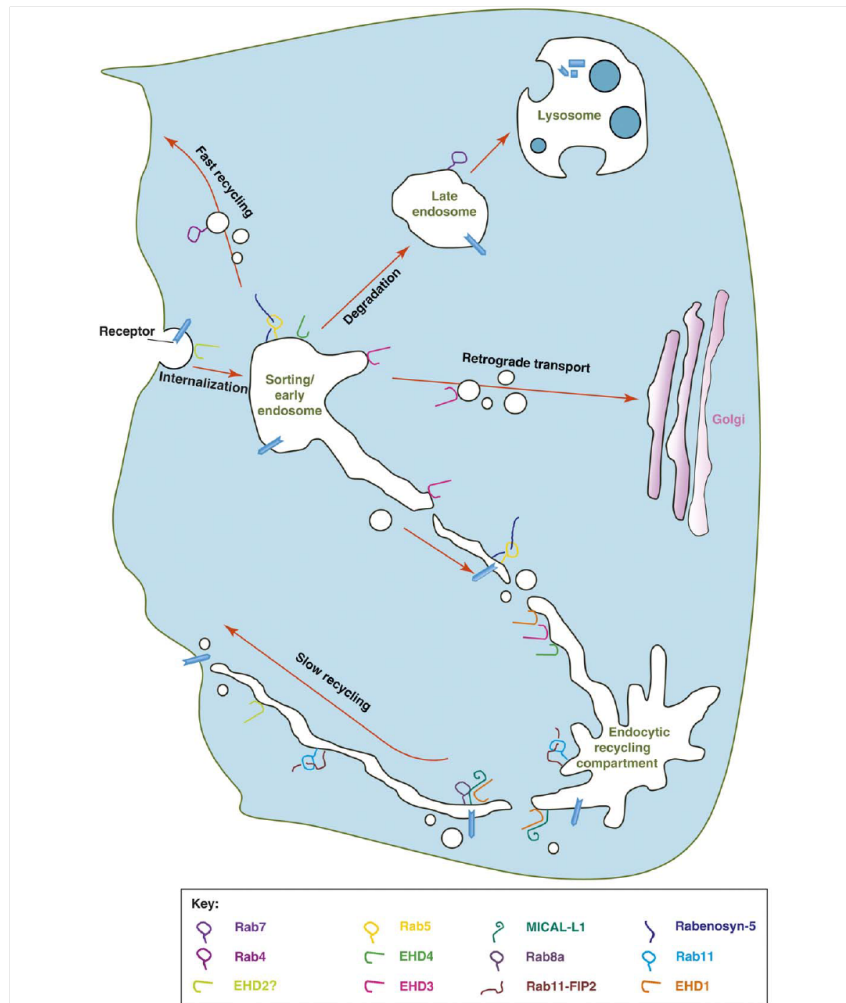


Figure 1.10: **Regulation of endocytic transport and proteins involved.** Internalized receptors are transported to the sorting/ early endosome (EE) where their future fate will be determined. They can either be directly **recycled** back to the surface via fast recycling or slowly, going into the perinuclear endocytic recycling compartment (ERC) first. Proteins destined for **degradation** can either be transported into the late endosome, from where they are moving on into lysosomes, or they are undergoing retrograde transport to the Golgi-apparatus. In all of these processes vesicles need to be labeled and transported to their final destination, which is mediated by trafficking proteins such as EHD-proteins, Rab-GTPases and Rab-like proteins. The figure was adapted from Naslavsky and Kaplan, 2011<sup>232</sup>.



the binding of the membrane<sup>282 233</sup>. Nevertheless it is not sure, yet, if the tubulation event also happens under endogenous gene expression (not overexpressed) *in vivo*. EHD1 and EHD4 are the only EHD-proteins that have been found on endogenous tubules in mammalian cells so far. EHD1 mutants that lacked the ability to bind to tubules created an impaired ability in these cells to recycle receptors indicating for a receptor-recycling function of these tubules<sup>234</sup>. But there is a question that remains to be answered: Do these EHD-proteins tubulate/stabilate the liposomes within the cells or do they only bind to the tubules after they have already formed<sup>232</sup>?

### Helical middle domain

The helical domain is located downstream of the G-domain and can bind to lipids with a polybasic stretch close to its N-terminal tip. Upon dimerization of the protein via the G-domain the lipid-binding site is exposed and forms an interaction site for lipids together with the second protein within the dimer (Fig. 1.11 A).

### EH-domain

The C-terminal Eps15-homology domain was named after three homologous domains at the N-terminus of the epidermal growth factor receptor tyrosine kinase substrate Eps15<sup>235 236</sup>. EH-domains contain two calcium-binding helix-loop-helix motifs (EF-hands) that give them a stable secondary structure. It has been shown that EH-domains are protein-protein-interaction domains that bind specifically to the tripeptide Asparagine-Proline-Phenylalanine (NPF)<sup>237 238</sup>. In addition to that, it has been shown that EH-domains can also interact with phosphorylated phosphoinositides<sup>239</sup>. Even though EH-domains of EHD-proteins and other proteins containing EH-domains are quite similar and all can possibly bind to NPF-motifs, there is a clear need for selectivity of the domains in these organisms. There need to be other factors involved in selecting to bind a specific protein via their EH-domain other than just the NPF-motif. There is a clear difference between EH-domains in EHD-proteins and in other proteins, respectively. In proteins where the EH-domain is located N-terminally, such as in Eps15, the surface of the domain is generally negatively charged, whereas it is positively charged in EHD-proteins<sup>240</sup>. Therefore both proteins can only bind to NPF-motifs that are surrounded by amino acids of the opposite charge<sup>241</sup>. It has been shown in addition, that EH-domains of EHD-proteins can not only bind to NPF- but also to GPF-motifs, even though with a much lower affinity<sup>242</sup>. During formation of homo-dimers of EHD2 the EH-domain of one monomer binds to a GPF motif in the linker region between the EH-domain and the helical domain of the other monomer<sup>282</sup>. In addition to the GPF motif in the linker of EHD2 there is also a KPFxxxNPF-motif within the G-domain that might be the connection point between the EH-domain of one dimer with the G-domain of another dimer during oligomerization<sup>282</sup>.

### 1.2.2 Function

The understanding of the function of EHD-proteins in mammalian cells have mainly derived from point mutations observed in the protein and changes in the expression level that lead to diseases in humans. It has been shown for example that in oral squamous cell carcinoma cells there is a more than 10-fold increase of the expression of EHD3 transcripts<sup>243</sup>. But EHD-proteins also seem to be involved during infections of cells with pathogens since for example human brain endothelial cells binding to *P. falciparum* infected red blood cells exhibit an almost 5-fold increase of EHD1 transcripts than compared to controls<sup>244</sup>. In general, the knock-out of EHD1 and EHD4 leads to only minor phenotypes in mouse models *in vivo*, leading to the conclusion that other EHD-proteins can take over the function and are at least partially redundant<sup>245 246 247</sup>.

#### EHD1

EHD1 presents the highest homology to the orthologs in invertebrate organisms and is the best characterized member of the four mammalian EHDs. It was shown to be involved in receptor-recycling processes regulating the recycling of transferrin receptors (Tfr) through a clathrin-dependent process<sup>248</sup> and other receptors such as major histocompatibility complex (MHC) class I and class II, the insulin-regulated GLUT4 glucose transporter, potassium-channels,  $\beta$ 1 integrins and other receptors through a clathrin-independent process<sup>231 249 250 251 252</sup>. EHD1 can interact with Rab11-FIP2 and localizes to peripheral endosomes<sup>229</sup>. Together with the fact that it is also linked to dynein motors that drive early endosome (EE) to ERC transport this suggests that EHD1 might be involved in the receptor-recycling transports from EE to ERC (Fig. 1.10)<sup>253 254 255</sup>. But EHD1 has also been shown to be involved in the retrograde transport of protein complexes from endosomes to the Golgi and endocytic trafficking events in neuronal cells in addition to its involvement in the regulation of cholesterol homeostasis and lipid droplet storage<sup>256</sup>. Together with EHD2, EHD1 has also recently been shown to interact with FER1L5, a ferlin-like protein, that mediates myoblast fusion for the generation and repair of muscle cells in mammals<sup>257</sup>.

#### EHD2

EHD2 appears to be unique among the mammalian EHD-proteins and shares only about 70% sequence identity with EHD1. EHD2 so far has only been found to form homo-oligomers<sup>282</sup>, whereas all other EHDs have been shown to form hetero-oligomers<sup>258 259 283</sup>, as well. Even though EHD2's function is not quite clear yet, it has been shown to be involved in a few different pathways of endocytic trafficking, most of them starting from the plasma membrane (Fig. 1.10). It was found to be associated with the cell's plasma membrane mainly, a localization crucially depending on ATP-binding of the G-domain<sup>260</sup>, and to be a binding partner of EHBP1,

a protein harbouring five different NPF-motifs, that is involved in internalization events of transferrin receptors and GLUT4<sup>261</sup>. Additionally, depleting EHD2 from mammalian cells leads to delayed recycling of transferrin receptors from the ERC in these cells<sup>262</sup>. It is likely, that in some tissues EHD2 shares a functional redundancy with EHD1 since also EHD2 has been shown to be involved in myoblast fusion and membrane resealing events by interacting with Fer1L5 and also Myoferlin<sup>263</sup>. More recently, it has been shown that in addition to trafficking events EHD2 oligomers can also act as scaffolding proteins stabilizing caveolae, special membrane invaginations and part of lipid rafts, at the plasma membrane via interaction with actin filaments and regulating the dynamics of the formation of these membrane invaginations<sup>264</sup><sup>265</sup>. Many endocytic proteins have been shown to regulate gene expression by undergoing nucleoplasmic shuttling into the nucleus. Whereas EHD1 and EHD3 did not show such a behaviour, EHD2 indeed possesses a nuclear localization signal (NLS), enters the nucleus and represses transcription<sup>266</sup>.

### EHD3

EHD3 is quite similar to EHD1 according to their sequence identities (86%), but nevertheless it seems to be more variably expressed in mammalian tissues, to a rather weak degree in most tissues. It is strongly expressed in the brain, the liver, the kidney and also myocytes of mice, where it seems to be important for the expression and function of the sodium/calcium exchangers on the heart muscle cells<sup>267</sup>. EHD3 has been shown to form hetero-oligomers with EHD1 and seems to cooperate with this protein and Rab8a to form a complex with Myosin Vb motors<sup>268</sup>. Like EHD1, EHD3 was found to be involved in retrograd transport from the EE to the Golgi (Fig. 1.10). This might represent a redundancy of function of both proteins and explain, why EHD1 knock-out mice do only show a modest phenotype. Therefore a generation of EHD1/EHD3 double-knock out mice would be interesting to study<sup>245</sup><sup>262</sup>.

### EHD4

Like EHD3, also EHD4 can hetero-oligomerize with EHD1<sup>259</sup><sup>246</sup>. Both proteins cooperate in the control of receptor-recycling events<sup>269</sup> in the nervous system and EHD4 has been assigned a tissue-specific role in the brain, even though no severe neurological symptoms have been seen in *ehd4* knockout mice. EHD4 depletion leads to enlarged EEs and has been shown to be involved in the regulation of receptor transport from EE to the ERC and from the ERC to the lysosomal pathway (Fig. 1.10) and it has been suggested that EHD4 functions at the EE, upstream of EHD4<sup>232</sup>.

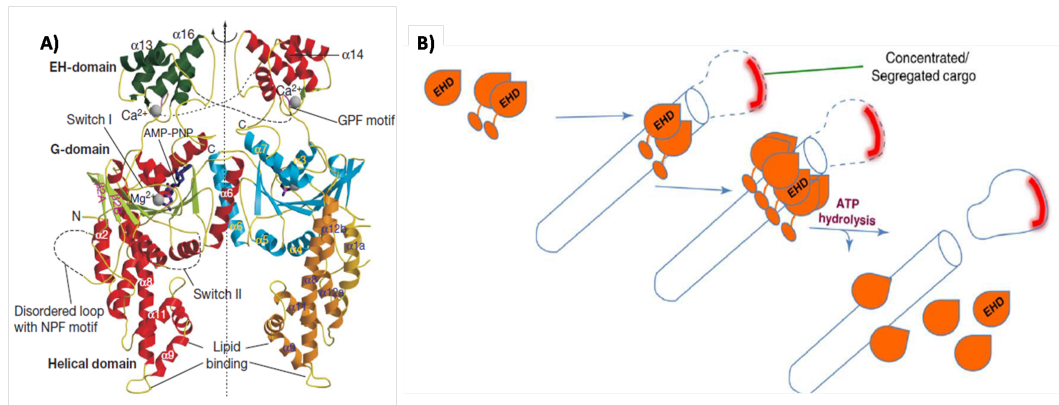


Figure 1.11: **EHD2 dimer architecture and proposed model of EHD-protein function.** **A)** Ribbon-type presentation of the EHD2 dimer. One of the molecules is coloured in red ( $\alpha$ -helices) and light green ( $\beta$ -strand). All structural interaction motifs are indicated. AMP-PNP: Non-hydrolysable ATP-analogue to solve the structure. **B)** Monomeric EHD-proteins in the cytoplasm bind ATP and dimerize. This causes the formation of a membrane binding-site at the dimer and the molecule associates with tubular membranes, undergoing oligomerization. The EHD oligomers form a ring-like structure around the tubule and ATP-hydrolysis finally leads to the abscission of vesicles containing cargo/receptors. (The figure was adapted from Daumke et al., 2007<sup>282</sup>, and from Naslavsky and Kaplan, 2011<sup>232</sup>)

### 1.3 Aim of this study

Apicomplexan protists are among the most important human and domestic animal parasites influencing our lives on an almost daily basis. Two of these organisms, *Toxoplasma* and *Plasmodium*, can cause severe diseases in humans but a promising vaccine against these parasites is still not available. Both parasites have a complex life-cycle involving both, asexual and sexual reproduction, that comes along with a change in hosts. The different environments in these hosts led to the evolutionary development of different parasite stages that are able to adapt to these different environmental conditions. The investigation of these stages will hopefully lead to the development of different anti-parasitic strategies to eradicate these diseases.

The investigation of *Plasmodium falciparum* exo-erythrocytic stages is a bottle neck in malaria research because of the rare availability of these stages under laboratory conditions. Only a few laboratories in the world have established a combined *in vivo/in vitro* *P. falciparum* life-cycle in their facilities to both generate and allow for the accessibility of the full array of *P. falciparum* stages. This is mainly because of technical issues. Therefore one aim during my thesis was to establish a constant combined *P. falciparum in vitro/in vivo* life-cycle that will enable researchers in the lab to work on different stages of *P. falciparum*, especially the elusive liver-stages.

One of the major obstacles for the apicomplexa parasites is the fact that they are replicating intracellularly. Even though this protects them from eradication by factors of the immune system of their hosts it prevents them from free access to sur-

rounding nutrients via several membranous barriers. Therefore the parasites have evolved specialized organelles and cellular mechanisms that eventually supply them with nutrients from the host cell to ensure their survival. One of the mechanisms by which nutrients can cross the parasite membrane is endocytosis. This process is not very well understood in apicomplexans so far. Therefore the aim of the second project of my thesis was to characterize an Eps15-homology-domain containing protein (EHD-protein) in both *Toxoplasma* and *Plasmodium*. Proteins of the EHD-protein family have been shown in other eukaryotic cells already to take part in endocytic trafficking and receptor-recycling. Therefore I hypothesized that the protein may be involved in endocytic events in *Plasmodium* and *Toxoplasma* parasites, respectively. One of my goals was to characterize the localization of the protein in different stages of *Toxoplasma gondii* and *Plasmodium berghei* by fluorescent tagging and immuno-fluorescence assays. By colocalization studies with proteins of subcellular localization, i.e. with organelles of the endocytic system of the parasites, will assist in confirming a putative role for Apicomplexan EHD in endocytic trafficking. Furthermore, endogenous depletion of the gene in both parasites will facilitate the phenotypical characterization and hence function for the parasite life cycle. A detailed characterization of this protein family in apicomplexan parasites will help to further understand the process of how these organisms can survive intracellularly and will ultimately pave the way to develop novel anti-parasitic strategies.

# Chapter 2

## Materials and Methods

### 2.1 Laboratory equipment

AMAXA Nucleofector II electroporation machine	Lonza, Koeln
Analytical scales BL510	Sartorius GmbH, Goettingen
Autoclave	Systec GmbH, Wettenberg
Binocular Niko SMZ 1500	Nikon, Tokyo, Japan
Camera, DC 120 Zoom digital	Kodak, New York, USA
Citation manager Endnote X	Thomso Scientific, USA
Electrophoresis System Horizon 11.14	Whatman Inc., USA
Electrophoresis Power Supply EPS 301	Amersham Pharmacia Biotech, Freiburg
Electroporation cuvettes plus	BTX, San Diego, USA
Film developer Hyperprocessor	Amersham Pharmacia Biotech, Freiburg
Film developing cassettes	Dr Goos suprema GmbH, Heidelberg
Freezer $-80^{\circ}\text{C}$	Sanyo
Freezers $-20^{\circ}\text{C}$	Liebherr, Biberach
Fridges	Liebherr, Biberach
Heat block thermomixer comfort	Eppendorf, Hamburg
Haemocytometer (Neubauer)	Labotec, Labor-Technik, Goettingen
Ice machine AF 30	Scotsman, Milano, Italy
Imaging software Image J 1.45s	National Institutes of Health, USA
Hera Cell Incubator	Heraeus Instruments, Hanau
Shaking Incubator Innova 4000/4300	New Brunswick Scientific Co. Inc.
Multi-gas incubator ( $\text{O}_2$ , $\text{CO}_2$ )	Mytron, Heiligenstadt
Liquid nitrogen tank	CBS, USA
Magnetic stirrer, Heidolph MR3001	NeoLab, Heidelberg
Megafuge 1.0R	Heraeus Instruments, Hanau
Microcentrifuges 5415 R, 5415 D	Eppendorf, Hamburg
Light optical microscope, Axiostar plus	Zeiss, Jena
Light optical microscope, Axioskop	Zeiss, Jena
Light optical microscope, Axiovert 25	Zeiss, Jena
DeltaVision Epifluorescence microscope	Applied Precision; Washington, USA
Microwave oven	MDA
Mosquito cages	BioQuip Products Inc, USA
Nikon TE200 Inverted Microscope	Nikon, Tokyo, Japan
GeneAmp PCR system 9700	Applied Biosystems, CA USA
Mastercycler Gradient	Eppendorf, Hamburg
pH-meter	Inolab, Heidelberg

Photometer	Eppendorf, Hamburg
Single channel pipettes	Abimed, Langenfeld
12-channel pipette 200 $\mu$ l	Abimed, Langenfeld
Pipetting aid pipetus	Hirschmann Laborgeraete, Eberstadt
Precision balance	Mettler Toledo, Switzerland
SDS-PAGE system Heidelberg	Amersham Pharmacia Biotech, Freiburg
SDS-PAGE system small Glasgow	CTI GmbH, Idstein
SDS-PAGE system big Glasgow	Biorad, Muenchen
Semi-dry blot apparatus	CTI GmbH, Idstein
Sterile work bench Gelaire X	Flow Laboratories, Meckenheim
Transmission electron microscope, 900	Zeiss, Jena
Ultra cryo-ultramicrotome	Leica
Vortex Genie 2	Scientific Industries Roth, Karlsruhe
Water bath Julabo U3	Julabo, Seelbach
Wet blot system	Amersham Pharmacia Biotech, Freiburg
Zeiss Axiovert 200M microscope	Carl Zeiss, Obernkirchen

## 2.2 Consumables

14 ml polystyrene round bottom tubes with lid	Greiner Bio-one, Frickenhausen
15 ml polypropylene tubes with lid	Sarstedt, Nuembrecht
50 ml polypropylene tubes with lid	Sarstedt, Nuembrecht
6-well cell culture plates, Cellstar	Greiner Bio-one, Frickenhausen
8-well chamber slides	Nunc, Langenselbold
96-well round bottom plates	Greiner Bio-one, Frickenhausen
Cell culture flasks:	
Cellstar (Filter Cap, 75 cm <sup>2</sup> )	Greiner Bio-one, Frickenhausen
Nunc Flasks Nuclon (Filter Cap, 25 cm <sup>2</sup> )	Nunc, Langenselbold
Cell strainer (70 $\mu$ m)	BD Biosciences, Heidelberg
Cuvettes	Sarstedt, Nuembrecht
Cryovials	Greiner Bio-one, Frickenhausen
Dialysis tube membrane Nadir	Carl Roth GmbH, Karlsruhe
Filter paper Whatman TM 3MM	Whatman, GE Healthcare, Dassel
Gloves, Peha-soft satin	Hartmann, Heidenheim
Immersion oil	Zeiss, Jena
Microscope cover slips	Marienfeld, Lauda-Koenigshofen
Needles, BD Microlance	Becton Dickinson; Heidelberg
Nitrocellulose membrane, Hybond ECL	Amersham, GE Healthcare, Freiburg
Glass slides	Marienfeld; Lauda-Koenigshofen
Parafilm	Pechiney Plastic Packaging; USA
Pasteur capillary pipettes	Wu; Mainz

Petri dishes (94/16 mm)	Greiner Bio-one, Frickenhausen
Pipette filter tips, Biosphere	Sarstedt, Nuembrecht
Pipette tips	Sarstedt, Nuembrecht
Reaction tubes (0.5 ml, 1.5 ml, 2.0 ml)	Sarstedt, Nuembrecht
Sterile filtration devices (500 ml)	Nalagene, Wiesbaden
Sterile pipettes (1 ml-25 ml) Cellstar	Greiner Bio-one, Frickenhausen
Sterile syringe filter, Filtropur (0.22 µm pore size)	Sarstedt, Nuembrecht
Syringe, BD Microlance	Becton Dickinson, Heidelberg
Thermo well PCR tubes (0.2 ml)	Sarstedt, Nuembrecht

## 2.3 Strains

### 2.3.1 Bacteria strains

<i>Escherichia coli</i> XL1 blue	Stratagene; Agilent Technologies Sales & Services GmbH & Co. KG
<i>Escherichia coli</i> XL10 Gold	Stratagene; Agilent Technologies Sales & Services GmbH & Co. KG

### 2.3.2 Cell lines

Huh7	human hepatoma cell line
HFF	human foreskin fibroblasts

### 2.3.3 Parasite strains

<i>P. falciparum</i> NF54	(Ponnudurai et al. 1981) <sup>270</sup>
<i>Plasmodium berghei</i> ANKA GFPcon	(Franke-Fayard et al. 2004) <sup>271</sup>
<i>Plasmodium berghei</i> ANKA cl15cy1	(Hall et al. 2005)
<i>Plasmodium berghei</i> NK65	(Yoeli and Most 1965) <sup>272</sup>
<i>Toxoplasma gondii</i> RHhxgprt(-)	(Donald et al. 1996) <sup>273</sup>

### 2.3.4 Mosquito strains

<i>Anopheles stephensi</i> NIJ	Nijmegen, Niederlande
--------------------------------	-----------------------

### 2.3.5 Mouse strains

Naval Medical Research Institute (NMRI), outbred	Charles River Laboratory, Sulzfeld, Germany
C57BL/6, inbred mice	Charles River Laboratory, Sulzfeld, Germany



## 2.4 Chemicals and reagents

Chemicals were typically purchased in p.a. quality from the companies Roth, Merck, Sigma, Serva and AppliChem. Chemicals and reagents from other companies are listed below.

Agarose	Invitrogen, Karlsruhe
AP Conjugate Substrate Kit	Biorad Laboratories, Muenchen
BactoTM-Agar	Difco Laboratories, Augsburg
BactoTM-Trypton	Difco Laboratories, Augsburg
BactoTM -Pepton	Difco Laboratories, Augsburg
Cellulose powder CF11 (fibrous)	Whatman, GE Healthcare, Dassel
CFSE	Invitrogen, Karlsruhe
Heparin	Braun, Melsungen
Nycodenz powder	Axis-Shield PoC, Oslo
PBS-pellets	Gibco Invitrogen, Karlsruhe
Sea salt	Alnatura
Streptavidin-ALP	Mabtech, Sweden

## 2.5 Oligonucleotides

Oligonucleotides were ordered as custom DNA oligonucleotides in a desalted purity from Invitrogen, Karlsruhe. Lyophilised oligonucleotides were dissolved in ddH<sub>2</sub>O in a concentration of 100  $\mu$ M and stored at  $-20^{\circ}\text{C}$ .

pDLPfullsenseAvrII	5'-CGCCTAGGAGTCGCTGGCTGCGAGGG-3'
pDLPfullantisensePacI	5'-CGTTAATTAATCGCTGAGTGGGTTT GAGTCTCCGG-3'
pDLP $\Delta$ ATPase_senseAvrII	5'-CGCCTAGGGACATGGTTTCCTACCAGCAGC TGATGCG-3'
pDLP $\Delta$ EH_antisensePacI	5'-CGTTAATTAACGTTTCGACGTCGAGCGGCTG GTGGAGAAATTTGTCG-3'
pPFC0190cAvrIIfor	5'-CGCCTAGGTCATTATATATGGTTGAAAG GATGAGG-3'
pPFC0190cPacIrev	5'-CGTTAATTAATTATTTAATAATATCCTTGG GAACCTTGGCAGG-3'
PbEHDkointegSacIIfor	5'-TCCCCGCGGAACCACTTCTCACAAGT GGTGAC-3'
PbEHDkointegSpeIrev	5'-CGGACTAGTGAACAGGTGGAAAATCAC CAAGTG-3'
T7	5'-TAATACGACTCACTATAGGG-3'
SP6	5'-ATTTAGGTGACACTATAGAA-3'
TgDHFR for	5'-CCCGCACGGACGAATCCAGATGG-3'
PbANKA_040280_KO_ _5UTR_for_KpnI-HF	5'-CGGGGTACCCAGTTTTGACAGAATATA TAATTTTC-3'
PbANKA_040280_KO_ _5UTR_for_KpnI-HF	5'-CGGGGTACCCAGTTTTGACAGAATAT ATAATTTTC-3'
PbANKA_040280_KO _3UTR_rev_XbaI	5'-CTAGTCTAGATAACTCAGGATTGTTGAT CTTATTTCA-3'
PbRME-1 RT-PCR F	5'-GCGGAATGAGAATAGGTCCA-3'
PbRME-1 RT-PCR R	5'-TTCCACTTAATACACCGGGAG-3'

## 2.6 Antibodies

### 2.6.1 Primary antibodies

Name	Species	Dilution	
		IFA	WB
$\alpha$ -proTgM2AP-AK (Harper et al. 2006)	R	1:500	
$\alpha$ -TgCatalase (Ding et al. 2000)	R		1:500
$\alpha$ -TgDrpB-AK (Breinich et al. 2009)	M	1:1000	
$\alpha$ -TgIMC-AK (Mann and Beckers 2001)	R	1:1000	
$\alpha$ -TgMic8EGF-AK (Meissner et al. 2002)	R	1:500	
$\alpha$ -TgNtRhop5-AK (T53E2; El Hajj et al. 2007)	M	1:1000	
$\alpha$ -ddFKBP12-AK (ABR, Rockford, USA)	R		1:500
$\alpha$ -PfEHD (T. Spielmann, BNI, Hamburg)	M	1:1000	
$\alpha$ -PbHSP70 (Hybridoma, supernatant)	M	undiluted	

## 2.6.2 Secondary antibodies

ALEXA Fluor antibodies were ordered from Invitrogen (Frankfurt). The gold labeled antibody for immuno-EM was ordered from BBIInternational.

Name	Species	Dilution	
		IFA/iEM	WB
ALEXA Fluor 488 $\alpha$ -mouse	goat	1:1000	
ALEXA FLuor 594 $\alpha$ -mouse	goat	1:1000	
ALEXA Fluor 488 $\alpha$ -rabbit	goat	1:1000	
ALEXA Fluor 594 $\alpha$ -rabbit	goat	1:1000	
$\alpha$ -rabbit IgG, HRP	goat		1:5000
gold (15nm) $\alpha$ -mouse IgG	goat	1:500	

## 2.7 Media, buffers and solutions

### 2.7.1 Media and buffers for molecular biological methods

**LB (Luria Broth) Medium:** 10 % trypton  
 5 % yeast extract  
 10 % NaCl  
 pH 7,5; autoklave

**LB Agar:** LB-medium; 15 g/l agar

**TAE (50 x):** 2 M TRIS  
 1M acetic acid  
 50mM EDTA; pH 8.0

**PBS (10 x):** 0.01 M KH<sub>2</sub>PO<sub>4</sub>  
 1.37 M NaCl  
 0.027 M KCl  
 pH 7.2; autoklave  
 or dissolve 20 PBS tablets (Gibco) in 1 l ddH<sub>2</sub>O; autoklave

**PBS (1 x):** 100 ml 10 x PBS, filled up with ddH<sub>2</sub>O to 1 l  
 or purchased from Invitrogen

**TfB I:** 30 mM potassium acetate  
 50 mM MnCl<sub>2</sub>

100 mM KCl  
10 mM CaCl<sub>2</sub>  
15 % glycerine

The pH was adjusted to 5.8 with acetic acid. The buffer was sterile filtered and stored at 4 °C.

**TfB II:** 10 mM MOPS  
75 mM CaCl<sub>2</sub>  
10 mM KCl  
15 % glycerine

The pH was adjusted to 7.0 with NaOH. The buffer was sterile filtered and stored at 4 °C.

**3 M sodium acetate (NaAc)-solution:** 24.06 g NaAc  
add 100 ml H<sub>2</sub>O  
pH 5.2

#### **IFA-solutions**

**PFA-fixation solution:** 4% PFA (w/v) in PBS

**Permeabilisation solution:** 0,2% Triton X-100 in PBS

**Blocking solution:** 2% BSA in permeabilization solution  
or 10% FCS in PBS

**Washing solution:** 1% FCS or BSA in PBS

### **2.7.2 Media and solutions for cell culture**

Cell culture media and supplements were purchased from Invitrogen or Gibco, Karlsruhe.

**Hepatocyte culture medium:** 1 x Dulbecco's Modified Eagle Medium  
(DMEM complete) 10 % FCS  
1 % penicillin/streptomycin;  
sterile, stored at 4 °C

**DMEM HFF culture:** 500 ml DMEM  
10% FCS (v/v)  
1% Glutamine (v/v)  
1x Gentamycin (20 µg/ml)

**Cell freezing solution:** 80 % FCS  
20 % DMSO

or

90 % FCS  
10 % DMSO

mixed 1 : 1 with complete culture medium

***P. falciparum* culture medium:** 500 ml 1 x RPMI 1640  
50 ml human serum A+  
550 µl 1000 x Hypoxanthine  
550 µl 1000 x Gentamycin (opt.)  
sterile filtered

***P. falciparum* thawing solutions:** Sterile 0.2% dextrose/0.9% NaCl  
Sterile 1.6% NaCl  
Sterile 12% NaCl

### 2.7.3 Media, buffers and solutions for parasitological methods

***P. berghei* transfection medium:** 160 ml RPMI 1640 medium  
(T-medium) 40 ml FCS (US certified)  
heat inactivated for 30 minutes 56 °C  
60 µl Gentamycin;  
sterile filtered

***P. berghei* freezing solution:** 10 % glycerine in Alsever's solution (Sigma)

**Nycodenz stock solution:** 110.4 g Nycodenz powder  
5 mM TRIS/HCl; pH 7.5  
3 mM KCl  
0.3 mM EDTA; pH 8.0  
fill up to 400 ml with ddH<sub>2</sub>O; autoclave; store at 4 °C

**Pyrimethamine stock solution:** 7 mg/ml Pyrimethamine in DMSO  
store at 4 °C

**Electroporationbuffer/Cytomix:** 10 mM K<sub>2</sub>HPO<sub>4</sub>/KH<sub>2</sub>PO<sub>4</sub>  
25 mM HEPES  
2 mM EGTA pH 7,6  
120 mM KCl  
0,15 mM CaCl<sub>2</sub>  
5 mM MgCl<sub>2</sub>  
together with 5 mM KOH to pH 7,6  
2 mM ATP  
3 mM GSH

**ATP (30 µl/ml)** 100 mM in water

**GSH (30 µl/ml)** 100 mM in water

#### 2.7.4 Buffers and solutions for biochemical methods

**Saponin buffer:** 1x PBS, 2% BSA, 0.5% Saponin; prepare fresh

**PAA-Stock solution:** 30% PAA  
0,8% Bis-AA

**Stacking gel buffer (SDS, 4x):** 0,5 M Tris/HCl pH 6,8  
0,4% SDS (w/v)  
sterile filter

**Stacking gel:** 4% PAA (v/v)  
25% 4x stacking gel buffer (v/v)  
0,1 % APS 10%(v/v)  
0,2% TEMED (v/v)

**Separating gel buffer (SDS, 4x):** 1,5 M Tris/ HCl auf pH 8,8  
0,4% SDS (w/v)  
sterile filter

**Separating gel:** 8-15% PAA (v/v)  
25% 4x separating gel buffer  
0,1% APS 10% (v/v)  
0,2% TEMED (v/v)

**5x SDS-PAGE running buffer:** 33 mM Tris/HCl pH 6,8  
190 mM Glycin  
0,1% SDS

**4x SDS-PAGE sample buffer:** 50% 4x Sammelgelpuffer (v/v)  
40% Glycerol (v/v)  
8% SDS (w/v)  
0,2% Bromphenolblau (w/v)  
400 mM DTT (w/v)

**RIPA lysis buffer:** 50 mM Tris-HCl, pH 7.5  
150 mM sodium chloride (NaCl)  
5 mM EDTA  
50 mM sodium fluoride (NaF)  
0.5% sodium deoxycholate (NaDOC)  
0.1% SDS  
1% Triton X-100  
freshly added 1 mM DTT  
protease inhibitor

**Semidry-Blot-Transfer buffer:** 48 mM Tris  
39 mM Glycin  
20% Methanol

**10x TBS:** 20 ml 1M Tris, pH 7.6  
80 g sodium chloride (NaCl)  
add 1 l H<sub>2</sub>O

1x TBST: 100 ml 10x TBS  
 900 ml ddH<sub>2</sub>O  
 1 ml Tween 20

### 2.7.5 Antibiotics

Ampicillin 1000x	100 mg/ml in ddH <sub>2</sub> O
Tetracyclin 1000x	5 mg/ml in 70% Ethanol
Chloramphenicol	1000x 10 mg/ml in Ethanol
MPA 500x	12,5 mg/ml Methanol
Xanthin 500x	20 mg/ml 1 M KOH
Pyrimethamin 1000x	1 mM in Ethanol
Gentamycin 500x	10 mg/ml in H <sub>2</sub> O

## 2.8 Molecular biological methods

### 2.8.1 Cloning of the targeting constructs for parasite transfection

For the *Toxoplasma* RME-1 expression construct pTub8DDmCherryTgRME-1FL (Fig. 2.1) the full length coding sequence of the gene TGME49\_031210 was amplified from *Toxoplasma gondii* RHΔHX cDNA using the oligo set pDLPfullsenseAvrII and pDLPfullantisensePacI. The PCR-fragment was introduced into the Tub8DDmCherry-HXGPRT plasmid via the restriction sites *AvrII* and *PacI*.

For the *Toxoplasma* RME-1 over-expression ATPase-domain deletion construct pTub8DDmCherryTgRME-1ΔATPase (Fig. 2.2) the coding sequence of the gene was amplified downstream of the sequence coding for the predicted ATPase domain using the oligo set pDLPΔATPasesenseAvrII and the same reverse primer as mentioned above for the full length construct. The PCR-product was subsequently introduced into the Tub8DDmCherry-HXGPRT plasmid via the restriction sites *AvrII* and *PacI*.

For generation of the *TgRME-1* EH-domain over-expression deletion mutant construct pTub8DDmCherryTgRME-1ΔEH (Fig. 2.3) the coding sequence of the gene was amplified upstream of the sequence coding for the predicted EH-domain with a stop-codon added to the reverse Primer. Primers pDLPΔEHantisensePacI and the full-length forward primer mentioned above were used to amplify the fragment which was introduced into the plasmid pTub8DDmCherry-HXGPRT via the restriction sites *AvrII* and *PacI*.

For generation of the construct pTub8DDmCherryPfc0190c (*PfEHD*) (Fig. 2.4) the full-length ORF of the gene PFC0190c/ PF3D7\_0304200 (*PfEHD*) was amplified from *Plasmodium falciparum* cDNA using the oligo set pPFC0190cAvrIIfor and pPFC0190cPacIrev. The PCR-product was subsequently introduced into the pTub8DDmCherry-HXGPRT plasmid via the restriction sites *AvrII* and *PacI*. For



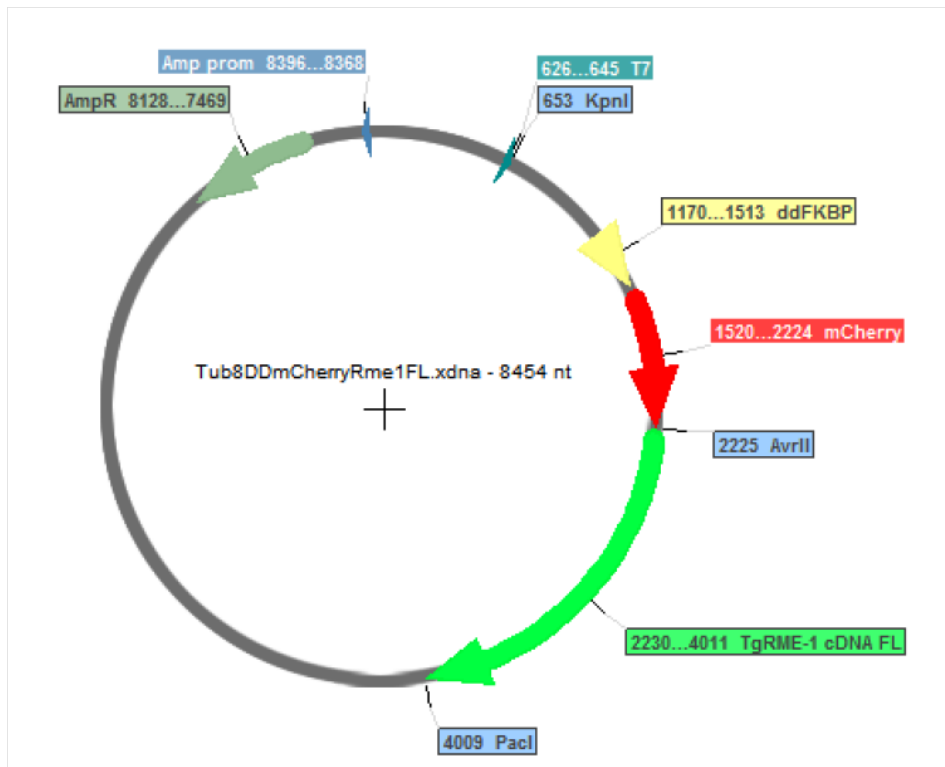


Figure 2.1: Vector map **Tub8DDmCherryRME-1 full length.**

transfection into *Toxoplasma gondii* parasites all Tub8DDmCherry-constructs were linearized by *KpnI* restriction enzyme.

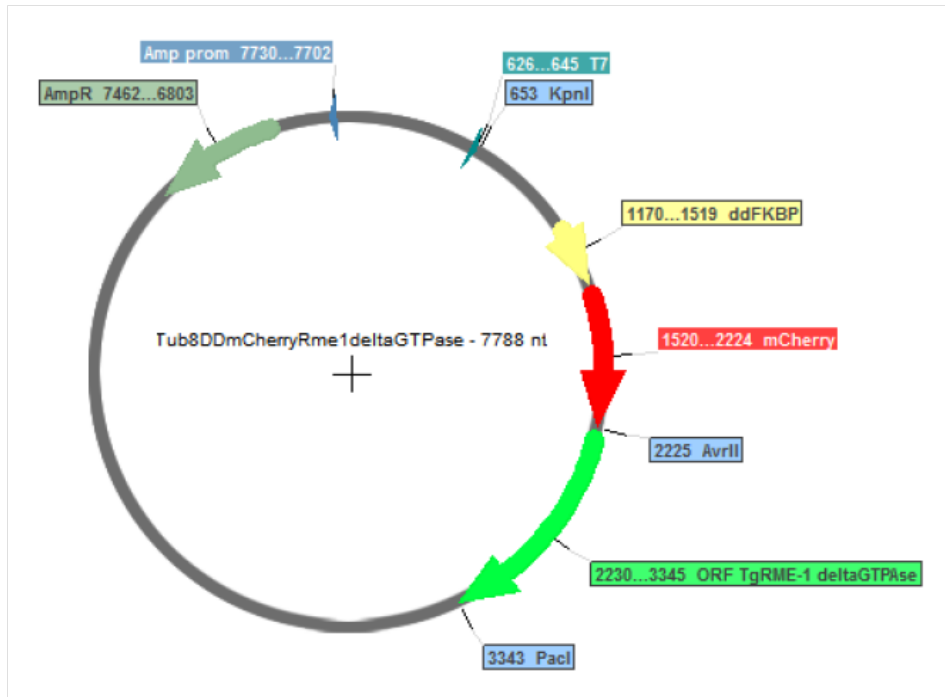
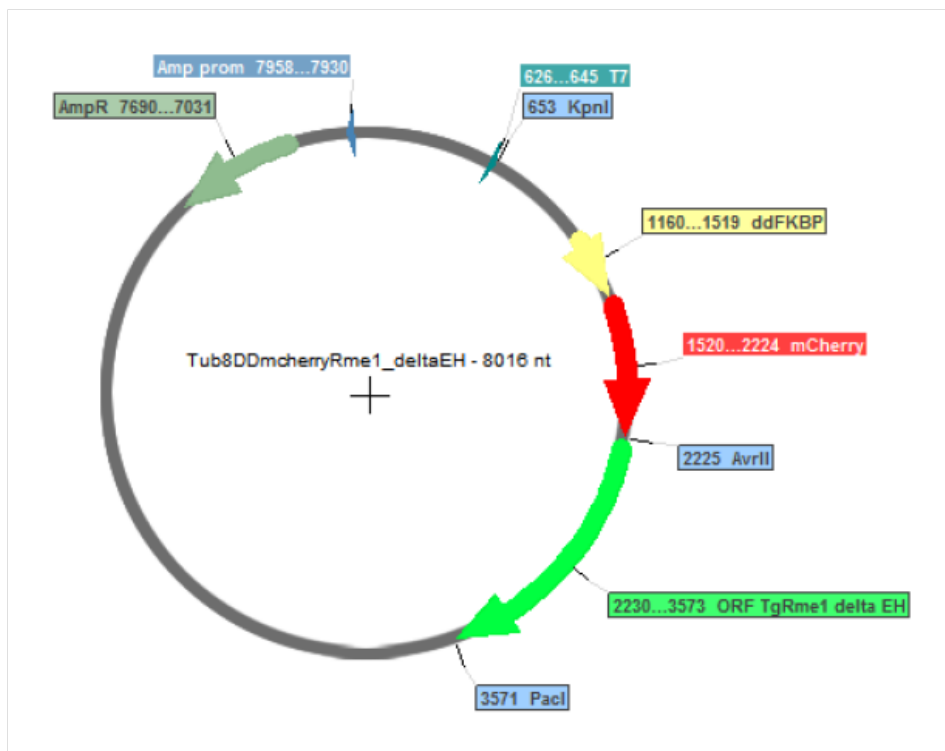
For generation of the single-crossover *pbehd* (-) targeting construct pFK01 (Fig. 2.5) a 1kb fragment of the middle part of the ORF of PbANKA\_040280 was amplified from genomic DNA using the oligo set PbEHDkointegSacIIfor and PbEHDkointegSpeIrev. The PCR-product was subsequently introduced into *P. berghei* transfection vector b3D.DT/H./D<sup>274</sup> via the restriction sites *SacII* and *SpeI*. For transfection the plasmid was linearized by *HpaI* restriction.

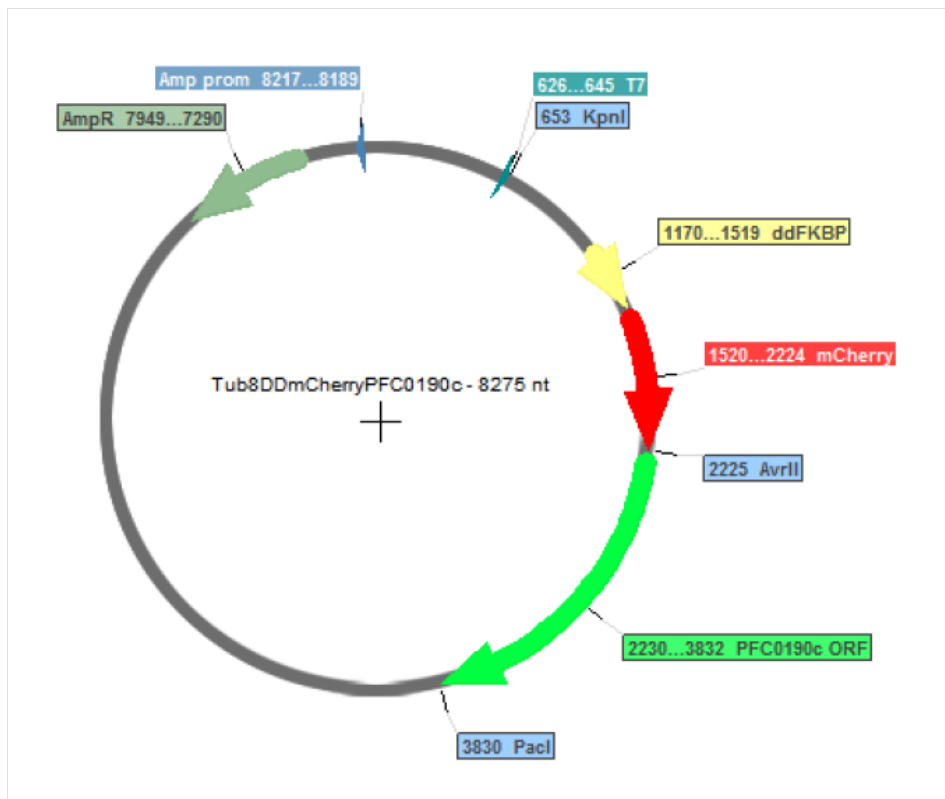
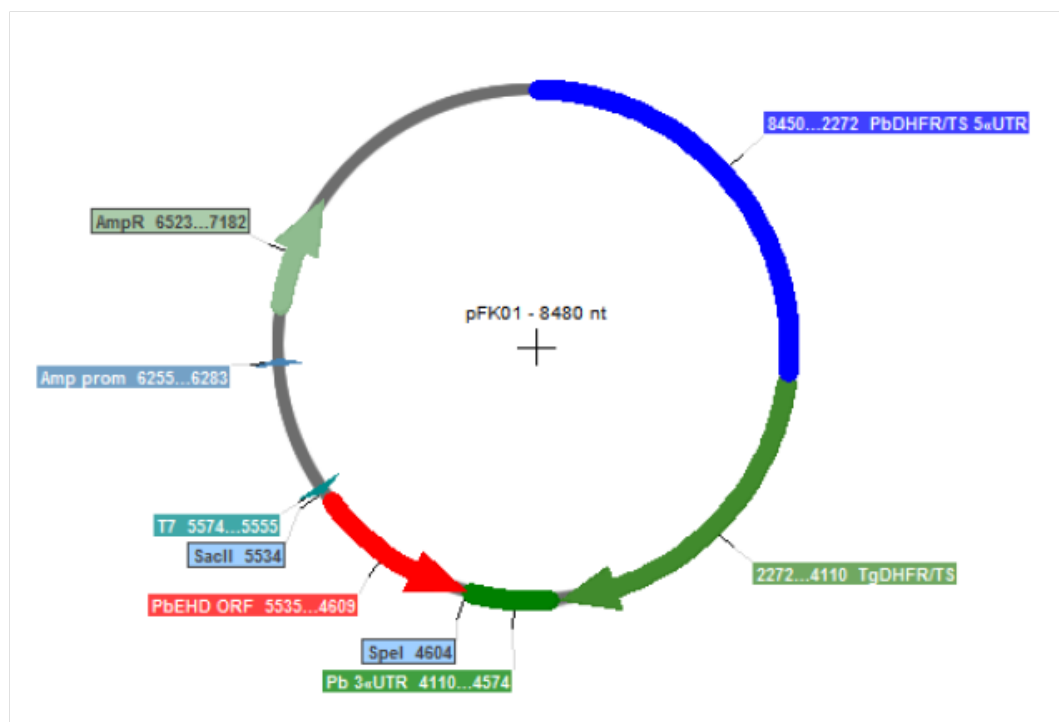
All vector maps were created using the *Serial Cloner Tool* (Version 2.5; Franck Perez, SerialBasics). Other used vectors in this thesis:

Plasmid	Source
Tub8ddmycGFP-TgDrpB	Breinich et al., 2009
Tub8ddmyc-Rab5a	AG Meissner
Tub8ddmyc-Rab7	AG Meissner
Tub8IMC-YFP	AG Meissner

### **Amplification of the specific DNA fragments by Polymerase chain reaction (PCR)**

Specific DNA fragments were amplified by Polymerase chain reaction (PCR) (Saiki et al. 1985) using specific oligonucleotides. All used oligonucleotides and their sequences are noted in section 2.5. As templates served *P. falciparum*, *P. berghei* or *T. gondii* gDNA or cDNA. For a standard PCR reaction 0.5 - 2  $\mu$ l parasite

Figure 2.2: Vector map **Tub8DDmCherryTgRME-1 $\Delta$ ATPase**.Figure 2.3: Vector map **Tub8DDmCherryTgRME-1 $\Delta$ EH**.

Figure 2.4: Vector map **Tub8DDmCherryPfc0190c**.Figure 2.5: Vector map **pFK01**.

gDNA/cDNA was used in a reaction volume of 10-50  $\mu$ l. Furthermore the reaction contained 50 pmol of the specific oligonucleotides (Invitrogen), 0.2 mM dNTPs, 1.5 mM MgCl<sub>2</sub>, 1 x Taq reaction buffer (+ KCl) and 2.5 U Taq polymerase (all Fermentas) filled up to 10-50 l with ddH<sub>2</sub>O. Reaction tubes were placed into a thermal cycler running the program with an initial denaturation of the dsDNA for 5 minutes at 95 °C, followed by 30 cycles with a denaturation at 94 °C for 30 seconds, annealing of the specific oligonucleotides at 45-60 C for 30 seconds and extension of the newly synthesised DNA strand 60 °C (72 °C in case of *P. falciparum* and *T. gondii*) for 1 minute per amplified kilobase. A final extension for 10 minutes at 72 °C was carried out and amplified DNA was stored at 4 °C for short-term and at -20 °C for long-term storage.

### **Analysis of DNA fragments by agarose gel electrophoresis**

Amplified DNA fragments were separated by size by agarose gel electrophoresis. For this 1% agarose was dissolved in 1 x TAE buffer by heating in the microwave. Ethidium bromide (Sigma, Taufkirchen) was added to a final concentration of 50 ng/ml. Samples were mixed with 1/5 volume of 6 x Orange Loading dye (Fermentas) and loaded along with 1  $\mu$ g GeneRuler 1 kb DNA Ladder (Fermentas) into the wells. The gel was run for 1 hour at 100-120 V in 1 x TAE buffer in a Whatman Horizon 11.14 electrophoresis chamber. Negatively charged DNA thereby migrates in direction of the anode. Separated DNA fragments were visualized by exposure of the DNA-intercalating ethidium bromide to UV-light and fluorescence was recorded with the Electrophoresis Documentation and Analysis System 120 (Kodak).

### **Purification of DNA with Qiaquick PCR purification Kit**

Amplified DNA fragments were purified with Qiaquick PCR purification Kit (Qiagen, Hilden) prior to digestion with restriction endonucleases and digested DNA fragments as well as plasmid DNA also prior to ligation according to the manufacturer's manual.

### **Digestion of double-stranded DNA**

Purified DNA fragments or plasmid DNA were digested with specific restriction endonucleases (New England Biolabs NEB, Frankfurt) prior to ligation (preparative digest) or after plasmid isolation (control digest). For the preparative digest the amplified and purified DNA fragments and the respective plasmid DNA were cut with the same restriction endonucleases. The complete purified DNA fragment or 1 - 3  $\mu$ g plasmid DNA were mixed with 10 - 20 Units of the respective restriction enzymes, 5  $\mu$ l of the matching buffer (10x) and 5  $\mu$ l of BSA (10x), if necessary, and filled up to 50  $\mu$ l with ddH<sub>2</sub>O. The digest was typically incubated over night at 37 °C (if not otherwise suggested by NEB). For the control digest of isolated plasmids the approach was typically scaled down to 20 l reaction volume, using only 0.5 - 1  $\mu$ g

DNA. The reaction was then incubated for 2 hours at 37 °C. All digested DNA was analysed by agarose gel electrophoresis as described in section 2.8.1 and preparative digested DNA was purified prior to ligation as described in section 2.8.1. Prior to parasite transfections 10 µg of the generated plasmids were digested completely with up to 40 units of the respective enzymes in a volume of 100 µl over night at 37 °C. Subsequently digested plasmid DNA was ethanol precipitated as described below.

### **Ligation of DNA**

Digested and purified DNA fragments were ligated with equally restricted plasmids in a ratio of 7:1 or 6:2 in a total reaction volume of 10 µl. 5 Units of the T4 ligase were used to catalyse the reaction in 1 x of the provided T4 ligase reaction buffer (10 x, Fermentas). The ligation reaction was incubated for 2 hours at room temperature or at 16 °C over night. Subsequently competent *E. coli* XL1 blue were directly transformed with the ligated DNA constructs.

### **Preparation of transformation competent *E. coli* XL1 blue**

*E. coli* XL1 blue were cultured over night in LB medium with tetracycline (5 µg/ml). The over night culture was diluted 1 : 100 in LB medium with tetracycline (5 µg/ml) and cultivated shaking at 37 °C until it reached an OD600 of 0.5. The culture was cooled down on ice and spun for 5 minutes at 1500 x g at 4 °C. The cell pellet of 100 ml culture was resuspended in 30 ml cold TfbI, incubated for 15 minutes on ice and spun again for 5 minutes at 1500 x g. The pellet was resuspended in 8 ml TfbII and incubated another 15 minutes on ice. 200 µl aliquots of the suspension were frozen at -80 °C.

### **Transformation of competent *E. coli* XL1 blue**

Transformation competent *E. coli* XL1 blue, either purchased from Stratagene or prepared as described above, were thawed on ice. 35 hboxµl of the purchased cells or 200 µl of the self-made competent cells were used for one transformation. Competent cells were either treated for 10 minutes on ice with 0.68 hboxµl -mercaptoethanol (1.42 M; Stratagene) and subsequently mixed with 2 µl of the ligation (Stratagene competent cells) or directly mixed with 10 µl ligation (self-made competent cells). The cells were incubated for 30 minutes on ice, followed by a heat-shock for 45 seconds at 42 °C in the water bath. Cells were incubated subsequently another 2 minutes on ice, then 1 ml pre-warmed LB medium was added and cells were incubated, shaking at 37 °C for 1 hour. The cells were spread on LB agar plates with ampicillin (100 µg/ml) and incubated over night at 37 °C.

### **Plasmid-isolation with Quiaprep Spin Miniprep Kit**

After transformation single colonies were used to inoculate 3 ml LB medium with ampicillin (100 µg/ml) each. These cultures were incubated shaking at 37 C over

night. The over night cultures were spun for 2 minutes at 16,000 x g in a table-top microcentrifuge. The plasmid isolation from the cell pellet was performed as described in the manufacturer's manual. Isolated plasmids were control digested as described under 4 and resulting DNA fragments were analysed by agarose gel electrophoresis (described above) to confirm successful integration of the DNA fragments.

### **Preparation of bacteria glycerol-stocks**

For conservation of transformed E. coli containing the generated plasmids over night cultures were prepared as described under 8. 850 µl of the over night culture were mixed with 150 µl glycerine (99.5 %, Roth) in a cryovial and stored at  $-80^{\circ}\text{C}$ .

### **Determination of DNA concentration by photometric measurement**

In order to determine the DNA concentration of a plasmid preparation the DNA was typically diluted 1 : 100 in ddH<sub>2</sub>O. The absorption of the DNA at 260 nm was measured in a photometer (Eppendorf) and DNA concentration was calculated according the following relation:

$$\text{OD}_{260} \times 50 \times \text{dilution factor} = \text{concentration dsDNA [g/ml]}$$

The purity of the DNA preparation was shown by the ratio of OD<sub>260</sub>/OD<sub>280</sub> and typically ranged from 1.8 to 2.0.

### **Ethanol precipitation of DNA**

Digested DNA was ethanol precipitated prior to parasite transfection. For this purpose 2.5 volumes 100 % ethanol and 1/10 volume 3 M sodium acetate, pH 5.2, were added to the DNA solution and incubated at least 30 minutes at  $-80^{\circ}\text{C}$ . After spinning for 15 minutes at 16,000 x g the DNA pellet was washed once with ice cold 70 % ethanol and again spun for 5 minutes at 16,000 x g. The ethanol was carefully removed and the DNA pellet was air dried. Finally the DNA was resuspended in 1 x PBS to a final DNA concentration of 1 µg/µl. Digested and precipitated DNA was once more analysed by agarose gel electrophoresis and stored at  $-20^{\circ}\text{C}$  until parasite transfection.

## **2.8.2 Stage-specific RNA isolation and cDNA synthesis for RT PCR**

Different parasite stages were isolated from infected mosquitos (2.10.2), in-vitro hepatocyte cultures (2.9) or infected blood (2.10.1).

### **Isolation of total RNA with RNeasy Mini Kit (Quiagen)**

Parasite cells were disrupted by addition of in 350 µl RLT buffer (supplied, Qiagen) supplemented with 1 % -mercaptoethanol (14.3 M) and homogenised by vortexing for 1 minute. Total RNA was isolated from the cell lysate according to the "Animal Cell Spin" protocol supplied in the manufacturer's manual. Isolated RNA was stored at  $-80^{\circ}\text{C}$ .

**Trizol extraction of total RNA**

Parasites were resuspended in 1 ml Trizol Reagent (Invitrogen), 200  $\mu$ l chloroform was added and carefully mixed by inverting. After 3 minutes incubation at room temperature it was mixed again and subsequently spun for 15 minutes at 12,000 x g at 4°C. The top aqueous layer, containing the RNA, was carefully transferred to a fresh RNase-free tube (Eppendorf). After addition of 500  $\mu$ l isopropanol (2-propanol) the solution was incubated for 10 minutes at room temperature and spun for 10 minutes at 12,000 x g at 4°C. The supernatant was discarded and the RNA pellet was washed with 75 % ethanol and thoroughly mixed by vortexing. After a final centrifugation for 5 minutes at 7,500 x g at 4°C the RNA pellet was air dried, resuspended in 10  $\mu$ l DEPC-treated H<sub>2</sub>O and incubated for 10 minutes at 60°C. Isolated RNA was stored at -80°C.

**DNase treatment of total RNA**

After RNA isolation remaining DNA contaminations were removed by digestion with DNase. The RNA was mixed with 1/10 volume of 10 x TURBO DNase buffer (Ambion) and 1  $\mu$ l TURBO DNase (Ambion) and incubated for 30 - 45 minutes at 30°C. 1/10 volume of the resuspended DNase Inactivation Reagent (Ambion) was added, mixed thoroughly and incubated for 2 minutes at room temperature. The reaction was centrifuged for 1 minute at 10,000 x g and the supernatant containing the RNA was transferred to a fresh RNase-free tube (Eppendorf). DNase treated RNA was stored at -80°C.

**First strand cDNA synthesis**

RNA was transcribed into complementary DNA (cDNA) with the Fermentas "First Strand cDNA Synthesis Kit" according to the manufacturer's manual using random hexamer oligonucleotides. The initial optional denaturation step of the total RNA for 5 minutes at 65°C was performed. For each transcribed RNA one approach without reverse transcriptase (-RT) was run to exclude DNA contaminations. The transcribed product was directly used for reverse transcriptase PCR (below) or stored at -20°C.

**Reverse transcriptase PCR (RT PCR)**

A standard PCR approach was prepared as described above. In a reaction volume of 20  $\mu$ l 0.5 - 2  $\mu$ l first strand cDNA of the different parasite stages were used as template together with *P. berghei* or *T. gondii* gene specific oligonucleotides. For each sample one tube with cDNA synthesised with reverse transcriptase (+ RT) and one - RT control tube were prepared. Oligonucleotides specific for the *P. berghei* aldolase, expressed constantly throughout the life cycle, were used as control. The amplification was performed in a thermal cycler using the standard PCR program as described above.

## 2.9 Cell culture

### 2.9.1 In vitro liver-stage development of *P. berghei* in human hepatoma cells Huh7

Frozen cell stocks of the human hepatoma cell line Huh7 were kept in 80% FCS, 20% DMSO in liquid nitrogen. Thawed cells were immediately transferred into pre-warmed DMEM culture medium containing 10% FCS and 1% Penicillin/Streptomycin (DMEM complete) and centrifuged for 5 minutes at 200 x g. The cell pellet was resuspended in fresh DMEM complete and transferred into a cell culture flask (25 cm<sup>2</sup> or 75 cm<sup>2</sup>). Cells were incubated at 37 °C, 5% CO<sub>2</sub> until a confluent monolayer was reached. For further cultivation medium was removed, attached cells were washed once with HBSS and detached with 0.25% Trypsin/EDTA (Gibco) for 3 - 5 minutes at 37 °C. After addition of 10 ml DMEM complete cells were transferred to a 15 ml tube and centrifuged for 5 minutes at 200 x g. The cell pellet was washed once with HBSS and finally resuspended in 10 ml DMEM complete. Depending on the approach an aliquot of 200 µl up to 2 ml of the cell suspension were transferred to a new culture flask and filled up to 15 ml with DMEM complete.

For the *Plasmodium berghei* in vitro liver cell development assay Huh7 cells cultivated to a confluent monolayer were detached with 0.25 % Trypsin/EDTA and washed as described. The cell pellet was resuspended in DMEM complete and counted diluted in Trypan blue (0.4 %) using a haemocytometer. Either 25,000 cells per well on a 8 well chamber slide (nunc) or 200,000 cells per well on a 6 well plate (greiner) were seeded and cultivated over night. Mature salivary gland sporozoites were purified (described in section 2.10.1) and 25,000 - 35,000 sporozoites or 100,000 - 200,000 sporozoites were added on the cultivated cells on the 8 well chamber slide or 6 well plate, respectively. Sporozoites were allowed to invade for at least 90 minutes, afterwards the sporozoite suspension was removed and cells were incubated in DMEM complete plus anti-contamination cocktail. Liver-stage development was stopped after different time points by either fixing them for 10 minutes with 4% PFA or Methanol (icecold) for IFA-studies or harvesting the cells with 0.25 % Trypsin/EDTA as described before. The harvested cells were then transferred into a 1.5 ml tube and centrifuged for 2 minutes at 16,000 x g and depending on the application resuspended in RLT buffer, Trizol or PBS.

### 2.9.2 *P. falciparum* culture - asexual parasites

A small culture flask (25 cm<sup>2</sup>) with 5 ml complete Medium (10% human heat inactivated A+ Serum, Gentamycin 50 µl/ml, Hypoxanthin; filtered through a 0,22 µm filter) and a final haematocrit of 5% (1:10 dilution out of stock: 50% weekly freshly purified erythrocytes in complete medium) was inoculated with a freshly thawed *P. falciparum* stock solution. Parasites were grown for several days while culture was checked every second day for its parasitemia. If erythrocytes reach a parasitemia between 5-10% the culture was split down to a new small culture flask



to a concentration of 1% parasitized erythrocytes per flask. Therefore the volume of the old culture that had to be transferred to a new culture flask was calculated as follows:  $y = 11,1 \times X \times 500 \mu\text{l}$  (X is the needed dilution to obtain 1% parasitaemia; for example 1:5 if the parasitaemia of the old culture is 5%). y was diluted in 5 - y ml complete medium and  $500 \mu\text{l} - y/11.1$  fresh erythrocyte solution (see above) was added. After at least 10 subculturing rounds the asexual culture was used to set up a gametocyte culture. The parasite culture was maintained at 37 °C and 5% O<sub>2</sub>/ 5% CO<sub>2</sub>/ 90% N<sub>2</sub>.

### 2.9.3 *P. falciparum* culture - gametocytes

To set up a gametocyte culture an asexual *P. falciparum* culture was grown to a parasitaemia of 6-10%. This culture was then transferred into a big culture flask (75 cm<sup>2</sup>) with the volume calculated as follows:  $y = 11,1 \times X \times 2000 \text{ l}$  (X is the needed dilution to obtain 1% parasitaemia; for example 1:8 if the parasitaemia of the asexual culture was 8%). y was diluted in 20 ml - (y+blood) complete medium (10% human heat inactivated A+ Serum, without Gentamycin, Hypoxanthin; filtered through a 0,22 m filter) and  $2000 \mu\text{l} - y/11.1$  blood was added. The culture medium was changed every day, first week after setting up 15 ml, later 25 ml. Occasional blood smears of the cultures were done from day 7 on to check for gametocyte production.

### 2.9.4 Cultivation of *Toxoplasma gondii* in human foreskin fibroblasts (HFFs)

The virulent *Toxoplasma gondii* strain RHΔHX was cultivated in vitro in human foreskin fibroblast (HFF) cells. HFF cells are primary culture cells that can not be maintained for longer than 30 passages in culture. They form a single confluent layer in cell culture flasks. The cells were kept in DMEM complete medium and were splitted into new flasks every 3-4 days in a ratio of 1:3 or seeded into 6-cm dishes in a ratio of 1:5 for *Toxoplasma* cultures. For parasites cultures a confluent HFF dish was infected with extracellular parasites and kept until complete lysis of the host cells under the conditions described above. After the lysis parasites keep viable for another 12-24 hours before they die if they can not invade new cells. If intracellular parasites are needed to be extracted from host cells for experiments the infected cells can be scratched off from the dish bottom. Afterwards they can be pressed through a 26G needle to release the parasites from the host cells. A washing step of about 5-30 min centrifugation at 1000 x g and RT can purify the parasites from surrounding medium for further experiments.

## 2.10 Parasitological methods

### 2.10.1 Plasmodium methods

#### Determination of parasitemia in giemsa stained blood smears

A small drop of blood was obtained from the tail of the infected mouse or the *P. falciparum* cell culture (spun down at 7000 rpm for 1 min) and a thin blood film was prepared on a glass slide. The blood smear was air dried and fixed for 10 seconds with methanol. The fixed blood smear was stained with giemsa, diluted 1 : 10 in deionised water, for 15 minutes. The stained blood smear was washed with water and parasites were examined under the light microscope using the 100 x objective with oil immersion. In order to determine the parasitemia the number of all erythrocytes and the infected erythrocytes were counted in 25 fields. Subsequently the parasitemia was calculated using the following formula:

Number of infected erythrocytes/ total number of erythrocytes x 100 = parasitemia (%)

#### Examination of exflagellating gametocytes

The hatching of male gametes from erythrocytes is called exflagellation, a process that can be observed under the light microscope. A high number of exflagellating parasites is important for a successful transmission to the mosquito and was hence examined routinely before parasite transmission. For this a drop of tail blood or a small volume (about 200 µl) of the *P. falciparum* cell culture was placed on a glass slide and carefully covered with a cover slip. The slide was incubated for 10 minutes at room temperature. Exflagellation was examined under the light microscope using the 40 x objective lenses with phase contrast (Ph2). For a successful transmission at least 3 to 5 exflagellation centres should be observed per field (*P. berghei*) or 1 exflagellation centre per field in the case of *P. falciparum*.

#### Cryopreservation of Plasmodium parasites

Plasmodium parasites were conserved during blood stage development, because infected blood can be stored for long periods in liquid nitrogen. For this purpose 100 µl freshly withdrawn blood was mixed with 200 µl parasite freezing solution (10% glycerine in Alsever's solution) in a cryo vial and immediately frozen in liquid nitrogen. Thawed parasite stocks can be reinjected into mice to continue the parasite growth.

#### Thawing of Plasmodium falciparum

Parasites vial (frozen culture) were taken from cold storage and thawed at 37 °C for 1-2 min. Culture was transferred to a 50ml centrifuge tubes with a sterile serological pipette. Blood volume = V was measured and 0.1x V of 12% NaCl slowly added,

drop wise while shaking the tube gently. Subsequently the tube rested 5 min before 10x V of 1.6% NaCl was added slowly, drop wise swirling the tube. Afterwards the tube was centrifuged at 1,500 rpm at room temperature for 5 min. To remove the supernatant a Pasteur pipette and the vacuum pump were used, carefully not to remove any red blood cells. 10X V of 0.2% dextrose/0.9% NaCl in a 10ml syringe was measured and added to the parasites slowly, drop wise mixing gently. The tube was again centrifuged at 1,500 rpm at room temperature for 5 min. To remove the supernatant a Pasteur pipette and the vacuum pump was used again, being careful not to remove any red blood cells. Finally the pellet was re-suspended with 3mL of complete RPMI medium with gentamycin, transferred to a 25cm<sup>2</sup> tissue culture flask and supplemented with two drops of 50% hematocrit washed blood. Incubation followed at 37 °C.

### **Plasmodium falciparum membrane feeding**

At day 16 after setting up a gametocyte culture, two cultures (16 and 14 days old) were mixed and centrifuged in a 50 ml falcon tube at 2000 rpm/ 37 °C. After that the resulting supernatant was removed and the pellet diluted 1:1 with freshly purified erythrocyte concentrate (O+, 37 °C). Finally this mixture of erythrocytes was diluted to a final haematocrit of 60% with pre-warmed (37 °C) heat inactivated human serum (O+), mixed by pipetting up and down and filled into a membrane glass feeder system by using a 1000-µl-ependorf pipette (prewarmed tip). *A. stephensi* mosquitoes were then allowed to feed through a parafilm membrane from the bottom of the feeder for 20 min. After the bloodmeal the mosquitoes were maintained in a humidity and temperature controlled incubator (80% humidity, 37 °C) and checked for oocysts at day 7. At day 8 after infection a second bloodmeal with freshly purified human uninfected blood (see asexual culture above) was performed to supply the mosquitoes with nutrients. An additional nutrient supply was provided every day through applied cotton pads that were soaked in glucose/PABA solution (10% glucose, 0,05% Para-aminobenzoic acid). At day 17 SGs were dissected from the infected mosquitoes and SG sporozoites were extracted.

### **Plasmodium berghei transfection**

The rodent *Plasmodium* parasite *P. berghei* was transfected with linearised DNA using the AMAXA transfection system (Lonza). By a crossing-over event between homolog regions the targeting constructs inserted into the targeted genomic loci.

**Overnight culture and merozoite purification** For one transfection typically 2 - 3 NMRI mice with a high level parasitemia (3 - 5% for *P. berghei* ANKA) were used. Mice were sacrificed and blood was collected by heart puncture (see below). The blood was combined in a 50 ml tube with 10 ml T-medium containing 250 µl Heparin (200 p.i. in PBS) and centrifuged for 8 minutes at 400 x g without brake. The medium was removed and the blood pellet was resuspended in 20 ml fresh T-

medium. The blood suspension was carefully dropped by gravity into a conical flask containing already 100 ml pre-warmed T-medium. The 50 ml tube was washed with 30 ml fresh T-medium and this was also dropped carefully into the flask without swirling the blood. The parasites were cultivated at 37 °C, 5% O<sub>2</sub>, 5% CO<sub>2</sub> and 90% N<sub>2</sub>, shaking at 70 rpm. To enrich schizonts in the blood culture the incubation took 16 to 18 hours for *P. berghei*. Mature schizonts were purified by a Nycodenz density gradient centrifugation. The Nycodenz stock solution was diluted to 55% or 60% working solutions in PBS for *P. berghei* purification. The over night parasite culture was transferred into four 50 ml tubes (approximately 35 ml per tube) and each tube was under-laid with 10 ml Nycodenz solution pre-warmed to room temperature. Tubes were exactly balanced and centrifuged for 25 minutes at 200 x g at room temperature without brake. The mature schizonts appeared as a brown ring at the interface and were carefully collected to two new 50 ml tubes. Tubes were filled up to approximately 40 ml with T-medium (from top of the gradient) and centrifuged for 8 minutes at 400 x g. The schizont pellet was resuspended in fresh T-medium, the volume depended on the size of the pellet and the number of constructs the parasites should be transfected with. For one transfection 1 ml resuspended schizonts were transferred in a 1.5 ml microcentrifuge tube and spun for 15 seconds.

**AMAXA transfection and selection for transformants** For each transfection, 100 µL of AMAXA human T cell nucleofactor solution (Lonza) was added to 5 - 10 µg of digested and precipitated plasmid DNA. The DNA solution was then added to the schizont pellet, mixed well, transferred to the AMAXA cuvette and pulsed once using the U-033 pre-programmed setting on the AMAXA machine. After pulsing 50 µl fresh T-medium was directly added into the cuvette and transfected parasites were immediately injected i.v. in nave NMRI mice. Typically 2 mice per construct were used. 24 hours post-infection a giemsa stained blood smear was prepared to record the starting parasitemia and pyrimethamine treatment of the mice was started. For this the pyrimethamine stock solution was diluted 1 : 100 in tap water (final concentration 70 µg/ml) and provided as drinking water. Parasitemia typically decreased to undetectable levels (blood smear) on day 2 post infection and first resistant parasites appeared in giemsa stained blood smears from day 7. When parasitemia reached at least 0.5 % mice were sacrificed and blood was withdrawn by heart puncture. Blood was transferred to new mice, cryopreserved and parasite gDNA was isolated (parental population). The transfer animals were further treated with pyrimethamine and mice were sacrificed as soon as parasitemia reached sufficient levels. The infected blood was again cryopreserved and purified for parasite DNA isolation (transfer population).

**Isolation of blood stage parasites for genomic DNA purification** To isolate parasites from infected blood a column was made using a 5 ml syringe. The syringe was closed with cotton wool at the bottom. Thereon a 2 - 3 cm thick layer of cellulose powder CF11 (Whatman) was put and the column was completed with around 1

cm glass beads (diameter 212 - 300  $\mu\text{m}$ , unwashed; Sigma). The column was equilibrated with 2 column volumes 1 x PBS and subsequently the infected blood was transferred on the column. The erythrocytes were washed off the column with 1 x PBS. Starting from the first red drop 15 ml erythrocyte suspension were collected in a respective tube. The suspension was centrifuged for 8 minutes at 400 x g, without brake, and the supernatant was carefully removed. The erythrocyte pellet was resuspended in 10 - 15 ml 0.2% saponin in PBS to lyse the red blood cells. The suspension was again centrifuged for 8 minutes at 1500 x g and the supernatant was discarded. The parasite pellet was resuspended in 1 ml PBS and transferred to a 1.5 ml microcentrifuge tube. The isolated parasites were once more centrifuged for 2 minutes at 4500 x g and finally resuspended in 200  $\mu\text{l}$  PBS. The parasite genomic DNA (gDNA) was subsequently isolated using the QIAamp Blood Mini Kit with the "Blood or Body Fluid Spin Protocol". For this 20  $\mu\text{l}$  Qiagen protease and 200  $\mu\text{l}$  buffer AL were added to 200  $\mu\text{l}$  parasites in PBS and thoroughly mixed by vortexing. All following steps were performed according to the manufacturer's instructions. The parasite gDNA was finally eluted in 100 - 150  $\mu\text{l}$  elution buffer AE (10 mM TRIS/HCl; 0.5 mM EDTA; pH 9.0) and stored at  $-20^\circ\text{C}$ .

**Genotyping PCR of transfected parasites** The isolated gDNA of parental and transfer transfectants was tested for integration of the targeting constructs by PCR. Templates for this genotyping PCR were typically 1 - 2  $\mu\text{l}$  parasite gDNA of the transfectants or wildtype (WT) parasites as control. As additional control the targeting constructs were diluted 1 : 100 in ddH<sub>2</sub>O and also used as template for the PCR. Usually three different oligonucleotide pairs were used for genotyping PCR. The integration test oligonucleotides (test) typically bind inside the selectable marker inserted and the parasite's genome. Resulting fragments therefore verify successful integration of the targeting construct inside the targeted genomic locus. Control oligonucleotide pairs are usually WT or open-reading frame (ORF) specific oligonucleotides and vector specific oligonucleotides (episomal). The PCR approach was prepared as described under above using the standard PCR program with an annealing temperature of usually  $54^\circ\text{C}$ . Resulting DNA fragments were analysed by agarose gel electrophoresis.

Genotyping of the obtained parasite populations for the *pbehd* (-) parasite was performed by specific PCRs using the following primer combinations:

PbANKA_040280_KO_5UTR_for_KpnI-HF/	PbANKA_040280_KO_3UTR_rev_XbaI
	for the <b>Wildtype</b> population
TgDHFRTS_for	PbANKA_040280_KO_5UTR_for_KpnI
	for the <b>Integration</b> population

### Parasite cloning

Successfully transfected parasite populations were selected for clonal parasites by limited dilution. For this a frozen blood stock of the parental or transfer population was injected i.p. into a naive NMRI mouse. Once the parasitemia ideally reached 0.3 - 0.5% the mouse was sacrificed and blood was withdrawn by heart puncture. Parasitemia was determined very exactly by counting at least 80 fields. Assuming on average  $7 \times 10^6$  erythrocytes per  $\mu\text{l}$  mouse blood the number of parasites was determined using the following formula:

$$7 \times 10^6 \times \text{parasitemia [\%]} \times 10^{-2} = \text{parasites}/\mu\text{l}$$

A dilution series was prepared in RPMI medium to inject theoretically one parasite per mouse. For this 100  $\mu\text{l}$  blood was diluted 1 : 10 in RPMI, this dilution was again diluted 1 : 10 in RPMI and so on. Typically the 1 :  $10^6$  dilution contained less than one parasite per  $\mu\text{l}$ . The calculated amount of this dilution that theoretically held one or in some cases three parasites was mixed with fresh RPMI medium and 10 naive NMRI mice were injected i.v. each with 100  $\mu\text{l}$  medium containing one parasite. Mice usually became blood stage positive from day 7 post infection on and as soon as sufficient levels of blood stage parasites were reached mice were sacrificed and blood was collected. Not all injected mice developed a blood stage parasitemia, typically mice were declared negative if there were no parasites visible in a giemsa-stained blood smear up to 21 days post infection. Clonal parasites were isolated from infected blood as described (above) and gDNA was tested for integration of the respective targeting construct by PCR (see above).

### Immuno-fluorescence analysis (IFA)

For the analysis of the expression and localization of the EHD-protein in *Plasmodium berghei* blood stages, sporozoites and liver stages the parasites were fixed and incubated with a primary  $\alpha$ -PfEHD antibody. For the investigation of the *P. berghei* liver-stage development a primary  $\alpha$ -PbHSP70 antibody was used, similar to the *P. falciparum* liver-stage development assay where a  $\alpha$ -PbHSP70 antibody was used. These primary antibodies were then detected by a secondary fluorescently labeled antibody. All antibodies used are listed in section 2.6.1 and 2.6.2.

In general, the parasites were fixed with 4% paraformaldehyde (PFA) at RT for 10-20 minutes and subsequently permeabilized with permeabilization solution for 20 minutes. Afterwards unspecific binding of the primary antibody was prevented by blocking unspecific binding sites via incubating the parasites with blocking solution for 20-60 minutes. Afterwards the primary antibody was incubated on the cells diluted in blocking solution and subsequently removed by washing the cells with washing solution 3 times for 5 minutes. Detection of the primary antibody via a fluorescent secondary antibody (diluted in blocking solution) followed for 30-60 minutes. Afterwards unbound secondary antibody was washed away by incubating the samples in PBS for 3 times for 5 minutes before the samples were mounted with a 50% glycerol/PBS solution and covered with a coverslip. If a nuclear staining was

desired a Hoechst-staining step incubating the cells with Hoechst diluted 1:1000 for one minute was added before the second last washing step of the protocol.

The analysis of the fixed fluorescent samples was performed using the microscopes listed in section 2.1.

### **Immuno-electron microscopy (iEM)**

For cryo-immunolabelling, overnight *P. berghei* schizonts were fixed in 0.1 M sodium cacodylate buffer, pH 7.2, containing 4% freshly prepared formaldehyde and embedded in gelatin. The samples were infiltrated overnight in 2.1 M sucrose and rapidly frozen by immersion in liquid nitrogen. Cryosections were obtained at  $-90^{\circ}\text{C}$  using an Ultracut cryo-ultramicrotome (Reichert). Cryosections were thawed in methylcellulose, blocked in PBS- 3% bovine serum albumin and then incubated in the presence of the antibody  $\alpha$ -PfEHD. The cryosections were then incubated with 15 nm, gold-labeled  $\alpha$ -mouse IgG (BBInternational), and observed in a Zeiss 900 transmission electron microscope. For a detailed protocol see Lemgruber et al., 2011<sup>275</sup>.

## **2.10.2 Anopheles mosquito methods**

### **Mosquito breeding**

*Anopheles stephensi* mosquitoes were bred at  $28^{\circ}\text{C}$ , 75% humidity under a 12-h light/12-h dark cycle. Larvae were raised in 1‰sea salt ddH<sub>2</sub>O, pupae were collected and allowed to hatch in mosquito cages (BioQuip Products Inc; USA). Adult mosquitoes were fed on a 10% sucrose/PABA solution provided on cotton wool pads. In order to maintain the mosquito life cycle, female *Anopheles* mosquitoes were blood fed on naive anaesthetized NMRI mice. Four days after the blood meal dishes with 1‰sea salt ddH<sub>2</sub>O soaked filter paper were put into the cages and female mosquitoes laid their eggs. Eggs were washed with 70% ethanol and twice with 1‰sea salt ddH<sub>2</sub>O and again put in trays filled with 1‰sea salt ddH<sub>2</sub>O. Hatched larvae were fed on cat food (Brekki) and split depending on the density.

### **Parasite transmission**

For transmission of *P. berghei* and *P. falciparum* parasites 4-7 day old female mosquitoes were blood fed on anaesthetized NMRI mice that had been infected i.p. with parasite blood stocks. Mice were assayed for high levels of parasitemia and the percentage of exflagellating male gametocytes was observed under the microscope. After the infective blood meal, mosquitoes were maintained at  $21^{\circ}\text{C}$ , 80% humidity. On day 10 post feeding, mosquitoes were dissected in RPMI 1640 medium/ 3% BSA, and isolated midguts were examined for the infection rate. From day 17 post infection mature sporozoites could be isolated from the salivary glands (below). In order to maintain a continuous *Plasmodium* cycle naive rodents could be exposed to bites of infected mosquitoes from day 17 post feeding, respectively.

### **Mosquito dissection**

Midguts of infected mosquitoes were dissected 10 days after the blood meal in order to observe oocyst formation, 12 -14 days post feeding midgut sporozoites were isolated from midgut oocysts. And 17 - 21 days post feeding salivary glands were isolated and infectious sporozoites were extracted (below). For all dissections infected mosquitoes were anaesthetised on ice. The dissection was performed in RPMI 1640 medium with 3% BSA under a stereo microscope in the insectary at 15 °C using two needles (27 G and 23 G). Midguts and salivary glands were kept in RPMI 1640 medium with 3% BSA on ice until sporozoite extraction.

### **Sporozoite extraction from salivary glands**

Mosquito midguts or salivary glands were disrupted mechanically in RPMI 1640 medium with or without 3% BSA using a pestle and spun for 3 minutes at 90 x g, 4 °C. The supernatant containing the sporozoites was transferred to a fresh tube and the pellet was again squeezed with a pestle in fresh RPMI. A second centrifugation was performed for 3 minutes at 100 x g, 4 °C and the supernatant was combined with the first collected. Extracted sporozoites were subsequently count under the microscope in a haemocytometer using the 40 x objective lenses with phase contrast (Ph2). For counting the sporozoite solution was typically diluted 1/10 in RPMI. The number of sporozoites was calculated with the following formula:

Number of sporozoites in 4 large squares / 4 x dilution factor x 10<sup>4</sup>

The quantity of a mosquito infection was typically expressed as number of sporozoites per mosquito.

### **2.10.3 Toxoplasma methods**

#### **Transient transfection of *T. gondii***

For a transient transfection of a plasmid into *Toxoplasma* parasites the plasmid was not linearized to allow the parasites to maintain it extra-chromosomally. Therefore, after some rounds of replication, the parasites lose the plasmid again since it lacked an origin of replication (parasite-specific) that would have allowed autonomous replication of the plasmid. Since the transient transfection does not require a selection procedure (described for the stable transfection below) it is a quicker procedure as the stable transfection and produces faster results. But in contrast to a stable transfection the transient one produces a very heterogenous transient population of parasites that can not be cloned out.

The DNA was transfected into the parasites via electroporation. Therefore freshly lysed tachyzoites were washed once with Cytomix and subsequently resuspended in 850 µl Cytomix. About 1x10<sup>7</sup> parasites were used for one single transfection with about 60 µg of DNA that was ethanol precipitated, resuspended in 50 µl Cytomix and supplemented with 25 µl ATP (100 mM) and 25 µl GSH (100 mM). This mix was then added to 700 µl of parasite suspension and the whole volume (800 µl) was



then transferred into electroporation cuvettes. The electroporation was subsequently done in an Electro Square Por 830 machine (BTX) with two pulses at 1,7 kV for 176  $\mu$ s. With the transfected parasites finally confluent HFF cells were inoculated.

### Stable transfection of *T. gondii*

For a stable transfection of a second copy of an endogenous gene into *Toxoplasma* parasites a linear plasmid (linearized in the backbone of the plasmid) was transfected and randomly integrated into the genome. To select parasites that successfully integrated the plasmid a selection marker (*dhfrts* or *hxgprt*) was cloned into the plasmid that carried the gene of interest. Via this selection marker the addition of selective drugs (pyrimethamine or mycophenolic acid, respectively) only leads to the death of parasites that do not possess the selection marker. In case of the mycophenolic acid (MPA) selection only the parasites carrying the HXGPRT-gene are able to use Xanthin (additionally added to the medium) instead of Hypoxanthin, that is blocked by MPA. The transfection procedure in general was carried out as described above for the transient transfection. But in contrast to this procedure for the stable transfection only 10 - 30  $\mu$ g of DNA was transfected that was also mixed with 10 U of the linearization enzyme previously to the transfection, a technique named REMI (*Restriction Enzyme Mediated Insertion*)<sup>276</sup>. After the transfection the parasites were inoculated on HFF cells and maintained under drug pressure starting 12-24 hours after inoculation. The selective drugs were used in the following concentrations:

**Mycophenolic acid:** 25  $\mu$ g/ml  
**Pyrimethamine:** 1  $\mu$ M  
**Xanthin:** 40  $\mu$ g/ml

After about 1 week, depending on the type of selective drug, all parasites not carrying the plasmid died and left a pool of transgenic parasites.

### Isolation of stable clones via limiting dilution

To isolate parasite clones from the stable transfections mentioned above a limiting dilution was performed in 96-well cell culture mikrotiter plates. After 5-7 days plaques of lysed cells are visible in the wells that represent a parasite clone, each. Only the wells that contained one plaque only from the beginning of the plaque formation are wells that contain only one clone. These clones were then isolated and expanded to 24-well cell culture plates and further characterized.

### Induction of expression of DD-tagged proteins

To induce overexpression of DDmCherry *TgRME-1* protein variants in *Toxoplasma gondii* a destabilization domain (ddFKBP) was cloned in front of the mCherry-tag under a strong promoter. In the absence of the ligand Shield-1 (Shld-1) the fusion

protein is not stable within the parasites and is degraded<sup>288</sup>. Thereby parasites carrying the modified or overexpressed protein of interest that might be toxic to the parasites can be maintained in culture. When Shld-1 is added to the culture medium it binds to the fusion protein and stabilizes the protein expression. Thereby protein localization and influence of the overexpression of the respective protein can be studied. Shld-1 was used in a concentration of 1  $\mu$ M to overexpress the TgRME-1 fusion proteins in this thesis.

### Plaque-assay

The intracellular replication of *T. gondii* leads to a lysis of the infected cell. The emerged parasites then infect surrounding cells and the ongoing replication finally leads to the generation of cell-free areas within a confluent cell layer, so-called *Plaques*. In a Plaque-assay<sup>277</sup> the ability of different parasite lines to grow, replicate and finally lyse the host cells can be investigated. By comparing the numbers and sizes of Plaques of WT parasites and parasites expressing the (modified) gene of interest an influence of the protein of interest on the replication of the parasites can be visualized. In this thesis 6-well titer plates with a confluent HFF cell layer were inoculated with 50 cells per well. The parasites were maintained under Shld-1 protein expression or without (control) to investigate the influence of the overexpression of DDmCherry TgRME-1 and the deletion mutants of the protein on parasite replication. After 6-8 days the cell layers were fixed with Methanol for 10 minutes and subsequently stained with Giemsa-solution (see section 2.10.1).

### Fluorescence-analysis of intracellular parasites

For the investigation of the fluorescent proteins investigated in this thesis in *Toxoplasma* intracellular parasites were induced with Shld-1 for 4-8 hours to express the DDmCherry-fusion proteins. If no co-labelling with an antibody-staining was performed the parasites were immediately fixed with 4% PFA for 10 minutes, shortly washed afterwards and finally mounted as described in section 2.10.1 for the *Plasmodium* IFAs. If an immuno-labelling was performed in addition to the expression of a fluorescent protein an IFA was done as described in section 2.10.1 for *Plasmodium* IFAs.

### Live-imaging

For live-imaging of *Toxoplasma* parasites HFF cells were grown in  $\mu$ -Dish<sup>35mm,high</sup> ESS coated live-cell dishes (ibidi, Martinsried). These dishes had a really thin bottom allowing an inverse objective of a fluorescent microscope to image through the bottom. The HFF coated dishes were one day prior to imaging infected with the DDmCherry TgRME-1 expressing parasites. About 4 hours before the live-imaging protein expression was induced via addition of Shld-1 to the medium. To image processes the mCherry-tagged TgRME-1 is involved in the dish carrying the infected

cells was transferred into a live-cell chamber at a DeltaVision RT epifluorescence microscope imaging system (Applied Precision; Washington, USA) at the imaging facility of the Institute of Infection, Immunity and Inflammation of the University of Glasgow (Glasgow, UK). This live-cell chamber was heated to 37 °C and in addition connected to a CO<sub>2</sub> supply. In a long-term imaging experiment pictures of the YFP-signal (IMC-YFP construct) and the mCherry-signal (DDmCherry TgRME-1) of a parasite cell of interest were taken every 10 or every 30 minutes for several hours or over night. An autofocus mode provided by the microscope software (SoftWx) was used to keep the moving cells in focus over time. An autotracking mode was switched off since it did not prove to be useful. Images were taken with a CoolSnap HQ camera and later put together to a movie with ImageJ. The same procedure was done for a short-term imaging study taking pictures of the DDmCherryTgRME-1 expressing parasites every 3-5 seconds to visualize rapid vesicular movement within the parasites.

## 2.11 Animal experimental methods

Mice were purchased from Charles River Laboratories, Germany or Janvier, France with a age of 18 - 20 days and animal care was done in a central facility of the University of Heidelberg (Interfakultäre Biomedizinische Forschungseinrichtung; IBF). All animal experiments were conducted according to the European regulations and approved by the state authorities (Regierungspraesidium Karlsruhe).

### 2.11.1 Administration of anaesthesia

Mice were anaesthetised with Ketamine (100 mg/ml)/Xylazine (3 mg/ml) (K/X) administered into the abdominal cavity (intraperitoneal; i.p.).

### 2.11.2 Infection of rodents with *Plasmodium* parasites

In order to transmit *Plasmodium* parasites to the rodent host the mice were either anaesthetized and exposed to bites of infected mosquitoes or isolated salivary gland sporozoites were injected in various numbers (1,000 - 10,000 spz) into the tail veins (*i.v.*). Furthermore blood stages injected either *i.v.* or *i.p.* established a *Plasmodium* infection, isolated schizonts, freshly isolated infected blood or frozen blood stocks were used.

### 2.11.3 Blood withdrawal by heart puncture

Mice were terminally anaesthetized with diethyl ether and the heart was uncovered preferably fast. Blood was withdrawn using a heparinized needle (23 G) and a 2 ml or 5 ml syringe from the right ventricle. Infected blood was immediately put on ice and processed as fast as possible. Typically 0.7 - 1.5 ml blood could be obtained from one mouse.

## 2.12 Biochemical methods

### 2.12.1 Preparation of parasite lysate for SDS-PAGE

For the preparation of parasite material for the detection of the DDmCherry *TgRME-1* protein on a western blot (time-dependent expression in response to Shield1) a confluent layer of HFF cells in a number of 6-cm cell culture dishes was inoculated with the recombinant parasites. These parasites were allowed to replicate until a great number of parasite vacuoles within the cell layer was visible but without allowing the generation of plaques in this layer. When a great number of intracellular parasites had formed Shield1 in a concentration of 1 M was added to the cell culture medium in the dishes. Thereby the expression of DDmCherry *TgRME-1* was induced in these parasites and the parasites could be harvested after the desired time of induction. The HFF cells including the intracellular parasites of each dish were then scratched off from the bottom of the dish and pressed through a syringe supplied with a 26G needle (BRAUN). Thereby the parasites were released from the host cell, could be washed with icecold PBS and then taken up in 1 ml PBS in an 1,5-ml-Eppendorf tube. Washed parasites were then counted in a Haemocytometer and subsequently pelleted in a centrifuge at 1000x g for 10 minutes at 4 °C. Afterwards the pellet was either frozen down at -80 °C or resuspended in RIPA buffer and incubated on ice for 5 minutes. The volume of the RIPA buffer was variable and adjusted to reach a final concentration of  $1,25 \times 10^5$  parasites per  $\mu\text{l}$ . After the incubation on ice the lysate was pelleted at full speed for 60 minutes at 4 °C and the supernatant was transferred to a new reaction tube and frozen down or directly mixed with SDS-PAGE loading buffer and loaded onto a protein gel (see below). Per lane  $6 \times 10^6$  of the DDmCherry *TgRME-1* parasites were loaded onto the gel.

### 2.12.2 SDS polyacrylamide gel electrophoresis (SDS-PAGE)

Proteins were separated according to their size by SDS polyacrylamide gel electrophoresis. Components of the gels are described in section 2.7.4 and were mixed in the indicated order there.

The addition of ammonium persulphate (APS) and TEMED starts the polymerisation. The anionic detergent SDS denatures the protein and applies a negative charge therefore by SDS-PAGE proteins run towards the anode. First the separating gel was poured between the two glass plates fixed in the gel caster (Amersham). The gel was overlaid with a thin layer of isopropanol and allowed to polymerise. The isopropanol was removed, the loading gel was poured on top of the separating gel and a comb was placed in order to create the wells. As soon as the loading gel is polymerized as well the comb can be removed and the gel is ready for electrophoresis. Protein samples were mixed 1 : 4 with 4 x SDS loading buffer and heated to 95 °C for 5 minutes prior to loading on the gel. Alongside 15 - 30  $\mu\text{l}$  of the samples 10  $\mu\text{l}$  PageRuler Prestained Protein Ladder (Fermentas) was loaded on the gel. The gel was fixed in the electrophoresis chamber (Amersham) and surrounded with running

buffer. Electrophoresis was performed for 1 hour at 80 V, 25 mA and subsequently for further 1 - 2 hours at 100 V. The proteins were then transferred to a nitrocellulose membrane via western blot and detected with specific antibodies.

### 2.12.3 Western blot analysis

For specific detection of *PbEHD* and *DDmCherryTgRME-1* with specific antibodies the separated proteins were transferred from the SDS gel to a nitrocellulose membrane. For this 4 x Whatman paper and 1 x nitrocellulose membrane were cut in gel size and wet together with 4 blotting sponges in 1 x transfer buffer. The Western blot sandwich was built starting with 2 blotting sponges on the cathode side of the blotting cassette (Amersham), followed by 2 x Whatman paper, the SDS gel, the nitrocellulose membrane, 2 x Whatman paper and finally 2 more blotting sponges. The cassette was closed with the anode plate and protein transfer occurred for 1 - 1.5 hours at 125 mA, approximately 20 V in 1 x transfer buffer. The membrane was subsequently blocked over night at 4 °C with 5% milk in TBST and washed three times for 10 minutes with 1 x TBST at room temperature. The incubation with the primary antibodies was carried out for 1 hour at room temperature or again over night at 4 °C under continuous shaking. The membrane was again washed three times for 10 minutes with TBST and the secondary HRP conjugated goat antibody (1 : 10,000 in TBST; Sigma) was added for 1 hour at room temperature, shaking. Washing was repeated as before. The chemiluminescent detection of the labeled protein was performed with the "ECL Western Blotting Detection Reagents" (GE Healthcare). For this the substrate solutions 1 and 2 were mixed 1 : 1 and incubated on the membrane for 1 minute. The membrane was subsequently transferred in a film cassette, a film (Kodak) was incubated in the dark for 5 seconds up to 25 minutes on the membrane and the light signal on the film was developed (Hyperprocessor Amersham Pharmacia Biotech, Freiburg).

## 2.13 In silico analysis of apicomplexan EHD-proteins

The *in silico* analysis of apicomplexan EHD-proteins was based on the published nucleotide and protein sequences of *Toxoplasma*, *Plasmodium* and vertebrate EHD-proteins using the online databases Genebank, Uniprot, ToxoDB and PlasmoDB and the prediction algorithms used in these databases. For alignments and further analysis of the sequences the program CLC genomics workbench (CLC bio EMEA, Denmark) was used.

# Chapter 3

## Results

### 3.1 Establishment of a combined *in vitro*/*in vivo* *P. falciparum* life-cycle

The investigation of *Plasmodium falciparum* exo-erythrocytic stages is a bottle neck in malaria research. To obtain these stages infectious sporozoites first have to develop in *Anopheles* mosquitoes that previously have been infected with sexual stages of the parasite. This includes the generation of a high number of *P. falciparum* gametocytes in an *in vitro* culture system and subsequently transferring these into the *in vivo* situation in *Anopheles* mosquitoes. Even though there are standard protocols<sup>278</sup> existing for that process only a few labs in the world are able to perform it and to successfully establish this process in our lab several factors had to be taken into account: 1) We had to generate a constantly high gametocytemia in the sexual *P. falciparum* cultures by optimizing the culture conditions to generate high infections of the mosquitoes. 2) A perfect timing of the gametocyte cultures and the mosquito breeding had to be established to match mature gametocyte cultures with the right age of the *Anopheles* mosquitoes. 3) The best breeding conditions and age for the susceptibility of the *Anopheles* mosquitoes for a *P. falciparum* infection had to be evaluated. 4) A membrane feeding protocol had to be established that is allowing the transfer of viable mature gametocytes from the cell culture into the midgut of the mosquitoes.

The aim of the whole project was to generate a constant combined *P. falciparum* *in vitro*/*in vivo* life-cycle (Fig. 3.1) that enables researchers in the lab to work on different stages of *P. falciparum*, especially liver-stages. In one of the projects the sporozoites obtained from the infected mosquitoes were administered to primary human hepatocytes to identify and characterize liver stage antigens of *P. falciparum*, a project I was not involved in (R. Frank. et al.)

#### 3.1.1 *Plasmodium falciparum* asexual and sexual bloodstage *in vitro* culture

To establish an *in vitro* *P. falciparum* life-cycle in our lab parasites of the NF54-strain were cultivated *in vitro* under gametocyte-inducing conditions such as high parasitemia to induce gametocytogenesis and a protocol was established to enrich mature gametocytes within the *in vitro* culture (see section 2.10.1). The highest gametocyte yields could be obtained when gametocyte-cultures were inoculated from an asexual culture of parasitemias between 4-5% (small culture flask, 25 cm<sup>2</sup>) and split down to a starting parasitemia of 1% in big culture flasks (75 cm<sup>2</sup>). Mature gametocytes were checked for maturity at day 15-17 via exflagellation assay and

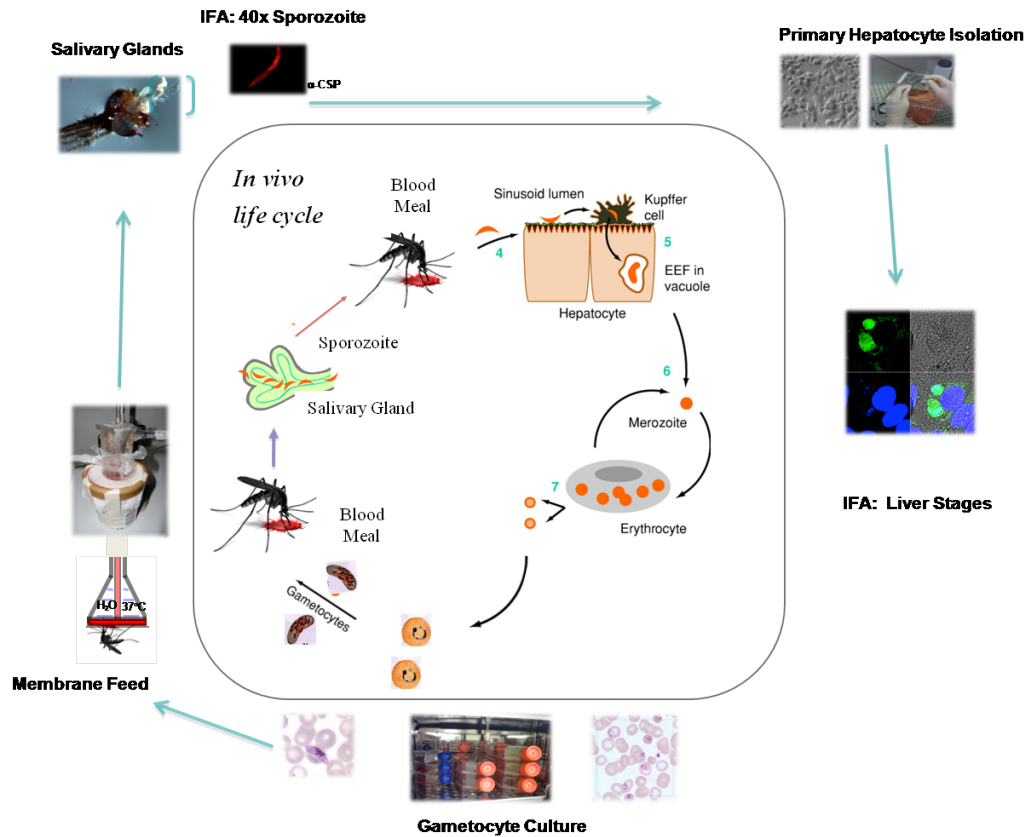


Figure 3.1: **Combined *in vitro/in vivo Plasmodium falciparum* life-cycle.** To investigate *Plasmodium falciparum* liver-stage antigens a combined *in vitro/in vivo* lifecycle was established. **Inner circle:** *In vivo* life-cycle. **Outer circle:** Combined life-cycle established in the lab. The generation of liver-stages started with cultivation of gametocytes in *in vitro* blood cell cultures followed by membrane feeding of *Anopheles stephensi* mosquitoes. *P. falciparum* sporozoites were later extracted from *A. stephensi* salivary glands and added to cultivated primary human hepatocytes, extracted beforehand from liver resections. Liver-stage development was finally confirmed by immuno-fluorescence analysis (IFA) detecting liver-stage specific antigens.

subsequently transferred to *A. stephensi* mosquitoes via membrane-feed.

### 3.1.2 Membrane feeding of mature gametocytes to *Anopheles stephensi* mosquitoes

To transfer mature gametocytes from the *in vitro* cell culture to *A. stephensi* mosquitoes a standard membrane feeding protocol<sup>279</sup> was optimized for our lab conditions (see section ). Throughout the course of the experiments described in Frank, R. et al. (*in preparation*) a stable transmission rate could be maintained that ceased again afterwards for reasons discussed in chapter 5. To evaluate the success of the *P. falciparum*-transmissions midguts and later salivary glands of a proportion of the infected mosquitoes were analyzed for the presence of oocysts and salivary gland sporozoites, respectively (Fig. 3.2). A high prevalence of infected midguts with a high number of oocyst per midgut could be achieved that led to a sufficient number of salivary glands sporozoites for subsequent experiments (Tab. 3.1).



Figure 3.2: Membrane transfer of *Plasmodium falciparum in vitro* cultures to *A. stephensi* mosquitoes and analysis of parasite development within the anophelene host. **A) Membrane-feeding.** Mature gametocytes were supplemented with fresh human blood and injected into a glass-feeder sealed by a parafilm membrane on the bottom. Mosquitoes were kept in paperboard cups and allowed to feed on the blood distributed over the membrane for up to 20 minutes. **B) Evaluation of the infection of mosquito midguts.** *P. falciparum* infected *A. stephensi* midguts were extracted from the mosquito carcass and stained with mercurochrome red. Black arrows show some of the parasite oocysts present in the midgut. **C) *P. falciparum* salivary gland sporozoites.** Salivary gland sporozoites were extracted from the mosquitoes and stained in an immuno-fluorescence assay (IFA) with rabbit  $\alpha$ -PfCSP/alexa594  $\alpha$ -rabbit antibodies. (Bar: 5  $\mu$ m)

Table 3.1: Prevalence and infectivity of *P. falciparum*-infected *A. stephensi* mosquitoes.

	Oocysts	Sporozoites (No.)
<b>Total amount</b>	78,5% prevalence	2.700.00
<b>Average number/individual</b>	27	28.000
<b>Total no. of individuals</b>	14	93



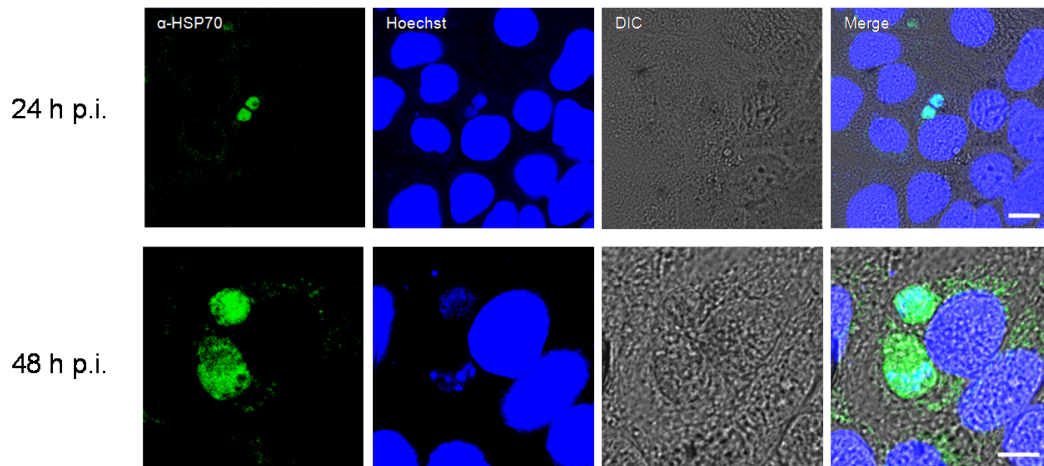


Figure 3.3: **Liver-stage development of *P. falciparum* parasites *in vitro* in hepatoma cells.** *P. falciparum* sporozoites were allowed to invade Huh7 hepatoma cells for 30-120 minutes and to develop for 24h (upper panel) or 48 h (lower panel), respectively. After liver-stage development parasites were fixed with Methanol and subsequently stained with mouse  $\alpha$ -PfHSP70/alexa488  $\alpha$ -mouse antibodies. As shown in both panels parasites were able to generate exo-erythrocytic forms in humane hepatoma cells and have started to undergo schizogony as shown by nuclear staining (Hoechst) in the lower panel. (Bar: 8  $\mu$ m)

### 3.1.3 Liver-stage development of *Plasmodium falciparum* in vitro

To obtain *P. falciparum* liver-stage parasites for further experiments described elsewhere (Roland Frank, PhD thesis; Frank, R. et al. *in preparation*) sporozoites were extracted from *A. stephensi* salivary glands and added to cultivated primary human hepatocytes (Frank, et al., *in preparation*). An isolation and cultivation of primary human hepatocytes was necessary since infection of immortalized liver cells such as HuH7 cells did not work effectively. After invasion of hepatocytes for 30-120 minutes for evaluation of liver-stage development liver-stage parasites were allowed to grow for 24-48 hours in primary cell culture and hepatoma cell lines (Huh7 cells) and were subsequently fixed and stained for immuno-fluorescence analysis (IFA; Fig. 3.3). The evaluation of the IFAs showed that *P. falciparum* sporozoites were able to invade both primary human hepatocytes and hepatoma cell lines and to develop into liver-stage trophozoites (Fig. 3.3, upper panel) and early schizonts (Fig. 3.3, lower panel).

## 3.2 Characterization of EHD-proteins in apicomplexan parasites

### 3.2.1 RME-1 encodes for a conserved EHD-family member in apicomplexan parasites

In an attempt to identify new Dynamin-related proteins in apicomplexan parasites we performed an *in silico* analysis of the *Toxoplasma gondii* genome searching for genes harboring a predicted G-domain-coding sequence in apicomplexan parasites. We identified a so far unknown member of the Eps15 homology (EH) domain-containing protein family in these organisms. Whereas mammalian cells and other higher eukaryotes possess several different EHD-proteins, *C. elegans* possesses only one member, i.e. *CeRME-1* (Receptor-mediated endocytosis protein 1)<sup>280</sup>. A phylogenetic analysis (kindly provided by Dr. Markus Meissner, Glasgow, UK) shown in Fig. 3.4 demonstrates that also apicomplexan parasites possess only one EHD-protein member, clustering tightly within this clade, that shows the characteristic primary structure of EHD-proteins (Fig. 3.5).

The apicomplexa protein is harboring a predicted p-loop containing nucleoside triphosphate hydrolase motif<sup>281</sup>, known to bind and hydrolase ATP in EHD-proteins instead of GTP in other G-domain proteins<sup>282 283</sup>, and a predicted EH-domain. It was named in *Toxoplasma* and *Plasmodium* *TgRME-1* and *PxEHD*, respectively.

### 3.2.2 *TgRME-1* localizes to not yet known subcellular structures within *Toxoplasma gondii*

According to the ToxoDB database, *TgRME1* transcripts as well as protein peptides are readily detected in tachyzoites and oocysts of the *Toxoplasma gondii* RH strain<sup>284 285</sup>. Additionally, transcriptomic analysis of the *Toxoplasma* tachyzoite intracellular replication cycle shows that the relative RNA-expression of the gene peaks with the mitosis phase of the parasite and decreases again upon G-phase entry<sup>286</sup>. In order to analyze the subcellular localization of the RME-1 protein, I generated a parasite line that expressed *TgRME-1* that was N-terminally fused to a fluorescent mCherry-tag. Therefore the full-length coding sequence of the gene was cloned downstream of the sequence of a destabilization-domain (ddFKBP) and a mCherry-tag (Fig. 3.6), controlled by a strong promoter (p5RT70), and the vector was subsequently transfected and randomly integrated into the genome of *Toxoplasma gondii* RH $\Delta$ HX parasites as a second copy of the gene. A selection marker within the plasmid carrying the just described genetic sequences allowed to select for parasites that successfully took up the linearized plasmid (restriction digest in the backbone) after transfection of the parasites. To remove any non-integrated episomal plasmids the selective drug was removed after resistant parasites were growing in a normal replication rate in cell culture. Since expression levels of genes in the integrated plasmids can vary depending on their genomic environment because of

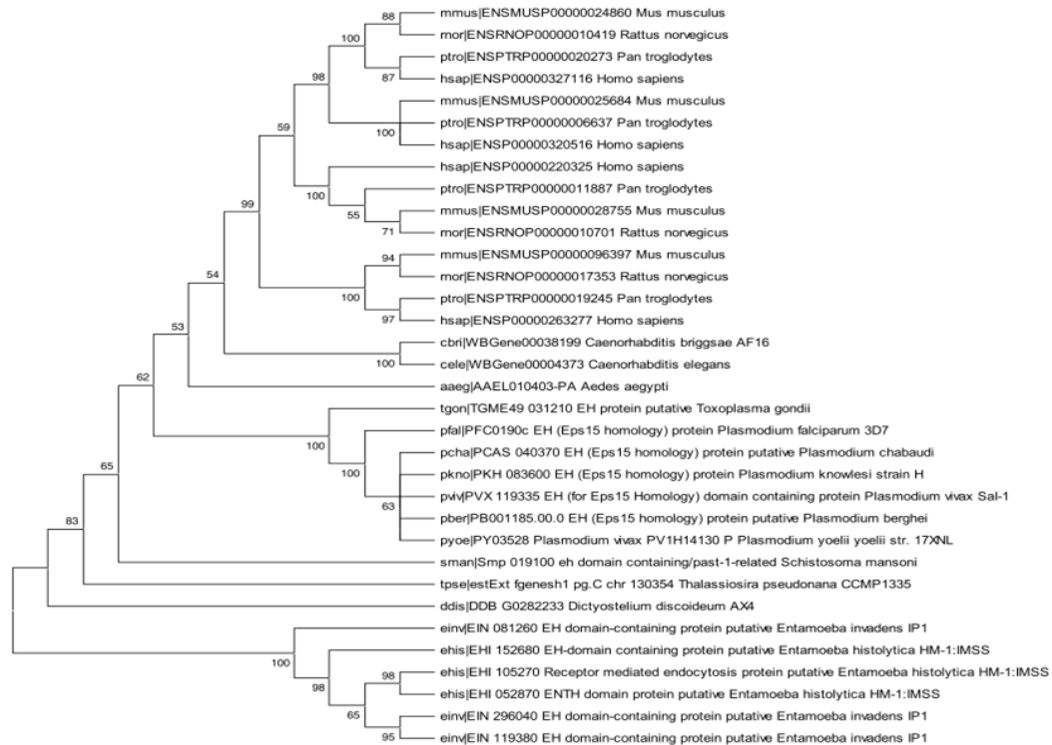


Figure 3.4: **Phylogenetic tree of EHD-proteins.** The evolutionary history was inferred using the Neighbor-Joining method (Saitou N. and Nei M. (1987). The neighbor-joining method: A new method for reconstructing phylogenetic trees. Molecular Biology and Evolution 4:406-425.). Both, ATPase- and EH-domain, were included into the analysis. The bootstrap consensus tree inferred from 500 replicates (Felsenstein J. (1985). Confidence limits on phylogenies: An approach using the bootstrap. Evolution 39:783-791.) is taken to represent the evolutionary history of the taxa analyzed. Branches corresponding to partitions reproduced in less than 50% bootstrap replicates are collapsed. The percentage of replicate trees in which the associated taxa clustered together in the bootstrap test (500 replicates) are shown next to the branches (Felsenstein J. (1985). Confidence limits on phylogenies: An approach using the bootstrap. Evolution 39:783-791.). The evolutionary distances were computed using the JTT matrix-based method (Jones D.T., Taylor W.R., and Thornton J.M. (1992). The rapid generation of mutation data matrices from protein sequences. Computer Applications in the Biosciences 8: 275-282.) and are in the units of the number of amino acid substitutions per site. The rate variation among sites was modeled with a gamma distribution (shape parameter 0.7693). The analysis involved 34 amino acid sequences. All positions containing gaps and missing data were eliminated. There were a total of 242 positions in the final dataset. Evolutionary analyses were conducted in MEGA5 (Tamura K., Dudley J., Nei M., and Kumar S. (2007). MEGA4: Molecular Evolutionary Genetics Analysis (MEGA) software version 4.0. Molecular Biology and Evolution 24:1596-1599.).



Figure 3.5: **General EHD-protein domain structure in apicomplexans.** The single predicted domains are represented by colored boxes. The aminoacid motifs of the G-domain that represent the P-loop nucleotide binding site (G...T) and the KPF, NKAD and PF protein-protein-interaction motifs that are all conserved between the apicomplexan EHDs and human EHD2 are shown in letters below the boxes (figure adapted from Daumke et al., 2007 [1]). aa: Amino-acids

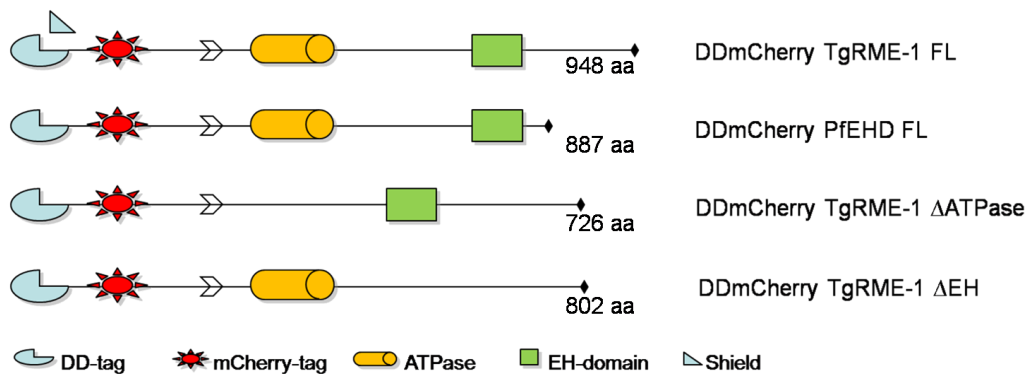


Figure 3.6: **Tagging approach for subcellular localization analysis.** *TgRME-1* and *PfEHD* were N-terminally tagged with a mCherry-tag and a destabilization-domain (DD) and expression of the gene was driven by a strong promotor (p5RT70). After addition of the Shield-1 ligand to the culture medium expression was induced via stabilization of the protein. To create dominant-negative effects two deletion mutants lacking either the ATPase-domain ( $\Delta$ ATPase) or the EH-domain ( $\Delta$ EH) were cloned and expressed within the parasites. FL, full length; aa, amino-acids

the random integration single parasite clones were selected for further analysis by limiting dilution. By adding the synthetic ligand Shield-1 to the cell culture medium a fluorescence could be observed in the parasite. The protein expression was analyzed by both Western blot and fluorescence assay. Through binding of the soluble ligand Shield-1 to the ddfKBP-domain the protein was stabilized within the parasite<sup>287 288</sup> and could be detected as early as 2h hours after induction by Western blot (Fig. 3.7). In a time-course fluorescence assay parasites were fixed with 4%

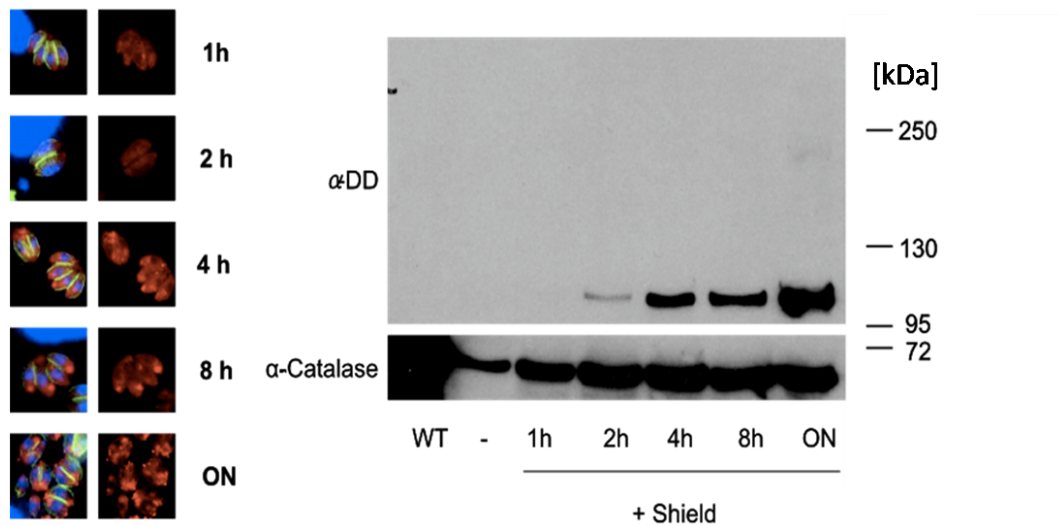


Figure 3.7: **Confirmation of the expression of DDmCherry *TgRME-1*.** Left: Fluorescence-microscopic analysis of PFA-fixed parasites in a time-dependent manner after addition of 1 $\mu$ M Shield-1. Right: Western-Blot analysis of the expression of DDmCherry *TgRME-1* protein in a time-dependent manner after addition of 1 $\mu$ M Shield-1. kDa: protein size; kilodalton

paraformaldehyde (PFA) and the mCherry signal was fluorescence-microscopically analyzed subsequently in response to the duration of Shield-1 exposure. Only a very weak background cytosolic mCherry signal could be seen for the first two hours after induction of protein expression. When the amount of protein increased over time a distinct spot labeled by the mCherry signal within the parasite became apparent (Fig. 3.7). In indirect immuno-fluorescence assay (IFA) colocalization studies, where the parasite's inner membrane complex (IMC) was labeled with an  $\alpha$ -IMC antibody detected by a green-fluorescent secondary antibody, we could show that the tagged *TgRME-1* localizes to an organelle-like compartment. This compartment within the parasite does not always correspond to the same coordinates within the cell (Fig. 3.8). The protein can be found in a single compartment at the apical end (arrow heads) as well as in a single compartment at the basal end of the parasite (arrows). In other occasions it localizes to the newly forming daughter-cells or can also be found in several smaller vesicle-like structures distributed over the whole parasite (Fig. 3.8). The localization of the over-expressed *TgRME-1* does also not seem to be synchronized between the single cells within the same vacuole. These

observations already led to the hypothesis that *TgRME-1* localization within the parasite may be dynamic. To investigate this, we applied two different live-imaging approaches, long- and short-term, to study localization of the tagged *TgRME-1* protein during parasite replication within the host cell. Via short-term imaging, taking a picture of the parasites every 4 seconds, we observed small mCherry-labeled vesicular structures within the parasites that are rapidly moving in a multi-directional manner, mainly circulating between the two poles of the parasite (suppl. video 2). These vesicles had not been observed previously in fixed samples. This movement of the *TgRME-1* protein-labeled vesicles dramatically increases upon formation of the daughter-cells within the mother cell. During long-term imaging studies, by taking a picture of the parasites every 10 minutes, mainly in parasites undergoing cellular division we observed dramatic structural re-organization of the *TgRME-1*-labeled compartment (Fig. 3.9). During an early time point of the formation of daughter-cells the *TgRME-1* compartment fragments and smaller vesicles are transported to the apical tip of the newly forming IMC (arrow heads, Fig. 3.9). At a late stage of the endodyogeny the main *TgRME-1* compartment within 30-40 minutes moves from the apical to the basal pole of the parasite, upon a so far unknown trigger (arrows, Fig. 3.9). When cytokinesis is completed *TgRME-1*-labeled compartments can be found again at the apical pole of the two newly formed daughter-cells as well as at their connection point at the residual body.

In order to confirm correlation of the long-term movement of the *TgRME-1* compartment with the formation of daughter-cells in live-imaging studies we co-transfected the DDmCherry *TgRME-1*-expressing parasites with a construct that leads to the expression of an IMC-YFP fusion protein. Through that we were able to image the formation of the IMC in daughter-cells and the movement of the *TgRME-1* compartment at the same time in living cells. In this approach again we were able to show a reorganization of the *TgRME-1* compartment upon formation of the IMC of the daughter-cells. A smaller mCherry-labeled structure is embodied by the IMC of the daughter-cells and the bigger compartment of the mother cell squeezes alongside the daughter IMC to the basal pole of the mother cell (Fig. 3.10). My attempts to colocalize the *TgRME-1* protein with any organelle of the endosomal system, the secretory system or any other organelle known in *Toxoplasma* failed so far (exemplary organelles shown in Fig. 3.11). Together my findings propose a localization of *TgRME-1* to a so far unknown organelle-like structure in *Toxoplasma gondii* that is undergoing dramatic reconstruction during formation of daughter-cells.

### 3.2.3 Functional analysis of RME-1 in *Toxoplasma gondii*

To study the biological function of *TgRME-1* in *Toxoplasma* parasites I created two different over-expression constructs where either the sequence coding for the predicted ATPase-domain or the predicted EH-domain was deleted. The truncated protein was fused to a N-terminal DD/mCherry-tag in order to create an inducible dominant-negative effect (Fig. 3.6). After transfection, random integration into

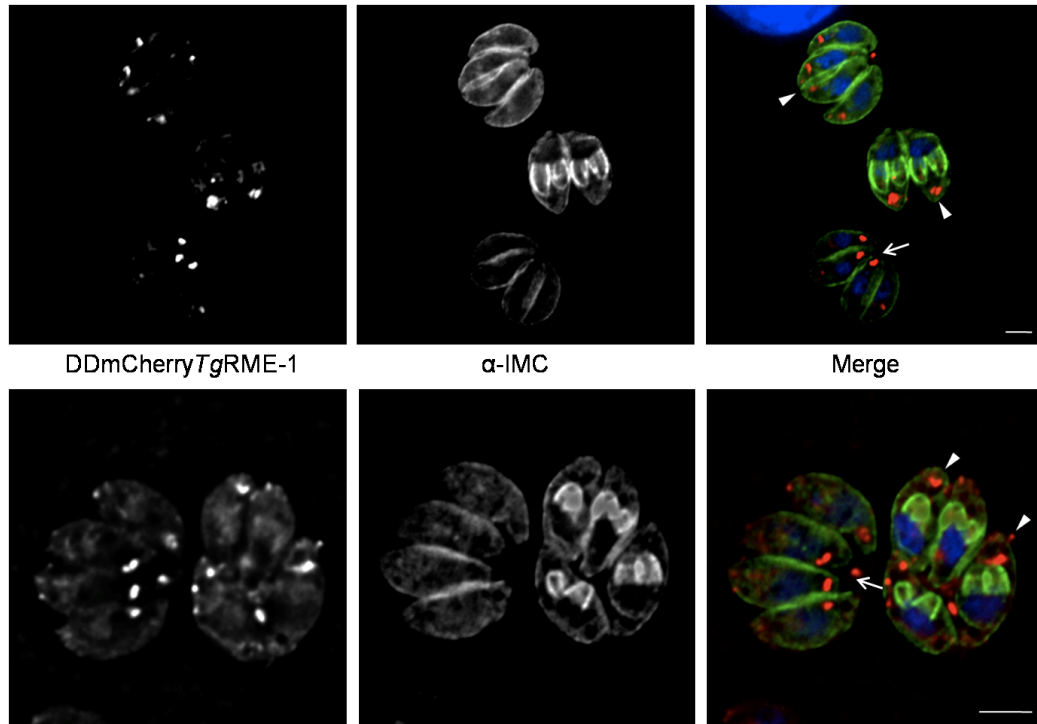


Figure 3.8: **Localization of DDmCherryTgRME-1 in *Toxoplasma*.** mCherry-tagged *TgRME-1* expression was induced via addition of Shield-1 for 4 hours. After fixation of the cells an indirect immuno-fluorescence assay was performed labeling the inner membrane complex (IMC) of the parasites with an  $\alpha$ -IMC antibody. Localization of the tagged *TgRME-1* was directly imaged via the mCherry signal. Localization of the mCherry-signal appeared in a dynamic vesicular labeling of the apical part of the parasites (arrow heads) as well as the basal part (arrows). (Bar: 4  $\mu$ m.)

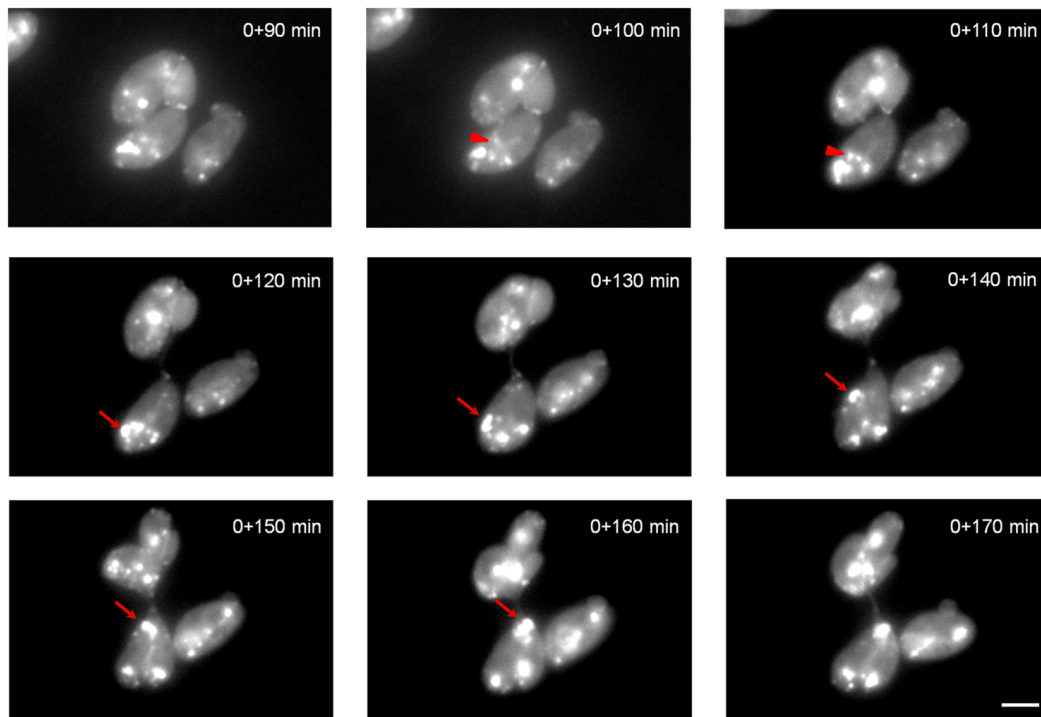


Figure 3.9: **Time-lapse analysis of DDmCherry *TgRME-1*.** 4h before imaging DDmCherry *TgRME-1* expression was induced via addition of Shield-1 to the culture. Intracellular parasites were then imaged in a live-cell chamber taking a picture of the mCherry-signal every 10 min starting at timepoint 0 (4h after induction of expression). Upon formation of daughter-cells (0+90min) the mCherry-labeled apical compartment fragments and smaller vesicles move to the apical end of the daughter-cells (arrow heads). About 40 min after initiation of daughter-cell formation (0+120min) the main apical *TgRME-1* compartment starts to move to the basal end of the parasite (arrows). (Bar: 4  $\mu\text{m}$ .)



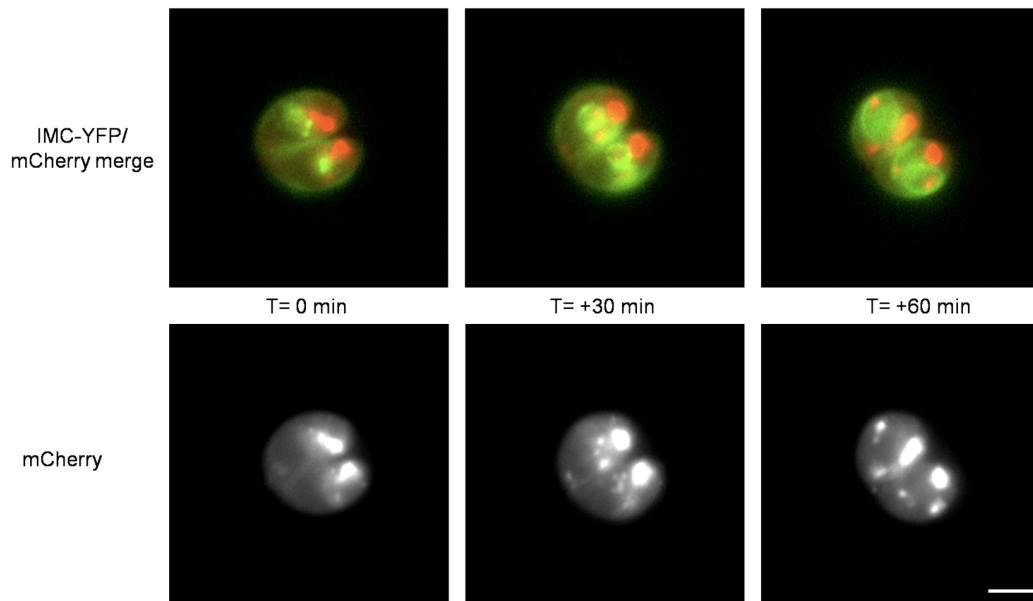


Figure 3.10: **Time-lapse analysis to investigate *TgRME-1*-IMC colocalization.** DDmCherry *TgRME-1* parasites were transiently co-transfected with a plasmid that allows constitutive expression of an IMC-YFP fusion protein within the parasites. This expression was used to visualize the formation of daughter-cells by live-cell imaging via visibility of the IMC (Yellow-fluorescent protein; YFP). Upon initiation of formation of the daughter-cells (T=0 min) the *TgRME-1* compartment (mCherry panel) fragments and smaller vesicular structures are incorporated by the IMC of the forming daughter-cells (T=30 min). About 60 min after initiation of daughter-cell formation the apical *TgRME-1* compartment starts to squeeze along the daughter-cell-IMC to move to the basal end of the mother cell. (Bar: 4  $\mu\text{m}$ .)

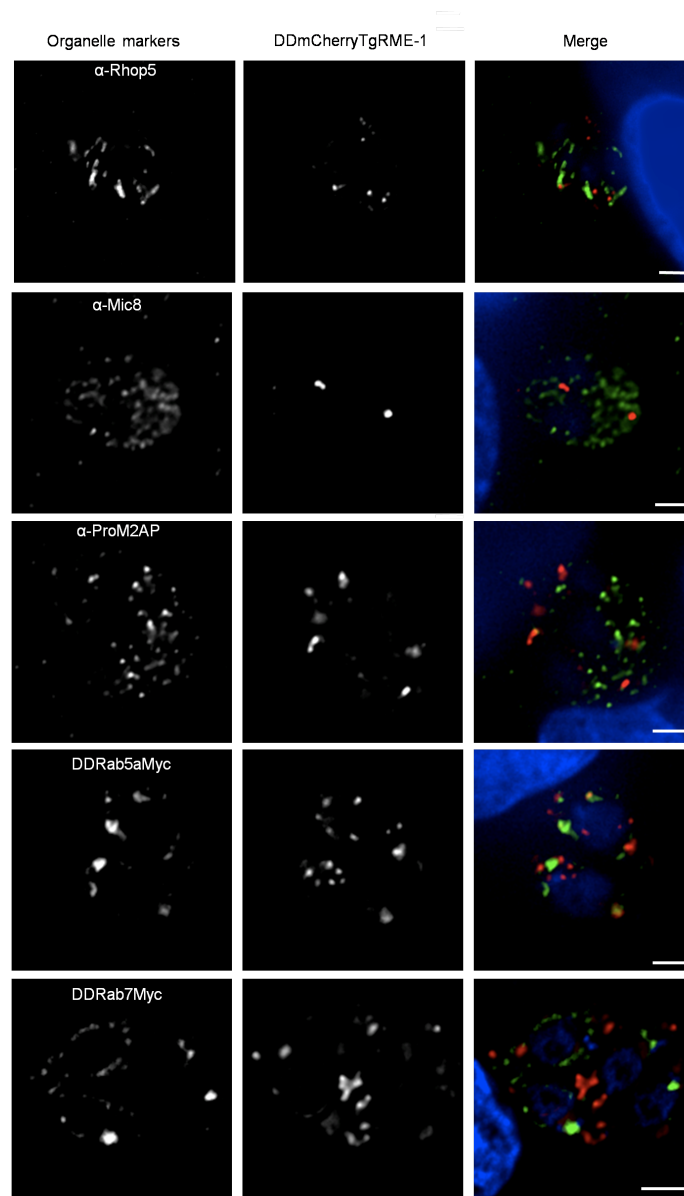


Figure 3.11: **Exemplified images of the colocalization of *TgRME-1* with organelles of the secretory and endosomal system, respectively.** Pictures show a selection of colocalization studies of *TgRME-1* with the secretory and the endosomal system. Co-localization was either analyzed via indirect immuno-fluorescence assay (IFA) of the organellar markers or via co-expression (DD-tag) of tagged proteins (Rhop5: Rhoptries; Mic8: Microneme subset; ProM2AP: Early endosome subset; Rab5A: Endosomal-like compartment; Rab7: late-endosomal like-compartment). No colocalization could be observed for any of the tested organelles. (Bar: 4  $\mu\text{m}$ .)

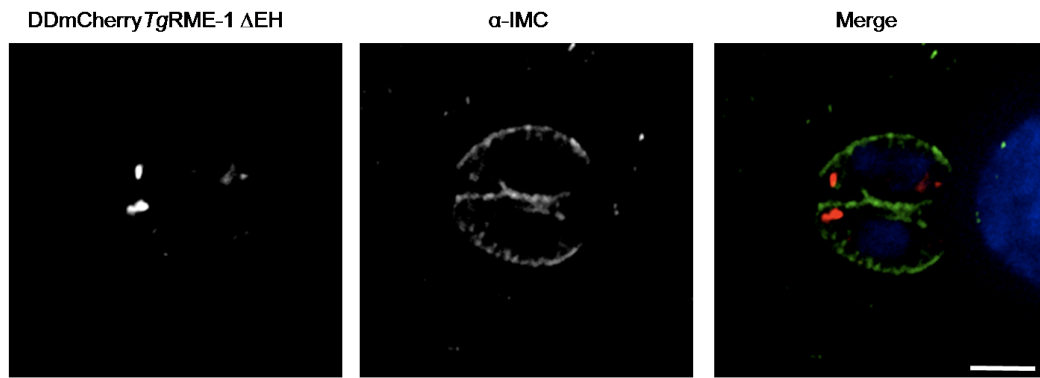


Figure 3.12: **Expression of the *TgRME-1*ΔEH deletion mutant.** *TgRME-1* lacking the Eps15-homology domain (EH) was N-terminally tagged with a destabilization domain (DD) and a mCherry-tag. Over-expression of the deletion mutant was induced via addition of 1  $\mu$ M Shield-1 for 6 h and the parasites were subsequently fixed with 4% PFA. The inner membrane complex (IMC) was detected via an indirect immunofluorescence assay (IFA) using an  $\alpha$ -IMC antibody. The localization of *TgRME-1*ΔEH was comparable to the full-length protein. (Bar: 4  $\mu$ m)

the genome and successful cloning of single parasite lines I initially examined the localization of the protein in the deletion mutants generated. Interestingly, whereas localization of the *TgRME-1*ΔEH protein was comparable to the wild-type localization (Fig. 3.12), the subcellular localization of the *TgRME-1*ΔATPase protein differed dramatically from the wild-type, in a sense that it appeared mainly cytosolic (Fig. 3.13). When the parasites were subsequently analyzed for their ability to grow while expressing the deletion mutant no growth defect was observed in standard plaque-assays (Fig. 3.14). All attempts to generate a potent knock-out of the *TgRME-1* gene in *Toxoplasma* parasites failed due to the inability to amplify the 3'UTR of the gene from genomic DNA for cloning.

### 3.2.4 Localization of *Plasmodium falciparum* EHD-protein PfEHD

To analyze the localization of the *Plasmodium falciparum* ortholog of *TgRME-1*, *PfEHD*, in collaboration with Florian Kruse (PhD-student, AG Spielmann, BNI-Hamburg), the *pfehd* open-reading frame was fused C-terminally to a sequence coding for a GFP-tag and stably expressed in *P. falciparum* blood-stage parasites. Analysis of the fixed transgene parasites under the fluorescence microscope revealed a localization of the GFP-fusion protein to the periphery of the parasites, in close association of the parasite plasma membrane (Fig. 3.15). A faint staining of the cytoplasm as well as a strong focal staining of some areas of the plasma membrane could be observed also.

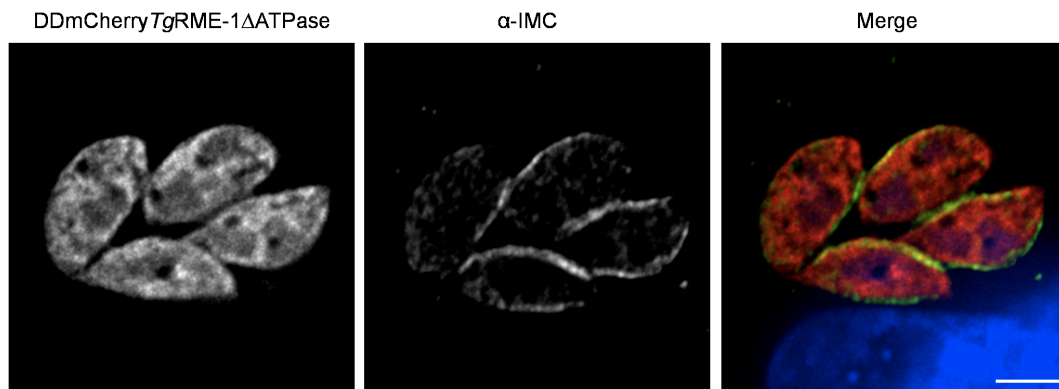


Figure 3.13: **Expression of the *TgRME-1*ΔATPase deletion mutant.** *TgRME-1* lacking the ATPase-domain was N-terminally tagged with a destabilization domain (DD) and with a mCherry-tag, respectively. Expression of the deletion version was induced via addition of 1  $\mu$ M Shield-1 for 6 h and parasites were subsequently fixed with 4% PFA. The inner membrane complex (IMC) was detected via an indirect immunofluorescence assay (IFA) using an  $\alpha$ -IMC antibody. Localization of *TgRME-1*ΔATPase was mainly cytosolic. (Bar: 4  $\mu$ m)

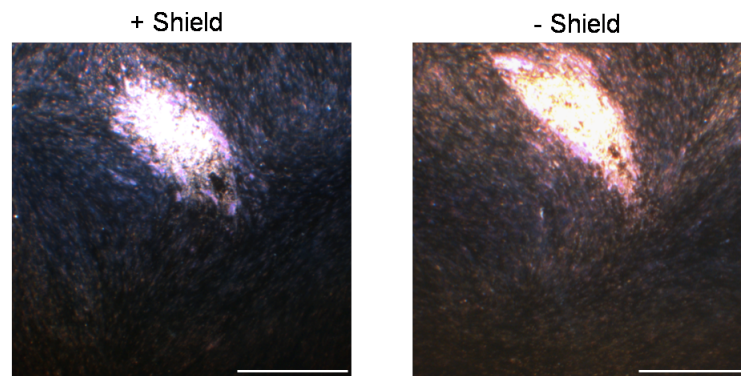


Figure 3.14: **Plaque-Assay of DDmCherry *TgRME-1*-expressing *Toxoplasma* parasites.** Human foreskin fibroblast monolayers were infected with *Toxoplasma* parasites expressing DDmCherry *TgRME-1* in presence or absence of Shield-1 for 7 days, fixed with Methanol and subsequently stained with Giemsa-stain solution. No difference in parasite growth could be observed between parasites that are expressing the fusion protein and that are not expressing it, respectively. (Bar: 1 mm)

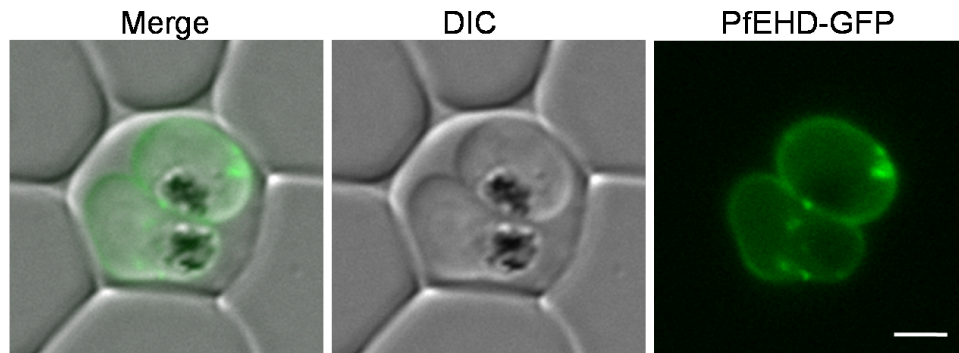


Figure 3.15: **Localization of *PfEHD-GFP* in *Plasmodium falciparum* trophozoites.** *PfEHD* was C-terminally tagged with a GFP-tag and expressed as additional copy to the endogenous protein in *P. falciparum*. Stably expressing parasites were fixed with 4% PFA and the GFP-signal was analyzed subsequently under a fluorescent microscope. The GFP-signal could be observed at the periphery of *P. falciparum* trophozoites closely and homogenously associated with the plasma membrane of the parasite, as well as at distinct focal spots. (Bar: 2  $\mu\text{m}$ )

### 3.2.5 Protein localization of *TgRME-1* and *PfEHD* is interchangeable between apicomplexans, but differs according to the intrinsic protein architecture

To analyze the overall conservation of the single EHD-protein for apicomplexan parasites regarding both its subcellular localization and hence functionality we carried out complementation studies by integrating the *TgRME-1* gene into *Plasmodium falciparum* and *vice versa*. Interestingly, when we transiently expressed *PfEHD* in *Toxoplasma* applying the exact same genetic strategy as for *TgRME-1* (DDmCherry-Tag, N-terminally, described in section 3.2.1), we observed a localization of *PfEHD* mainly concentrated to the parasite's plasma membrane (Fig. 3.16). This is consistent with the localization of *PfEHD* in *P. falciparum* as shown in Fig. 3.15 and described in section 3.2.4. When we stably expressed *TgRME-1* in *P. falciparum* fused to a C-terminal GFP-tag the protein localized to a distinct spot within the *Plasmodium* parasite, similar to its defined localization observed in *Toxoplasma* parasites (Fig. 3.17; in collaboration with Florian Kruse, AG Spielmann, BNI-Hamburg). Both experiments suggest a localization of each protein specific for a distinct structure in apicomplexan parasites, that is interchangeable between both parasites, meaning the cellular localization for *PfEHD* and *TgRME-1*, respectively, is the same in both organisms. Each apicomplexan EHD-protein localizes to the same structure within both parasites, but this localization differs from the other apicomplexan EHD-protein member, respectively. Therefore the localization of the protein seems to be defined by its intrinsic architecture rather than its parasite-specific interaction partners. This is consistent with the above mentioned finding that deletion of the EH-domain of *TgRME-1*, generally known to be an important site for protein-protein-interactions in other EHD-proteins<sup>289</sup>, does not lead to a

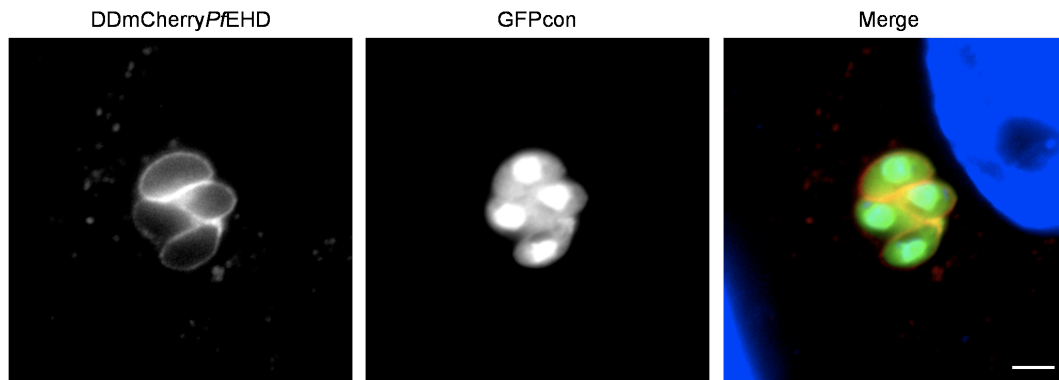


Figure 3.16: **Localization DDmCherryPfEHD in *Toxoplasma*.** *Plasmodium falciparum* EHD was tagged N-terminally with a destabilization domain (DD) and an mCherry-tag and transiently transfected into *Toxoplasma gondii* RH $\Delta$ HX GFPcon (conditional cytosolic GFP-expressing) parasites. PfEHD-protein expression was induced with Shield-1 for 6 h and parasites were fixed subsequently. The mCherry-tagged protein localized to the cytoplasmic membrane of the *Toxoplasma* parasites. (Bar: 4  $\mu$ m)

different localization of the protein. Furthermore, an alignment of the three apicomplexan EHD-protein family members of the human malaria pathogen *P. falciparum*, the murine malarial parasite *P. berghei* and human Toxoplasmosis causing agent *T. gondii* shows that, even though all three proteins are very similar regarding their primary protein architecture, solely *TgRME-1* harbors a long C-terminal stretch downstream of the EH-domain (Fig. 3.18). This stretch seems to be highly phosphorylated as described recently by Treek et al.<sup>290</sup>.

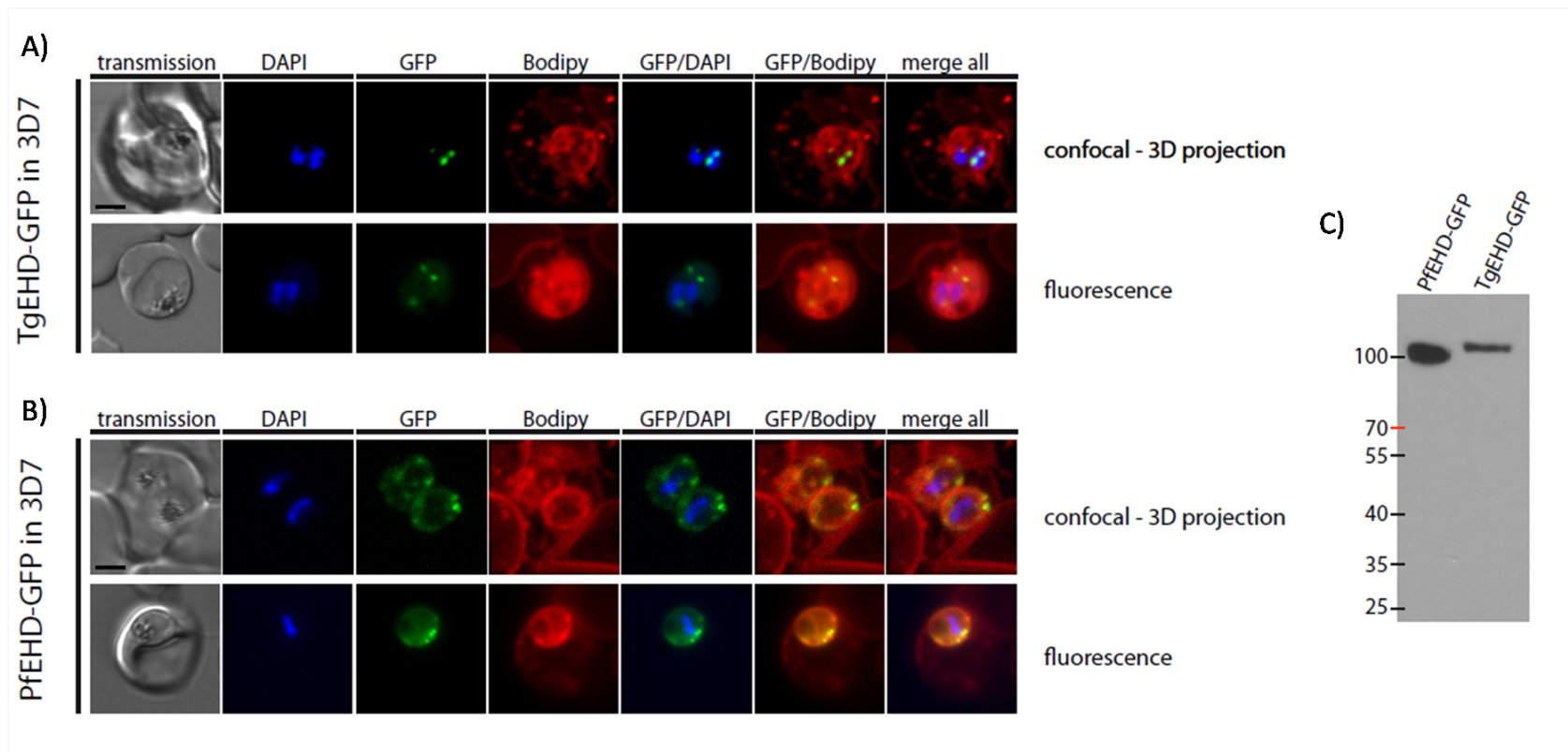


Figure 3.17: **Comparison of the expression of GFP-tagged *TgRME-1* (*TgEHD*) and *PfEHD* in *Plasmodium falciparum* 3D7 parasites.** *TgRME-1* and *PfEHD* were both C-terminally GFP-tagged and this version of the protein was stably expressed in addition to the endogenous protein in *Plasmodium falciparum*. **A) Expression of *TgRME-1*/*TgEHD*-GFP in *P. falciparum*.** *TgEHD*-GFP is expressed in distinct organelle-like compartments within the parasite as shown by fluorescence microscopy (lower panel) and confocal 3D-reconstruction (upper panel) in blood-stage trophozoites. Some of the labeled spots seem to be associated with the nucleus of the parasite. The parasite cytoplasm was co-stained with bodipy-stain in addition to DAPI-staining of the nucleus (Bar: 2  $\mu$ m). **B) Expression of *PfEHD*-GFP in *Plasmodium falciparum*.** *PfEHD*-GFP localizes to the periphery, likely the plasma membrane, of the parasite and concentrates at few distinct spots at this membrane. In addition to that some of the protein can also be found in the parasite cytoplasm (Bar: 2  $\mu$ m). **C)** Western blot detecting the fusion proteins *TgEHD*-GFP and *PfEHD*-GFP with an  $\alpha$ -GFP antibody. The marker on the lefthand side indicates protein sizes in kDa.



### 3.2.6 Expression and localization of the EHD-protein in *P. berghei*

In order to analyse expression and localisation of the EHD-protein in the rodent malaria parasite *Plasmodium berghei* an antibody against the amino-acids 339-533 (compare Fig. 3.18) of the *PfEHD*-protein was generated (kindly provided by Dr. Tobias Spielmann, BNI Hamburg) and tested against the *P. berghei* protein in IFA studies. In summary it could be shown that *PbEHD* is expressed on protein level in bloodstages (BS), salivary gland sporozoites (SGS) and liver-stages (LS). When BS were analysed on immuno-EM level a gold labeling of the parasite's plasmamembrane (PM) as well as structures within the parasite could be observed (Fig. 3.19). When a number of EM-sections (N100) were analyzed for the number of events in which certain organelles were labeled by gold particles combined with  $\alpha$ -*PfEHD* antibodies in a semi-quantitative analysis (Fig. 3.20) a preferred localization of *PbEHD* to the parasite cytoplasm, vesicles, the endoplasmic reticulum (ER) and the parasite nucleus could be shown (Fig. 3.21). In less frequent occasions also a labeling of the parasite's mitochondria, the cytostome, the apicoplast and the surrounding membranes (PM/PVM) and even a labeling of the red blood-cell lumen and membrane could be seen (Fig. 3.21 and Fig. 3.20). When blood-stage parasites (schizont overnight culture) were analyzed in an IFA only a very weak expression of the protein could be observed (Fig. 3.22). When SGS were labeled with the antibody a vesicular staining could be observed that is homogenously distributed over the whole cytoplasm of the parasite (Fig. 3.23). This staining changes after the parasites invade HuH7 hepatoma cells *in vitro* and develops into early extra-erythrocytic forms (EEFs). After development of EEF trophozoites for 24h the protein can be found in a single compartment of the parasite (Fig. 3.24). This compartment is aligning with the plasma membrane (PM) of the parasite and appears to be dynamic since it is forming extensions into the cytoplasm of the parasite. In most of the images observed the localization of this compartment is polarized within the parasite towards the host cell nucleus, where the labeling of the compartment by  $\alpha$ -*PfEHD* antibodies appears to be stronger. After 48 h of EEF development, when schizogony has taken place and first-generation merozoites begin to form, the EHD-labeled compartment splits up into vesicular structures that are distributed non-homogenously over both the whole parasite and the PM (Fig. 3.25). Similar to what was observed for *TgRME-1* the localization of *PbEHD* seems to be highly dynamic, as well, since tubular structures could also be seen in *P. berghei* (Fig. 3.25, bottom panel).

### 3.2.7 EHD gene deletion in murine *P. berghei* is not essential for blood-stage development

Since functional studies in *Toxoplasma* failed (described above) and in order to study the importance of EHD during the malarial life-cycle, I generated loss-of-function mutants in the rodent *Plasmodium* parasite, *P. berghei*. I therefore applied an integration strategy in order to disrupt the endogenous EHD gene locus by a single cross-over homologous recombination<sup>291</sup>. For targeted gene-disruption a plas-



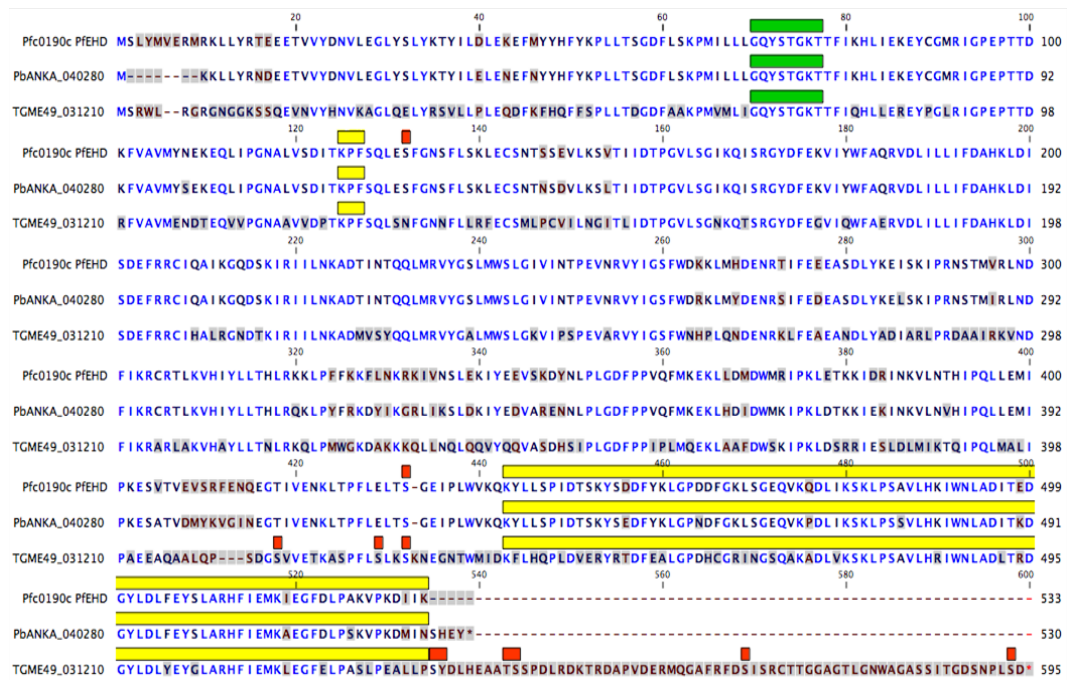


Figure 3.18: Alignment of selected apicomplexan EHD-proteins. *PfEHD*, *PbEHD* and *TgRME-1* were aligned according to their primary structure. Main sequence motifs coding for known functional domains are shown in colored bars above the sequences (predicted p-loop containing nucleoside triphosphate hydrolase motif, green; KPF-binding motif; short yellow bar; EH-domain, long yellow bar; phosphorylation sites, red bars).

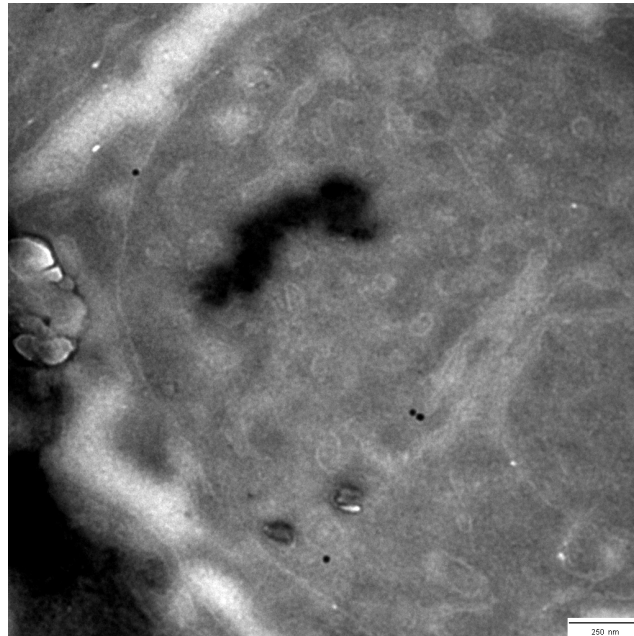


Figure 3.19: Immuno-EM of *P. berghei* bloodstage parasites labeling *PbEHD*. *P. berghei*-infected red blood cells (iRBC) were fixed and embedded using the Tokuyasu-method, cryo-sectioned (100nm) and labeled using an anti-*PfEHD* primary antibody detected by 10nm gold-bead conjugated secondary antibodies. Gold-beads can be found at the parasite's plasma membrane as well as in the cytoplasm and at vesicles.

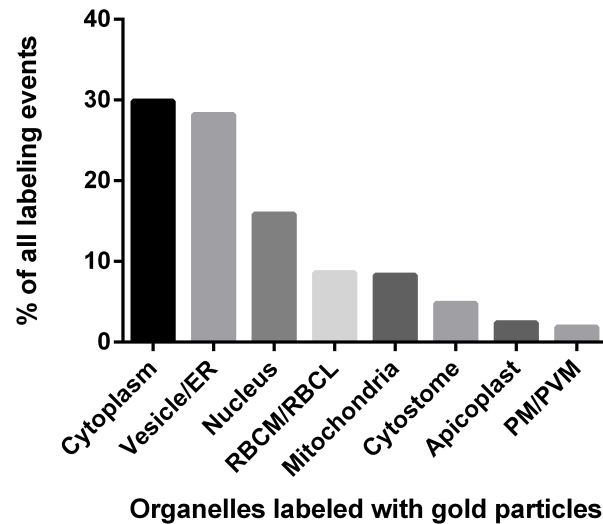


Figure 3.20: **Semiquantitative analysis of *PbEHD* localization in *P. berghei* blood-stages in electron microscopy studies.** The number of events of labeled organellar structures on the EM sections were counted and plotted as percentage of the total number of events (N=100). Labeling of one organellar structure by several gold particles within the same section was counted as only one event. ER: Endoplasmic reticulum; RBCM: Red blood cell membrane; RBCL: Red blood cell lumen; PM: Parasite membrane; PVM: Parasitophorous vacuole membrane;

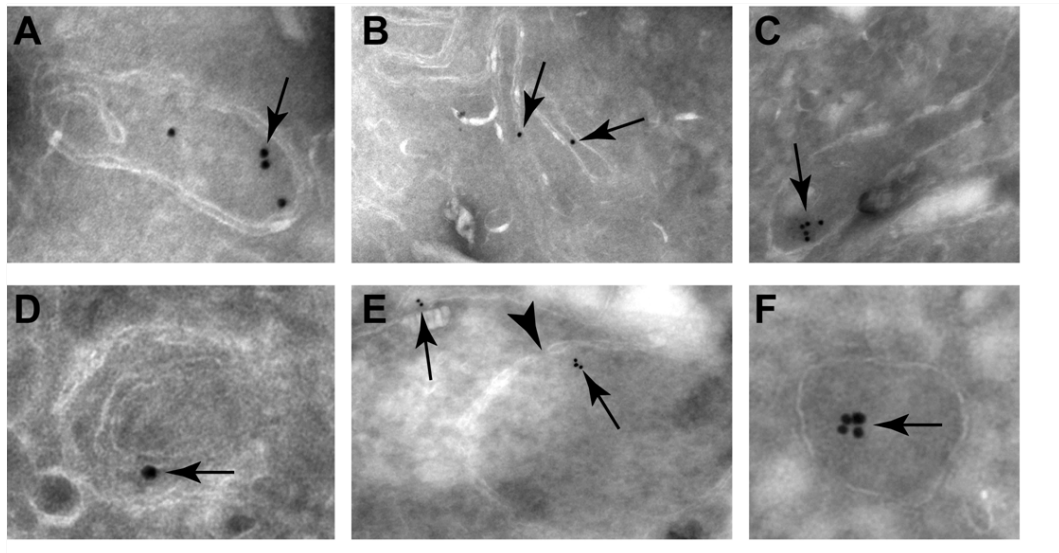


Figure 3.21: **Overview of the labeling of different organelles by  $\alpha$ -*PbEHD* antibodies in immuno-EM studies of blood-stages.** Arrows point to the gold-beads attached to antibodies labeling *PbEHD*. Pictures A-F show examples of the organelles labeled by the antibodies. A: Mitochondrion; B: ER (endoplasmic reticulum) profiles; C: Cytostome; D: Apicoplast; E: PM/PVM (parasite membrane and parasitophorous vacuole membrane) and nucleus - arrowhead points to nuclear pore; F: Vesicle.

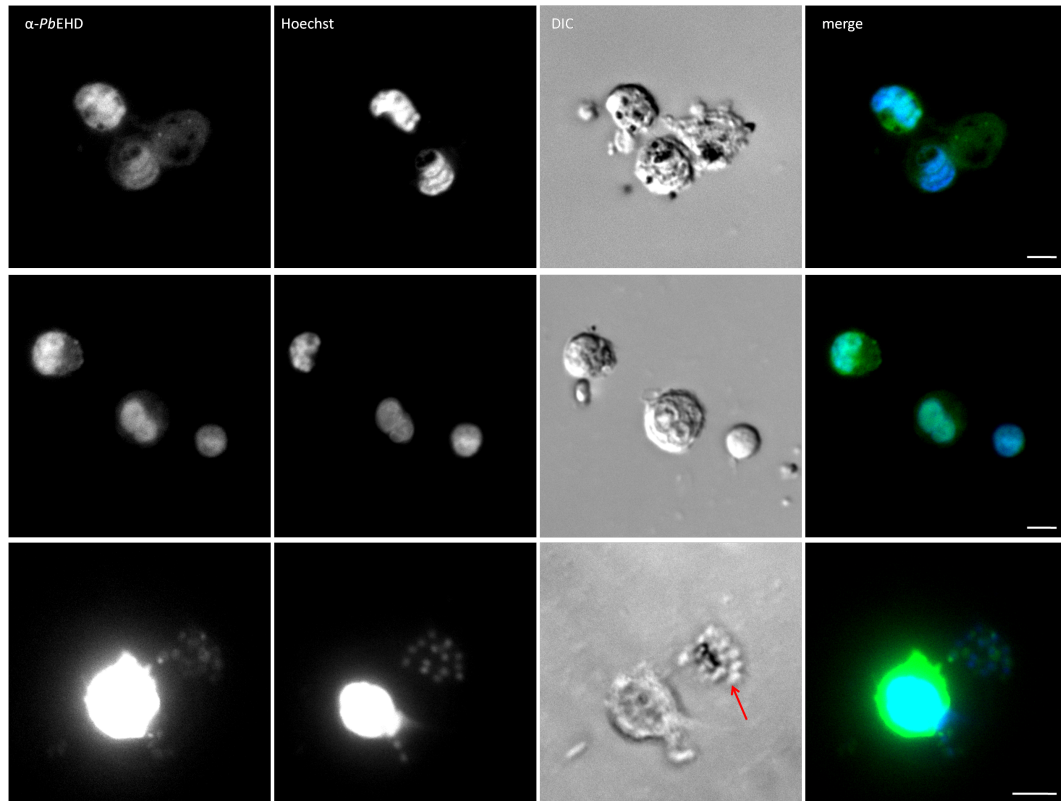


Figure 3.22: **Localisation of *PbEHD* in blood-stage parasites.** Blood-stage parasites enriched during a 15h over-night culture were fixed with 4% PFA and subsequently stained with mouse  $\alpha$ -*PfEHD*/ $\alpha$ -mouse Alexa488 antibodies. Only a weak staining of the parasites could be observed in ring-stage trophozoites (upper and middle panel) and blood-stage schizonts (arrow, lower panel). (Bar: 4  $\mu$ m)

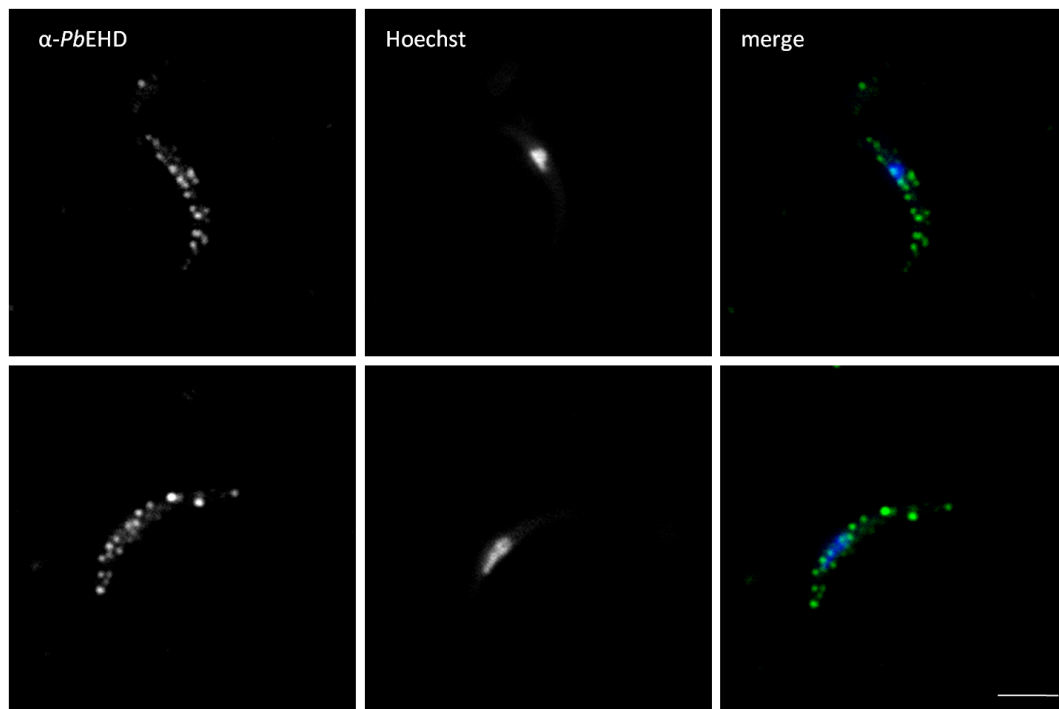


Figure 3.23: **Localisation of *PbEHD* in salivary gland sporozoites.** *PbANKA* sporozoites were extracted from salivary glands of *A. stephensi* mosquitoes and allowed to glide on BSA-coated slides for 30 min. After fixation in PFA an IFA was performed detecting *PbEHD* with the mouse  $\alpha$ -*PfEHD*/ $\alpha$ -mouse Alexa488 antibody. A vesicular staining covering the entire cytoplasm of the parasites was observed. (Bar: 4  $\mu$ m)

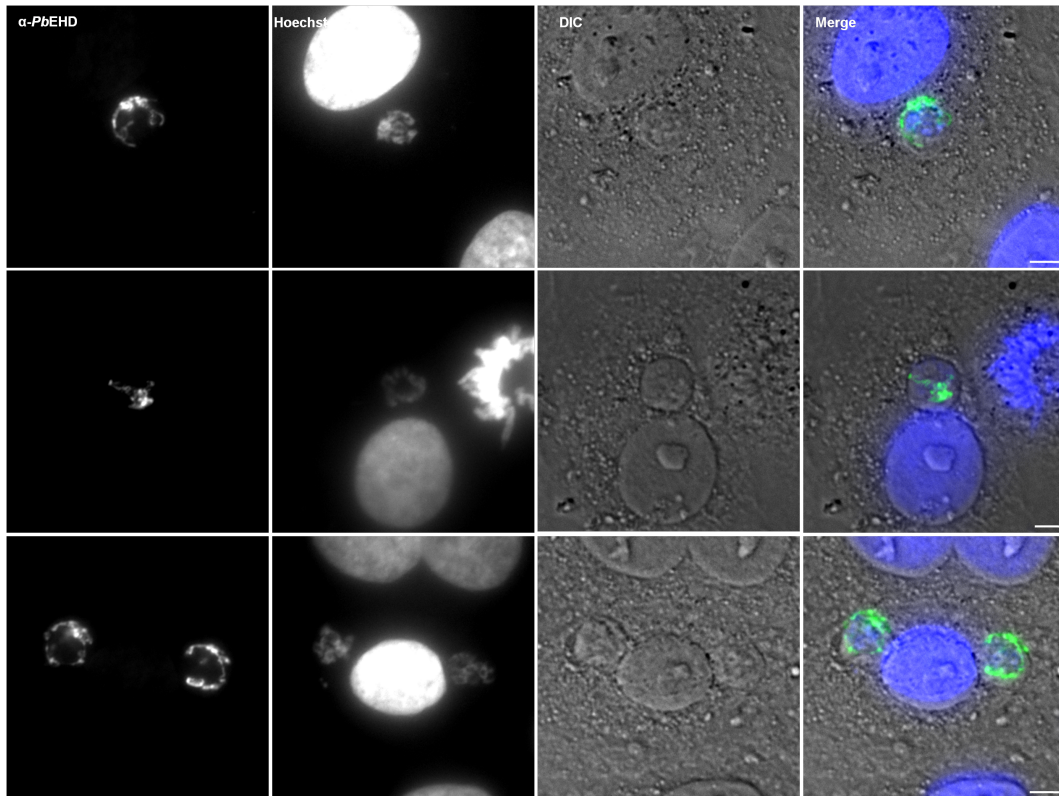


Figure 3.24: **Localization of *PbEHD* EEFs after development of 24h *in vitro*.** *P. berghei* parasites were allowed to develop within Huh7 hepatoma cells *in vitro* for 24h post invasion. In an IFA  $\alpha$ -*PfEHD* antibodies were applied after PFA-fixation to visualize localization of the protein within the parasites. A strong labeling of one compartment within the parasites could be observed that has a polar orientation directed to the host cell nucleus. Extensions of the compartment into the parasite cytoplasm can be detected. (Bar: 8  $\mu$ m)



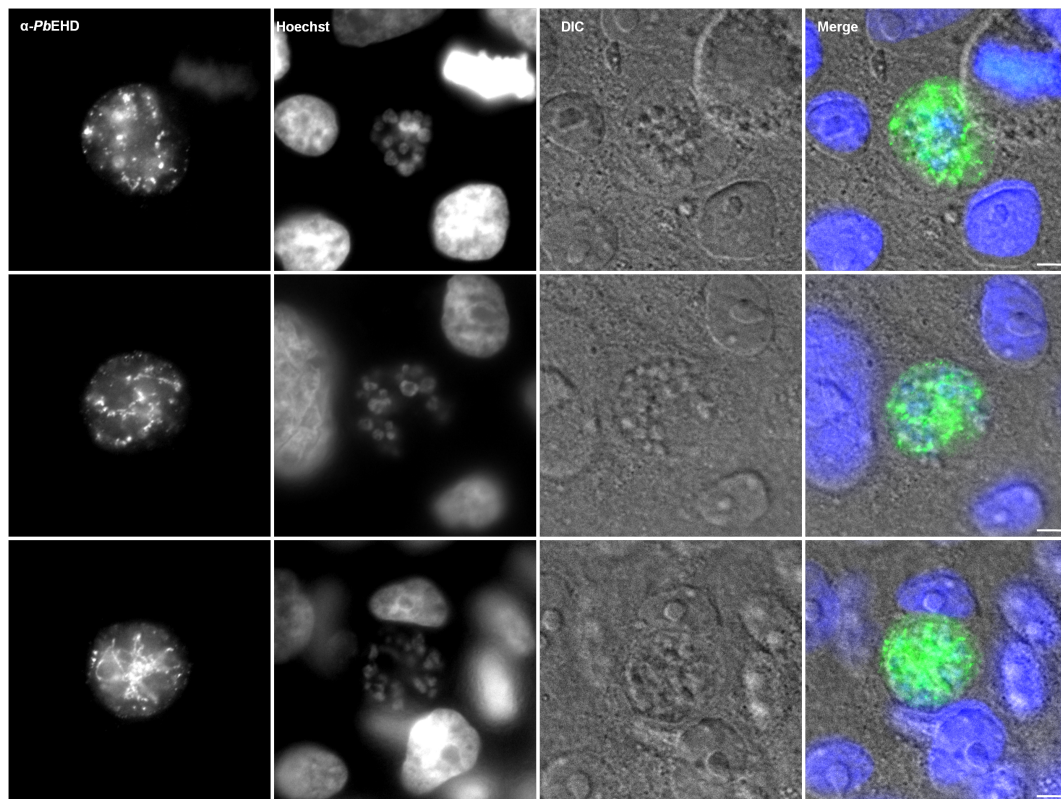


Figure 3.25: **Localization of *PbEHD* EEFs after development of 48h *in vitro*.** *P. berghei* parasites were allowed to develop for 24h post invasion and an IFA was performed as described in Fig. 3.24. A labeling of vesicular structures within the parasites can be seen as merozoites start to form. The structure is dynamic (vesicular and tubular; bottom panel) and non-homogenously distributed over the whole parasite. (Bar: 8  $\mu$ m)

mid carrying a fragment of the *pbehd* open-reading frame (ORF) and a selectable marker (*tgdhfr/ts*) was linearized within the homologous region and transfected into parasites of the *P. berghei* ANKA (PbA) reference line (Fig. 3.26A). By successful integration of the full-length plasmid into the *pbehd* locus via homologous recombination the gene was truncated making it unlikely for the full-length mRNA of the gene of interest (GOI) to be expressed. Applying a double cross-over strategy to replace the endogenous locus of the GOI was however not possible, since the 3' untranslated region of the gene could not be amplified by PCR-reaction. This is consistent with recent data from Pfander et al. who were also not able to include the 3' part of the *pbehd* ORF into their plasmogEM database recombination vectors<sup>292</sup>. Transfected parasites were selected with the antifolate Pyrimethamine and the parental blood-stage population from a successful transfection, verified by genotyping-PCR, was subsequently used to isolate four independent knock-out clonal lines, two of which were used for phenotypical analyses (*pbehd(-)#4/1* and *pbehd(-)#4/2*; Fig. 3.26B). Since stable clones of the *pbehd* (-) strain could be obtained after transfection the protein does not seem to be essential for the blood-stage phase of the parasite.

### 3.2.8 EHD mutant *P. berghei* parasites develop indistinguishable from wildtype parasites during the intra-mosquito life-cycle

Blood-stage positive *pbehd* (-) and WT infected mice were analyzed for the existence of mature gametocytes via exflagellation assay. When at least 2-5 exflagellation centers per field could be observed at 400x magnification 5-7 days old *Anopheles stephensi* mosquitoes were allowed to feed for 15 min on the anesthetized infected mice. After 12 days 10 mosquitoes per group were killed and midguts were analyzed for the numbers of oocysts present. The same midguts were afterwards combined and mashed within an eppendorf reaction tube. Through that oocyst derived sporozoites (ODS) were extracted and could be counted afterwards. At day 19 after the blood meal 15-20 mosquitoes were killed, salivary glands combined and mashed in an eppendorf reaction tube. After that salivary gland sporozoites (SGS) were counted at 400x magnification.

In summary we observed no significant difference between wildtype parasites and the *pbehd* (-) strain during development of the parasites within *A. stephensi* mosquitoes as shown by similar numbers of oocysts, ODS and SGS (Fig. 3.27).

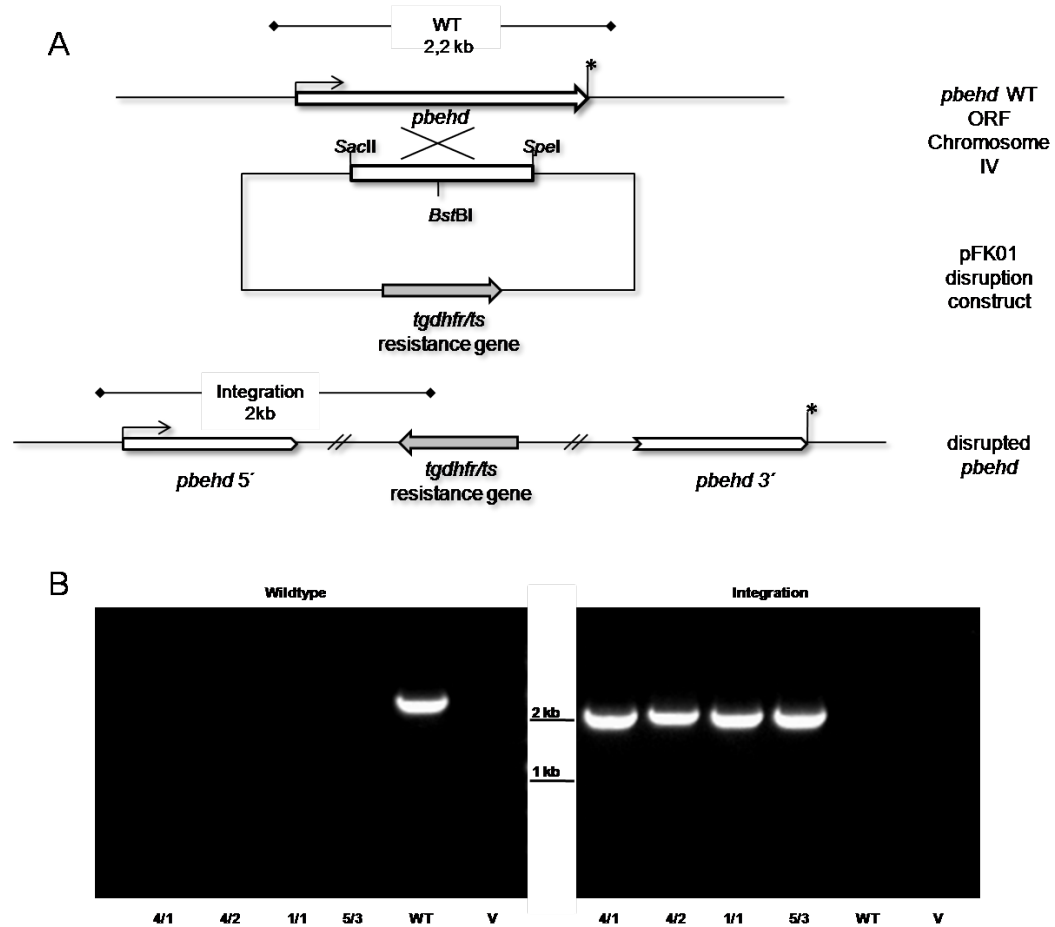


Figure 3.26: **A) Endogenous gene depletion resulted in *pbehd* (-) parasites.** *pbehd* was deleted via single cross-over integration strategy. For transfection pFK01 was linearized with *Bst*BI and the homologues sequence of the *pbehd* ORF cloned into pFK01 (*Sac*II/*Spe*I) was allowed to recombine with the endogenous gene locus. Thereby the *pbehd* 5' and 3' fragments were separated and a resistance gene (*Tgdhfr/ts*) was integrated. Parasites stably carrying the integrated plasmid were selected with Pyrimethamine and successful integration was confirmed via PCR (WT fragment 2,2 kb, Integration fragment 2,0 kb). **B) Confirmation of the integration of pFK01 into the *pbehd* locus.** Clonal parasite lines from two independent transfections and limited dilutions were tested for the existence of the wildtype or the *pbehd* (-) locus (integration) via PCR. Depicted below the lanes are the respective templates chosen for the PCR. Numbers 4/1 and 4/2 represent clones from the 1st transfection; Numbers 1/1 and 5/3 represent clones from the 2nd transfection. Left: Primer combination to detect the WT locus chosen. Right: Primer combination to detect the recombined locus chosen. WT: wildtype; V: vector.



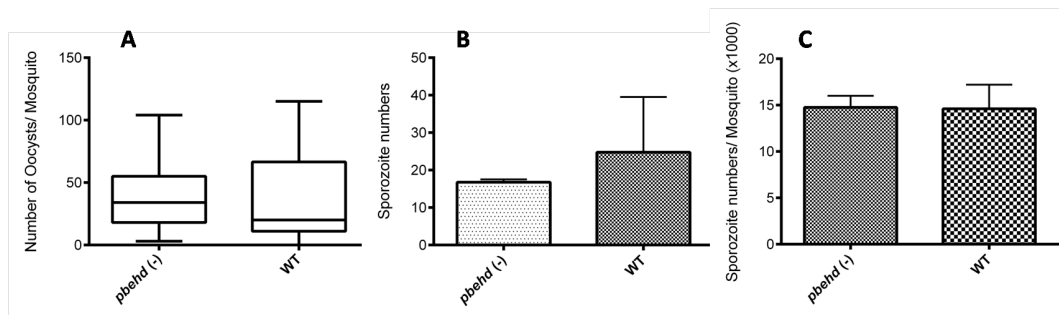


Figure 3.27: **Analysis of *pbehd*<sup>-/-</sup> parasite development in the mosquito vector.** A) Analysis of the oocyst formation in *A. stephensi* midguts. B) Number of oocyst derived sporozoites per mosquitoes (numbers x 1000). C) Number of mature sporozoites per *A. stephensi* salivary gland at day 19 after blood meal.

Parasite	Oocyst, no. d12 mean (range)	Sporozoite no. per oocyst d12 (mean)	Sporozoite no. per salivary gland d19 (mean)	Sporozoite injection (10.000); no. of infected mice	Sporozoite injection (1.000); no. of infected mice	Liver trophozoites at 48 h in vitro, no. mean	Liver trophozoites at 48 h in vitro, size Area (Pixel <sup>2</sup> , mean)	Prepatency after Sporozoite challenge (days, mean)	No. of infected mice developing ECM, spz challenge	No. of infected mice developing ECM, BS challenge
WT <i>PbANKA</i>	40,0 (0-120)	24750	14300	9/9	3/3	145± 12	<b>0,35 ± 0,013</b>	<b>3,5 ± 0,5</b>	<b>100% (N=12)</b>	<b>3/3</b>
<i>pbehd</i> (-)	37,78 (0-110)	16750	14450	9/9	2/3	127± 15	<b>0,28 ± 0,013</b>	<b>4,5 ± 0,5</b>	<b>0% (N=11)</b>	<b>2/3</b>

Figure 3.28: Analysis of *pbehd* (-) parasite development throughout the lifecycle (significant value differences shown in bold)

### 3.2.9 Depletion of EHD results in developmental slow-down during late liver-stage development in *P. berghei* and protection of severe pathology in C57BL/6 mice

When C57BL/6 mice were infected with salivary gland sporozoites (SGS) intravenously a significant delay in prepatency of approximately 1 day in mice infected with *pbehd* (-) parasites in comparison to the WT could be shown by examination of blood smears. An *in vitro* liver-stage development assay showed a slowed down development of *pbehd* (-) parasites during the liver phase since the knock-out parasites were significantly smaller than the wildtype at 48h after invasion (Fig. 3.29). When C57BL/6 mice infected with sporozoites became blood-stage patent interestingly, in addition to the delay in prepatency, also a striking difference in disease outcome was observed. Infection of C57BL/6 mice with *Plasmodium berghei* ANKA parasites represents a well-accepted murine model of experimental cerebral malaria (ECM), which reflects symptoms observed in patients suffering from human cerebral malaria (HCM)<sup>293</sup>. Mice in this model usually suffer from a neurological syndrom characterized by paralysis, deviation of the head, ataxia, convulsions and coma between six and 10 days after inoculation with parasitized red blood cells. Infection leads to death in 60-100% of mice despite relatively low parasitemia<sup>294</sup>. In our approach, whereas all *PbANKA* (PbA) wildtype-infected mice developed ECM around day 8 post infection at parasitemias not higher than 5%, none of the *pbehd* (-) infected mice did show any signs of ECM rather going into hyper-parasitemia instead and dying much later in result of anaemia (Fig. 3.30A and Fig. 3.30B). The protection from ECM in *pbehd* (-) infected mice could be shown to be solely dependent on the liver phase of the parasite since animals challenged with  $1 \times 10^6$  iRBC of *pbehd*(-) (blood-stage knock-out) parasites were not protected from developing ECM similar to those infected with PbA iRBC (blood-stages) (Fig. 3.28). When brains of infected mice were analyzed via Evan's blue staining at the coma stage (in the case of a PbA wildtype infection) or after the mice were sacrificed (*pbehd*(-) infection), a leakage of the blood brain barrier was observed for the PbA-infected mice as had been shown previously<sup>295</sup>, whereas no leakage could be observed for the *pbehd* (-) infected mice (Fig. 3.30D). All of these results were confirmed for a second clone and are summarized in Fig. 3.28. Since observations by Lewis et al. (unpublished observations) indicated that IL-10 induction in the host might play a role in the protection from ECM during the liver stage we depleted IL-10 via an IL-10 depletion antibody in 3 mice during the liverstage phase of *pbehd* (-) infected mice. Interestingly, 2 out of 3 *pbehd* (-) infected mice developed ECM when depleted from IL-10 confirming a protective role for IL-10 in this model.

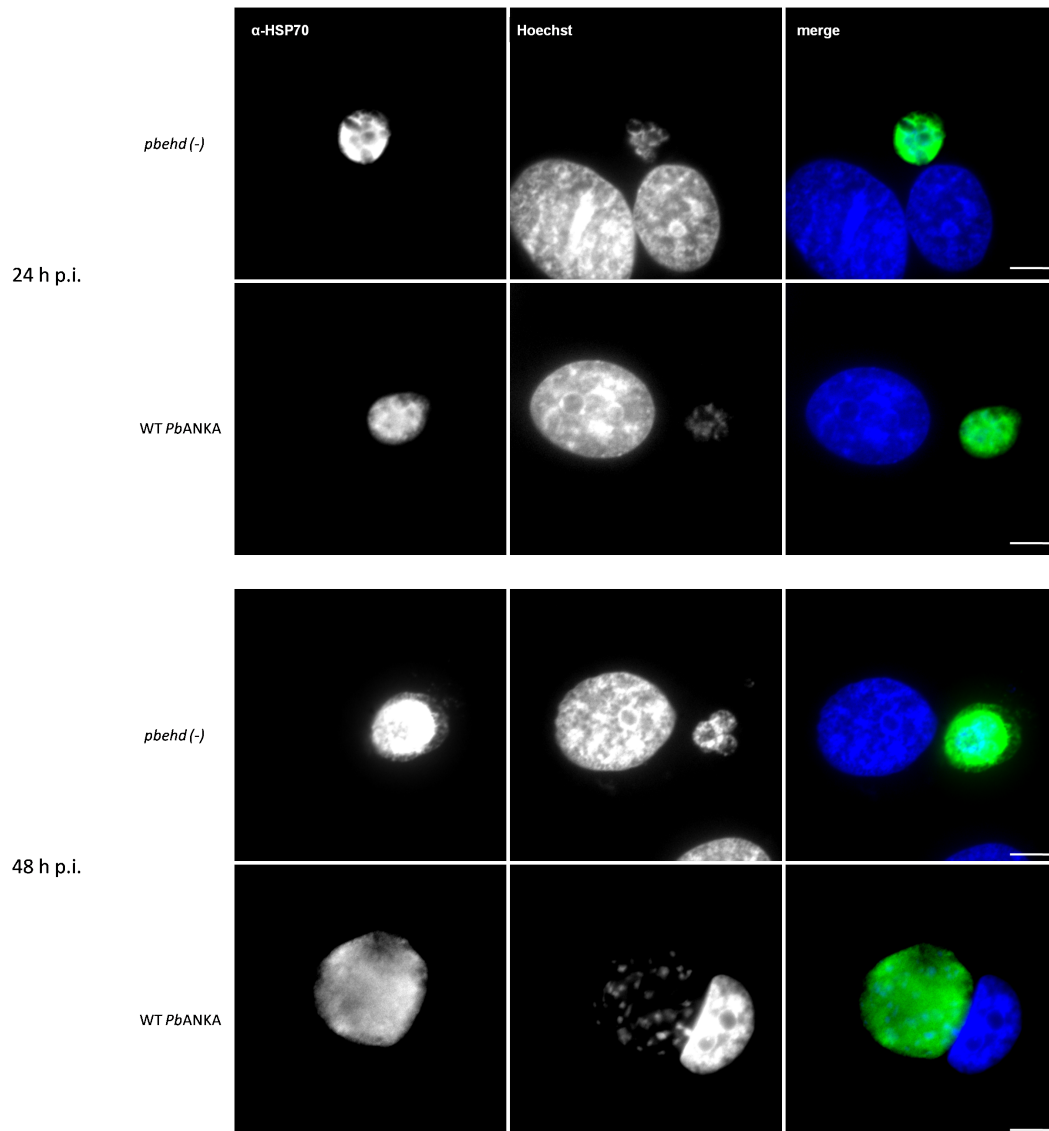


Figure 3.29: Liverstage development assay comparing *pbehd* (-) and WT parasites. Parasites were treated as described in Fig.3.30 C and sizes of the EEFs were analyzed at 24h and 48h post invasion.

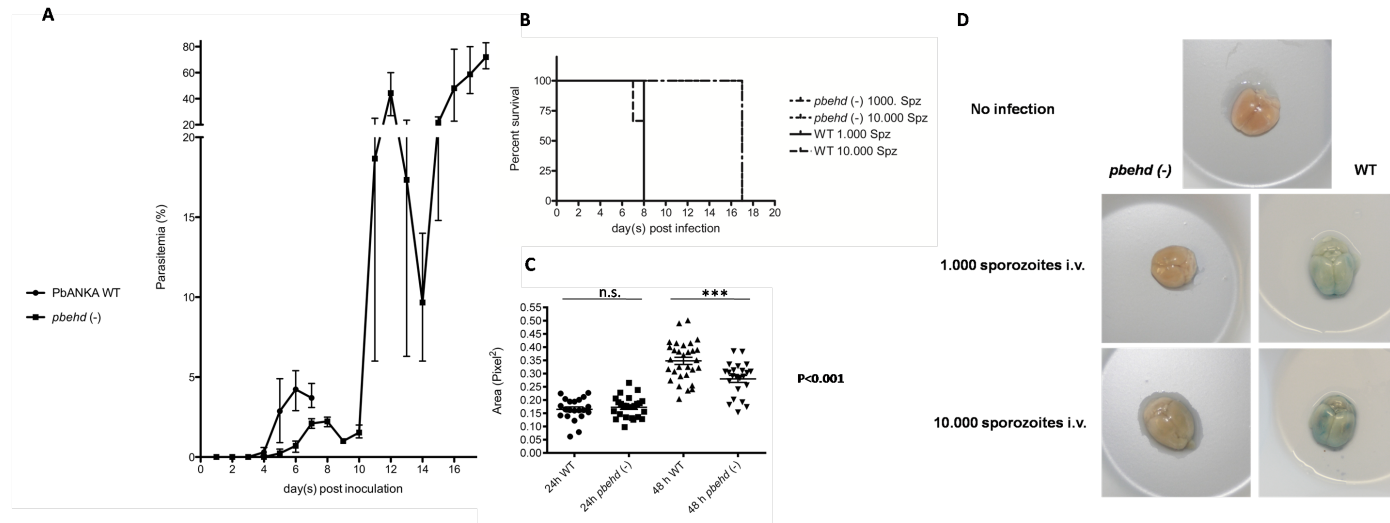


Figure 3.30: **A) Parasitemia curve after challenge of C57BL/6 mice with 10.000 sporozoites of WT and *pbehd* (-).** 10.000 sporozoites were injected intravenously into C57BL/6 mice (N=6). WT parasites died at low parasitemia around day 7 whereas *pbehd* (-) parasites developed slower, were delayed in reaching the blood-stage phase, finally developed hyperparasitemia and died later of anemia symptoms. **B) Survival rate of mice after sporozoite inoculation.** 1.000 and 10.000 sporozoites of wt and *pbehd* (-), respectively, were intravenously injected into 3 C57BL/6 mice each. Whereas WT mice died around d7-8 post infection, showing strong symptoms of experimental cerebral malaria (ECM), *pbehd* (-)-infected mice died of hyper-parasitemia around day 17, at no point during infection showing symptoms of ECM. Spz: Sporozoites. **C) In vitro liver-stage development.** 10.000 sporozoites of wt and *pbehd* (-) parasites were inoculated on Huh7 cells and developed for 24 h and 48 h. Parasites were stained with  $\alpha$ -HSP70 antibodies and analyzed by indirect immuno-fluorescence assay (IFA). Images were taken at a confocal-microscope and sizes of the parasites measured using the ImageJ (Version 1.4.3.67) polygon selection tool. A highly significant difference ( $P < 0.001$ ) was detectable between liver-stage sizes of WT parasites and *pbehd* (-) at 48 h post invasion. **D) Evans Blue staining of brains of infected mice.** Evan's Blue Dye (EBD) was injected into mice when mice were showing ECM symptoms in the wt group and 2 hours later brains were taken out and pictures shot. Leakage of EBD into the brains of wt infected C57BL/6 mice indicates damage of the blood brain barrier (BBB) in these mice, whereas the BBB in *pbehd* (-) infected mice seems to be intact. *Statistical analysis and plotting of the results was performed with GraphPad Prism V.6.00.*

# Chapter 4

## Discussion

The aim of the work presented in this thesis was a twofold approach: **1)** The establishment of a *P. falciparum in vitro* life-cycle in the host department and **2)** the characterization of a newly identified protein in apicomplexans of the EHD-protein family in the two parasites *Toxoplasma* and *Plasmodium*.

### 4.1 Plasmodium falciparum transmission

The protocol established in this thesis led to *P. falciparum* infections of *A. stephensi* mosquitoes that were sufficient (sporozoite numbers and prevalence) to infect primary human hepatocytes as well as immortalized hepatoma cell lines and to isolate *Plasmodium* liver-stage RNA from these to investigate gene expression. We were able to keep the mosquito infections high enough during the course of the experiments but could not maintain a constant infection rate for more than just a few months. Since the feeding procedure, the membrane transfer of mature gametocyte cultures onto *A. stephensi* mosquitoes, was standardized only the change in the quality of the *Plasmodium* gametocyte cell culture or the mosquitoes may have led to the decline in the infection rate. Since it has been observed before that the age of the mosquitoes at the feeding day is quite crucial (Van de Vegte-Bolmer, M. and van Gemert, G.J., Radboud University Nijmegen Medical Center, *personal communication*) we tried to standardize the feeding procedure in regard to that. Unfortunately, the periodic **mosquito breeding** routine and the fluctuating availability of mosquitoes in the lab did not always allow to create the perfect timing of the generation of a mature *P. falciparum* gametocyte culture (characterized by a certain number of exflagellating gametes) with the correct mosquito age. Therefore the susceptibility of the mosquitoes to a *P. falciparum* infection for some feeding procedures might not have been high enough, even though it was always made sure that the mosquitoes are feeding enough blood. The susceptibility of mosquitoes is not only influenced by their pure age alone, but also by other factors. One of it being the innate-immune system of the *Anopheles* mosquito, for example, that has been shown to get alerted by *Plasmodium* ookinetes when these try to traverse the midgut epithelium. As a result many of the ookinetes are killed by complement-like mosquito-proteins or reactive oxygen species<sup>296 297 298 299</sup>. The immune system is determined by genetic factors of the mosquito strains and might be influenced by long rounds of inbreeding under laboratory conditions. In addition to that, a recently published study showed that the gut microbiota of *Anopheles gambiae* has a strong impact on the susceptibility of the mosquitoes to *P. falciparum* infections<sup>300</sup>. In this study the authors could show that the gut microbiota in different adult wild-bred mosquito populations differed widely due to bacterial contamination of their differ-

ent larval habitats. The difference in the gut microbiota also correlated with the ability of these mosquitoes to transmit *Plasmodium* parasites. Indeed, some of the bacteria were actually needed by the parasites for a successful transmission, whereas others correlated with non-susceptibility. The authors also compared insectary-bred mosquitoes to field-collected ones and found great difference in the bacteria strains mainly prominent in these mosquitoes. The authors speculate that the reason for that might be the diverse mosquito-diet under both conditions is favouring different bacteria species, something that has been shown to influence the gut microbiota before already<sup>301 302 303</sup>. Quite recently the inhibitory effect on *Plasmodium* parasite transmission through destroying commensal gut microbes or alerting the mosquito immune system by introducing unusual alpha-proteobacteria (*Wolbachia*) in *Anopheles* has also been described as a transmission blocking tool<sup>304 305</sup>. In summary, it is not surprising that our insectary-bred mosquitoes are influenced by environmental factors such as their diet, the larvae breeding water etc., that vary over time and thereby lead to a change in the mosquito immune-system and their gut microbiota. This might have influenced the susceptibility of the mosquitoes to a *Plasmodium* infection and thereby might explain the drop in the infection rate in our experiments. This leads to the conclusion that for constantly high *Plasmodium falciparum* transmission rates the mosquito-breeding needs to be standardized and factors such as the pH of the breeding water, contamination of the larvae trays with bacteria and sources of other bacterial contaminations that might influence the growth of a gut " *Plasmodium*-unfavorable" microbiota need to be controlled and maintained at a constant level. Another factor that might have influenced the *P. falciparum* infection rate in our experimental setup is the **quality of the gametocyte culture** produced *in vitro* for the feeding of the mosquitoes. The aim for a sexual stage *P. falciparum* gametocyte culture is to create a large percentage of infected erythrocytes that form gametocytes within the culture. Therefore an asexual culture flask that is usually kept in a small volume and by replacement of iRBCs with fresh RBCs is maintained at a parasitemia below 5 %, is expanded into a larger volume and no fresh RBCs are added anymore. Thereby the parasitemia increases dramatically and gametocytes are formed as a result of density stress<sup>306</sup>. The maturity of a gametocyte culture is represented by a high number of stage V gametocytes<sup>307</sup> that are able to form gametes when activated by external triggers such as pH-change of the surrounding medium, temperature drop and a mosquito molecule, the xanthurenic acid<sup>308 309 310 311 312</sup>. During this process that can be visualized under a light microscope the male gametocytes form eight exflagellated gametes (exflagellation center) that possess highly motile flagella<sup>309</sup>. We used this process to evaluate the maturity of our gametocyte culture by examining the number of exflagellation centers per volume induced by temperature drop (cell culture to lab room temperature) under a light microscope. Even though we kept this number at a constant range for the feeding over time and therefore the quality of the culture should have been constant, this procedure might have been misleading. The exflagellation rate is only provid-

ing information about the maturity of male gametocytes, not female. As has been shown, though, a ratio of at least 50% of female gametocytes is needed to confer high infection rates<sup>313</sup>. It has been reported, for example, that sex ratios in *Plasmodium* sexual parasites vary in response to environmental factors such as host hormones etc. and that this influences the transmission success<sup>314</sup>. Important to note hereby is, that the human serum taken for the parasite *in vitro* culture in our setup was ordered from the Heidelberg University Hospital Blood Bank. This serum is expired donated material from donors of various genetic and health background and therefore the content is not standardized. Hence, the different batches of serum used for the parasite cultures might have had an influence on the gametocyte production. Therefore our evaluation of the maturity of our cultures by checking exflagellation may have been wrong since the sex ratio of the gametocytes may have been wrong. This may also have been influenced by the fact that the culture maintenance (exchange of the medium, inoculation of the cultures) was performed manually and not standardized. Other laboratories that have established a constantly running *P. falciparum*-transmission system therefore installed an automated cell-culture system that allows them to rely on perfectly mature cultures at certain timepoints and to time their maturity with the maturity of the *Anopheles* mosquitoes. In this setup they can also control the number of passages that have been made for maintaining the asexual cultures and check, if the rate of the gametocytogenesis, the formation of gametocytes, has dropped. This can happen if a parasite population has been passaged for many times in asexual cultures without having had to go through the mosquito cycle from time to time<sup>315</sup> (Marga van de Vegte-Bolmer, Radboud University Nijmegen Medical Center, *personal communication*).

## 4.2 Characterization of EHD-proteins in apicomplexa

In this thesis I was able for the first time to identify a member of the EHD-protein family in apicomplexan parasites by *in silico* analysis. Subsequently, I was able to characterize the protein in regard to its localization and function in the parasites *Toxoplasma gondii* and *Plasmodium berghei/Plasmodium falciparum*. The results of my thesis have contributed to a better understanding of EHD-proteins in apicomplexan parasites. It is not quite clear yet, if the results obtained for the single investigated organisms can be combined to one full picture or rather need to be viewed separately. Especially, if it comes to the comparison of EHD-proteins in *Toxoplasma* and *Plasmodium* it might not be possible to compare localization and function of EHD-proteins in both organisms, because of the different lifestyle of both. Therefore most of the interesting results will be discussed individually in the following.



### 4.2.1 The apicomplexan EHD-protein family

The *in silico* analysis in this thesis has revealed that the apicomplexan parasites *Toxoplasma* and *Plasmodium* each possess a single ortholog of proteins of the EHD-protein family (Fig. 3.4). The protein clusters tightly within the apicomplexan clade and is closely related to their orthologs in *C. elegans* and in vertebrates (Fig. 3.4). While *C. elegans* and apicomplexa only seem to have one predicted member of the EHD-protein family each, vertebrates have four paralogs. One of the reasons for the number of different paralogous proteins in vertebrates could be their higher organisation into different tissues. It has been shown for mammalian EHD-proteins that some have different functions in different tissues (see 1.2.2). EHD3 and EHD4 for example are specifically expressed in the glomerular endothelium of kidney cells whereas the other two family members are not<sup>316</sup>. In other mammalian cells at least some of the EHD-protein functions are redundant and depletion of just one member does not lead to major defects in these cells (see 1.2.2). The fact that also other protozoan single cellular organisms like *Entamoeba* are also predicted to have more than just one EHD-protein member (Fig. 3.4) seems to argue against this "complexity-theory". But so far only *in silico* data are existing for *Entamoeba* EHD-proteins making it difficult to interpret their existence. One could argue further against it, that also the multicellular worm *C. elegans* possesses only one EHD-protein, Rme-1, a protein shown to be involved in receptor-recycling events and also other cellular processes<sup>280</sup>. But it has been shown that *C. elegans* can produce several different isoforms of Rme-1 by alternative splicing that can likely exert different functions<sup>280</sup>. In addition to that, also the Drosophila ortholog Past-1 has shown to be differentially expressed in different transcripts<sup>317</sup>. Most of the studies on mammalian EHD-proteins have lead to a clear picture of the EHD-protein function during one specific process, the endocytic recycling in cells. Here, different EHD-proteins take over a function in different endocytic trafficking events such as trafficking from the plasma membrane to the early endosome (EE), from EE to the endocytic-recycling compartment (ERC) or from the ERC back to the membrane or into protein degradation (see Fig. 1.10). Human EHD-1 exhibits the highest level of sequence homology to the single EHD ortholog expressed in invertebrate organisms and the sequence similarity of these orthologs is higher than between the EHD-paralogs in humans themselves. This leads to the conclusion that an ancestral cell had only one protein, quite similar to EHD-1, that later became multiplied in higher organisms to fulfill different roles in the increasingly complex organisms. It seems to be very unlikely that a complex process like endocytic recycling could be driven by just one EHD-protein member in apicomplexans alone, since protein and receptor-recycling needs to be tightly regulated. And it is not known whether isoforms of the EHD-protein in apicomplexa may exist, something that will have to be investigated in the future. But if there is only one EHD-protein version in these single-celled protozoans this is leading me to the following conclusion: Either the EHD-protein has only one specialized function in these organisms in a process that is not as complex as the

endocytic-recycling of higher eukaryotes, or different proteins than EHDs are taking part in this complex process.

#### 4.2.2 Structure of the apicomplexan EHD-proteins

The *in silico* analysis performed in this thesis predicted that all characteristic domains of EHD-proteins are also present in the apicomplexa member. The analysis of the predicted amino-acid sequence showed a characteristic P-loop containing nucleotide binding site in the **G-domain** that possibly binds and hydrolyses ATP, even though this was not investigated in the present study. It has been shown for human EHD2 that the binding of ATP by the G-domain is required for the dimerization of two monomers (see chapter 1.2.1 and Fig. 1.11). Only upon dimerization the EHD2 homo-dimer is then able to bind to membranes of target organelles or structures via the helical middle domain of the protein. The ATP-binding and dimerization/oligomerization of the apicomplexan EHD-protein itself has not been investigated in this thesis but there are other results that lead to the assumption that also the apicomplexan EHD-protein might be able to dimerize: I was able to show that the deletion of the G-domain of *TgRME-1* leads to a cytosolic localization of the fluorescently tagged protein in *Toxoplasma gondii* (see chapter 3.2.3 and Fig. 3.13)). This stood in contrast to the localization of the full-length protein tagged by the same strategy which localized to distinct punctated and tubular structures within the parasite (discussed in 4.2.3). A similar phenotype has been shown for the non-ATP-binding mutant T72A of human EHD2<sup>282</sup>. In this study the mutation of Threonin to Alanin in the nucleotide-binding site prevented ATP-binding of the protein and thereby inhibited the dimerization of the protein *in vitro*. The overexpression of a tagged version of the same mutant *in vivo* led to a cytoplasmic localization of the protein in HeLa cells instead of a localization at tubules and punctated structures as seen for the full-length protein<sup>282</sup>. The authors assumed that the lacking ability of the mutated protein to bind ATP and to oligomerize prevented it from binding to membranes. Therefore the protein did not show a localization to membranous structures anymore. The ability of membrane binding can also be assumed for the apicomplexan EHD-protein from its primary structure and homology to the human EHD-proteins and also from the localization studies shown in section 3.2. Certainly the depletion results in this thesis show that the G-domain of *TgRME-1* is essential for its localization. But in addition, similar to human EHD2, *TgRME-1* depleted from its G-domain and thereby from its ATP-binding site is losing its ability to bind to membranes and remains cytosolic, indicating also for a need of the protein to dimerize via the G-domain to bind to membranes. One might argue that deleting the whole G-domain of *TgRME-1* might destroy a lot more interactions of the protein by removing parts of its secondary structure than just preventing the ATP-binding of the protein. This is certainly the case and in future studies a mutation of just the ATP-binding site in this protein seems to be a more elegant method to narrow down the domain-function on its ability to bind ATP. Nevertheless, the depletion of the

G-domain in this thesis gives a first hint on the function of the G-domain in the *Toxoplasma* TgRME-1 and probably the orthologous EHDs in apicomplexa in general, as well. Another important feature of the G-domain is the side-to-side KPFxxxNPF amino acid motif. This motif is important in the mammalian EHD2 protein for the oligomerization of the homodimer with other EHD2 proteins<sup>282</sup>. In this oligomer the EHD-domain of one dimer is interacting with the NPF motif of another to form the oligomer. Upon oligomerization the ATPase-activity is stimulated by the interaction. Interestingly, the apicomplexan EHD-protein ortholog does possess only the KPF motif, not the NPF (see chapter 1.2.1 and Fig. 3.18). Even more surprising is the fact that the second amino acid in the NPF tripeptide in both organisms, *Toxoplasma* and *Plasmodium*, is mutated from the hydrophobic amino acid Proline to a hydrophilic amino acid. In *Toxoplasma* Proline is mutated into Asparagine and in *Plasmodium* into Serine. This is surprising since EH-domains have been found to form a hydrophobic pocket that binds the hydrophobic residues of the xPF motif. This leads to the hypothesis that oligomerization does not play a major role in the working mechanism of the apicomplexan EHD or rather a weak interaction of the oligomers is present since only one of the side-to-side xPF motifs is conserved in this protein. An additional hypothesis is presented by the fact that, whereas the first of the two side-to-side xPF motifs is also present in EHD1, EHD3 and EHD4, the NPF motif is, like in apicomplexa, also not found in these paralogs of EHD2 even though they are thought to form oligomers<sup>318</sup>. Therefore it has been hypothesized that in these oligomers maybe other proteins that possess NPF motifs and interact with the EH-domains of the dimers provide a scaffold for oligomer-formation, something that still has to be experimentally confirmed. The G-domain of EHD-proteins is followed downstream of the domain by a helical middle domain and further downstream by an **EH-domain** (see chapter 1.2.1). The helical middle domain, that is known to bind to lipid membranes, and the EH-domain are connected by a linker sequence. This sequence comprises another xPF motif in all mammalian EHDs (GPF) that was shown to be an interaction site for both EH-domains in the dimer with the opposite monomer (see chapter 1.2.1). Interestingly, this xPF motif within the linker is also present in the apicomplexan EHD-protein which could be another indicator for the apicomplexan EHD-protein also being able to dimerize (Fig. 1.11). Nevertheless, in both, *Toxoplasma* and *Plasmodium*, respectively, the first amino acid of the xPF motif has mutated from a hydrophobic amino acid in mammalian EHDs (Glycine) to a hydrophilic amino acid (Serine or Threonine, respectively). It is not quite sure, yet, which impact this could have for the binding properties since most of the interaction is mediated by the Proline and the phenylalanine<sup>289</sup>. To investigate the function of the EH-domain of TgRME-1 in this thesis I generated an overexpression-mutant of the protein tagged with a N-terminal fluorescent tag that lacked the EH-domain (see chapter 3.2.3). The experiments showed, that deletion of the EH-domain in this protein did not change its localization to a punctate structure within the parasite, similar to the full-length protein (localization discussed in chapter 4.2.3). From the

literature about human and other EHD-proteins it is known that the deletion of the EH-domain could have several impacts on the protein: **1)** The EH-domain is known to be the interaction domain of an EHD-protein through which it binds to other proteins that harbour NPF motives. A deletion of the EHD-domain therefore would stop the proteins' ability to interact with possible interaction partners. So far no data are present suggesting a specific interaction partner of the apicomplexan EHD-protein. Nevertheless, since the localization to the specific punctum structure of the parasite is not affected in the EH-domain deletion mutant this localization does not seem to be dependent on interaction partners mediated by an EH-domain-NPF motif-interaction. **2)** The EH-domain has been shown to be important for oligomerization of human EHD-proteins as discussed above. Additionally, without certain amino acid motives present in the apicomplexan EHD-protein it is not quite clear, to which extent oligomerization is happening for these proteins at all. Nevertheless, if at all happening in the full-length protein, deletion of the EH-domain should inhibit oligomerization of the apicomplexan protein. This means, that also oligomerization is not necessary for the localization of the apicomplexan EHD-protein to the punctum structure within the parasite. This is in agreement with a third consideration: **3)** EH-domains, in addition to binding to NPF motives in proteins, have also been shown to be interacting with lipid-molecules such as phosphoinositides. The binding of these lipids leads to a localization of EHD1 to long tubular endosomal membranes. I was able to show a localization of *TgRME-1* in tachyzoites and *PbEHD* in liver-stage parasites on tubular structures, as well (discussed in chapter 4.2.3). Both, the mutation of the lipid-binding site in the EH-domain and also the truncation of the whole domain of mammalian EHD1 led to a change in the cellular localization of the protein from a punctum-tubular intermediar phenotype to a solely punctated phenotype<sup>239</sup>. This indicates, that the EH-domain, via the binding to phosphoinositides, is mediating the binding of EHD-proteins to tubular structures in the cell, whereas the localization to punctate endosomes is not affected by this<sup>239</sup>. The same seems to be true for the *Toxoplasma TgRME-1* that also still showed localization to the punctum when the EH-domain was deleted (Fig. 3.12). Since localization of the *TgRME-1* $\Delta$ EH deletion mutant to tubules was not further investigated in this thesis a future investigation will be needed to confirm the assumptions made above (Fig. 3.12). Most data gained in this thesis about the structural features of the apicomplexan EHD-protein were obtained in *Toxoplasma*. Can they be transferred to *Plasmodium* as well? Is there a difference in both proteins? Even though both proteins share a high sequence similarity of almost 60% and their similarity of the G- and EH-domains is even higher there is one striking difference about both proteins and even all other EHD-proteins (Fig. 3.18). *Toxoplasma RME-1*, in contrast to all other EHD-proteins investigated so far, has a long C-terminal stretch downstream of its EH-domain (Fig. 3.18). This stretch is more than 60 amino acids long and possesses 6 experimentally confirmed phosphorylation sites<sup>290</sup>. Since all other EHD-proteins do not have this stretch it seems unlikely that *Toxoplasma* kept it if

it does not fulfill a defined purpose. The strong phosphorylation and its expression profile (upregulation during cytokinesis) could indicate for a function in signal transduction, cell-cycle related activation or an interaction of this C-terminal tail with other proteins via the phosphorylated sites. But an *in silico* analysis of this C-terminal stretch did not show significant homology with special protein domains known or any other protein sequence in other organisms. Therefore it will need further analysis to narrow down a specific function on this protein sequence.

### 4.2.3 Localization and function of EHD-proteins in apicomplexa

The localization of the apicomplexan EHD-protein was investigated in this thesis in the three different organisms *Toxoplasma gondii*, *Plasmodium berghei* and *Plasmodium falciparum*. The studies were performed applying different techniques in different organisms (*T. gondii* and *P. falciparum*: Fluorescently tagged EHD, live-imaging and fixed parasites; *P. berghei*: EHD antibody detection, fixed parasites only) and in different parasite stages. Therefore the results will be discussed separately for each organism in the following and in the end compared to each other, as far as possible. To localize the *Toxoplasma TgRME-1* within intracellular tachyzoite cell cultures a second copy of the endogenous *rme-1* gene was integrated randomly into to parasite's genome. Upstream of the open-reading frame of the gene a sequence encoding a destabilization domain (DD) followed by a sequence encoding a mCherry fluorescent tag were cloned (compare Fig. 3.6). A time-course assay of the DDmCherry *TgRME-1*-expression after Shield-1-induction (1 $\mu$ M) showed a time dependent expression of the protein by western blot in relation to the amount of time spent after addition of Shield-1 (Fig. 3.7). The fusion protein blotted on a western blot under reducing conditions revealed a molecular weight of slightly higher than 100 kDa which is in the range of the calculated weight (TGME49\_031210 66,7 kDa; mCherry-tag 28.8 kDa; DD-tag 12 kDa). After two hours of protein expression only a weak cytosolic mCherry signal in IFA-studies could be observed within the parasite. This changed after 4 hours of expression when few fluorescently labeled puncta occurred within the parasites (Fig. 3.7). Over time these puncta became more apparent but even though there was still an increasing amount of protein produced between 8 and 24 hours (ON) after start of the induction as seen on the western blot, there was no change in the localization of the fluorescent signal of the parasites after 8 hours. This indicates for a saturated location of the protein on the cellular level and that further overexpression of the protein does not change the phenotype anymore. This was supported by the fact that also the increase of the Shield1-concentration did not change the localization of the protein in the cell. Most of the times in fixed parasites the mCherry signal could be found on only few puncta within the parasites, one bigger punctum (a few hundred nanometer in diameter) and some smaller ones. These structures could either be located at the apical end of the parasites or at the basal end. To determine the origin of the labeled puncta a colocalization study was performed co-labeling known parasite organelles of the

secretory and endosomal system in addition to the fluorescently tagged *TgRME-1* (Fig. 3.11). The endosomal system was chosen since EHD-proteins in mammalian cells have been shown to localize to this network. No colocalization of the mCherry-labeled organelle could be found for parasite secretory organelles such as Rhoptries, Micronemes and compartments of the endosomal system such as the early endosome, endosomal-like compartment and the late endosomal-like compartment. Nevertheless, the resolution of the images might have been too low to show partial colocalization of the smaller vesicular mCherry-labeled puncta with some of these organelles. But the big punctum labeled by the mCherry-tagged protein could not be seen colocalizing with one of the mentioned organelles in any parasite. There is no hint so far which compartment within the parasite *TgRME-1* could localize to since also another round shaped compartment, the apicoplast, of about the same size of the big RME-1-punctum could not be colocalized. Another similar structure has been seen before for the EHD-protein related protein dynamin-related protein B (DrpB)<sup>319</sup> (both share a dynamin-like G-domain). A tagged overexpressed version of this protein in *Toxoplasma* tachyzoites also showed an accumulation of the DrpB close to but distinct from the Golgi-apparatus. The protein, in addition, has been proven to be important for the biogenesis of secretory organelles in this study. During replication of the parasites the DrpB accumulation breaks up and reassembles again within the newly formed daughter-cells. The same dynamics were shown for the DDMCherry *TgRME-1* labeled compartment in this thesis when living parasites were imaged live under a fluorescent microscope in a live-cell chamber. Most of the time of the replication cycle the big punctum remained at a distinct focus at the apical part of the parasite. Via short-term live-imaging I was able to show that during this phase small mCherry-labeled vesicles are rapidly shuttling between the big punctum and the back end of the parasite (supplementary movie 2). When the parasites start to form daughter-cells, analogous to DrpB, the big punctum fragments and smaller fragments localize to the apical tips of the daughter-cells, as shown by long term imaging (Fig. 3.9 and Fig. 3.10; supplementary movie 1). At a later timepoint during the replication phase the apical mCherry-labeled compartment of the mother cell moved to the back end of the cell, squeezing alongside the IMC of the newly forming daughter parasites. After cytokinesis the *TgRME-1* compartment has reemerged at the apical tip of the parasite but also remained at the basal part of the vacuole of the two newly formed parasites. Since dynamics and localization of DrpB and *TgRME-1* appeared quite similar a colocalization of both proteins was investigated in this thesis (supplementary data; Fig. 5.1). Unfortunately, no colocalization could be observed for both protein compartments. This leads to the conclusion that both proteins probably localize to different cytosolic pool-like structures but nevertheless undergo similar dynamics and might exhibit comparable functions during endodyogeny of the parasites. Another recently identified new compartment in *Toxoplasma gondii* (VAC) was shown to harbour a cathepsin-like protease, *TgCPL*<sup>320</sup>. The authors showed a function for the protease in the proteolytic processing of propeptides

destined to the secretory organelles of the parasite. They speculated about the punctate structure it localizes to it might be a lysosome or a lytic vacuole. Whereas the VAC did not colocalize with the DrpB-accumulation within the parasite either, it showed at least partial colocalization with endocytic organelles. Interestingly, also this VAC-compartment was shown to be a dynamic organelle that undergoes structural reorganisation during the cell cycle in their study. Comparable to *TgRME-1* in this thesis, also small *TgCPL* positive structures in the study of Parussini et al.<sup>320</sup> are forming during fragmentation of the VAC upon daughter-cell formation and can soon be found in the apical part of the daughter-cells. The authors could not distinguish in their study, if these structures move to the apical end of the daughter-cells or rather to the posterior end of the mother cell where they might take part in the proteolytical processing of proteins in the basal body. In the latter case the VAC compartment in the daughter-cells would be formed and loaded with *TgCPL de novo* or filled up with material from the compartment at the basal end. The same question could also not be answered for the *TgRME-1* labeled compartment in this thesis where at least a movement of the compartment to the basal end of the parasite could be shown. But here also smaller compartments appear at the apical pole of the daughter-cells before the movement of the big compartment to the posterior pole has been initiated. It will be interesting to study in the future, if the *TgRME-1* labeled compartment might be the VAC identified in the study mentioned above. But the comparison of the localization and colocalization in both studies, the one from Parussini et al. and results of my thesis, lead to the hypothesis that both might rather be two different vacuolar structures within the *Toxoplasma* parasite and both possibly members of the endosomal system. The similar dynamics during the replicative phase of the parasite leads to the hypothesis that there might be a general inheritance mechanism used in *Toxoplasma* to distribute organelle members of the endosomal system into the daughter-cells or a common specialized function for the proteins inhabited by these organelles during replication. If VAC and the *TgRME-1* compartment are not the same structure then what the latter consists of could not be defined in this thesis but will be interesting to study in the future.

One possibility for the functionality of the compartment identified in this thesis would be that of an **endosomal recycling compartment (ERC)**. Since vertebrate EHD-proteins have been found to localize to the ERC (see chapter 1.2.2) a colocalization with this organelle might be possible. Nevertheless, an ERC has never been identified in *Toxoplasma* so far and its existence would raise the question: What would be recycled or transported to the ERC? The intracellular forms of apicomplexan parasites reside within a parasitophorous vacuole in mammalian cells. This means their internal organelles are surrounded by three membranes that block them from nutrients in the surrounding medium: The plasmamembrane of the host cell (HPM), the parasitophorous vacuole membrane (PVM) and the parasite membrane (PM) (see chapter 1.1.2). To acquire nutrients they can not synthesize themselves *de novo*. Therefore the parasites need to take up nutrients from their host cell cross-

ing the lipid bilayers of the PVM and the PM. Whereas the PVM contains pores facilitating passive diffusion of low molecular weight molecules into the PV the PM is not permeable and needs active processes to be crossed<sup>321</sup>. One of these active processes is endocytosis, still a mystery in apicomplexa today and hence not fully understood. Nevertheless, first evidence has been found almost two decades ago already that endocytosis is in fact occurring at a special site in the anterior half of the parasite at the parasite membrane, the micropore<sup>322</sup>. This invagination of the plasma membrane penetrates the parasite cytoskeleton, the IMC, to allow vesicular trafficking into the parasite cytosol. In eukaryotic cells the endocytosis of nutrients from the outside of the cells can be mediated either via fluid-phase endocytosis or receptor-mediated endocytosis. During receptor-mediated endocytosis a receptor on the surface of the cell is internalized via endocytosis while having bound a ligand. This allows a specific uptake of molecules that are existing in a low concentration at a high rate from outside the cell. The vesicles containing the receptors having bound (or not having bound) their ligand are then transported to the early endosome (EE) from where their content will be further transported to the final destination (see Fig. 1.10). The receptors internalized together with their ligands will be recycled back to the surface for several additional rounds of receptor-mediated endocytosis via the fast route directly back from the early endosome, or through a slower process that is organized at the endosomal recycling compartment (ERC)<sup>223</sup>. In these receptor-mediated endocytosis and receptor-recycling processes many proteins of the EHD-family are involved (see chapter 1.2.2). It is not clear because of the lack of knowledge about endocytosis in apicomplexa, though, if receptor-mediated endocytosis also occurs in these organisms and which receptors would be recycled. But a conserved sorting motif in apicomplexa for intracellular trafficking known from mammalian cells indeed indicates this process might also be conserved in apicomplexans<sup>323</sup>. Neither is it known, if an ERC exists in these parasites in addition to early and late endosomes. But in addition to recycling receptors back to the cell surface the ERC and recycling endosomes have been shown to play an important role in cytokinesis, as well<sup>324 325</sup>. By trafficking of recycling endosomes and Golgi-derived vesicles the cells contribute membrane to the cleavage furrow. In addition, they have been shown to facilitate abscission during the last phase of the cytokinesis, an ability that is also known for EHD-proteins. Interestingly, the live-imaging studies of the TgRME-1 in *Toxoplasma* have shown a localization of the protein to the very end of the parasites after the cellular division has occurred. Here the protein localized to the connection point of the two daughter-cells and the residual body where abscission might be facilitated by the TgRME-1 protein.

Another nutrient uptake different to receptor-mediated endocytosis the apicomplexan EHD-protein might be involved in is the scavenging and uptake of lipids from host cells. It has been shown for *Toxoplasma gondii* for example that the parasite can mobilize lipid resources from the host cell for its intracellular growth. The PVM of the parasite after formation inside the host cell becomes rapidly associated to sites



of the host cell lipid biosynthesis such as the ER and mitochondrial membranes<sup>326 327 328 329</sup>. In addition, it has been shown that *Toxoplasma gondii* scavenges lipid resources such as low-density lipoprotein (LDL) and cholesterol from the host cell to use them as a lipid source for the mass production of membranes<sup>330 331</sup>. Therefore the parasite stores the uptaken lipids in so-called lipid bodies and endomembranes and thereby maintains its lipid homeostasis. During replication neutral lipids are transported from the lipid body to the ER and the Golgi to incorporate them into the lipid metabolism. But the exact composition of lipid bodies is not yet known<sup>331</sup>. Even though the parasites are able to produce fatty acids, precursors of all kinds of lipids, through a special FASII-pathway, some parasite stages and some parasite strains do need take up host-cell derived lipids to ensure optimal growth (see chapter 1.1.2). EHD-proteins in apicomplexans might be mediators of the uptake, storage and/or trafficking of these lipids before and especially during cellular division. At this timepoint in the lifecycle there is a very high demand of lipids for the production of membranous structures in daughter-cells. Because of their lipid-binding ability and their ability to pinch off vesicles from membranes apicomplexan EHD-proteins might be a very good motor to help sort and distribute lipid resources during replication of the parasite. EHD1 for example has already been shown to be involved in the regulation of cholesterol homeostasis and lipid droplet storage in mammalian cells<sup>256</sup>. The *TgRME-1* labeled compartment together with the structures seen for *Plasmodium* liver stages discussed below might represent lipid storage compartments of these parasites that are reorganized and trafficked during replication to the newly forming membranous structures. To investigate localization of the EHD-protein in *Plasmodium berghei* an antibody, generated against the amino-acids 339-533 of the *Plasmodium falciparum* EHD-protein (kindly provided by Dr. Tobias Spielmann, BNI Hamburg), was used in IFA studies on sporozoites, liver-stages and blood-stages. Since the respective amino acid sequences of both orthologous proteins, *PbEHD* and *PfEHD*, respectively, are highly similar the *PfEHD*-specific antibody promised to be detecting the protein in *P. berghei*, as well. Indeed, using the antibody on PFA-fixed *P. berghei* **sporozoites** led to a specific signal of *PbEHD* in a vesicular pattern within the sporozoites (see Fig. 3.23). This staining looked very similar in all salivary gland sporozoites observed, indicating for rather static dynamics, and the vesicles seemed to be distributed more or less homogenously over the whole body of the parasite. Most of the vesicles located at the periphery of the cytosol of the parasite in close association with the plasma membrane, even though a lack of antibodies generated in a background other than mouse did not allow a costaining with this membrane and other cellular markers. Depleting parasites from *PbEHD* (discussed in detail further below) did not lead to a impaired development of *P. berghei* salivary gland sporozoites which leads to the conclusion that the protein is not needed during this phase of the parasites' lifecycle. Therefore the abundance of the *PbEHD*-labeled vesicles suggests them being a storage compartment harboring proteins or nutrients such as lipids etc. that are needed in later stages. It has

been shown before that parasite stages already prepare themselves molecularly before they are transmitted to a new host that has different environmental conditions. There they establish as different stages that require a rapid molecular and cellular re-programming of the parasite. For example gametocytes have been shown to store translationally repressed mRNAs and proteins that are required much later during formation of ookinets in the mosquito<sup>332 333 334</sup>. In addition, protein storage has been shown in *Plasmodium* sporozoites, as well. Most of these stored proteins known so far are required for gliding motility, invasion of liver cells and formation of the parasitophorous vacuole of the parasites and are released only by specific triggers in the mammalian host. For example TRAP, a protein essential for the sporozoite motility and cell invasion is stored in secretory organelles, the micronemes, and released from the parasite upon a calcium trigger<sup>335 336 337</sup>. Most of the known proteins stored in sporozoites are secretory proteins released from secretory apical organelles, since they are needed immediately upon contact with host cells. The fact that the *PbEHD* pattern in sporozoites suggests no localization of the protein to apical organelles leads, together with the lack of any indication that it might be secreted at all, to the assumption, that the protein is not secreted and needed upon host cell contact.

Nevertheless, the presence and abundance of the protein in IFA studies in this thesis during the sporozoite stage argues for a function of the protein shortly after the entry into the host. This is in concordance with the results obtained during liver-stage development for a *pbehd* (-) parasite created in this thesis. In these parasites the *pbehd* open reading frame (ORF) was disrupted by integrating a plasmid carrying a resistance marker via single-crossover into it (see chapter 3.2.7). Thereby, even though transcription might still occur, translation of the protein is most unlikely. A double crossover replacement strategy was also followed up to completely remove the open-reading frame from the parasite but was not successful because of an inability to amplify the 3'UTR from the ORF of the gene. This goes in line with the results of Pfander et al.<sup>292</sup> who were also not able to include the 3'-part of the gene into their recombination vectors. A reason for that might be a tight regulation of the gene expression of this gene and the resulting tight packaging of the gene by histones and other DNA-binding proteins on genomic level. Thereby the secondary structure of the locus at the 3' part of the gene might not be accessible for amplification and cloning strategies. In this thesis, by integration of the whole plasmid into the *pbehd* ORF the sequence was disrupted. A single-crossover integration can be reversible and removed by the parasite from its genome. Therefore the parasites were checked again for the existence of a wildtype population after having completed a lifecycle. No reversion to the wildtype could be observed in these cases. The recombinant parasites did not show any growth defect during *in vivo* blood-stage and mosquito-stage development and during *in vitro* liver-stage development 24 hours after invasion of hepatocytes. But they were significantly smaller after 48 hours growth *in vitro* in comparison to wildtype parasites. The invasion of sporozoites into hepatoma cells

did not seem to be affected since the numbers of liver-stages in this setup did not differ from the ones obtained for wildtype parasites. This also indicates that *PbEHD* has a function for *Plasmodium* parasites during the liver phase. In addition, the delay in liver stage growth was also confirmed by *in vivo* data showing a significant delay of prepatency of mice infected with the *pbehd* (-) sporozoites in comparison to wildtype-infected mice.

When the localization of *PbEHD* was investigated in wildtype **liverstages** *in vitro* using the antibody described above an interesting pattern could be observed (see Fig. 3.24 and Fig. 3.25). The dynamics of this pattern seemed to be similar to the ones observed for the *TgRME-1* compartment in *Toxoplasma gondii* discussed above. In liver stage trophozoites 24 hours after invasion the protein localized to a single compartment within the parasite. This compartment had a strongly antibody-labeled core, indicating for a great amount of protein, and tubulated structures that emerged from the core into the cytosol of the parasite. Interestingly, in most of the parasites the core located to the periphery of the parasites in close association with the host cell nucleus. In later stages 48 hours after invasion, when schizogony is taking place, the *PbEHD* compartment fragmented and split up into vesicular structures and tubules that seemed to localize around the nuclei of the newly forming daughter merozoites. Together with the fact, that in *pbehd* (-) parasites the growth of the liver parasites between 24 and 48 hours is slowed down I would hypothesize a function of *PbEHD* in liverstages for the supply of the parasites with nutrients. Scavenging of nutrients from the host cell has already been shown for *P. berghei* liver stages. Quite recently, it has been shown that an essential cofactor for enzymes, lipoic acid, is most likely taken up via the close association of the parasite and the host cell endoplasmic reticulum<sup>338</sup>, though the exact mechanism is not known, yet. In this study the blockage of the lipoic acid uptake via an lipoic acid analogue did have a great impact on the liver stage parasites during later stages of development, when schizogony was occurring, and led to an impaired but not complete blockage of full liver stage development<sup>338</sup>. The fact that these data are quite similar to the ones observed in this thesis for *PbEHD* does not necessarily mean that *PbEHD* is involved in lipoic acid uptake. The localizations of lipoic acid and *PbEHD* in liver stages differ to some extent, anyways. But it underlines again how important nutrient uptake for schizogony and maturation of liver stages is and that depletion of some nutrients can lead to a phenotype observed for *pbehd* (-) parasites.

Another process that eukaryotic cells are using for nutrient supply is **autophagy**. Even though the process is one of three different cell-death mechanisms it can also be used to degrade the cell's own constituents upon nutrients starvation or changing surrounding conditions<sup>339</sup>. During macroautophagy cytoplasmic components or organelles are engulfed by lysosomal membranes for degradation<sup>340</sup>. This process requires complex membrane dynamics<sup>340</sup>. Autophagosome formation is a process that is mediated by autophagy-related proteins (Atg)<sup>341 342</sup> that have interestingly also been identified in apicomplexan parasites<sup>340</sup>. It has been shown for *Toxoplasma*

for example that depletion of *TgAtg3* causes growth inhibition of the parasites<sup>343</sup>. Also, the mitochondria in these parasites show anomalies indicating for a defect in the autophagy of these organelles<sup>343</sup>. Furthermore, *Plasmodium berghei* liver-stage parasites have been shown to harbour autophagosome-like double-membrane structures that might be involved in degradation of of micronemes<sup>344 345</sup>. In addition to that, Atg8 localizes to abundant vesicles that are organized in a reticular network in *P. berghei*<sup>345</sup>. During the erythrocytic stage, in contrast, Atg8 was found to localize to the apicoplast<sup>340</sup>. Autophagy in exo-erythrocytic stages, even though not well studied yet, might represent an important step of the transition of Sporozoites into liver-stages and from these into merozoites. During both transformation steps organelles and structures such as the secretory organelles, the IMC, the nucleus and mitochondria need to be degraded or built up and segregated. In *Plasmodium berghei* liver-stage parasites it has been shown for example that during a so-called cytomere-stage the parasite apicoplast begins to reorganize and to be segregated to the newly forming merozoites<sup>346</sup>. The segregation pattern of the apicoplast shown in the study of Stanway et al.<sup>346</sup> looks very similar to that of *PbEHD* in liver-stages. In addition to that, also in *Toxoplasma* parasites autophagic vesicles have been shown to exist especially in intracellular dividing parasites<sup>343</sup>, similar to *TgRME-1*. Therefore the *TgRME-1*-labelled compartment in *Toxoplasma* and the *PbEHD-1* compartment in *Plasmodium berghei* liver-stage trophozoites might represent either an autophagosomal-like compartment or might at least take part in the degradation and segregation of organelles during the replication of the parasites. The *PbEHD*-protein's catalytic abilities might help to structure the complex membrane dynamics of these processes.

The ability of EHD-proteins to bind and bend membranes and to transport lipids as discussed above for *TgRME-1* would make it likely to assume a lipid supply function for *PbEHD*. *Plasmodium* parasites, like *Toxoplasma* as well, are in great need of lipids throughout their lifecycle. During schizogony in the liver one mothercell can produce thousands of merozoites that all are individual cells requiring membranes to surround them. This phase represents one of the fastest growth rates among eukaryotic cells known so far<sup>93</sup>. To provide itself with enough lipids (and precursors such as fatty acids) to built membranes the parasite has established two different methods, a *de novo* synthesis and in addition a mechanism to scavenge lipid resources like fatty acids from the host cell (see chapter 1.1.2 and Fig. 1.3). The scavenging of lipid resources does likely involve host cell specific proteins that interact with parasite-specific proteins to recruit lipids to the parasite. It has been shown for example that UIS3, a parasite-specific protein upregulated in invasive sporozoites and known to be essential for the liver stage development<sup>347 348</sup>, is located within the PVM<sup>349</sup> with its C-terminal tail reaching into the cytoplasm of the liver cell. Thereby it can interact indirectly with fatty acids via direct interaction with liver fatty acid binding protein (L-FABP)<sup>349 350</sup>. Deletion of UIS3 in the parasites also renders the parasites unable to develop into fully mature liver shizonts. Furthermore, downregulation of

L-FABP in liver cells by RNAi greatly inhibits proliferation of *Plasmodium* parasites whereas overexpression promotes growth<sup>349</sup>. By binding to L-FABP UIS3 may help to recruit fatty acids to the PVM and into the PV, but how these are reaching the cytosol of the parasite is not known. The further investigation of *PbEHD* may help to solve this mystery. Besides, other proteins like EXP-1 (Nyboer et al., unpublished observations) and *PfE1590w*<sup>351</sup> have been shown to interact with apolipoproteins in liver cells. Both parasite proteins are located within the PVM and even though apolipoproteins have rather shown to be involved in parasite invasion into host cells it cannot be ruled out that they are also serving as a lipid source for liver stage parasites. The data acquired in this thesis together with the recent literature suggest that *PbEHD* might be involved in storage and trafficking of lipid storage compartments/vesicles or liposomes within the liver stage parasite and in later liver stages to help tubulate and form membranes around the merozoites building up within the mother cell.

Localization of the EHD-protein in *Plasmodium* **blood stages** was carried out in two different ways: *Plasmodium falciparum* EHD was N-terminally tagged with a GFP-tag and its localization was analyzed in fixed parasites (see chapter 3.2.5). This strategy revealed a localization mainly to the plasma membrane of the parasites and more prominent to a distinct spot close to it. In contrast to that, using an antibody against the protein in *Plasmodium berghei* in IFA and immuno-EM (iEM) studies showed a localization of the protein distributed over the whole parasite, but mainly associated with membranous structures (compare Fig. 3.19). The signal obtained from both was rather low, though, indicating for a low abundance of the protein in blood stages. A semi-quantitative analysis of the structures labeled by anti-EHD antibodies in the iEM revealed that most of the protein seems to be locating to structures in the cytoplasm followed by vesicular structures/endoplasmic reticulum and the nucleus. Interestingly, also mammalian EHD2 has recently shown to be travelling to the nucleus where it represses transcription<sup>266</sup>. Most interestingly, the iEM analysis also showed a localization of *PbEHD* to the red blood cell membrane and the red blood cell lumen, leading to the assumption that this protein might also be exported in blood stages. Even though both techniques to identify the localization of the EHD-protein in both, *P. berghei* and *P. falciparum*, differed, a similar localization to membranes could be observed. Whereas in *P. falciparum* the tagging revealed a prominent localization of the protein to the parasite membrane and likely the cytostome (Dr. Tobias Spielmann, BNI Hamburg, *personal communication*), an assumed hotspot for endocytosis in blood stages, the data obtained with antibody labeling from *PbEHD* indicated the protein might be located at different intra- and extracellular organelles, probably shuttling between them. For the comparison of both, *PfEHD* and *PbEHD* in blood stages, it has to be kept in mind that the tagging of the *PfEHD* (data provided by Dr. Tobias Spielmann, BNI Hamburg) was carried out C-terminally. This strategy might interfere with the interaction of the protein with interaction partners and therefore may lead to a mislocalization of the protein.

Therefore future studies in *P. falciparum* should also include antibody labeling of the PfEHD in blood stages. The only low amount of data obtained for blood stages in this study does not explain the protein's function in these stages. But the normal viability of the *pbehd* (-) blood stages leads to the conclusion that the protein is not essential for these stages. Nevertheless, the affects might be more subtle and not visible in a parasite growth curve.

In a **complementation** experiment I tried to investigate if both proteins, the *Toxoplasma* TgRME-1 and the *Plasmodium falciparum* PfEHD can be transferred into the other respective organism. If so the localization of both was to be compared. This localization then should have led to a conclusion about the comparability of the function and similarity of the protein structure of both orthologs. Meaning, that if the orthologous protein localizes in a same pattern than the endogenous protein both probably have the same architecture, the same interaction partners and the same structures they can localize to and thereby they would be functional in the respective other apicomplexan parasite, as well. This complementation project was performed together with Florian Kruse (BNI, Hamburg) who conducted the experiment in *P. falciparum*. To allow the comparison between the orthologs, both proteins, the TgRME-1 and the PfEHD, were expressed with the exact same strategy within the respective organism (DDmCherry N-terminal tag in *T. gondii* tachyzoites; GFP-tag C-terminal in *P. falciparum* blood-stages). Interestingly, the orthologous proteins did not localize to the same compartment within the same organism but each protein localized to the same parasite structure regardless of the parasite. This means, first of all, that both proteins are determined to localize to distinct subcellular structure by their intrinsic protein architecture. Alternatively it could mean, that, if interaction proteins are also needed to direct the proteins to distinct structures, these interaction partners also seem to be present in the sister apicomplexan parasite. Nevertheless, I was never able to stably express the tagged version of PfEHD in *Toxoplasma gondii* and the parasites did not seem to grow very well. This could indicate that, even though PfEHD does not localize to the same spot within *Toxoplasma* as the endogenous protein, it still might be inhibiting processes within the parasite or block interaction partners away from the endogenous protein and therefore is toxic to the parasite. One of the problems of complementing both, TgRME-1 and PfEHD, might have been the selection of the wrong stage for the comparison. Both parasites, *Toxoplasma* and *Plasmodium*, have different life-cycles with different developmental stages and host-cells they are residing in (chapter 1.1.3). *Toxoplasma gondii* tachyzoites and *Plasmodium falciparum* asexual blood-stages were chosen for complementation and localization studies because of technical issues. But even though they are both asexual intracellular stages of their life-cycle tachyzoites are residing in nucleated humane foreskin fibroblasts (in cell culture) whereas *P. falciparum* asexual stages are growing within non-nucleated human red blood cells. Both cells represent totally different environments for the parasites and under such different conditions the need and function of EHD-proteins might be different. From the

localization studies of PbEHD in *Plasmodium berghei* liver-stages and from the more similar cellular environment of liver-stage parasites and tachyzoites it seems likely that they might share a more common EHD-protein profile than the one observed for tachyzoites and blood-stages. Therefore a complementation study of TgRME-1 in *Plasmodium* liver-stages in future might lead to a more secure hypothesis about the comparability of function and localization of both orthologs in apicomplexa. **In summary** it can be concluded from this thesis that EHD-proteins in apicomplexan parasites most likely take part in the nutrient supply of the intracellular parasites and/or in autophagocytotic-like events to promote organelle-segregation. During the growth phase of the parasite the protein localizes to a single compartment within the parasite that may represent a storage compartment such as a lipid droplet or an ERC-like compartment for lipids, recycling endosomes or other nutrients. During this phase the EHD-protein takes part in vesicular trafficking most probably from hotspots of endocytosis to the storage compartment and may also be involved in the uptake of lipids from the host cell. Upon cellular division of the parasites, during endodyogeny and schizogeny, the storage or autophagosome-like compartment fragments and is distributed to the forming daughter-cells and locates to tubules as well as vesicular structures. During this phase the protein is most-likely assisting to distribute nutrients via recycling endosomes to the forming cells or building up new membranes and segregating organelles. In addition, it is creating a new pool of nutrients within the daughter-cell. During the late stage of the cytokinesis the apicomplexan EHD-protein might also assist with the abscission of the parasites from each other.

#### 4.2.4 Virulence of the *P. berghei* ANKA strain depleted of PbEHD

When *pbehd* (-) sporozoites (discussed in chapter 4.2.3) were injected into C57BL/6 naive mice a delay in prepatency in these mice of about one day in comparison to wildtype PbA infected mice was observed. This is in agreement with the observations made for the *pbehd* (-) liver stage development observed in *in vitro* development assays where I could show that the deletion of PbEHD leads to a slowed-down liver-stage development of the parasites. The fact that the parasites reach the blood of the mice *in vivo* at all, only later than the wildtype, shows that they are in general able to fully mature in the liver cell to produce merozoites and to infect RBCs. The *pbehd* (-) parasites were generated in the PbANKA (PbA) background. The wildtype PbA parasites normally are able to induce experimental cerebral malaria (ECM) in C57BL/6 and CBA mice (ECM model explained in chapter 1.1.4). Very surprisingly, when C57BL/6 mice were infected with *pbehd* (-) sporozoites they were protected from developing ECM in 100% of the cases, went into hyperparasitaemia and died several days later than expected. In contrast all of the mice inoculated with PbA wildtype parasites developed ECM and died around day 7-8. But what is the connection between the development of ECM and PbEHD? From what is known about the generation of CM in the mouse model (chapter 1.1.4) two scenarios can

be envisaged: Either *pbehd* (-) parasites are different to the wildtype in their ability **1**) to **sequester** as bloodstages or **2**) to alert the **immune system** of their host.

**1)** Which role could *PbEHD* play in the sequestration of bloodstages? Even though in this thesis a role for *PbEHD* in receptor-recycling was not investigated, there is still the possibility that the protein is involved in this process, at least in blood-stages. As discussed in chapter 1.1.4 a role for parasite-specific receptors on the surface of infected red blood cells (iRBCs) has been shown in the generation of human cerebral malaria. By binding to endothelial receptors via parasite-specific surface proteins the iRBCs sequester and block capillaries in the brain that block blood the flow and lead to the recruitment of immune cells. Even though the role of sequestration for the generation of ECM is not as clear as in human CM a few observed factors have led to the conclusion that parasite-specific receptors might be involved in this model as well (compare chapter 1.1.4). Therefore the possibility exists that *PbEHD* is involved in the receptor-recycling of adhesion molecules on the surface of RBCs. The depleted expression of the protein in *pbehd* (-) parasites would then lead to a reduced expression of surface markers of the iRBC because the recycling and trafficking back to the surface is not possible anymore. It has been shown for example, that siRNA knock-down experiments of human EHD-proteins resulted in a blockage of the transferrin receptor-recycling of HeLa cells that remained within the perinuclear region of the cell instead of trafficking to the cytoplasmic membrane as shown for EHD-expressing wildtype cells<sup>262</sup>. Nevertheless, since no receptor has been identified in *P. berghei* so far that is mediating iRBC-endothelium contact this receptor-recycling hypothesis could not be tested in this thesis. But to test if solely the bloodstage phase is responsible for the protection from ECM symptoms in *pbehd* (-) infected mice I circumvented the liver phase by directly transferring blood containing  $1 \times 10^6$  iRBCs to naive C57BL/6 animals. But surprisingly 2 out of 3 mice in this setup were not protected from severe symptoms and died from ECM. This means that even though the bloodstage phase and receptor-recycling therein might play a partial role in the protection from ECM in the *pbehd* (-) C57BL/6 model the main protection is mediated by the liverstage phase. During the liverstage the second factor that is involved in the generation of human CM and ECM might play a role, the immune system.

**2)** The immune system has been shown to play an important role in the generation of human CM and ECM (chapter 1.1.4). But it is mostly unknown so far which role the immune-reaction generated by the liverstage parasites is playing in the generation of CM. Nevertheless, the results obtained from the *pbehd* (-) bloodstage transfer discussed above indicate for a strong correlation between the liverstage and protection from ECM. But what is the difference between the liverstages of *pbehd* (-) and wildtype liverstage parasites and how could this difference influence the outcome of ECM? The only difference between both parasite strains determined



in this thesis was the growth rate during their liverstage development and as a result the time they spent within the liver cell. In contrast to the wildtype PbA parasites *pbehd* (-) parasites spent about 24 hours longer within these cells in average. Could that lead to a difference in the generation of an immune reaction against the parasites? Yes it could. Comparing the ECM-generating strain PbA to the non-ECM strain NK65 shows, that also NK65 develops slower within the liver. Comparing the immunological profile of both parasites showed that NK65 is inducing a higher level of the anti-inflammatory cytokine IL-10 in infected mice than PbA and that could then lead to a prevention of the generation of ECM symptoms (Lewis and Joschko, *unpublished observations*). In fact, when IL-10 knockout mice were infected with NK65 parasites ECM symptoms were induced (Lewis and Joschko, *unpublished observations*). To test, if IL-10 also plays a role for the protection of mice infected with *pbehd* (-) parasites from ECM, mice were depleted from IL-10 via an anti-IL10 depletion antibody during the liverstage phase. Indeed, 3 out of 3 mice infected with *pbehd* (-) parasites and depleted from IL-10 did develop ECM whereas control mice not depleted did not show ECM symptoms.

These results indicate that the slow down of the liverstage development of *pbehd* (-) parasites does lead to a prevention of ECM in infected C57BL/6 mice. This prevention is mediated by the anti-inflammatory cytokine IL-10. It is not clear, if the prolonged development of the parasites in the liver generates a higher level of IL-10 during this phase or if the later appearance of the parasites in the blood gives the immune system more time to act against an overshooting immune-response resulting in a cytokine storm. Higher mouse numbers for the statistical analysis and an evaluation of the immunological profile of the mice will lead to a better understanding of this phenomenon in the future.

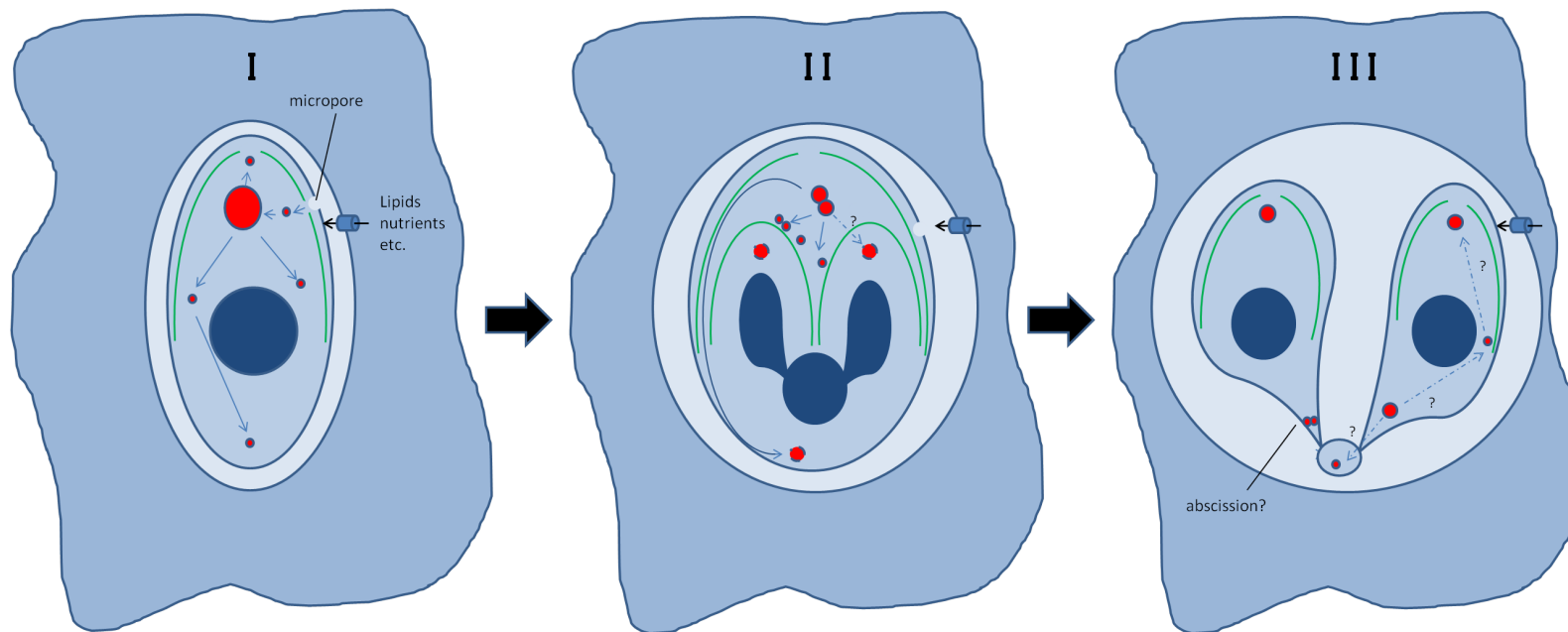


Figure 4.1: **Summary of the working hypothesis for apicomplexan EHD-proteins in parasite stages residing in nucleated cells - *Toxoplasma*.** **I)** After invasion of the host cell a *Toxoplasma* tachyzoite is scavenging lipids and other nutritional factors from the host cell that can not be synthesized *de novo* by the parasite itself. These factors are passively diffusing into the PV by pores inside the PVM or actively transported by transmembrane transporters. From the PV the factors are then endocytosed by the parasite into the parasite cytosol, most likely at the micropore of the parasite. The endocytosed or autophagic vesicles are trafficked to the endosomal system via EHD-proteins (red small circles) and other proteins and some will end up in the storage compartment labeled by the *TgRME-1*-protein (red oval-shaped structure) or will be distributed by *TgRME-1*-vesicles to other organelles. **II)** During cytokinesis the storage compartment fragments and *TgRME-1* distributes nutrients (possibly lipids etc.) to the cleavage furrow. In addition, a part of the storage compartment migrates to the back end of the parasite and also appears in the apical part of the newly formed daughter-cells (shown by the green IMC). It is not clear if this compartment in the daughter-cells is synthesized *de novo* (possibly as a autophagosome-like structure) or transported into the cell in step III. **III)** After cellular division the daughtercells are still connected via a residual body at the basal part and the *TgRME-1* protein localizes to the locus where abscission takes place. Through oligomerization *TgRME-1* might assist during abscission of the membranes. In addition, a compartment in the back end *TgRME-1* localizes to might be used to fill up a new storage compartment at the apical end of the daughter cells with nutrients. (dark blue lines: membranes; red: *TgRME-1*; green: IMC; dark blue circle: nucleus; light blue space: PV)

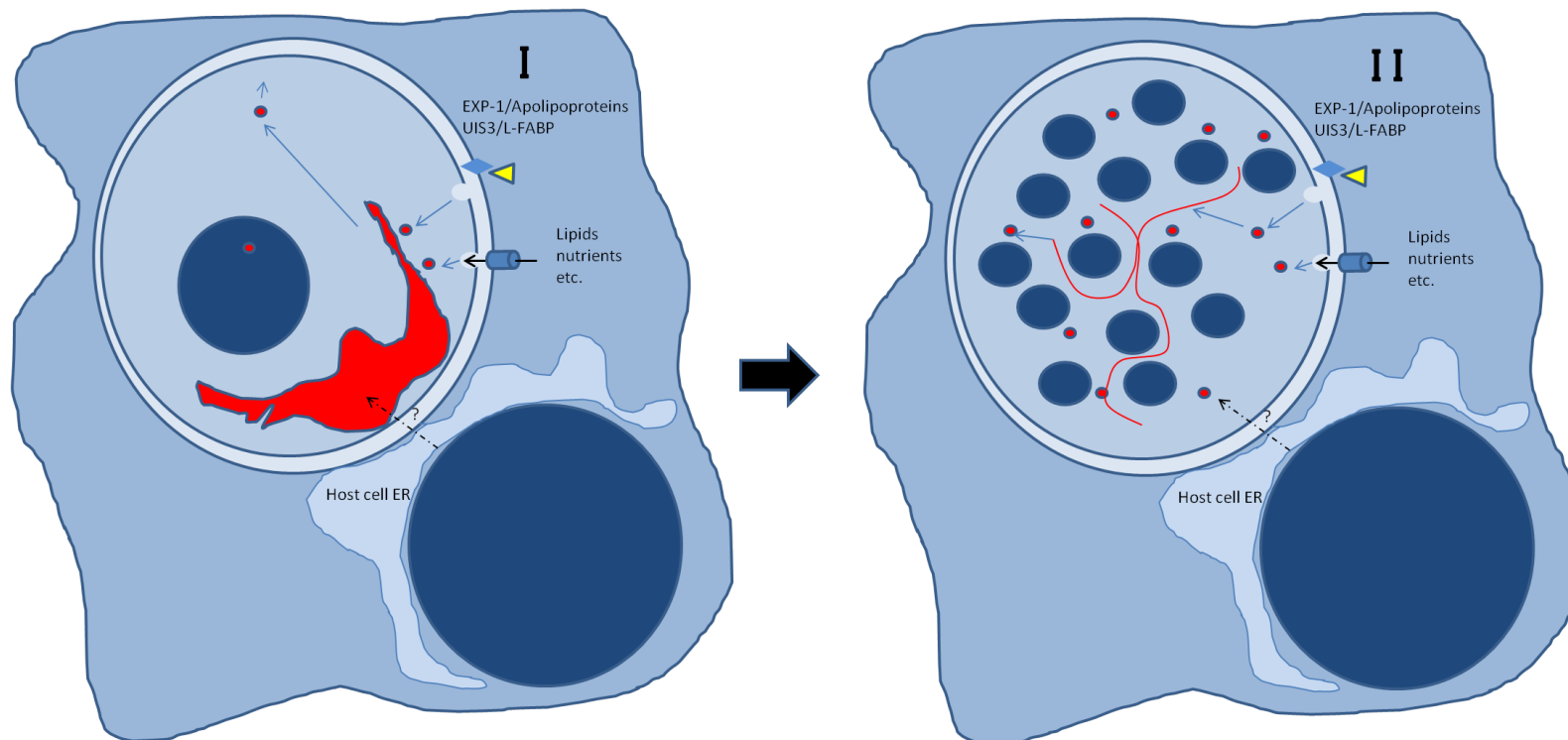


Figure 4.2: **Summary of the working hypothesis for apicomplexan EHD-proteins in parasite stages residing in nucleated cells - *Plasmodium* liver stages.** **I)** After invasion *Plasmodium* liver stages scavenge lipids and other nutrients from the host cell. Uptake of lipids into the PV might occur through the interaction of PVM resident proteins (EXP-1, UIS3) with L-FABP or apolipoproteins. From the PV the taken up factors are then most likely endocytosed and stored inside the parasite, a process likely mediated by the apicomplexan EHD-protein. The storage compartment (possibly an autophagosome-like structure) is directed towards the host cell nucleus and possibly closely associated with the host cell ER. It is not known, yet, if there is a mechanism for direct trafficking between the host cell ER and the EHD-storage compartment. **II)** During schizogony the EHD-labeled compartment is fragmenting and trafficking to the newly forming daughter merozoites and either assisting with organelle segregation (ER, apicoplast) or transporting lipids to form the new merozoite membranes. The protein can also be found on tubules that are not identified yet, but might represent membrane accumulations or the mother cell ER that are/is segregated/autophagocytosed and separated by the EHD-protein. (dark blue lines: membranes; red: *Px*EHD; dark blue circle: nucleus; light blue space: PV)

# Chapter 5

## Supplementary data

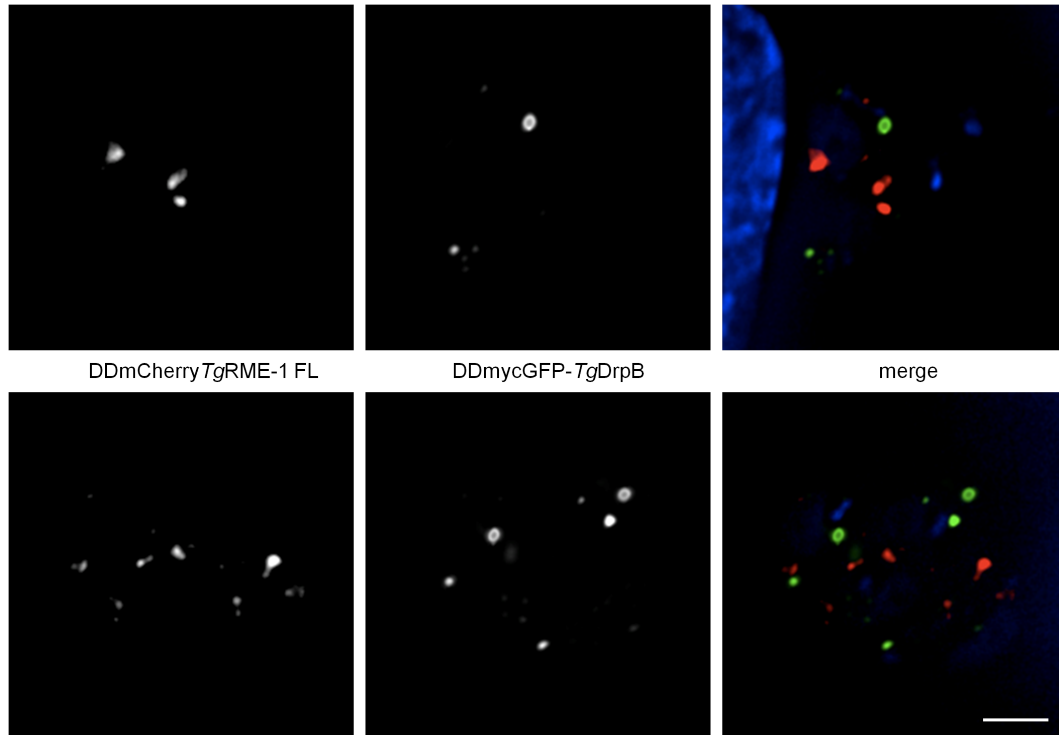


Figure 5.1: **Colocalization study of *TgRME-1* with *DrpB*.** *Toxoplasma gondii* Dynamin-related protein B tagged with a DDmycGFP-tag was episodically expressed in stably DDmCherry *TgRME-1* expressing parasites. Protein expression was induced with 1  $\mu$ M Shield-1 in intracellular parasites 6 hours before the parasites were fixed with 4%PFA and imaged under a epifluorescence microscope. (Bar: 4  $\mu$ m)

**Supplementary movie 1:** Long-term live-imaging of DDmCherry *TgRME-1* expressing parasites. Parasites were imaged as described in section 2.10.3. A picture was taken every 10 minutes and subsequently put together as a video sequence in ImageJ.

**Supplementary movie 2:** Short-term live-imaging of DDmCherry *TgRME-1* expressing parasites. Parasites were imaged as described in section 2.10.3. A picture was taken every 3 seconds and subsequently put together as a video sequence in ImageJ.

The supplementary movies can be found on the attached DVD.

# Chapter 6

## References

### References

<sup>1</sup>Cavalier-Smith T (2004) Only six kingdoms of life. *Proceedings Biological sciences / The Royal Society* 271: 1251-1262.

<sup>2</sup>Adl SM, Simpson AG, Farmer MA, Andersen RA, Anderson OR, et al. (2005) The new higher level classification of eukaryotes with emphasis on the taxonomy of protists. *The Journal of eukaryotic microbiology* 52: 399-451.

<sup>3</sup>Kuvarina ON, Leander BS, Aleshin VV, Myl'nikov AP, Keeling PJ, et al. (2002) The phylogeny of colpodellids (Alveolata) using small subunit rRNA gene sequences suggests they are the free-living sister group to apicomplexans. *The Journal of eukaryotic microbiology* 49: 498-504.

<sup>4</sup>Janouskovec J, Horak A, Obornik M, Lukes J, Keeling PJ (2010) A common red algal origin of the apicomplexan, dinoflagellate, and heterokont plastids. *Proceedings of the National Academy of Sciences of the United States of America* 107: 10949-10954.

<sup>5</sup>Wilson RJ (2002) Progress with parasite plastids. *Journal of molecular biology* 319: 257-274.

<sup>6</sup>Moore RB, Obornik M, Janouskovec J, Chrudimsky T, Vancova M, et al. (2008) A photosynthetic alveolate closely related to apicomplexan parasites. *Nature* 451: 959-963.

<sup>7</sup>Dlugonska H (2008) *Toxoplasma* rhoptries: unique secretory organelles and source of promising vaccine proteins for immunoprevention of toxoplasmosis. *Journal of biomedicine and biotechnology* 2008: 632424.

<sup>8</sup>Dvorak JA, Miller LH, Whitehouse WC, Shiroishi T (1975) Invasion of erythrocytes by malaria merozoites. *Science* 187: 748-750.

<sup>9</sup>Miller LH, Aikawa M, Johnson JG, Shiroishi T (1979) Interaction between cytochalasin B-treated malarial parasites and erythrocytes. Attachment and junction formation. *The Journal of experimental medicine* 149: 172-184.

<sup>10</sup>Carruthers VB, Tomley FM (2008) Microneme proteins in apicomplexans. *Subcellular biochemistry* 47: 33-45.

<sup>11</sup>Shaw MK, Roos DS, Tilney LG (2002) Cysteine and serine protease inhibitors block intracellular development and disrupt the secretory pathway of *Toxoplasma gondii*. *Microbes and infection / Institut Pasteur* 4: 119-132.

<sup>12</sup>Bradley PJ, Ward C, Cheng SJ, Alexander DL, Collier S, et al. (2005) Proteomic analysis of rhoptry organelles reveals many novel constituents for host-parasite interactions in *Toxoplasma gondii*. *The Journal of biological chemistry* 280: 34245-34258.

<sup>13</sup>Hakansson S, Charron AJ, Sibley LD (2001) *Toxoplasma* vacuoles: a two-step process of secretion and fusion forms the parasitophorous vacuole. *The EMBO journal* 20: 3132-3144.

<sup>14</sup>Besteiro S, Michelin A, Poncet J, Dubremetz JF, Lebrun M (2009) Export of a *Toxoplasma gondii* rhoptry neck protein complex at the host cell membrane to form the moving junction during invasion. *PLoS pathogens* 5: e1000309.

<sup>15</sup>Saeij JP, Boyle JP, Collier S, Taylor S, Sibley LD, et al. (2006) Polymorphic secreted kinases are key virulence factors in toxoplasmosis. *Science* 314: 1780-1783.

<sup>16</sup>Taylor S, Barragan A, Su C, Fux B, Fentress SJ, et al. (2006) A secreted serine-threonine kinase determines virulence in the eukaryotic pathogen *Toxoplasma gondii*. *Science* 314: 1776-1780.

<sup>17</sup>Soldati D, Lassen A, Dubremetz JF, Boothroyd JC (1998) Processing of *Toxoplasma* ROP1 protein in nascent rhoptries. *Molecular and biochemical parasitology* 96: 37-48.

<sup>18</sup>Hoppe HC, Ngo HM, Yang M, Joiner KA (2000) Targeting to rhoptry organelles of *Toxoplasma gondii* involves evolutionarily conserved mechanisms. *Nature cell biology* 2: 449-456.

<sup>19</sup>Ngo HM, Yang M, Joiner KA (2004) Are rhoptries in Apicomplexan parasites secretory granules or secretory lysosomal granules? *Molecular microbiology* 52: 1531-1541.

<sup>20</sup>Singh S, Alam MM, Pal-Bhowmick I, Brzostowski JA, Chitnis CE (2010) Distinct external signals trigger sequential release of apical organelles during erythrocyte invasion by malaria parasites. *PLoS pathogens* 6: e1000746.

<sup>21</sup>Mercier C, Dubremetz JF, Rauscher B, Lecordier L, Sibley LD, et al. (2002) Biogenesis of nanotubular network in *Toxoplasma* parasitophorous vacuole induced by parasite proteins. *Molecular biology of the cell* 13: 2397-2409.

<sup>22</sup>Paredes-Santos TC, de Souza W, Attias M (2012) Dynamics and 3D organization of secretory organelles of *Toxoplasma gondii*. *Journal of structural biology* 177: 420-430.

<sup>23</sup> Nam HW (2009) GRA proteins of *Toxoplasma gondii*: maintenance of host-

parasite interactions across the parasitophorous vacuolar membrane. The Korean journal of parasitology 47 Suppl: S29-37.

<sup>24</sup>Kilejian A (1975) Circular mitochondrial DNA from the avian malarial parasite *Plasmodium lophurae*. *Biochimica et biophysica acta* 390: 276-284.

<sup>25</sup>Gardner MJ, Feagin JE, Moore DJ, Spencer DF, Gray MW, et al. (1991) Organisation and expression of small subunit ribosomal RNA genes encoded by a 35-kilobase circular DNA in *Plasmodium falciparum*. *Molecular and biochemical parasitology* 48: 77-88.

<sup>26</sup>Gardner MJ, Williamson DH, Wilson RJ (1991) A circular DNA in malaria parasites encodes an RNA polymerase like that of prokaryotes and chloroplasts. *Molecular and biochemical parasitology* 44: 115-123.

<sup>27</sup>Gardner MJ, Feagin JE, Moore DJ, Rangachari K, Williamson DH, et al. (1993) Sequence and organization of large subunit rRNA genes from the extrachromosomal 35 kb circular DNA of the malaria parasite *Plasmodium falciparum*. *Nucleic acids research* 21: 1067-1071.

<sup>28</sup>Wilson RJ, Denny PW, Preiser PR, Rangachari K, Roberts K, et al. (1996) Complete gene map of the plastid-like DNA of the malaria parasite *Plasmodium falciparum*. *Journal of molecular biology* 261: 155-172.

<sup>29</sup>Moore RB, Obornik M, Janouskovec J, Chrudimsky T, Vancova M, et al. (2008) A photosynthetic alveolate closely related to apicomplexan parasites. *Nature* 451: 959-963.

<sup>30</sup>Obornik M, Vancova M, Lai DH, Janouskovec J, Keeling PJ, et al. (2011) Morphology and ultrastructure of multiple life cycle stages of the photosynthetic relative of apicomplexa, *Chromera velia*. *Protist* 162: 115-130.

<sup>31</sup>Zhu G, Marchewka MJ, Keithly JS (2000) *Cryptosporidium parvum* appears to lack a plastid genome. *Microbiology* 146 ( Pt 2): 315-321.

<sup>32</sup>Abrahamsen MS, Templeton TJ, Enomoto S, Abrahante JE, Zhu G, et al. (2004) Complete genome sequence of the apicomplexan, *Cryptosporidium parvum*. *Science* 304: 441-445.

<sup>33</sup>Xu P, Widmer G, Wang Y, Ozaki LS, Alves JM, et al. (2004) The genome of *Cryptosporidium hominis*. *Nature* 431: 1107-1112.

<sup>34</sup>Toso MA, Omoto CK (2007) *Gregarina niphandrodes* may lack both a plastid genome and organelle. *The Journal of eukaryotic microbiology* 54: 66-72.

<sup>35</sup>Kohler S, Delwiche CF, Denny PW, Tilney LG, Webster P, et al. (1997) A plastid of probable green algal origin in Apicomplexan parasites. *Science* 275: 1485-1489.

<sup>36</sup>Fichera ME, Roos DS (1997) A plastid organelle as a drug target in apicomplexan parasites. *Nature* 390: 407-409.

<sup>37</sup>He CY, Shaw MK, Pletcher CH, Striepen B, Tilney LG, et al. (2001) A plastid segregation defect in the protozoan parasite *Toxoplasma gondii*. *The EMBO journal* 20: 330-339.

<sup>38</sup>Waller RF, Keeling PJ, Donald RG, Striepen B, Handman E, et al. (1998) Nuclear-encoded proteins target to the plastid in *Toxoplasma gondii* and *Plasmodium falciparum*. *Proceedings of the National Academy of Sciences of the United States of America* 95: 12352-12357.

<sup>39</sup>Ramakrishnan S, Docampo MD, Macrae JI, Pujol FM, Brooks CF, et al. (2012) Apicoplast and endoplasmic reticulum cooperate in fatty acid biosynthesis in apicomplexan parasite *Toxoplasma gondii*. *The Journal of biological chemistry* 287: 4957-4971.

<sup>40</sup>Vaughan AM, O'Neill MT, Tarun AS, Camargo N, Phuong TM, et al. (2009) Type II fatty acid synthesis is essential only for malaria parasite late liver stage development. *Cellular microbiology* 11: 506-520.

<sup>41</sup>Yu M, Kumar TR, Nkrumah LJ, Coppi A, Retzlaff S, et al. (2008) The fatty acid biosynthesis enzyme FabI plays a key role in the development of liver-stage malarial parasites. *Cell host & microbe* 4: 567-578.

<sup>42</sup>Zhu G, Li Y, Cai X, Millership JJ, Marchewka MJ, et al. (2004) Expression and functional characterization of a giant Type I fatty acid synthase (CpFAS1) gene from *Cryptosporidium parvum*. *Molecular and biochemical parasitology* 134: 127-135.

<sup>43</sup>Zhu G, Shi X, Cai X (2010) The reductase domain in a Type I fatty acid synthase from the apicomplexan *Cryptosporidium parvum*: restricted substrate preference towards very long chain fatty acyl thioesters. *BMC biochemistry* 11: 46.

<sup>44</sup>Mazumdar J, Striepen B (2007) Make it or take it: fatty acid metabolism of apicomplexan parasites. *Eukaryotic cell* 6: 1727-1735.

<sup>45</sup>Goodman CD, McFadden GI (2007) Fatty acid biosynthesis as a drug target in apicomplexan parasites. *Current drug targets* 8: 15-30.

<sup>46</sup>Tarun AS, Vaughan AM, Kappe SH (2009) Redefining the role of de novo fatty acid synthesis in *Plasmodium* parasites. *Trends in parasitology* 25: 545-550.

<sup>47</sup>Morrisette NS, Sibley LD (2002) Cytoskeleton of apicomplexan parasites. *Microbiology and molecular biology reviews* : MMBR 66: 21-38; table of contents.

<sup>48</sup>Adams JH, Todd KS, Jr. (1983) Transmission electron microscopy of intracellular sporozoites of *Eimeria vermiformis* (Apicomplexa, Eucoccidiida) in the mouse. *The Journal of protozoology* 30: 114-118.



<sup>49</sup>Beaudoin RL, Strome CP (1973) Plasmodium lophurae: the ultrastructure of the exoerythrocytic stages. *Experimental parasitology* 34: 313-336.

<sup>50</sup>Desser SS (1980) An ultrastructural study of the asexual development of a presumed *Isoospora* sp. in mononuclear, phagocytic cells of the evening grosbeak (*Hesperiphona vespertina*). *The Journal of parasitology* 66: 601-612.

<sup>51</sup>Nichols BA, Chiappino ML (1987) Cytoskeleton of *Toxoplasma gondii*. *The Journal of protozoology* 34: 217-226.

<sup>52</sup>Roberts WL, Hammond DM, Anderson LC, Speer CA (1970) Ultrastructural study of schizogony in *Eimeria callospermophili*. *The Journal of protozoology* 17: 584-592.

<sup>53</sup>Stokkermans TJ, Schwartzman JD, Keenan K, Morrissette NS, Tilney LG, et al. (1996) Inhibition of *Toxoplasma gondii* replication by dinitroaniline herbicides. *Experimental parasitology* 84: 355-370.

<sup>54</sup>Russell DG, Burns RG (1984) The polar ring of coccidian sporozoites: a unique microtubule-organizing centre. *Journal of cell science* 65: 193-207.

<sup>55</sup>Foussard F, Gallois Y, Tronchin G, Robert R, Mauras G (1990) Isolation of the pellicle of *Toxoplasma gondii* (Protozoa, Coccidia): characterization by electron microscopy and protein composition. *Parasitology research* 76: 563-565.

<sup>56</sup>Moore J, Sinden RE (1974) Fine structure of *Plasmodium mexicanum*. *The Journal of parasitology* 60: 825-834.

<sup>57</sup>Kelley GL, Hammond DM (1972) Fine structural aspects of early development of *Eimeria ninakohlyakimovae* in cultured cells. *Zeitschrift fur Parasitenkunde* 38: 271-284.

<sup>58</sup>Schrevel J, Asfaux-Foucher G, Bafort JM (1977) [Ultrastructural study of multiple mitoses during sporogony of *Plasmodium b. berghei*]. *Journal of ultrastructure research* 59: 332-350.

<sup>59</sup>Striepen B, Crawford MJ, Shaw MK, Tilney LG, Seeber F, et al. (2000) The plastid of *Toxoplasma gondii* is divided by association with the centrosomes. *The Journal of cell biology* 151: 1423-1434.

<sup>60</sup>Mann T, Beckers C (2001) Characterization of the subpellicular network, a filamentous membrane skeletal component in the parasite *Toxoplasma gondii*. *Molecular and biochemical parasitology* 115: 257-268.

<sup>61</sup>Dubremetz JF, Torpier G (1978) Freeze fracture study of the pellicle of an eimerian sporozoite (Protozoa, Coccidia). *Journal of ultrastructure research* 62: 94-109.

<sup>62</sup>Porchet E, Torpier G (1977) [Freeze fracture study of *Toxoplasma* and *Sarcocystis* infective stages (author's transl)]. *Zeitschrift für Parasitenkunde* 54: 101-124.

<sup>63</sup>Wesseling JG, Snijders PJ, van Someren P, Jansen J, Smits MA, et al. (1989) Stage-specific expression and genomic organization of the actin genes of the malaria parasite *Plasmodium falciparum*. *Molecular and biochemical parasitology* 35: 167-176.

<sup>64</sup>Dobrowolski JM, Niesman IR, Sibley LD (1997) Actin in the parasite *Toxoplasma gondii* is encoded by a single copy gene, ACT1 and exists primarily in a globular form. *Cell motility and the cytoskeleton* 37: 253-262.

<sup>65</sup>Poupel O, Tardieux I (1999) *Toxoplasma gondii* motility and host cell invasiveness are drastically impaired by jasplakinolide, a cyclic peptide stabilizing F-actin. *Microbes and infection / Institut Pasteur* 1: 653-662.

<sup>66</sup>Shaw MK, Tilney LG (1999) Induction of an acrosomal process in *Toxoplasma gondii*: visualization of actin filaments in a protozoan parasite. *Proceedings of the National Academy of Sciences of the United States of America* 96: 9095-9099.

<sup>67</sup>Schmitz S, Grainger M, Howell S, Calder LJ, Gaeb M, et al. (2005) Malaria parasite actin filaments are very short. *Journal of molecular biology* 349: 113-125.

<sup>68</sup>Sahoo N, Beatty W, Heuser J, Sept D, Sibley LD (2006) Unusual kinetic and structural properties control rapid assembly and turnover of actin in the parasite *Toxoplasma gondii*. *Molecular biology of the cell* 17: 895-906.

<sup>69</sup>Higgs HN, Pollard TD (2001) Regulation of actin filament network formation through ARP2/3 complex: activation by a diverse array of proteins. *Annual review of biochemistry* 70: 649-676.

<sup>70</sup>Weaver AM, Young ME, Lee WL, Cooper JA (2003) Integration of signals to the Arp2/3 complex. *Current opinion in cell biology* 15: 23-30.

<sup>71</sup>Morahan BJ, Wang L, Coppel RL (2009) No TRAP, no invasion. *Trends in parasitology* 25: 77-84.

<sup>72</sup>Heintzelman MB, Schwartzman JD (2001) Myosin diversity in Apicomplexa. *The Journal of parasitology* 87: 429-432.

<sup>73</sup>Bergman LW, Kaiser K, Fujioka H, Coppens I, Daly TM, et al. (2003) Myosin A tail domain interacting protein (MTIP) localizes to the inner membrane complex of *Plasmodium* sporozoites. *Journal of cell science* 116: 39-49.

<sup>74</sup>Hettmann C, Herm A, Geiter A, Frank B, Schwarz E, et al. (2000) A dibasic motif in the tail of a class XIV apicomplexan myosin is an essential determinant of plasma membrane localization. *Molecular biology of the cell* 11: 1385-1400.

<sup>75</sup>Soldati D, Meissner M (2004) Toxoplasma as a novel system for motility. *Current opinion in cell biology* 16: 32-40.

<sup>76</sup>Meissner M, Schluter D, Soldati D (2002) Role of Toxoplasma gondii myosin A in powering parasite gliding and host cell invasion. *Science* 298: 837-840.

<sup>77</sup>Beattie CP (1982) The ecology of toxoplasmosis. *Ecology of disease* 1: 13-20.

<sup>78</sup>Lingelbach K, Joiner KA (1998) The parasitophorous vacuole membrane surrounding Plasmodium and Toxoplasma: an unusual compartment in infected cells. *Journal of cell science* 111 ( Pt 11): 1467-1475.

<sup>79</sup>Sibley LD (2004) Intracellular parasite invasion strategies. *Science* 304: 248-253.

<sup>80</sup>Carruthers V, Boothroyd JC (2007) Pulling together: an integrated model of Toxoplasma cell invasion. *Current opinion in microbiology* 10: 83-89.

<sup>81</sup>Cowman AF, Crabb BS (2006) Invasion of red blood cells by malaria parasites. *Cell* 124: 755-766.

<sup>82</sup>Aikawa M, Miller LH, Johnson J, Rabbege J (1978) Erythrocyte entry by malarial parasites. A moving junction between erythrocyte and parasite. *The Journal of cell biology* 77: 72-82.

<sup>83</sup>Santos JM, Lebrun M, Daher W, Soldati D, Dubremetz JF (2009) Apicomplexan cytoskeleton and motors: key regulators in morphogenesis, cell division, transport and motility. *International journal for parasitology* 39: 153-162.

<sup>84</sup>Carruthers VB, Sibley LD (1997) Sequential protein secretion from three distinct organelles of Toxoplasma gondii accompanies invasion of human fibroblasts. *European journal of cell biology* 73: 114-123.

<sup>85</sup>Foussard F, Leriche MA, Dubremetz JF (1991) Characterization of the lipid content of Toxoplasma gondii rhoptries. *Parasitology* 102 Pt 3: 367-370.

<sup>86</sup>Coppens I, Vielemeyer O (2005) Insights into unique physiological features of neutral lipids in Apicomplexa: from storage to potential mediation in parasite metabolic activities. *International journal for parasitology* 35: 597-615.

<sup>87</sup>Boothroyd JC, Dubremetz JF (2008) Kiss and spit: the dual roles of Toxoplasma rhoptries. *Nature reviews Microbiology* 6: 79-88.

<sup>88</sup>Dluzewski AR, Mitchell GH, Fryer PR, Griffiths S, Wilson RJ, et al. (1992) Origins of the parasitophorous vacuole membrane of the malaria parasite, Plasmodium falciparum, in human red blood cells. *Journal of cell science* 102 ( Pt 3): 527-532.

<sup>89</sup>Caffaro CE, Boothroyd JC (2011) Evidence for host cells as the major contributor of lipids in the intravacuolar network of Toxoplasma-infected cells. *Eukaryotic*

cell 10: 1095-1099.

<sup>90</sup>Magno RC, Lemgruber L, Vommaro RC, De Souza W, Attias M (2005) Intravacuolar network may act as a mechanical support for *Toxoplasma gondii* inside the parasitophorous vacuole. *Microscopy research and technique* 67: 45-52.

<sup>91</sup>Magno RC, Straker LC, de Souza W, Attias M (2005) Interrelations between the parasitophorous vacuole of *Toxoplasma gondii* and host cell organelles. *Microscopy and microanalysis : the official journal of Microscopy Society of America, Microbeam Analysis Society, Microscopical Society of Canada* 11: 166-174.

<sup>92</sup>Spielmann T, Montagna GN, Hecht L, Matuschewski K (2012) Molecular make-up of the *Plasmodium* parasitophorous vacuolar membrane. *International journal of medical microbiology : IJMM*.

<sup>93</sup>Bano N, Romano JD, Jayabalasingham B, Coppens I (2007) Cellular interactions of *Plasmodium* liver stage with its host mammalian cell. *International journal for parasitology* 37: 1329-1341.

<sup>94</sup>Aikawa M (1971) Parasitological review. *Plasmodium: the fine structure of malarial parasites*. *Experimental parasitology* 30: 284-320.

<sup>95</sup>Bannister LH, Mitchell GH (1995) The role of the cytoskeleton in *Plasmodium falciparum* merozoite biology: an electron-microscopic view. *Annals of tropical medicine and parasitology* 89: 105-111.

<sup>96</sup>Hepler PK, Huff CG, Sprinz H (1966) The fine structure of the exoerythrocytic stages of *Plasmodium fallax*. *The Journal of cell biology* 30: 333-358.

<sup>97</sup>Jura WG, Brown CG, Rowland AC (1983) Ultrastructural characteristics of in vitro parasite-lymphocyte behaviour in invasions with *Theileria annulata* and *Theileria parva*. *Veterinary parasitology* 12: 115-134.

<sup>98</sup>Shaw MK, Tilney LG (1992) How individual cells develop from a syncytium: merogony in *Theileria parva* (Apicomplexa). *Journal of cell science* 101 ( Pt 1): 109-123.

<sup>99</sup>Sinden RE, Strong K (1978) An ultrastructural study of the sporogonic development of *Plasmodium falciparum* in *Anopheles gambiae*. *Transactions of the Royal Society of Tropical Medicine and Hygiene* 72: 477-491.

<sup>100</sup>Gavin MA, Wanko T, Jacobs L (1962) Electron microscope studies of reproducing and interkinetic *Toxoplasma*. *The Journal of protozoology* 9: 222-234.

<sup>101</sup>Hemphill A, Gottstein B, Kaufmann H (1996) Adhesion and invasion of bovine endothelial cells by *Neospora caninum*. *Parasitology* 112 ( Pt 2): 183-197.

<sup>102</sup>Lindsay DS, Speer CA, Toivio-Kinnucan MA, Dubey JP, Blagburn BL (1993)

Use of infected cultured cells to compare ultrastructural features of *Neospora caninum* from dogs and *Toxoplasma gondii*. *American journal of veterinary research* 54: 103-106.

<sup>103</sup>Sheffield HG, Melton ML (1968) The fine structure and reproduction of *Toxoplasma gondii*. *The Journal of parasitology* 54: 209-226.

<sup>104</sup>Entzeroth R, Chobotar B, Scholtyseck E (1982) Ultrastructure of *Sarcocystis* sp. from the muscle of a white-tailed deer (*Odocoileus virginianus*). *Zeitschrift fur Parasitenkunde* 68: 33-38.

<sup>105</sup>Read M, Sherwin T, Holloway SP, Gull K, Hyde JE (1993) Microtubular organization visualized by immunofluorescence microscopy during erythrocytic schizogony in *Plasmodium falciparum* and investigation of post-translational modifications of parasite tubulin. *Parasitology* 106 ( Pt 3): 223-232.

<sup>106</sup>Mehlhorn H, Heydorn AO (1978) The sarcosporidia (Protozoa, Sporozoa): life cycle and fine structure. *Advances in parasitology* 16: 43-91.

<sup>107</sup>Vivier E, Petitprez A (1969) [The outer membrane complex and its development at the time of the formation of daughter-cells in *Toxoplasma gondii*]. *The Journal of cell biology* 43: 329-342.

<sup>108</sup>Robert-Gangneux F, Darde ML (2012) Epidemiology of and diagnostic strategies for toxoplasmosis. *Clinical microbiology reviews* 25: 264-296.

<sup>109</sup>Afonso E, Thulliez P, Gilot-Fromont E (2006) Transmission of *Toxoplasma gondii* in an urban population of domestic cats (*Felis catus*). *International journal for parasitology* 36: 1373-1382.

<sup>110</sup>Tenter AM, Heckeroth AR, Weiss LM (2000) *Toxoplasma gondii*: from animals to humans. *International journal for parasitology* 30: 1217-1258.

<sup>111</sup>Afonso E, Poulle ML, Lemoine M, Villena I, Aubert D, et al. (2007) Prevalence of *Toxoplasma gondii* in small mammals from the Ardennes region, France. *Folia parasitologica* 54: 313-314.

<sup>112</sup>Dabritz HA, Miller MA, Gardner IA, Packham AE, Atwill ER, et al. (2008) Risk factors for *Toxoplasma gondii* infection in wild rodents from central coastal California and a review of *T. gondii* prevalence in rodents. *The Journal of parasitology* 94: 675-683.

<sup>113</sup>Smith K, Shah A, Wright K, Lewis G (1995) The prevalence and costs of psychiatric disorders and learning disabilities. *The British journal of psychiatry : the journal of mental science* 166: 9-18.

<sup>114</sup>Montoya JG, Liesenfeld O (2004) Toxoplasmosis. *Lancet* 363: 1965-1976.

<sup>115</sup>Cook AJ, Gilbert RE, Buffolano W, Zufferey J, Petersen E, et al. (2000) Sources of toxoplasma infection in pregnant women: European multicentre case-control study. European Research Network on Congenital Toxoplasmosis. *BMJ* 321: 142-147.

<sup>116</sup>Dubey JP (1988) Long-term persistence of *Toxoplasma gondii* in tissues of pigs inoculated with *T gondii* oocysts and effect of freezing on viability of tissue cysts in pork. *American journal of veterinary research* 49: 910-913.

<sup>117</sup>Dubey JP, Kotula AW, Sharar A, Andrews CD, Lindsay DS (1990) Effect of high temperature on infectivity of *Toxoplasma gondii* tissue cysts in pork. *The Journal of parasitology* 76: 201-204.

<sup>118</sup>Lambert H, Barragan A (2010) Modelling parasite dissemination: host cell subversion and immune evasion by *Toxoplasma gondii*. *Cellular microbiology* 12: 292-300.

<sup>119</sup>Barragan A, Hitziger N (2008) Transepithelial migration by *Toxoplasma*. *Sub-cellular biochemistry* 47: 198-207.

<sup>120</sup>Bierly AL, Shufesky WJ, Sukhumavasi W, Morelli AE, Denkers EY (2008) Dendritic cells expressing plasmacytoid marker PDCA-1 are Trojan horses during *Toxoplasma gondii* infection. *Journal of immunology* 181: 8485-8491.

<sup>121</sup>Miller CM, Boulter NR, Ikin RJ, Smith NC (2009) The immunobiology of the innate response to *Toxoplasma gondii*. *International journal for parasitology* 39: 23-39.

<sup>122</sup>Liesenfeld O, Dunay IR, Erb KJ (2004) Infection with *Toxoplasma gondii* reduces established and developing Th2 responses induced by *Nippostrongylus brasiliensis* infection. *Infection and immunity* 72: 3812-3822.

<sup>123</sup>Mosser DM (2003) The many faces of macrophage activation. *Journal of leukocyte biology* 73: 209-212.

<sup>124</sup>Palanisamy M, Madhavan B, Balasundaram MB, Andavar R, Venkatapathy N (2006) Outbreak of ocular toxoplasmosis in Coimbatore, India. *Indian journal of ophthalmology* 54: 129-131.

<sup>125</sup>Robert-Gangneux F, Gangneux JP, Vu N, Jaillard S, Guiguen C, et al. (2011) High level of soluble HLA-G in amniotic fluid is correlated with congenital transmission of *Toxoplasma gondii*. *Clinical immunology* 138: 129-134.

<sup>126</sup>Laliberte J, Carruthers VB (2008) Host cell manipulation by the human pathogen *Toxoplasma gondii*. *Cellular and molecular life sciences : CMLS* 65: 1900-1915.

<sup>127</sup>Saeij JP, Collier S, Boyle JP, Jerome ME, White MW, et al. (2007) *Toxoplasma* co-opts host gene expression by injection of a polymorphic kinase homologue. *Nature*

445: 324-327.

<sup>128</sup>Vutova P, Wirth M, Hippe D, Gross U, Schulze-Osthoff K, et al. (2007) Toxoplasma gondii inhibits Fas/CD95-triggered cell death by inducing aberrant processing and degradation of caspase 8. *Cellular microbiology* 9: 1556-1570.

<sup>129</sup>Bowie WR, King AS, Werker DH, Isaac-Renton JL, Bell A, et al. (1997) Outbreak of toxoplasmosis associated with municipal drinking water. The BC Toxoplasma Investigation Team. *Lancet* 350: 173-177.

<sup>130</sup>Burnett AJ, Shortt SG, Isaac-Renton J, King A, Werker D, et al. (1998) Multiple cases of acquired toxoplasmosis retinitis presenting in an outbreak. *Ophthalmology* 105: 1032-1037.

<sup>131</sup>Gilbert RE, Stanford MR, Jackson H, Holliman RE, Sanders MD (1995) Incidence of acute symptomatic toxoplasma retinochoroiditis in south London according to country of birth. *BMJ* 310: 1037-1040.

<sup>132</sup>Carme B, Bissuel F, Ajzenberg D, Bouyne R, Aznar C, et al. (2002) Severe acquired toxoplasmosis in immunocompetent adult patients in French Guiana. *Journal of clinical microbiology* 40: 4037-4044.

<sup>133</sup>Botterel F, Ichai P, Feray C, Bouree P, Saliba F, et al. (2002) Disseminated toxoplasmosis, resulting from infection of allograft, after orthotopic liver transplantation: usefulness of quantitative PCR. *Journal of clinical microbiology* 40: 1648-1650.

<sup>134</sup>Martina MN, Cervera C, Esforzado N, Linares L, Torregrosa V, et al. (2011) Toxoplasma gondii primary infection in renal transplant recipients. Two case reports and literature review. *Transplant international : official journal of the European Society for Organ Transplantation* 24: e6-12.

<sup>135</sup>Rogers NM, Peh CA, Faull R, Pannell M, Cooper J, et al. (2008) Transmission of toxoplasmosis in two renal allograft recipients receiving an organ from the same donor. *Transplant infectious disease : an official journal of the Transplantation Society* 10: 71-74.

<sup>136</sup>Luft BJ, Remington JS (1992) Toxoplasmic encephalitis in AIDS. *Clinical infectious diseases : an official publication of the Infectious Diseases Society of America* 15: 211-222.

<sup>137</sup>Rabaud C, May T, Lucet JC, Leport C, Ambroise-Thomas P, et al. (1996) Pulmonary toxoplasmosis in patients infected with human immunodeficiency virus: a French National Survey. *Clinical infectious diseases : an official publication of the Infectious Diseases Society of America* 23: 1249-1254.

<sup>138</sup>Hofman P, Bernard E, Michiels JF, Thyss A, Le Fichoux Y, et al. (1993) Extracerebral toxoplasmosis in the acquired immunodeficiency syndrome (AIDS).

Pathology, research and practice 189: 894-901.

<sup>139</sup>Abbasi M, Kowalewska-Grochowska K, Bahar MA, Kilani RT, Winkler-Lowen B, et al. (2003) Infection of placental trophoblasts by *Toxoplasma gondii*. The Journal of infectious diseases 188: 608-616.

<sup>140</sup>Dunn D, Wallon M, Peyron F, Petersen E, Peckham C, et al. (1999) Mother-to-child transmission of toxoplasmosis: risk estimates for clinical counselling. Lancet 353: 1829-1833.

<sup>141</sup>WHO (2011). World Malaria Report 2011.

<sup>142</sup>Sturm A, Amino R, van de Sand C, Regen T, Retzlaff S, et al. (2006) Manipulation of host hepatocytes by the malaria parasite for delivery into liver sinusoids. Science 313: 1287-1290.

<sup>143</sup>Graewe S, Rankin KE, Lehmann C, Deschermeier C, Hecht L, et al. (2011) Hostile takeover by *Plasmodium*: reorganization of parasite and host cell membranes during liver stage egress. PLoS pathogens 7: e1002224.

<sup>144</sup>Sadanand S (2010) Malaria: an evaluation of the current state of research on pathogenesis and antimalarial drugs. The Yale journal of biology and medicine 83: 185-191.

<sup>145</sup>Miller LH, Baruch DI, Marsh K, Doumbo OK (2002) The pathogenic basis of malaria. Nature 415: 673-679.

<sup>146</sup>Trampuz A, Jereb M, Muzlovic I, Prabhu RM (2003) Clinical review: Severe malaria. Critical care 7: 315-323.

<sup>147</sup>Kyes S, Horrocks P, Newbold C (2001) Antigenic variation at the infected red cell surface in malaria. Annual review of microbiology 55: 673-707.

<sup>148</sup>Miller LH, Baruch DI, Marsh K, Doumbo OK (2002) The pathogenic basis of malaria. Nature 415: 673-679.

<sup>149</sup>Taylor HM, Kyes SA, Newbold CI (2000) Var gene diversity in *Plasmodium falciparum* is generated by frequent recombination events. Molecular and biochemical parasitology 110: 391-397.

<sup>150</sup>Freitas-Junior LH, Bottius E, Pirrit LA, Deitsch KW, Scheidig C, et al. (2000) Frequent ectopic recombination of virulence factor genes in telomeric chromosome clusters of *P. falciparum*. Nature 407: 1018-1022.

<sup>151</sup>Smith JD, Gamain B, Baruch DI, Kyes S (2001) Decoding the language of var genes and *Plasmodium falciparum* sequestration. Trends in parasitology 17: 538-545.



<sup>152</sup>Kraemer SM, Smith JD (2003) Evidence for the importance of genetic structuring to the structural and functional specialization of the *Plasmodium falciparum* var gene family. *Molecular microbiology* 50: 1527-1538.

<sup>153</sup>Rowe JA, Kyes SA, Rogerson SJ, Babiker HA, Raza A (2002) Identification of a conserved *Plasmodium falciparum* var gene implicated in malaria in pregnancy. *The Journal of infectious diseases* 185: 1207-1211.

<sup>154</sup>Salanti A, Staalsoe T, Lavstsen T, Jensen AT, Sowa MP, et al. (2003) Selective upregulation of a single distinctly structured var gene in chondroitin sulphate A-adhering *Plasmodium falciparum* involved in pregnancy-associated malaria. *Molecular microbiology* 49: 179-191.

<sup>155</sup>Bull PC, Berriman M, Kyes S, Quail MA, Hall N, et al. (2005) *Plasmodium falciparum* variant surface antigen expression patterns during malaria. *PLoS pathogens* 1: e26.

<sup>156</sup>Newbold C, Warn P, Black G, Berendt A, Craig A, et al. (1997) Receptor-specific adhesion and clinical disease in *Plasmodium falciparum*. *The American journal of tropical medicine and hygiene* 57: 389-398.

<sup>157</sup>Turner GD, Morrison H, Jones M, Davis TM, Looareesuwan S, et al. (1994) An immunohistochemical study of the pathology of fatal malaria. Evidence for widespread endothelial activation and a potential role for intercellular adhesion molecule-1 in cerebral sequestration. *The American journal of pathology* 145: 1057-1069.

<sup>158</sup>Carlson J, Helmby H, Hill AV, Brewster D, Greenwood BM, et al. (1990) Human cerebral malaria: association with erythrocyte rosetting and lack of anti-rosetting antibodies. *Lancet* 336: 1457-1460.

<sup>159</sup>Lavstsen T, Salanti A, Jensen AT, Arnot DE, Theander TG (2003) Sub-grouping of *Plasmodium falciparum* 3D7 var genes based on sequence analysis of coding and non-coding regions. *Malaria journal* 2: 27.

<sup>160</sup>de Souza JB, Hafalla JC, Riley EM, Couper KN (2010) Cerebral malaria: why experimental murine models are required to understand the pathogenesis of disease. *Parasitology* 137: 755-772.

<sup>161</sup>Craig AG, Grau GE, Janse C, Kazura JW, Milner D, et al. (2012) The role of animal models for research on severe malaria. *PLoS pathogens* 8: e1002401.

<sup>162</sup>Teasdale G, Jennett B (1974) Assessment of coma and impaired consciousness. A practical scale. *Lancet* 2: 81-84.

<sup>163</sup>Artavanis-Tsakonas K, Tongren JE, Riley EM (2003) The war between the malaria parasite and the immune system: immunity, immunoregulation and im-

munopathology. *Clinical and experimental immunology* 133: 145-152.

<sup>164</sup>Haldar K, Murphy SC, Milner DA, Taylor TE (2007) Malaria: mechanisms of erythrocytic infection and pathological correlates of severe disease. *Annual review of pathology* 2: 217-249

<sup>165</sup>Patnaik JK, Das BS, Mishra SK, Mohanty S, Satpathy SK, et al. (1994) Vascular clogging, mononuclear cell margination, and enhanced vascular permeability in the pathogenesis of human cerebral malaria. *The American journal of tropical medicine and hygiene* 51: 642-647.

<sup>166</sup>Newbold C, Craig A, Kyes S, Rowe A, Fernandez-Reyes D, et al. (1999) Cytoadherence, pathogenesis and the infected red cell surface in *Plasmodium falciparum*. *International journal for parasitology* 29: 927-937.

<sup>167</sup>Chakravorty SJ, Craig A (2005) The role of ICAM-1 in *Plasmodium falciparum* cytoadherence. *European journal of cell biology* 84: 15-27.

<sup>168</sup>Ockenhouse CF, Ho M, Tandon NN, Van Seventer GA, Shaw S, et al. (1991) Molecular basis of sequestration in severe and uncomplicated *Plasmodium falciparum* malaria: differential adhesion of infected erythrocytes to CD36 and ICAM-1. *The Journal of infectious diseases* 164: 163-169.

<sup>169</sup>Udomsangpetch R, Taylor BJ, Looareesuwan S, White NJ, Elliott JF, et al. (1996) Receptor specificity of clinical *Plasmodium falciparum* isolates: nonadherence to cell-bound E-selectin and vascular cell adhesion molecule-1. *Blood* 88: 2754-2760.

<sup>170</sup>Adams S, Turner GD, Nash GB, Micklem K, Newbold CI, et al. (2000) Differential binding of clonal variants of *Plasmodium falciparum* to allelic forms of intracellular adhesion molecule 1 determined by flow adhesion assay. *Infection and immunity* 68: 264-269.

<sup>171</sup>Ockenhouse CF, Tegoshi T, Maeno Y, Benjamin C, Ho M, et al. (1992) Human vascular endothelial cell adhesion receptors for *Plasmodium falciparum*-infected erythrocytes: roles for endothelial leukocyte adhesion molecule 1 and vascular cell adhesion molecule 1. *The Journal of experimental medicine* 176: 1183-1189.

<sup>172</sup>Silamut K, Phu NH, Whitty C, Turner GD, Louwrier K, et al. (1999) A quantitative analysis of the microvascular sequestration of malaria parasites in the human brain. *The American journal of pathology* 155: 395-410.

<sup>173</sup>Udomsangpetch R, Reinhardt PH, Schollaardt T, Elliott JF, Kubes P, et al. (1997) Promiscuity of clinical *Plasmodium falciparum* isolates for multiple adhesion molecules under flow conditions. *Journal of immunology* 158: 4358-4364.

<sup>174</sup>McCormick CJ, Craig A, Roberts D, Newbold CI, Berendt AR (1997) Intercellular adhesion molecule-1 and CD36 synergize to mediate adherence of *Plasmodium*

falciparum-infected erythrocytes to cultured human microvascular endothelial cells. *The Journal of clinical investigation* 100: 2521-2529.

<sup>175</sup>van der Heyde HC, Nolan J, Combes V, Gramaglia I, Grau GE (2006) A unified hypothesis for the genesis of cerebral malaria: sequestration, inflammation and hemostasis leading to microcirculatory dysfunction. *Trends in parasitology* 22: 503-508.

<sup>176</sup>Rae C, McQuillan JA, Parekh SB, Bubb WA, Weiser S, et al. (2004) Brain gene expression, metabolism, and bioenergetics: interrelationships in murine models of cerebral and noncerebral malaria. *FASEB journal : official publication of the Federation of American Societies for Experimental Biology* 18: 499-510.

<sup>177</sup>Penet MF, Viola A, Confort-Gouny S, Le Fur Y, Duhamel G, et al. (2005) Imaging experimental cerebral malaria in vivo: significant role of ischemic brain edema. *The Journal of neuroscience : the official journal of the Society for Neuroscience* 25: 7352-7358.

<sup>178</sup>unt NH, Golenser J, Chan-Ling T, Parekh S, Rae C, et al. (2006) Immunopathogenesis of cerebral malaria. *International journal for parasitology* 36: 569-582.

<sup>179</sup>Clark IA, Awburn MM, Whitten RO, Harper CG, Liomba NG, et al. (2003) Tissue distribution of migration inhibitory factor and inducible nitric oxide synthase in falciparum malaria and sepsis in African children. *Malaria journal* 2: 6.

<sup>180</sup>Taylor TE, Fu WJ, Carr RA, Whitten RO, Mueller JS, et al. (2004) Differentiating the pathologies of cerebral malaria by postmortem parasite counts. *Nature medicine* 10: 143-145.

<sup>181</sup>Seydel KB, Milner DA, Jr., Kamiza SB, Molyneux ME, Taylor TE (2006) The distribution and intensity of parasite sequestration in comatose Malawian children. *The Journal of infectious diseases* 194: 208-205.

<sup>182</sup>Schofield L, Grau GE (2005) Immunological processes in malaria pathogenesis. *Nature reviews Immunology* 5: 722-735.

<sup>183</sup>Good MF, Xu H, Wykes M, Engwerda CR (2005) Development and regulation of cell-mediated immune responses to the blood stages of malaria: implications for vaccine research. *Annual review of immunology* 23: 69-99.

<sup>184</sup>John CC, Panoskaltis-Mortari A, Opoka RO, Park GS, Orchard PJ, et al. (2008) Cerebrospinal fluid cytokine levels and cognitive impairment in cerebral malaria. *The American journal of tropical medicine and hygiene* 78: 198-205.

<sup>185</sup>Elhassan IM, Hviid L, Satti G, Akerstrom B, Jakobsen PH, et al. (1994) Evidence of endothelial inflammation, T cell activation, and T cell reallocation in uncomplicated *Plasmodium falciparum* malaria. *The American journal of tropical*

medicine and hygiene 51: 372-379.

<sup>186</sup>de Souza JB, Riley EM (2002) Cerebral malaria: the contribution of studies in animal models to our understanding of immunopathogenesis. *Microbes and infection / Institut Pasteur* 4: 291-300.

<sup>187</sup>Lackner P, Beer R, Helbok R, Broessner G, Engelhardt K, et al. (2006) Scanning electron microscopy of the neuropathology of murine cerebral malaria. *Malaria journal* 5: 116.

<sup>188</sup>Rest JR (1982) Cerebral malaria in inbred mice. I. A new model and its pathology. *Transactions of the Royal Society of Tropical Medicine and Hygiene* 76: 410-415.

<sup>189</sup>Hearn J, Rayment N, Landon DN, Katz DR, de Souza JB (2000) Immunopathology of cerebral malaria: morphological evidence of parasite sequestration in murine brain microvasculature. *Infection and immunity* 68: 5364-5376.

<sup>190</sup>Engwerda CR, Mynott TL, Sawhney S, De Souza JB, Bickle QD, et al. (2002) Locally up-regulated lymphotoxin alpha, not systemic tumor necrosis factor alpha, is the principle mediator of murine cerebral malaria. *The Journal of experimental medicine* 195: 1371-1377.

<sup>191</sup>Desruisseaux MS, Gulinello M, Smith DN, Lee SC, Tsuji M, et al. (2008) Cognitive dysfunction in mice infected with *Plasmodium berghei* strain ANKA. *The Journal of infectious diseases* 197: 1621-1627.

<sup>192</sup>Carroll RW, Wainwright MS, Kim KY, Kidambi T, Gomez ND, et al. (2010) A rapid murine coma and behavior scale for quantitative assessment of murine cerebral malaria. *PloS one* 5.

<sup>193</sup>Delahaye NF, Coltel N, Puthier D, Barbier M, Benech P, et al. (2007) Gene expression analysis reveals early changes in several molecular pathways in cerebral malaria-susceptible mice versus cerebral malaria-resistant mice. *BMC genomics* 8: 452.

<sup>194</sup>Lovegrove FE, Gharib SA, Patel SN, Hawkes CA, Kain KC, et al. (2007) Expression microarray analysis implicates apoptosis and interferon-responsive mechanisms in susceptibility to experimental cerebral malaria. *The American journal of pathology* 171: 1894-1903.

<sup>195</sup>Oakley MS, McCutchan TF, Anantharaman V, Ward JM, Faucette L, et al. (2008) Host biomarkers and biological pathways that are associated with the expression of experimental cerebral malaria in mice. *Infection and immunity* 76: 4518-4529.

<sup>196</sup>rest

<sup>197</sup>Jennings VM, Lal AA, Hunter RL (1998) Evidence for multiple pathologic and

protective mechanisms of murine cerebral malaria. *Infection and immunity* 66: 5972-5979.

<sup>198</sup>Lovegrove FE, Gharib SA, Pena-Castillo L, Patel SN, Ruzinski JT, et al. (2008) Parasite burden and CD36-mediated sequestration are determinants of acute lung injury in an experimental malaria model. *PLoS pathogens* 4: e1000068.

<sup>199</sup>Franke-Fayard B, Janse CJ, Cunha-Rodrigues M, Ramesar J, Buscher P, et al. (2005) Murine malaria parasite sequestration: CD36 is the major receptor, but cerebral pathology is unlinked to sequestration. *Proceedings of the National Academy of Sciences of the United States of America* 102: 11468-11473.

<sup>200</sup>Amante FH, Stanley AC, Randall LM, Zhou Y, Haque A, et al. (2007) A role for natural regulatory T cells in the pathogenesis of experimental cerebral malaria. *The American journal of pathology* 171: 548-559.

<sup>201</sup>Randall LM, Amante FH, McSweeney KA, Zhou Y, Stanley AC, et al. (2008) Common strategies to prevent and modulate experimental cerebral malaria in mouse strains with different susceptibilities. *Infection and immunity* 76: 3312-3320.

<sup>202</sup>Nie CQ, Bernard NJ, Norman MU, Amante FH, Lundie RJ, et al. (2009) IP-10-mediated T cell homing promotes cerebral inflammation over splenic immunity to malaria infection. *PLoS pathogens* 5: e1000369.

<sup>203</sup>Favre N, Da Laperousaz C, Ryffel B, Weiss NA, Imhof BA, et al. (1999) Role of ICAM-1 (CD54) in the development of murine cerebral malaria. *Microbes and infection / Institut Pasteur* 1: 961-968.

<sup>204</sup>Li J, Chang WL, Sun G, Chen HL, Specian RD, et al. (2003) Intercellular adhesion molecule 1 is important for the development of severe experimental malaria but is not required for leukocyte adhesion in the brain. *Journal of investigative medicine : the official publication of the American Federation for Clinical Research* 51: 128-140.

<sup>205</sup>Combes V, Rosenkranz AR, Redard M, Pizzolato G, Lepidi H, et al. (2004) Pathogenic role of P-selectin in experimental cerebral malaria: importance of the endothelial compartment. *The American journal of pathology* 164: 781-786.

<sup>206</sup>del Portillo HA, Fernandez-Becerra C, Bowman S, Oliver K, Preuss M, et al. (2001) A superfamily of variant genes encoded in the subtelomeric region of *Plasmodium vivax*. *Nature* 410: 839-842.

<sup>207</sup>Carlton JM, Angiuoli SV, Suh BB, Kooij TW, Perteau M, et al. (2002) Genome sequence and comparative analysis of the model rodent malaria parasite *Plasmodium yoelii yoelii*. *Nature* 419: 512-519.

<sup>208</sup>Janssen CS, Barrett MP, Turner CM, Phillips RS (2002) A large gene family

for putative variant antigens shared by human and rodent malaria parasites. *Proceedings Biological sciences / The Royal Society* 269: 431-436.

<sup>209</sup>Cunningham DA, Jarra W, Koernig S, Fonager J, Fernandez-Reyes D, et al. (2005) Host immunity modulates transcriptional changes in a multigene family (*yir*) of rodent malaria. *Molecular microbiology* 58: 636-647.

<sup>210</sup>Lou J, Gasche Y, Zheng L, Critico B, Monso-Hinard C, et al. (1998) Differential reactivity of brain microvascular endothelial cells to TNF reflects the genetic susceptibility to cerebral malaria. *European journal of immunology* 28: 3989-4000.

<sup>211</sup>Monso-Hinard C, Lou JN, Behr C, Juillard P, Grau GE (1997) Expression of major histocompatibility complex antigens on mouse brain microvascular endothelial cells in relation to susceptibility to cerebral malaria. *Immunology* 92: 53-59.

<sup>212</sup>Kossodo S, Monso C, Juillard P, Velu T, Goldman M, et al. (1997) Interleukin-10 modulates susceptibility in experimental cerebral malaria. *Immunology* 91: 536-540.

<sup>213</sup>Nie CQ, Bernard NJ, Schofield L, Hansen DS (2007) CD4+ CD25+ regulatory T cells suppress CD4+ T-cell function and inhibit the development of *Plasmodium berghei*-specific TH1 responses involved in cerebral malaria pathogenesis. *Infection and immunity* 75: 2275-2282.

<sup>214</sup>Saeftel M, Krueger A, Arriens S, Heussler V, Racz P, et al. (2004) Mice deficient in interleukin-4 (IL-4) or IL-4 receptor alpha have higher resistance to sporozoite infection with *Plasmodium berghei* (ANKA) than do naive wild-type mice. *Infection and immunity* 72: 322-331.

<sup>215</sup>Nitcheu J, Bonduelle O, Combadiere C, Tefit M, Seilhean D, et al. (2003) Perforin-dependent brain-infiltrating cytotoxic CD8+ T lymphocytes mediate experimental cerebral malaria pathogenesis. *Journal of immunology* 170: 2221-2228.

<sup>216</sup>Yanez DM, Manning DD, Cooley AJ, Weidanz WP, van der Heyde HC (1996) Participation of lymphocyte subpopulations in the pathogenesis of experimental murine cerebral malaria. *Journal of immunology* 157: 1620-1624.

<sup>217</sup>Belnoue E, Kayibanda M, Vigario AM, Deschemin JC, van Rooijen N, et al. (2002) On the pathogenic role of brain-sequestered alpha beta CD8+ T cells in experimental cerebral malaria. *Journal of immunology* 169: 6369-6375.

<sup>218</sup>Hermesen C, van de Wiel T, Mommers E, Sauerwein R, Eling W (1997) Depletion of CD4+ or CD8+ T-cells prevents *Plasmodium berghei* induced cerebral malaria in end-stage disease. *Parasitology* 114 ( Pt 1): 7-12.

<sup>219</sup>Hansen DS, Bernard NJ, Nie CQ, Schofield L (2007) NK cells stimulate recruitment of CXCR3+ T cells to the brain during *Plasmodium berghei*-mediated cerebral malaria. *Journal of immunology* 178: 5779-5788.

<sup>220</sup>Belnoue E, Potter SM, Rosa DS, Mauduit M, Gruner AC, et al. (2008) Control of pathogenic CD8+ T cell migration to the brain by IFN-gamma during experimental cerebral malaria. *Parasite immunology* 30: 544-553.

<sup>221</sup>Finley R, Weintraub J, Louis JA, Engers HD, Zubler R, et al. (1983) Prevention of cerebral malaria by adoptive transfer of malaria-specific cultured T cells into mice infected with *Plasmodium berghei*. *Journal of immunology* 131: 1522-1526.

<sup>222</sup>Conner SD, Schmid SL (2003) Regulated portals of entry into the cell. *Nature* 422: 37-44.

<sup>223</sup>Maxfield FR, McGraw TE (2004) Endocytic recycling. *Nature reviews Molecular cell biology* 5: 121-132.

<sup>224</sup>Grant BD, Donaldson JG (2009) Pathways and mechanisms of endocytic recycling. *Nature reviews Molecular cell biology* 10: 597-608.

<sup>225</sup>Pfeffer S, Aivazian D (2004) Targeting Rab GTPases to distinct membrane compartments. *Nature reviews Molecular cell biology* 5: 886-896.

<sup>226</sup>Grosshans BL, Ortiz D, Novick P (2006) Rabs and their effectors: achieving specificity in membrane traffic. *Proceedings of the National Academy of Sciences of the United States of America* 103: 11821-11827.

<sup>227</sup>Novick P, Medkova M, Dong G, Hutagalung A, Reinisch K, et al. (2006) Interactions between Rabs, tethers, SNAREs and their regulators in exocytosis. *Biochemical Society transactions* 34: 683-686.

<sup>228</sup>Naslavsky N, Boehm M, Backlund PS, Jr., Caplan S (2004) Rabenosyn-5 and EHD1 interact and sequentially regulate protein recycling to the plasma membrane. *Molecular biology of the cell* 15: 2410-2422.

<sup>229</sup>Naslavsky N, Rahajeng J, Sharma M, Jovic M, Caplan S (2006) Interactions between EHD-proteins and Rab11-FIP2: a role for EHD3 in early endosomal transport. *Molecular biology of the cell* 17: 163-177.

<sup>230</sup>Sharma M, Giridharan SS, Rahajeng J, Naslavsky N, Caplan S (2009) MICAL-L1 links EHD1 to tubular recycling endosomes and regulates receptor recycling. *Molecular biology of the cell* 20: 5181-5194.

<sup>231</sup>Caplan S, Naslavsky N, Hartnell LM, Lodge R, Polishchuk RS, et al. (2002) A tubular EHD1-containing compartment involved in the recycling of major histocompatibility complex class I molecules to the plasma membrane. *The EMBO journal* 21: 2557-2567.

<sup>232</sup>Naslavsky N, Caplan S (2011) EHD-proteins: key conductors of endocytic transport. *Trends in cell biology* 21: 122-131.

- <sup>233</sup>Campelo F, Fabrikant G, McMahon HT, Kozlov MM (2010) Modeling membrane shaping by proteins: focus on EHD2 and N-BAR domains. *FEBS letters* 584: 1830-1839.
- <sup>234</sup>Jovic M, Kieken F, Naslavsky N, Sorgen PL, Caplan S (2009) Eps15 homology domain 1-associated tubules contain phosphatidylinositol-4-phosphate and phosphatidylinositol-(4,5)-bisphosphate and are required for efficient recycling. *Molecular biology of the cell* 20: 2731-2743.
- <sup>235</sup>Fazioli F, Minichiello L, Matoskova B, Wong WT, Di Fiore PP (1993) eps15, a novel tyrosine kinase substrate, exhibits transforming activity. *Molecular and cellular biology* 13: 5814-5828.
- <sup>236</sup>Wong WT, Schumacher C, Salcini AE, Romano A, Castagnino P, et al. (1995) A protein-binding domain, EH, identified in the receptor tyrosine kinase substrate Eps15 and conserved in evolution. *Proceedings of the National Academy of Sciences of the United States of America* 92: 9530-9534.
- <sup>237</sup>Paoluzi S, Castagnoli L, Lauro I, Salcini AE, Coda L, et al. (1998) Recognition specificity of individual EH domains of mammals and yeast. *The EMBO journal* 17: 6541-6550.
- <sup>238</sup>Salcini AE, Confalonieri S, Doria M, Santolini E, Tassi E, et al. (1997) Binding specificity and in vivo targets of the EH domain, a novel protein-protein interaction module. *Genes & development* 11: 2239-2249.
- <sup>239</sup>Naslavsky N, Rahajeng J, Chenavas S, Sorgen PL, Caplan S (2007) EHD1 and Eps15 interact with phosphatidylinositols via their Eps15 homology domains. *The Journal of biological chemistry* 282: 16612-16622.
- <sup>240</sup>Kieken F, Jovic M, Naslavsky N, Caplan S, Sorgen PL (2007) EH domain of EHD1. *Journal of biomolecular NMR* 39: 323-329.
- <sup>241</sup>Kieken F, Sharma M, Jovic M, Giridharan SS, Naslavsky N, et al. (2010) Mechanism for the selective interaction of C-terminal Eps15 homology domain proteins with specific Asn-Pro-Phe-containing partners. *The Journal of biological chemistry* 285: 8687-8694.
- <sup>242</sup>Kieken F, Jovic M, Tonelli M, Naslavsky N, Caplan S, et al. (2009) Structural insight into the interaction of proteins containing NPF, DPF, and GPF motifs with the C-terminal EH-domain of EHD1. *Protein science : a publication of the Protein Society* 18: 2471-2479.
- <sup>243</sup>Chen C, Mendez E, Houck J, Fan W, Lohavanichbutr P, et al. (2008) Gene expression profiling identifies genes predictive of oral squamous cell carcinoma. *Cancer epidemiology, biomarkers & prevention : a publication of the American Association for Cancer Research, cosponsored by the American Society of Preventive Oncology*



17: 2152-2162.

<sup>244</sup>Tripathi AK, Sha W, Shulaev V, Stins MF, Sullivan DJ, Jr. (2009) Plasmodium falciparum-infected erythrocytes induce NF-kappaB regulated inflammatory pathways in human cerebral endothelium. *Blood* 114: 4243-4252.

<sup>245</sup>Rapaport D, Auerbach W, Naslavsky N, Pasmanik-Chor M, Galperin E, et al. (2006) Recycling to the plasma membrane is delayed in EHD1 knockout mice. *Traffic* 7: 52-60.

<sup>246</sup>George M, Rainey MA, Naramura M, Ying G, Harms DW, et al. (2010) Ehd4 is required to attain normal prepubertal testis size but dispensable for fertility in male mice. *Genesis* 48: 328-342.

<sup>247</sup>Rainey MA, George M, Ying G, Akakura R, Burgess DJ, et al. (2010) The endocytic recycling regulator EHD1 is essential for spermatogenesis and male fertility in mice. *BMC developmental biology* 10: 37.

<sup>248</sup>Lin SX, Grant B, Hirsh D, Maxfield FR (2001) Rme-1 regulates the distribution and function of the endocytic recycling compartment in mammalian cells. *Nature cell biology* 3: 567-572.

<sup>249</sup>Jovic M, Naslavsky N, Rapaport D, Horowitz M, Caplan S (2007) EHD1 regulates beta1 integrin endosomal transport: effects on focal adhesions, cell spreading and migration. *Journal of cell science* 120: 802-814.

<sup>250</sup>Guilherme A, Soriano NA, Furcinitti PS, Czech MP (2004) Role of EHD1 and EHBP1 in perinuclear sorting and insulin-regulated GLUT4 recycling in 3T3-L1 adipocytes. *The Journal of biological chemistry* 279: 40062-40075.

<sup>251</sup>Chung HJ, Qian X, Ehlers M, Jan YN, Jan LY (2009) Neuronal activity regulates phosphorylation-dependent surface delivery of G protein-activated inwardly rectifying potassium channels. *Proceedings of the National Academy of Sciences of the United States of America* 106: 629-634.

<sup>252</sup>Gao Y, Balut CM, Bailey MA, Patino-Lopez G, Shaw S, et al. (2010) Recycling of the Ca<sup>2+</sup>-activated K<sup>+</sup> channel, KCa2.3, is dependent upon RME-1, Rab35/EPI64C, and an N-terminal domain. *The Journal of biological chemistry* 285: 17938-17953.

<sup>253</sup>Allaire PD, Marat AL, Dall'Armi C, Di Paolo G, McPherson PS, et al. (2010) The Connecdenn DENN domain: a GEF for Rab35 mediating cargo-specific exit from early endosomes. *Molecular cell* 37: 370-382.

<sup>254</sup>Sato M, Sato K, Liou W, Pant S, Harada A, et al. (2008) Regulation of endocytic recycling by *C. elegans* Rab35 and its regulator RME-4, a coated-pit protein. *The EMBO journal* 27: 1183-1196.

<sup>255</sup>Rahajeng J, Giridharan SS, Naslavsky N, Caplan S (2010) Collapsin response mediator protein-2 (Crmp2) regulates trafficking by linking endocytic regulatory proteins to dynein motors. *The Journal of biological chemistry* 285: 31918-31922.

<sup>256</sup>Naslavsky N, Rahajeng J, Rapaport D, Horowitz M, Caplan S (2007) EHD1 regulates cholesterol homeostasis and lipid droplet storage. *Biochemical and biophysical research communications* 357: 792-799.

<sup>257</sup>Posey AD, Jr., Pytel P, Gardikiotes K, Demonbreun AR, Rainey M, et al. (2011) Endocytic recycling proteins EHD1 and EHD2 interact with fer-1-like-5 (Fer1L5) and mediate myoblast fusion. *The Journal of biological chemistry* 286: 7379-7388.

<sup>258</sup>Galperin E, Benjamin S, Rapaport D, Rotem-Yehudar R, Tolchinsky S, et al. (2002) EHD3: a protein that resides in recycling tubular and vesicular membrane structures and interacts with EHD1. *Traffic* 3: 575-589.

<sup>259</sup>Sharma M, Naslavsky N, Caplan S (2008) A role for EHD4 in the regulation of early endosomal transport. *Traffic* 9: 995-1018.

<sup>260</sup>Benjamin S, Weidberg H, Rapaport D, Pekar O, Nudelman M, et al. (2011) EHD2 mediates trafficking from the plasma membrane by modulating Rac1 activity. *The Biochemical journal* 439: 433-442.

<sup>261</sup>Guilherme A, Soriano NA, Bose S, Holik J, Bose A, et al. (2004) EHD2 and the novel EH domain binding protein EHBP1 couple endocytosis to the actin cytoskeleton. *The Journal of biological chemistry* 279: 10593-10605.

<sup>262</sup>George M, Ying G, Rainey MA, Solomon A, Parikh PT, et al. (2007) Shared as well as distinct roles of EHD-proteins revealed by biochemical and functional comparisons in mammalian cells and *C. elegans*. *BMC cell biology* 8: 3.

<sup>263</sup>Doherty KR, Demonbreun AR, Wallace GQ, Cave A, Posey AD, et al. (2008) The endocytic recycling protein EHD2 interacts with myoferlin to regulate myoblast fusion. *The Journal of biological chemistry* 283: 20252-20260.

<sup>264</sup>Stoeber M, Stoeck IK, Hanni C, Bleck CK, Balistreri G, et al. (2012) Oligomers of the ATPase EHD2 confine caveolae to the plasma membrane through association with actin. *The EMBO journal* 31: 2350-2364.

<sup>265</sup>Moren B, Shah C, Howes MT, Schieber NL, McMahon HT, et al. (2012) EHD2 regulates caveolar dynamics via ATP-driven targeting and oligomerization. *Molecular biology of the cell* 23: 1316-1329.

<sup>266</sup>Pekar O, Benjamin S, Weidberg H, Smaldone S, Ramirez F, et al. (2012) EHD2 shuttles to the nucleus and represses transcription. *The Biochemical journal* 444: 383-394.

<sup>267</sup>Gudmundsson H, Hund TJ, Wright PJ, Kline CF, Snyder JS, et al. (2010) EH

domain proteins regulate cardiac membrane protein targeting. *Circulation research* 107: 84-95.

<sup>268</sup>Roland JT, Kenworthy AK, Peranen J, Caplan S, Goldenring JR (2007) Myosin Vb interacts with Rab8a on a tubular network containing EHD1 and EHD3. *Molecular biology of the cell* 18: 2828-2837.

<sup>269</sup>Yap CC, Lasiecka ZM, Caplan S, Winckler B (2010) Alterations of EHD1/EHD4 protein levels interfere with L1/NgCAM endocytosis in neurons and disrupt axonal targeting. *The Journal of neuroscience : the official journal of the Society for Neuroscience* 30: 6646-6657.

<sup>270</sup>Ponnudurai T, Leeuwenberg AD, Meuwissen JH (1981) Chloroquine sensitivity of isolates of *Plasmodium falciparum* adapted to in vitro culture. *Tropical and geographical medicine* 33: 50-54.

<sup>271</sup>Franke-Fayard B, Trueman H, Ramesar J, Mendoza J, van der Keur M, et al. (2004) A *Plasmodium berghei* reference line that constitutively expresses GFP at a high level throughout the complete life cycle. *Molecular and biochemical parasitology* 137: 23-33.

<sup>272</sup>Yoeli M, Most H (1965) Pre-Erythrocytic Development of *Plasmodium Berghei*. *Nature* 205: 715-716.

<sup>273</sup>Donald RG, Carter D, Ullman B, Roos DS (1996) Insertional tagging, cloning, and expression of the *Toxoplasma gondii* hypoxanthine-xanthine-guanine phosphoribosyltransferase gene. Use as a selectable marker for stable transformation. *The Journal of biological chemistry* 271: 14010-14019.

<sup>274</sup>Silvie O, Goetz K, Matuschewski K (2008) A sporozoite asparagine-rich protein controls initiation of *Plasmodium* liver stage development. *PLoS pathogens* 4: e1000086.

<sup>275</sup>Lemgruber L, Lupetti P, Martins-Duarte ES, De Souza W, Vommaro RC (2011) The organization of the wall filaments and characterization of the matrix structures of *Toxoplasma gondii* cyst form. *Cellular microbiology* 13: 1920-1932.

<sup>276</sup>Black M, Seeber F, Soldati D, Kim K, Boothroyd JC (1995) Restriction enzyme-mediated integration elevates transformation frequency and enables co-transfection of *Toxoplasma gondii*. *Molecular and biochemical parasitology* 74: 55-63.

<sup>277</sup>Roos DS, Donald RG, Morrissette NS, Moulton AL (1994) Molecular tools for genetic dissection of the protozoan parasite *Toxoplasma gondii*. *Methods in cell biology* 45: 27-63.

<sup>278</sup>Carter R., Ranford-Cartwright L. C., and Alano P. (1993). The culture and preparation of gametocytes of *Plasmodium falciparum* for immunochemical, molec-

ular, and mosquito infectivity studies. In "Methods in Molecular Biology, Vol. 21: Protocols in Molecular Parasitology." (J. E. Hyde, Ed.), pp. 67-89. Humana Press Inc., Totowa, New Jersey.

<sup>279</sup>Carter, R., Ranford-Cartwright, L. C., and Alano, P. 1993. The culture and preparation of gametocytes of *Plasmodium falciparum* for immunochemical, molecular, and mosquito infectivity studies. In "Methods in Molecular Biology, Vol. 21: Protocols in Molecular Parasitology." (J. E. Hyde, Ed.), pp. 67-89. Humana Press Inc., Totowa, New Jersey.

<sup>280</sup>Grant B, Zhang Y, Paupard MC, Lin SX, Hall DH, et al. (2001) Evidence that RME-1, a conserved *C. elegans* EH-domain protein, functions in endocytic recycling. *Nature cell biology* 3: 573-579.

<sup>281</sup>Saraste M, Sibbald PR, Wittinghofer A (1990) The P-loop -a common motif in ATP- and GTP-binding proteins. *Trends in biochemical sciences* 15: 430-434.

<sup>282</sup>Daumke O, Lundmark R, Vallis Y, Martens S, Butler PJ, et al. (2007) Architectural and mechanistic insights into an EHD ATPase involved in membrane remodelling. *Nature* 449: 923-927.

<sup>283</sup>Lee DW, Zhao X, Scarselletta S, Schweinsberg PJ, Eisenberg E, et al. (2005) ATP binding regulates oligomerization and endosome association of RME-1 family proteins. *The Journal of biological chemistry* 280: 17213-17220.

<sup>284</sup>Fritz HM, Bowyer PW, Bogyo M, Conrad PA, Boothroyd JC (2012) Proteomic analysis of fractionated *Toxoplasma* oocysts reveals clues to their environmental resistance. *PloS one* 7: e29955.

<sup>285</sup>Xia D, Sanderson SJ, Jones AR, Prieto JH, Yates JR, et al. (2008) The proteome of *Toxoplasma gondii*: integration with the genome provides novel insights into gene expression and annotation. *Genome biology* 9: R116.

<sup>286</sup>Behnke MS, Wootton JC, Lehmann MM, Radke JB, Lucas O, et al. (2010) Coordinated progression through two subtranscriptomes underlies the tachyzoite cycle of *Toxoplasma gondii*. *PloS one* 5: e12354.

<sup>287</sup>Banaszynski LA, Chen LC, Maynard-Smith LA, Ooi AG, Wandless TJ (2006) A rapid, reversible, and tunable method to regulate protein function in living cells using synthetic small molecules. *Cell* 126: 995-1004.

<sup>288</sup>Herm-Gotz A, Agop-Nersesian C, Munter S, Grimley JS, Wandless TJ, et al. (2007) Rapid control of protein level in the apicomplexan *Toxoplasma gondii*. *Nature methods* 4: 1003-1005.

<sup>289</sup>de Beer T, Hoofnagle AN, Enmon JL, Bowers RC, Yamabhai M, et al. (2000) Molecular mechanism of NPF recognition by EH domains. *Nature structural biology*

7: 1018-1022.

<sup>290</sup>Treeck M, Sanders JL, Elias JE, Boothroyd JC (2011) The phosphoproteomes of *Plasmodium falciparum* and *Toxoplasma gondii* reveal unusual adaptations within and beyond the parasites' boundaries. *Cell host & microbe* 10: 410-419.

<sup>291</sup>Menard R, Janse C (1997) Gene targeting in malaria parasites. *Methods* 13: 148-157.

<sup>292</sup>Pfander C, Anar B, Schwach F, Otto TD, Brochet M, et al. (2011) A scalable pipeline for highly effective genetic modification of a malaria parasite. *Nature methods* 8: 1078-1082.

<sup>293</sup>White NJ, Turner GD, Medana IM, Dondorp AM, Day NP (2010) The murine cerebral malaria phenomenon. *Trends in parasitology* 26: 11-15.

<sup>294</sup>Engwerda C, Belnoue E, Gruner AC, Renia L (2005) Experimental models of cerebral malaria. *Current topics in microbiology and immunology* 297: 103-143.

<sup>295</sup>Chang-Ling T, Neill AL, Hunt NH (1992) Early microvascular changes in murine cerebral malaria detected in retinal wholemounts. *The American journal of pathology* 140: 1121-1130.

<sup>296</sup>Oliveira Gde A, Lieberman J, Barillas-Mury C (2012) Epithelial nitration by a peroxidase/NOX5 system mediates mosquito antiplasmodial immunity. *Science* 335: 856-859.

<sup>297</sup>Blandin S, Shiao SH, Moita LF, Janse CJ, Waters AP, et al. (2004) Complement-like protein TEP1 is a determinant of vectorial capacity in the malaria vector *Anopheles gambiae*. *Cell* 116: 661-670.

<sup>298</sup>Kumar S, Christophides GK, Cantera R, Charles B, Han YS, et al. (2003) The role of reactive oxygen species on *Plasmodium melanotic* encapsulation in *Anopheles gambiae*. *Proceedings of the National Academy of Sciences of the United States of America* 100: 14139-14144.

<sup>299</sup>Molina-Cruz A, DeJong RJ, Charles B, Gupta L, Kumar S, et al. (2008) Reactive oxygen species modulate *Anopheles gambiae* immunity against bacteria and *Plasmodium*. *The Journal of biological chemistry* 283: 3217-3223.

<sup>300</sup>Boissiere A, Tchioffo MT, Bachar D, Abate L, Marie A, et al. (2012) Midgut microbiota of the malaria mosquito vector *Anopheles gambiae* and interactions with *Plasmodium falciparum* infection. *PLoS pathogens* 8: e1002742.

<sup>301</sup>Maslowski KM, Mackay CR (2011) Diet, gut microbiota and immune responses. *Nature immunology* 12: 5-9.

<sup>302</sup> Damiani C, Ricci I, Crotti E, Rossi P, Rizzi A, et al. (2010) Mosquito-bacteria

symbiosis: the case of *Anopheles gambiae* and *Asaia*. *Microbial ecology* 60: 644-654.

<sup>303</sup>Moll RM, Romoser WS, Modrzakowski MC, Moncayo AC, Lerdthusnee K (2001) Meconial peritrophic membranes and the fate of midgut bacteria during mosquito (Diptera: Culicidae) metamorphosis. *Journal of medical entomology* 38: 29-32.

<sup>304</sup>Favia G, Ricci I, Marzorati M, Negri I, Alma A, et al. (2008) Bacteria of the genus *Asaia*: a potential paratransgenic weapon against malaria. *Advances in experimental medicine and biology* 627: 49-59.

<sup>305</sup>Jin C, Ren X, Rasgon JL (2009) The virulent *Wolbachia* strain wMelPop efficiently establishes somatic infections in the malaria vector *Anopheles gambiae*. *Applied and environmental microbiology* 75: 3373-3376.

<sup>306</sup>Bruce MC, Alano P, Duthie S, Carter R (1990) Commitment of the malaria parasite *Plasmodium falciparum* to sexual and asexual development. *Parasitology* 100 Pt 2: 191-200.

<sup>307</sup>Hawking F, Wilson ME, Gammage K (1971) Evidence for cyclic development and short-lived maturity in the gametocytes of *Plasmodium falciparum*. *Transactions of the Royal Society of Tropical Medicine and Hygiene* 65: 549-559.

<sup>308</sup>Nijhout MM, Carter R (1978) Gamete development in malaria parasites: bicarbonate-dependent stimulation by pH in vitro. *Parasitology* 76: 39-53.

<sup>309</sup>Sinden RE (1983) The cell biology of sexual development in plasmodium. *Parasitology* 86 (Pt 4): 7-28.

<sup>310</sup>Nijhout MM (1979) *Plasmodium gallinaceum*: exflagellation stimulated by a mosquito factor. *Experimental parasitology* 48: 75-80.

<sup>311</sup>Billker O, Lindo V, Panico M, Etienne AE, Paxton T, et al. (1998) Identification of xanthurenic acid as the putative inducer of malaria development in the mosquito. *Nature* 392: 289-292.

<sup>312</sup>Billker O, Lindo V, Panico M, Etienne AE, Paxton T, et al. (1998) Identification of xanthurenic acid as the putative inducer of malaria development in the mosquito. *Nature* 392: 289-292.

<sup>313</sup>Robert V, Read AF, Essong J, Tchuinkam T, Mulder B, et al. (1996) Effect of gametocyte sex ratio on infectivity of *Plasmodium falciparum* to *Anopheles gambiae*. *Transactions of the Royal Society of Tropical Medicine and Hygiene* 90: 621-624.

<sup>314</sup>Mitri C, Thierry I, Bourgouin C, Paul RE (2009) Density-dependent impact of the human malaria parasite *Plasmodium falciparum* gametocyte sex ratio on mosquito infection rates. *Proceedings Biological sciences / The Royal Society* 276: 3721-3726.

<sup>315</sup>Ponnudurai T, Meuwissen JH, Leeuwenberg AD, Verhave JP, Lensen AH (1982)

The production of mature gametocytes of *Plasmodium falciparum* in continuous cultures of different isolates infective to mosquitoes. *Transactions of the Royal Society of Tropical Medicine and Hygiene* 76: 242-250.

<sup>316</sup>George M, Rainey MA, Naramura M, Foster KW, Holzapfel MS, et al. (2011) Renal thrombotic microangiopathy in mice with combined deletion of endocytic recycling regulators EHD3 and EHD4. *PloS one* 6: e17838.

<sup>317</sup>Olswang-Kutz Y, Gertel Y, Benjamin S, Sela O, Pekar O, et al. (2009) *Drosophila* Past1 is involved in endocytosis and is required for germline development and survival of the adult fly. *Journal of cell science* 122: 471-480.

<sup>318</sup>Grant BD, Caplan S (2008) Mechanisms of EHD/RME-1 protein function in endocytic transport. *Traffic* 9: 2043-2052.

<sup>319</sup>Breinich MS, Ferguson DJ, Foth BJ, van Dooren GG, Lebrun M, et al. (2009) A dynamin is required for the biogenesis of secretory organelles in *Toxoplasma gondii*. *Current biology* : CB 19: 277-286.

<sup>320</sup>Parussini F, Coppens I, Shah PP, Diamond SL, Carruthers VB (2010) Cathepsin L occupies a vacuolar compartment and is a protein maturase within the endo/exocytic system of *Toxoplasma gondii*. *Molecular microbiology* 76: 1340-1357.

<sup>321</sup>Schwab JC, Beckers CJ, Joiner KA (1994) The parasitophorous vacuole membrane surrounding intracellular *Toxoplasma gondii* functions as a molecular sieve. *Proceedings of the National Academy of Sciences of the United States of America* 91: 509-513.

<sup>322</sup>Nichols BA, Chiappino ML, Pavesio CE (1994) Endocytosis at the micropore of *Toxoplasma gondii*. *Parasitology research* 80: 91-98.

<sup>323</sup>Hoppe HC, Joiner KA (2000) Cytoplasmic tail motifs mediate endoplasmic reticulum localization and export of transmembrane reporters in the protozoan parasite *Toxoplasma gondii*. *Cellular microbiology* 2: 569-578.

<sup>324</sup>Glotzer M (2005) The molecular requirements for cytokinesis. *Science* 307: 1735-1739.

<sup>325</sup>Montagnac G, Echard A, Chavrier P (2008) Endocytic traffic in animal cell cytokinesis. *Current opinion in cell biology* 20: 454-461.

<sup>326</sup>Endo T, Pelster B, Piekarski G (1981) Infection of murine peritoneal macrophages with *Toxoplasma gondii* exposed to ultraviolet light. *Zeitschrift fur Parasitenkunde* 65: 121-129.

<sup>327</sup>Jones TC, Yeh S, Hirsch JG (1972) The interaction between *Toxoplasma gondii* and mammalian cells. I. Mechanism of entry and intracellular fate of the parasite. *The Journal of experimental medicine* 136: 1157-1172.

<sup>328</sup>Sinai AP, Joiner KA (2001) The *Toxoplasma gondii* protein ROP2 mediates host organelle association with the parasitophorous vacuole membrane. *The Journal of cell biology* 154: 95-108.

<sup>329</sup>Sinai AP, Webster P, Joiner KA (1997) Association of host cell endoplasmic reticulum and mitochondria with the *Toxoplasma gondii* parasitophorous vacuole membrane: a high affinity interaction. *Journal of cell science* 110 ( Pt 17): 2117-2128.

<sup>330</sup>Coppens I, Sinai AP, Joiner KA (2000) *Toxoplasma gondii* exploits host low-density lipoprotein receptor-mediated endocytosis for cholesterol acquisition. *The Journal of cell biology* 149: 167-180.

<sup>331</sup>Charron AJ, Sibley LD (2002) Host cells: mobilizable lipid resources for the intracellular parasite *Toxoplasma gondii*. *Journal of cell science* 115: 3049-3059.

<sup>332</sup>Mair GR, Braks JA, Garver LS, Wiegant JC, Hall N, et al. (2006) Regulation of sexual development of *Plasmodium* by translational repression. *Science* 313: 667-669.

<sup>333</sup>Mair GR, Lasonder E, Garver LS, Franke-Fayard BM, Carret CK, et al. (2010) Universal features of post-transcriptional gene regulation are critical for *Plasmodium* zygote development. *PLoS pathogens* 6: e1000767.

<sup>334</sup>Khan SM, Franke-Fayard B, Mair GR, Lasonder E, Janse CJ, et al. (2005) Proteome analysis of separated male and female gametocytes reveals novel sex-specific *Plasmodium* biology. *Cell* 121: 675-687.

<sup>335</sup>Gantt S, Persson C, Rose K, Birkett AJ, Abagyan R, et al. (2000) Antibodies against thrombospondin-related anonymous protein do not inhibit *Plasmodium* sporozoite infectivity in vivo. *Infection and immunity* 68: 3667-3673.

<sup>336</sup>Kappe S, Bruderer T, Gantt S, Fujioka H, Nussenzweig V, et al. (1999) Conservation of a gliding motility and cell invasion machinery in Apicomplexan parasites. *The Journal of cell biology* 147: 937-944.

<sup>337</sup>Sultan AA, Thathy V, Frevert U, Robson KJ, Crisanti A, et al. (1997) TRAP is necessary for gliding motility and infectivity of *Plasmodium* sporozoites. *Cell* 90: 511-522.

<sup>338</sup>Deschermeier C, Hecht LS, Bach F, Rutzel K, Stanway RR, et al. (2012) Mitochondrial lipoic acid scavenging is essential for *Plasmodium berghei* liver stage development. *Cellular microbiology* 14: 416-430.

<sup>339</sup>Mizushima N, Klionsky DJ (2007) Protein turnover via autophagy: implications for metabolism. *Annual review of nutrition* 27: 19-40.

<sup>340</sup>Kitamura K, Kishi-Itakura C, Tsuboi T, Sato S, Kita K, et al. (2012) Autophagy-



related Atg8 localizes to the apicoplast of the human malaria parasite *Plasmodium falciparum*. *PloS one* 7: e42977.

<sup>341</sup>Nakatogawa H, Suzuki K, Kamada Y, Ohsumi Y (2009) Dynamics and diversity in autophagy mechanisms: lessons from yeast. *Nature reviews Molecular cell biology* 10: 458-467.

<sup>342</sup>Mizushima N, Yoshimori T, Ohsumi Y (2011) The role of Atg proteins in autophagosome formation. *Annual review of cell and developmental biology* 27: 107-132.

<sup>343</sup>Besteiro S, Brooks CF, Striepen B, Dubremetz JF (2011) Autophagy protein Atg3 is essential for maintaining mitochondrial integrity and for normal intracellular development of *Toxoplasma gondii* tachyzoites. *PLoS pathogens* 7: e1002416.

<sup>344</sup>Duszenko M, Ginger ML, Brennand A, Gualdron-Lopez M, Colombo MI, et al. (2011) Autophagy in protists. *Autophagy* 7: 127-158.

<sup>345</sup>Brennand A, Gualdron-Lopez M, Coppens I, Rigden DJ, Ginger ML, et al. (2011) Autophagy in parasitic protists: unique features and drug targets. *Molecular and biochemical parasitology* 177: 83-99.

<sup>346</sup>Stanway RR, Witt T, Zobiak B, Aepfelbacher M, Heussler VT (2009) GFP-targeting allows visualization of the apicoplast throughout the life cycle of live malaria parasites. *Biology of the cell / under the auspices of the European Cell Biology Organization* 101: 415-430, 415 p following 430.

<sup>347</sup>Kaiser K, Matuschewski K, Camargo N, Ross J, Kappe SH (2004) Differential transcriptome profiling identifies *Plasmodium* genes encoding pre-erythrocytic stage-specific proteins. *Molecular microbiology* 51: 1221-1232.

<sup>348</sup>Mueller AK, Labaied M, Kappe SH, Matuschewski K (2005) Genetically modified *Plasmodium* parasites as a protective experimental malaria vaccine. *Nature* 433: 164-167.

<sup>349</sup>Mikolajczak SA, Jacobs-Lorena V, MacKellar DC, Camargo N, Kappe SH (2007) L-FABP is a critical host factor for successful malaria liver stage development. *International journal for parasitology* 37: 483-489.

<sup>350</sup>Sharma A, Yogavel M, Akhouri RR, Gill J (2008) Crystal structure of soluble domain of malaria sporozoite protein UIS3 in complex with lipid. *The Journal of biological chemistry* 283: 24077-24088.

<sup>351</sup>Vignali M, McKinlay A, LaCount DJ, Chettier R, Bell R, et al. (2008) Interaction of an atypical *Plasmodium falciparum* ETRAMP with human apolipoproteins. *Malaria journal* 7: 211.